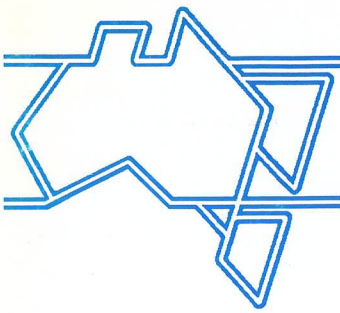

THIRD A-NZ YOUNG GEOTECHNICAL PROFESSIONALS CONFERENCE

Melbourne, 1998

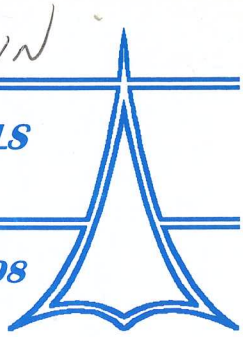

PROCEEDINGS OF THE THIRD AUSTRALIA - NEW ZEALAND YOUNG GEOTECHNICAL PROFESSIONALS CONFERENCE

18 - 21 February 1998
Queens College
Melbourne Australia

Edited by:

Grant Cameron
Ben Collingwood
Jim Slatter

AUSTRALIAN GEOMECHANICS SOCIETY

NEW ZEALAND GEOTECHNICAL SOCIETY

Golder FOUNDATION

A gift in support of

Golder's commitment to technical

knowledge and excellence

Max Ervin

PROCEEDINGS OF THE THIRD AUSTRALIA - NEW ZEALAND YOUNG GEOTECHNICAL PROFESSIONALS CONFERENCE

18 - 21 February 1998
Queens College
Melbourne Australia

Edited by:

Grant Cameron
Ben Collingwood
Jim Slatter

AUSTRALIAN GEOMECHANICS SOCIETY

NEW ZEALAND GEOTECHNICAL SOCIETY

Sponsored by:

COFFEY PARTNERS INTERNATIONAL PTY LTD

FRANKIPILE AUSTRALIA PTY LTD

GEOTECHNICAL SYSTEMS AUSTRALIA PTY LTD

GEOTEST PTY LTD

GOLDER ASSOCIATES PTY LTD

MONASH UNIVERSITY, DEPARTMENT OF CIVIL ENGINEERING

RUST PPK CONSULTANTS PTY LTD

THE NEW ZEALAND GEOTECHNICAL SOCIETY

UNIVERSITY OF NSW, SCHOOL OF CIVIL ENGINEERING

UNIVERSITY OF WA, DEPARTMENT OF CIVIL ENGINEERING

VIBROPILE (AUST.) PTY LTD

WOODWARD-CLYDE CONSULTANTS PTY LTD

The ***Centre for Offshore Foundation Systems (COFS)*** at The University of Western Australia and The University of Sydney, undertakes fundamental research into the properties of offshore soils and the response of foundation systems for offshore oil and gas production facilities. It has been established under the direction of Professor Mark Randolph (UWA).

COFS three major research streams are. (1) micro-mechanics and stress strain response of calcareous soil, (2) response of foundation systems, particularly under cyclic loading, and (3) soil-structure-fluid interaction for thin-walled shells and pipelines

COFS brings together top Australian and international researchers to advise and assist industry in all aspects of safe and economic foundation design and operation. COFS also supervises PhD students.

Complex tests are conducted using sophisticated facilities and COFS research personnel utilise world-class modelling capabilities. These include two geotechnical centrifuges, a large calibration chamber and advanced laboratory testing equipment. COFS houses the only centrifuge modelling facility in Australia.

For further information on COFS, its capacity to assist industry or the possibility of undertaking research work as a PhD student or postdoctoral fellow please contact: Suzanne Preston, Centre for Offshore Foundation Systems, UWA, Nedlands, WA, 6907. Phone: 61 (0)8 93807319, Fax: 61(0)8 93807320 or email: cofs@uwa.edu.au.

COFFEY

Coffey Partners International Pty Ltd

As one of Australasia's leading providers of earthsciences engineering, Coffey is proud to be a sponsor of the Third A-NZ Young Geotechnical Professionals Conference, Melbourne 1998.

With a commitment to "advance the knowledge of our industry", Coffey continue to develop and put in practice new and innovative technologies to serve practices in:

- Geotechnics;
- Geophysics;
- Groundwater Studies;
- Mining; &
- Environmental Sciences.

To talk to us about innovation in our industry, contact the Coffey office in your capital city.

"The Conference Organising Committee thanks all sponsors for the valuable contribution they have made to the success of the event, and for the commitment they have shown to the development of young professionals in their industry."

Table of Contents

Welcome

Welcome to the *Third Australia - New Zealand Young Geotechnical Professionals Conference,* Mebourne, 1998. This conference is a continuation of the highly successful series of YGP events, which are a joint initiative of the Australian Geomechanics Society and the New Zealand Geotechnical Society. The Institute of Engineers, Australia, has assisted in the organisation of this event by providing seed capital and underwriting.

Rather than adopting any particular technical focus, the YGP conferences are designed to encourage the broader professional development of delegates through sharing in the knowledge and experience of senior professionals and peers. An important aim of these events is to foster communication and understanding amongst younger members of the geotechnical professions, and to encourage them to take an active role in the activities of their technical societies.

The success of this conference, as with all YGP events, is critically dependent upon the level of support offered by the geotechnical community. Without some financial commitment and considerable goodwill from the profession at large, events such as this simply could not take place. It gives me great pleasure to report that the level of support offered for this event from all quarters of the geotechnical community has been unquestioning and extensive. The conference has been generously sponsored and will be strongly attended. Delegates will be given the opportunity to visit one of Australia's most ambitious construction projects, and will benefit from the participation of some of our region's foremost researchers and practitioners. It is noteworthy that not a single senior person who was invited to be involved in the conference declined. Delegates can take great heart in the fact that their professional community has seen fit to invest heavily in this event and their futures.

Numerous people have played a role in bringing the conference to fruition. The support of all paper reviewers and sponsors is gratefully appreciated. Many thanks are due to past and present organising committee members: Grant Cameron, David Collings, Don Richardson and Jim Slatter; who have contributed considerable time and effort in the past twelve months or more. Thanks must also go to conference mentors, Assoc. Prof. Chris Haberfield and Mr Max Ervin, who provided valuable advice to the organising committee and will participate in event. The Transurban consortium and Transfield-Obayashi Joint Venture are facilitating a first-class site visit, for which we are very appreciative. Finally, the conference is indebted to all its senior participants, who have been so generously supportive; particularly keynote speakers Prof. Harry Poulos, Mr Charles Waterton, Mr Max Ervin, and Mr Bruce Hutchison. Prof. Ian Johnston and Mr Warren Pump have also contributed their time as session participants.

Having set the scene for the conference ahead, I would like to congratulate all delegates on being the nominated representative of their organisation for this event. I encourage you to make the most of conference sessions, and to participate as enthusiastically in a social sense as in the more formal aspects of the conference. Organising committee members and myself look forward to joining you in a productive and enjoyable three days.

Ben Collingwood.
Organising Committee Chairman

Geotechnical Investigations and Construction in Active Geothermal Areas: Rotorua, New Zealand.

JAIME BEVIN
Foundation Engineering Limited
Auckland, New Zealand

SUMMARY

The Whakarewarewa thermal area in Rotorua, New Zealand, is an active geothermal area and major tourist attraction. Current upgrade of the facility includes a 1.8 km paved and suspended timber deck track, three shallow cut and cover tunnels, two new bridges and an upgrade of an existing glulam bridge, all constructed on difficult and dynamic ground conditions well beyond the range of conventional geotechnical engineering design solutions. Construction of three new architecturally designed buildings is also programmed to begin in 1998. Comprehensive field and laboratory investigations over a four year span were undertaken, complimented by ongoing design during the construction phase.

1. INTRODUCTION AND DEVELOPMENT PROPOSALS

Civil construction in active geothermal areas is recognised as a challenging and demanding undertaking requiring detailed, creative and sometimes unique design solutions to overcome difficult and dynamic ground conditions. The Whakarewarewa thermal area in Rotorua, New Zealand, is an active geothermal area and major tourist attraction. Three new architecturally designed buildings are in the process of being constructed on a terrace area south-west of the current New Zealand Maori Arts and Crafts Institute complex, together with a 1.8 km paved and suspended timber deck track carrying tourists in electric powered vehicles looping around the adjacent thermal reserve. The track development also involved three shallow 'cut and cover' tunnels, two new bridges and an upgrade of the existing Pohutu Geyser bridge as well as specialist construction measures to deal with geothermal ground conditions.

Detailed geotechnical and geological investigations were undertaken prior and during track design to establish suitable design parameters, construction methodologies and the best track location.

An "observational method" approach was adopted for the construction phase of the development to account for variations in ground conditions and unforeseen construction difficulties.

2 GEOLOGY

The Whakarewarewa thermal area (Figure 1) is located inside the southern wall of a large circular rhyolitic caldera, about 15 km in diameter, with Lake Rotorua offset towards the northern end. The caldera formed following collapse during and after the eruption of the Mamaku Ignimbrite some 220 ka ago.

Lake Rotorua has been dammed on may occasions since the Mamaku ignimbrite eruption by deposits from the Okataina Volcanic Centre, forming larger and deeper lakes than that of the present day Lake Rotorua. During 26.5 ka to 20 ka ago, water levels fell progressively to that of present day, exposing much of the Whakarewarewa area above water (1).

In terms of immediate site stratigraphy there are a least two surficial volcanic airfall ashes comprising orange/ brown/yellow, loose, uncompacted silty sands/sandy silts with age ranges between 5 and 10 ka. Beneath these is a 2 to 3 metre thick coarse gravel pumice ash with an age of around 13.5 ka.

Underlying both the above is a sequence of stiff, moderately dense, alluvial (lake terrace) very fine grained silica silts and pumice lapilli, forming much of the higher ground over the development. This unit is highly impermeable, with the upper part of the unit exhibiting thixotrophic properties when disturbed. It acts as a cap to the underlying geothermal activity contained within the basal Huka Group sediments, essentially hydrothermally altered and silicified alluvial sands, silts and coarse pumice/rhyolite gravels.

The Whakarewarewa thermal area has a high vertical conductive heatflow with thermal activity concentrated along the many faults which parallel the Puarenga Stream and criss-cross the area (1). There are two main classes of hot springs: alkali-chloride springs, including geysers, which usually have a high fluid discharge at or near boiling point, and semi-stagnant acid sulphate mudpools, with little or no discharge (2). The physical and chemical differences between them are mainly due to their positions relative to the water table.

Chloride springs emerge close to the water table and at Whakarewarewa they are concentrated where the faults intersect the water table close to the Puarenga Stream. The

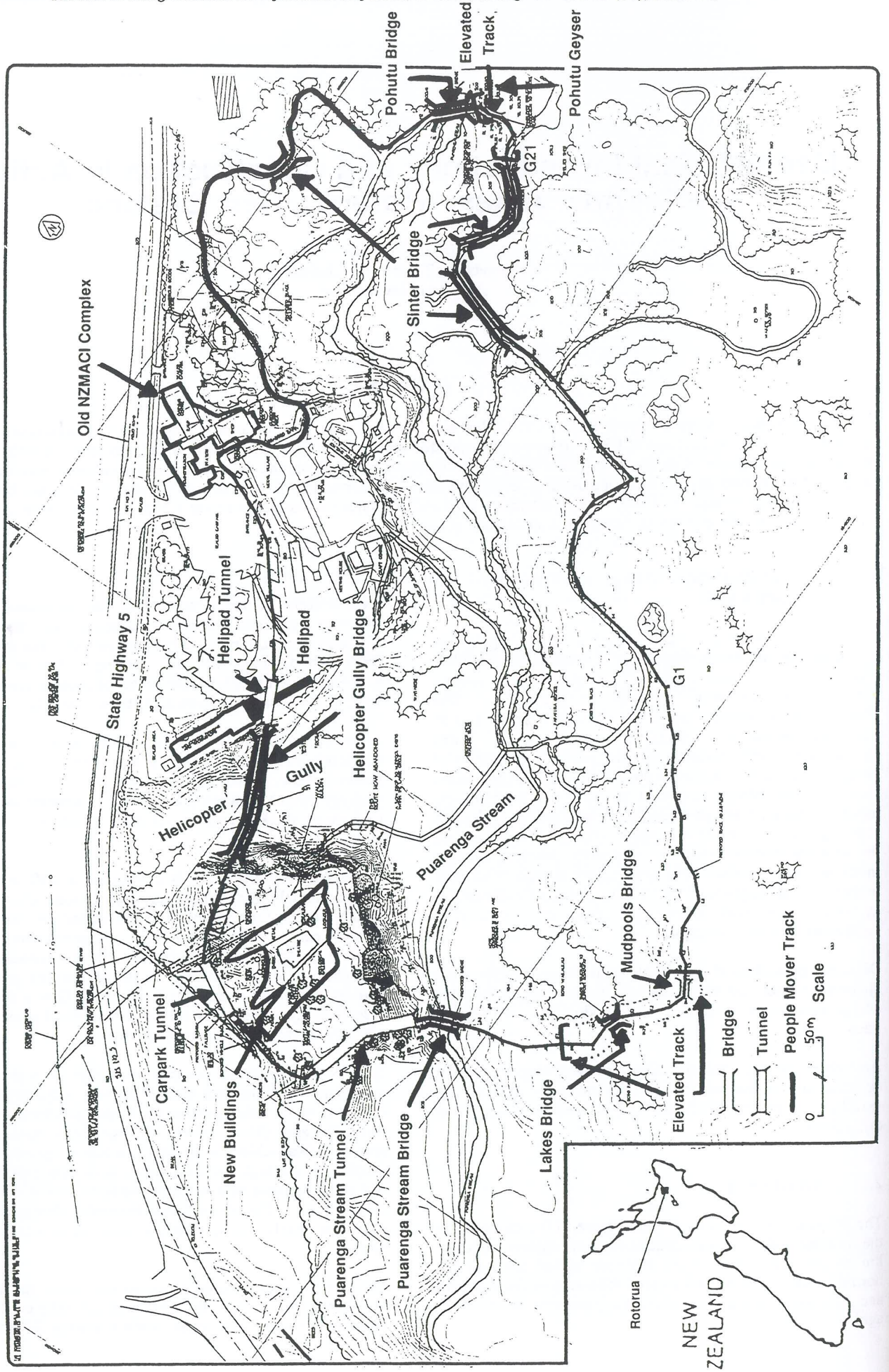
Pohutu Bridge
Elevated Track
Pohutu Geyser
G21
Sinter Bridge
Old NZMACI Complex
State Highway 5
Hellpad Tunnel
Hellpad
Helicopter Gully Bridge
Gully
Helicopter
Puarenga Stream
G1
Mudpools Bridge
Carpark Tunnel
New Buildings
Puarenga Stream Tunnel
Puarenga Stream Bridge
Lakes Bridge
Elevated Track
Bridge
Tunnel
People Mover Track
0
50m
Scale
Rotorua
NEW ZEALAND

water and gases are flushed from the system before they are oxidised and precipitate out silica to form sinter deposits. However, on the higher ground where the water table is deeper, little or no water, or only steam and gases can reach the surface. Ground conditions are invariably very acidic (sulphurous acids) due to oxidation of sulphide gas from out of the geothermal system; steam heating makes this acid attack even more aggressive. This attack causes ongoing decomposition of rock and soil minerals, resulting in multi-coloured clays stained with iron minerals, gradual void or cavity formation, subsidence and boiling mudpools.

From an engineering viewpoint, wide spread hydrothermal alteration of constituent soil and rock masses has resulted in areas of fragile ground conditions with poor bearing capacity, having potential for both extensive total and differential settlement and potentially rapid ground collapse.

3 FIELD & LABORATORY INVESTIGATION

Fieldwork for the Whakarewarewa project began in late 1993 as part of a preliminary geotechnical feasibility study for the overall development. More intensive investigations were carried out in November 1996 with additional investigations in early and mid 1997. These were designed to investigate geotechnical conditions and the engineering implications of constructing structures on an active, dynamic geothermal field. Distinct operations were carried out to investigate ground conditions on the building platform, bridge foundations, tunnel cuts, suspended track and on-grade pavement areas (Figure 1). The 1993 and 1996/1997 field work is summarised in Table 1, with laboratory testing summarised in Table 2.

Table 1: Summary of Field Investigation

Date	Investigation Method	Quantity	Maximum Depth (m)
1993	100mm HQ Wireline Machine Borehole	3	14.5m
	Cone Penetrometer Test	10	17.5m
	50mm Ø Hand Auger Borehole with in-situ soil strength test	64	4.2m
	Scala Penetrometer Test	59	5.0m
1996	100mm HQ Wireline Machine Borehole	6	15.2m
	Plate Load Test	11	0.4m
	50mm Ø Hand Auger Borehole with in-situ soil strength test	40	7.0m
	Scala Penetrometer Test	67	5.0m
	California Bearing Ratio (in-situ CBR's)	6	surface
	Ground Penetration Radar Survey	approx. 300m	2.2m
1997	100mm HQ Wireline Machine Borehole	2	13.5m
	Scala Penetrometer Test	Several 100	1.0m
	50mm Ø Hand Auger Borehole with in-situ soil strength test	8	2.4 m

NB: Further hand auger boreholes and scala penetrometer tests were carried out as ground conditions were exposed during the construction phase.

All results were Telarc endorsed where appropriate. Plate load tests were carried out in accordance with ASTM D1194 and in-house methods where appropriate.

Table 2: Summary of Laboratory Testing

Description	Test Number	No.
Atterberg Limits	NZS 4402, 1986: various	1
NZ Standard Compaction Test	NZS 4402, 1986: 4.1.1	1
Effective Stress - consolidated undrained triaxial compression test with pore pressure measurement	FEL in house test 19(b)	2
Solid Density	NZS 4402 1986: 2.7.2	1
Undrained Triaxial Compression Test	NZS 4402:1986 Test 6.2.1	3
Unconfined Compression Test	NZS 3112:1986 Test 9	7
Particle Size Analysis	NZS 4402:1986 Test 2.8.4	1
Nuclear Density	NZS 4407:1991 Test 4.2	20-30

3.1 Machine boreholes and cone penetrometer testing

Machine boreholes and CPT probes were undertaken to establish vertical soil stratigraphy, recover undisturbed samples for laboratory testing, obtain relative soil densities via SPT's, and log geothermal conditions including soil temperatures and hot/steaming ground at depth.

3.2 Hand auger boreholes and scala penetrometers

Extensive use of hand auger boreholes and scalas was undertaken to investigate shallow ground conditions, especially in difficult access areas or on the track alignment itself.

3.3 Plate Load & In-situ CBR Tests

Eleven plate load tests utilising a 500 mm diameter steel plate were undertaken, with seven tests on areas of predominantly geothermally altered soils around the track alignment and three further tests on the airfall ashes over the building platform. Two large tanks on a loading frame were used as reaction mass for the plate load tests, the tanks and frame being flown in by helicopter to each test site. Water was pumped to each site and placed in the tanks to increase reaction mass.

Loads at 20 mm deflection for the track alignment ranged from 55 to 159 kPa (Figure 2), while loads at 15 mm deflection over the building platform ranged from 65 to 110 kPa (Figure 3).

Six in-situ California Bearing Ratio (CBR) tests were also carried out adjacent to the plate load tests. CBR's ranged from 1.0 to 1.5.

3.4 Ground Radar Survey

The ground radar survey was carried out along part of the existing walkway track from G1-G21 (Figure 1). Interpretation of the survey traces suggested there were at least six to seven areas along the existing track of thin sinter crust overlying boiling mud or alkaline springs which would not be able to support the proposed paved track. These were confirmed by additional hand auger boreholes and scala penetrometers.

3.5 Stratigraphy, Soils Distribution & Engineering Properties

Field investigations revealed a 1 to 2 metre thick layer of generally soft to loose, non-plastic, orange/brown/yellow

airfall volcanic ashes, typically silty sands/sandy silts ("type 1" soils) overlying pumiceous and rhyolitic sands and gravels to around 4 metres depth ("type 2" soils). Thixotrophic/sensitive hydrothermally altered lacustrine silts and clayey silts ("type 3" soils) underlie the surficial airfall deposits, which are in turn underlain by weak to moderately silica cemented sands and gravel breccia's ("type 4").

Ground conditions beneath the track alignment were somewhat more variable than those outlined for the building platform. Soft, non-plastic, acid leached and geothermally altered silts ("type 5" soils) and loose to weakly cemented silica sinters ("type 6" soils) were also encountered in the intervening lower lying areas. Descriptions, distribution and the engineering properties of each soil type is summarised in Table 3.

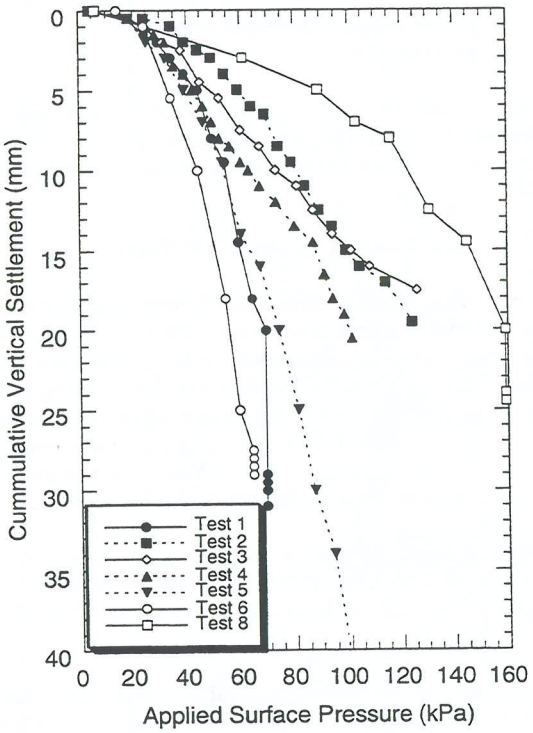

Figure 2: Track alignment plate load tests

3.6 Laboratory Results

Atterberg limit tests and particle size gradings confirmed the sandy/silty nature of the overlying surficial ashes (type 1). Compaction testing of type 1 soils returned a maximum dry density of 1.02 t/m^3 at an optimum water content of 47%. Further in-situ density tests yielded dry densities of 0.50 and 0.52 t/m^3 at water contents of between 103% and 112% for type 1 soils and dry densities of 0.80 to 0.90 t/m^3 at water contents of between 59% and 67% for type 3 soils.

The variability in strength of the type 3 soils with depth was illustrated from in-situ Standard Penetration Tests (SPT's), and undrained triaxial compression tests carried out on recovered block samples from the lower part of the type 3 unit. SPT's in type 3 soils ranged from N=0 (at the top of the unit) to N=21, increasing with depth. Confined compressive strengths in the base of the unit ranged from 0.4 to 2.2 MPa, at axial strains of 0.49 to 0.64%. Within the type 4 materials unconfined compressive strengths measured for pile design ranged from 2.2 to 30 MPa.

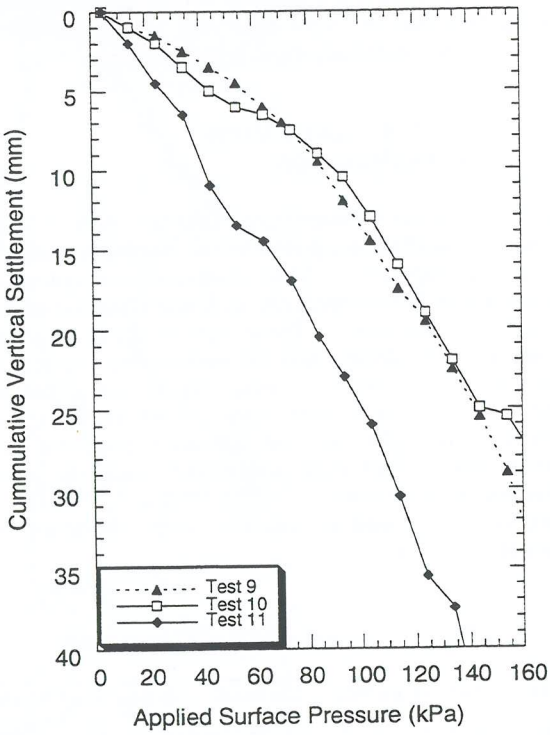

Figure 3: Building platform plate load tests

4 BUILDING PLATFORM CONSTRUCTION

4.1 Proof Rolling

Construction of the reinforced concrete floor slab for the new building began in June 1997, essentially being completed by late September. Actual building construction is programmed to commence in early 1998. The buildings are to be constructed of lightweight glulam timber portal frames and beams, with laminated veneer lumber (LVL) beams, purlins and girts to accommodate the curved nature of the building. The floor slab and foundations were designed for dead plus live loads of 40 kPa allowing for ground improvement via proof rolling to limit differential settlement.

Static proof rolling trials of the building platform began in early July 1997, following partial clearing of bush and scrub.

Table 3: Summary of ground conditions encountered at Whakarewarewa

Unit No.	Geological Description	"Engineering" Description	Distribution	Engineering Properties	Comment
Type 1	Whakatane and Mamuku ashes	Airfall volcanic ashes. Soft, loose, friable, non plastic, orange/brown/yellow fine sandy silts and silty fine sands.	Surface to between 1.6 & 2.2m depth. Average thickness approx 1.8m. Mantles building site as well as other remnant terrace areas across Whakarewarewa thermal area.	Loose, compacts under vehicle tyres. Shear vanes (SV's) range from 10-60 kPa, average 30 kPa. Sensitivities to disturbance 1.8-7.0, typical values 3.5-4.5. Equivalent CBRs almost all <1 for top 0.8-1.2 m. SPT results all N=0.	Seriously unfavourable load bearing characteristics. Hand auger boreholes 3 & 5 have 4+ m of this unit at northern end of building platform - material was hot and moderately altered. Airfall deposit mantles pre-existing topography, expect variable thicknesses across site.
Type 2	Rotoma and Rotorua ashes. Note Rotoma ash locally absent in some areas	Airfall volcanic ashes. Loose, non-plastic, orange/cream/brown, fine to coarse pumice sands & fine-medium pumice gravels with inclusions of fine gravel size rhyolitic lithic fragments. All particles angular to subangular.	Typically between 1.8 & 3.6m depth but ranging from 1.6 & 2.2m to 3.1 & 4.1m depth. Average thickness 1.8m.	Loose pumice sands and gravels. Highly permeable. Equivalent CBRs range <1 to 5, typical values CBR=3. Note values quite variable across building platform. SPT results all N=0 or at best N=1.	Highly permeable unit inferred to rapidly drain rainfall infiltration and hence enhance bank stability. Loose gravelly nature likely to substantially compact where exposed in building platform benches. Airfall deposit - mantles pre-existing topography, expect variable thicknesses across site.
Type 3	Oruanui breccia. Note erosional break between overlying ashes (Type 1 and 2) and this unit/soil type	Lacustrine terrace deposit, range of soil types: Soft to firm, non to moderately plastic, orange/red/ pink/ brown/cream silts and clayey silts. Beds and bands of 5-15mmØ lapilli pumice gravels. Bands of abundant amorphous silica, sensitive, thixotrophic - collapses on disturbance. Areas of hydrothermally altered montmorillite clays, swelling potential when unloaded. Increasing strength with depth, becoming stiff to very stiff and weakly cemented below 10-12 m depth	Top of unit typically 3.6m depth but ranging from 3.1-4.1 m. Base of unit variable range approx 11.1-13.6 m in machine boreholes. Mean thickness 8.5 m ranging from 7.2-10.4 m.	Firm to stiff, becoming weakly silica cemented at depth. SV's range from 10 to >140 kPa, mean approx 50 kPa. SV values higher than in two overlying units. Sensitivities to disturbance range 1.8 to >20 (extremely sensitive - quick). Equivalent CBRs range 3-10+, typical values CBR = 5. SPT results variable, range N=0-N=21, average N=6	Lacustrine terrace deposit , deposited approx 22,000 years BP when lake level was approx 40 metres higher. Some sedimentary structures seen in stream bank exposures. Sorting and grading of particles by size and density seen in borehole core. Highly impermeable unit effectively caps and seals off underlying geothermal aquifer and consequent activity.
Type 4	Huka Group sediments	Pre 65,000 year BP lacustrine sediments. Very weak to weak, weakly to moderately silica cemented fine to coarse grained silica sandstones, cemented gravels and weak, weakly cemented siltstones. Variable cementation.	Exposed along Puarenga Stream banks at bridge and in base of some machine boreholes. Inferred top of unit 11.1-13.6m depth but difficult to define precisely due to altered and weakly cemented nature of overlying Oruanui breccia unit	Very weak to weak, (non) to weakly to moderately cemented, soft rock. Bands of uncemented sands, interbeds of silicified sediments and sinter. SPTs range from N=3 to N>50. UCS range 2.2-29.9 MPa.	Good founding conditions for Puarenga Stream bridge but variable depth to top of competent founding surface. Undercutting and backfilling with site concrete or aggregate likely to be required.
Type 5	Acid geothermal muds and silts, hot barren ground, geothermally altered terrace deposits and airfall ashes	Soft to very soft, non plastic, cream/grey silts, often moist and hot. In places muds, actively bubbling. Thin, 0.2-1.0m thick crust of cool to warm, non plastic (white) silts, typically firm, in places friable, loose, prone to collapse where undermined by active acidic activity. Often mantled with 0.4-0.8m of moderately altered orange/brown/yellow ashes (type 1 soils)	Areas of site typically below RL 310m.	Very difficult founding conditions, poor ground bearing and high settlement characteristics coupled with elevated temperatures and on-going ground decay and settlement. SV's range 10-30 kPa, mean approx 15-20 kPa. Equivalent CBRs <1 (in places considerably <1!). Actual CBRs (done in conjunction with plate loads) 1-1.5. At best CBR = 1 available for design. Some ground modification will be required in some areas.	Ground conditions at absolute limit of conventional geomechanics applications.
Type 6	Boiling alkaline springs, active geyser areas, alkaline sinters	Loose, non-plastic, cream/ grey coarse silty sands and sandy fine gravels. Weak, weakly cemented cream/grey silica sinters interbedded with type 1, 2 and 3 soils above. Actively depositing amorphous silica sinter from boiling geothermal fluid.	Predominantly existing developed area of Whakarewarewa, southern abutment of Pohutu Bridge. Some older sinters adjacent to Puarenga Stream bridge area.	Where present without overlying ashes, silica sinter has relatively better engineering characteristics than much of higher ground. Shear vanes typically 5-80 kPa but obvious problems due to nature of substrata. Sensitivities to disturbance range from 2-8, typically 4. Equivalent CBRs range 1-5, typically CBR=2.	Ground conditions at absolute limit of conventional geomechanics applications. Potential for collapse of sinters, especially around existing developed area

Various types of equipment were trialed including excavators, rollers, graders, front end loaders and log loaders of up to 30 tonnes in weight. The most effective machine was found to be a medium sized log loader.

Approximately 50 to 100 mm induced compaction occurred in the type 1 and type 2 soils, with isolated areas of over 600 mm occurring where underlying pumice gravels were close to the surface and weakened by low grade geothermal activity. Due to the wet winter vehicle traction was a problem and 150 mm of GAP 65 rhyolite was laid down prior to further proof rolling. Areas of excess deflection (i.e. greater than 50 to 100 mm) were further undercut, and backfilled. Finally, a further 100 mm layer of rhyolite was added.

4.2 Building Foundations

Continuous external strip footings for the buildings were excavated to 0.8 metres depth by 1.8 metres wide and proof rolled. Further undercutting was undertaken where excess deflections occurred. Typical scala results at cut invert were 1 to 2 blows per 1500 mm penetration with several tests falling under self weight to 2 metres depth. A layer of Polyweave HR geotextile was placed at the base of the footings followed by 600 mm of compacted GAP 65 rhyolite. Concrete footings 800 mm wide by 600 mm deep were then constructed (Figure 4).

Further excavation occurred along the front (north-west) of the building platform adjacent to an area of hot steaming ground, and was built back up with Polyweave HR and compacted pumice. Pumice is more resistant to geothermal attack and was used in areas of elevated activity. The polyweave HR was used in the area as a construction expedient, and was not expected to survive beyond 6 to 8 weeks.

The south-eastern footprint of the building was also piled on account of being inside an 18 metre building restriction zone recommended from stability analyses on the adjacent steep bank above the Puarenga Stream. Eight, 600 mm diameter bored and concreted piles were constructed to depths of between 5.0 and 5.7 metres, socketing into the stiffer, weakly cemented lower type 3 unit.

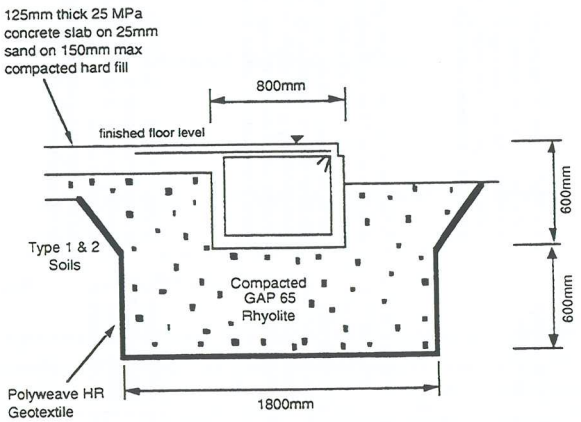

Figure 4: External strip footings of building

5 TRACK CONSTRUCTION

5.1 Main Track Design

The people mover fleet consists of five battery powered electric vehicles, each seating up to 36 people. The articulated trams are 14 metres in length and will operate continuously for a ten hour day throughout the year, charging at the main station during passenger pick up/drop off periods, and overnight. It is estimated the people mover will transport around one million visitors annually, the technology a world first in terms of its innovative engineering design. Typical axle loads are in the order of 2.0 tonnes (20 kN), approximately 25% of standard design axle loads. Considerable effort was expended in pavement design taking into account the lower vehicle induced stresses due to lighter loadings and low CBR's available for design.

Due to the low CBR and bearing capacity of the type 1 and 2 soils over parts of the track alignment (CBR's in places less than 1, and as low as 15 kPa safe bearing available on unimproved ground) and the presence of geothermal mudpools, several options were considered to prevent subgrade failures and provide safe passage for the people mover. These included increased basecourse hardfill thickness, use and selection of appropriate geotextile reinforcing, subgrade cement stabilisation and the use of specialised structures to overcome the very challenging conditions.

Approximately 1.8 km of paved and elevated timber deck track was constructed for the people mover. Much of the track was relatively straightforward to construct apart from a 400 metre stretch of track adjacent to two lakes at the southern end of the site and areas of relatively thin silica sinter on the main existing track, adjacent to and south of the Pohutu geyser.

5.2 Paved Track Alignment

The paved part of the track alignment was constructed on the elevated terrace areas where ground conditions, although soft or loose in places due to the overlying type 1 ashes, were sufficiently cool and competent to accommodate standard track construction of undercutting and backfilling with compacted hardfill. Construction of the paved track section consisted of 60 mm cobble block pavers, laid in a herringbone pattern, overlying CBR dependant depths (typically 150 to 400 mm) of compacted GAP 65 rhyolite hardfill subbase.

Paved track design was based on plate load, in-situ CBR and scala penetrometer test results carried out over the whole track alignment. Basecourse depths were also based on design charts and output from software supplied by the manufacturers of the cobble pavers as well as methods given by Giroud and Noiray (3), AUSTROADS (4) and Transit New Zealand (5). To limit basecourse volumes and costs, geotextiles were used where ground conditions permitted. Where excess deflections occurred from construction traffic, additional undercutting and backfilling with compacted rhyolite was undertaken. Cement stabilisation was not considered a viable option due to expense and accessibility for stabilisation gear.

5.3 Elevated Track Structure

Some 400 metres of glulam timber decking on an elevated timber frame structure was constructed on the southern part of

the development and adjacent to the Pohutu geyser, predominantly on hot geothermally affected and altered ground. Bearing capacity on these areas was as low as 15 kPa, with CBR's of less than 1.

The timber framed structure was bolted onto 600 mm by 300 mm fabriform bags filled with lightweight pumped concrete (Figure 5). Where excessively uneven ground was encountered, the underlying ground was benched and shotcrete used to 'lock' the fabriform bags in, although the majority of the of bags were laid on the ground surface. The elevated track structures were designed for dead plus live loads of 12 to 15 kPa.

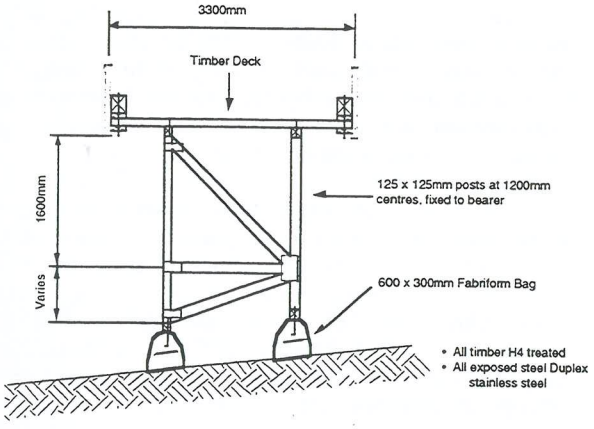

Figure 5: Elevated track structure

Two small glulam timber bridges were also constructed as part of the elevated track. The Lakes Bridge (10 metres long) spans between the narrow isthmus of two lakes, while the Mudpools Bridge (12 metres long) spans a narrow ridge with active mudpools on either side. Both bridges were designed for 15 kPa safe bearing, the Lakes Bridge having additional piles to account for seismic bearing capacity and possible liquefiable ground conditions.

Both the Lakes and Mudpools bridges have grouting ports inserted into the bridge footings to allow for future compaction grouting if required.

5.4 Sinter Bridges

Up to seven areas of inferred shallow crust were revealed by the ground radar survey from G1 to G21, typically on type 5 and 6 soils. To span these areas of thin sinter overlying possible cavities, three on-grade "sinter bridges" of 4 metres width were constructed, consisting of 100 mm thick 35 MPa concrete with fibreglass rod reinforcing. The Sinter bridges were up to 38 metres in length.

6 BRIDGES

6.1 Helicopter Gully Bridge

This 3.4 metre wide bridge spans from the helipad tunnel portal to the building terrace area, a distance of some 78 metres (Figure 1). Apart from two tunnel portal abutment positions, there are two bridge piers in the gully area, located 28 metres apart. Ground conditions at each bridge pier consisted of a veneer of type 1 ashes underlain by hydrothermally altered silts, muds and clays (type 5) to around 6 metres depth, which were in turn underlain by silica cemented sands and gravel breccia's (type 4). Unconfined compressive strengths in the underlying type 4 materials ranged from 2.2 to 30 MPa.

Due to high lateral loads and to enable adequate loading capacity under static and seismic loading conditions (only 20 kPa available on unimproved ground at the surface) four, 600 mm diameter piles at each bridge pier were initially pendulum drilled through the surficial ashes and type 5 soils, then percussion hammer drilled to enable piles to be socketed at least 1.5 metres into the silicified type 4 materials (Figure 6). The bridge entry and exit portal tunnel piles were drilled to approximately 7 metres depth.

Due to the extreme ground conditions encountered at the base of each pile hole (steam venting and groundwater in excess of 90°C, pH approximately 2-3, and 400-600 ppm sulphate), and mudpools adjacent to the eastern pier, duracem cement, a blend of cement and ground granulated blastfurnace slag, was specified for all piles and bridge footing concrete.

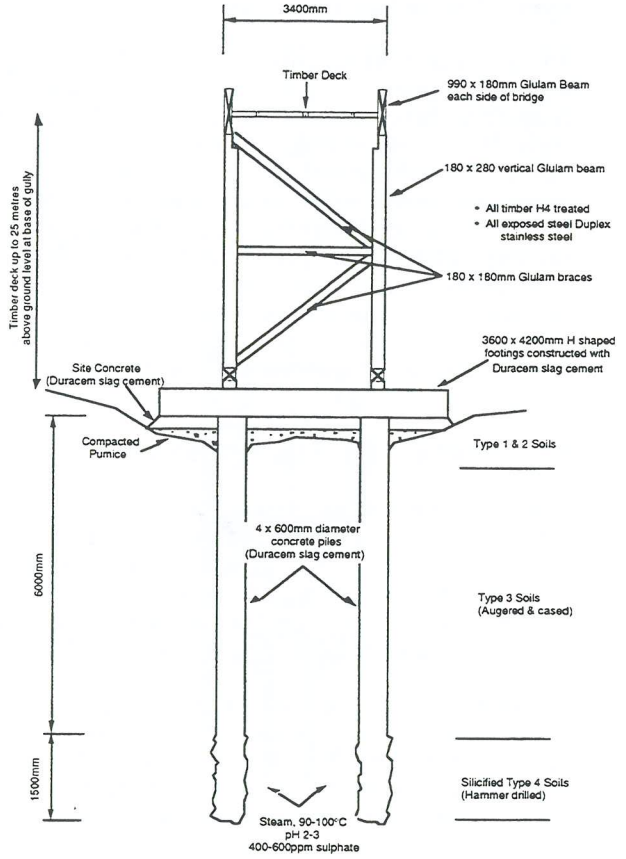

Figure 6: Helicopter Gully bridge foundations

6.2 Puarenga Stream Bridge

The glulam timber Puarenga Stream bridge runs some 33 metres from the southern portal of the Puarenga Stream Bridge tunnel across the stream. Due to low bearing pressures and proximity to the steep bank, piles were drilled to depths of between 1.7 and 5 metres to found on competent basal type 3 materials under individual footings.

6.3 Pohutu Bridge Upgrade

The existing glulam beam timber bridge adjacent to the Pohutu Geyser was widened by 2.2 metres to allow access for both the people mover and pedestrian traffic. Despite the age of the bridge (around 20 years old) and the hot ground conditions (in excess of 80°C beneath surficial sinter and gravel fill) the existing foundations have performed well.

7 TUNNELS

Three shallow 2.5 metre high by 3 metre wide box culvert cut and cover tunnels were constructed, primarily to ease approach and exit gradients from some of the bridges. Tunnel design had to take into account seismic and soil lateral loads, especially in the type 3 soils which are prone to swelling when unloaded. Stability of the temporary batters also required careful monitoring during construction.
Available CBR's along tunnel subgrades ranged from 4 to less than 1. Up to 800 mm of compacted hardfill and Polyweave HR geotextile was placed under all tunnel sections with selective undercutting and further backfilling with hardfill where soft ground was encountered.

All tunnel cuts were backfilled with hardfill following tunnel section placement. Backfill material was specifically designed to prevent internal soil erosion. 110 mm diameter draincoils were placed along the tunnel invert line along either side to control subsurface groundwater. Expanded polystyrene panels were initially specified for back filling where type 3 soils were encountered to account for any swelling pressures developed within this unit. However, due to the length of time tunnel cuts were open (up to 3 months) and size of excavations on either side (up to 2 metres) polystyrene panels were not used. Backfill over the tunnel sections consisted of reworked type 1 and 2 soils.

8 RETAINING STRUCTURES

Three flexible gabion basket retaining structures were constructed mainly to retain filled ground above tunnel entrances and exits. PVC coated galvanised mesh gabions were used, backfilled with 150/80 gap graded rhyolite fill. Gabions were founded on either compacted GAP 65 rhyolite or compacted pumice, depending on ground conditions.

Several areas of the track required cuts of up to 3.5 metres to achieve requisite track gradients of 12% downslope and 10% upslope. Cut slopes were battered back to 60° for slopes up to 2 metres high, and 50° for slopes greater than 2 metres in height. Punga logs were then laid over the batter slopes.

Battering the cut slopes versus fully retaining slopes with crib walls or similar was seen as a risk-cost trade off. The cost savings in leaving steeper batters will be offset by the future risk of having to repair any instabilities that may occur. There were also issues of safety for the public in terms of leaving slopes steeper than ideal, although to some extent these will be offset by regular detailed safety surveys and maintenance/observation procedures put in place to monit track conditions.

9. CONCLUSIONS

The Whakarewarewa project has proven how difficult civ construction in active geothermal areas can be, with grour conditions well beyond the range of conventional geotechnic engineering design solutions. Despite an extensiv geotechnical investigation, there was an expectation th ground conditions would vary from what the project designe had assumed. Thus, design values for geotechnical aspec of the buildings, structures, and the roadways were based c anticipated worst case conditions, imposing minimu practical construction loads. The adopted "observation method" approach allowed the design to be modified durir the construction phase by finding the best way out, implementing design alternatives when unexpected grour conditions were encountered.

A commissioning process is to be undertaken prior to th development being open to the public. This process wi involve monitoring dynamic loadings on the structures by th people mover. While failure/collapse of structures is n expected, there may be some excessive live load differenti movements. Contingencies for such problems incluc compaction grouting through grout ports installed in bridg footings and additional retaining structures.

10. ACKNOWLEDGEMENTS

The author gratefully acknowledges the permission of th New Zealand Maori Arts and Crafts Institute to report on th findings of the investigation and assistance provided by Lak Engineering Limited.

11. REFERENCES

1. Cody, A. (1996): NZMACI redevelopment conse application: geological and geotherma considerations. Unpublished Report.

2. Lloyd, E.F. (1975): Geology of Whakarewarewa h springs. Information Series No. 111. N.Z Department of Scientific and Industrial Research.

3. Giroud, J-P., and Noiray, L. (1981): Geotextile-reinforce unpaved road design. Journal of the Geotechnic Engineering Division. Vol. 107, No. GT9, p 1233-1254.

4. AUSTROADS. (1992): Pavement design - A guide to th structural design of road pavements AUSTROADS, Sydney, Australia.

5. Transit New Zealand. (1989): State Highway Pavemer Design and Rehabilitation Manual. Transit Ne Zealand, Wellington, New Zealand.

Centrifuge Modelling of Driven Piles in Dense Sand

Mr. Davide Bruno
Geomechanics Group, The University of Western Australia, Nedlands, W.A., Australia

SUMMARY

Reliable data on the axial bearing capacity of piles in dense sand is required in order to understand the complex bearing failure mechanisms which occur during pile installation and subsequent loading. The high cost of field testing necessitates that such experimental research is undertaken at model scale, at least initially, allowing fundamental load-displacement behaviour to be investigated. This paper outlines the apparatus and testing regime adopted in the axial loading of driven piles, performed in the geotechnical centrifuge at the University of Western Australia. Typical test results are also presented, which demonstrate the usefulness of the centrifuge as a modelling device for field-scale pile tests.

1. INTRODUCTION

The main reason for the lack of field scale pile test data is due to the high costs associated with such an undertaking. Whilst the extrapolation of centrifuge pile tests to field scale tests (and hence design) is still questionable, the centrifuge remains the principal modelling tool available to researchers in this field.

The centrifuge is ostensibly the only modelling tool that correctly scales the stress gradient due to soil self-weight. This scaling applies to both the free field, and more importantly, to the soil plug within the pile. Centrifuge model tests have a number of advantages over alternative modelling techniques. They allow the accurate reproduction of soil profiles, and permit a wide range of soil and pile parameters to be varied independently.

2. PILE DRIVING APPARATUS

The experimental work presented in this paper was carried out on the fixed beam geotechnical centrifuge facility at the University of Western Australia. The facility houses an Acutronic 661 centrifuge with a capacity of 40 g-tonnes and a platform radius of 1.8 m. A detailed account of the geotechnical centrifuge and associated equipment may be found in Randolph et al., (1).

2.1 Miniature Pile Driving Hammer Actuator

In the centrifuge, the model piles have been installed in-flight using an unique pneumatically operated drop hammer, that simulates a prototype drop-hammer of up to 70 tonnes (ram-mass) such as would be used for an equivalent prototype pile. This piece of equipment has been described in detail by de Nicola, (2) so only the key features are summarised here. A schematic of the moving parts of the actuator is shown in Figure 1. Two double acting pneumatic solenoid valves direct pressurised air into the top and bottom compartments of a piston chamber which forces a piston to pick up the ram mass on its upward trajectory and then allows it to free-fall under the centrifuge acceleration on its downward trajectory. As a consequence, the hammer impact is correctly modelled.

In addition to permitting in-flight pile installation, the carriage is also capable of pushing or pulling the model pile at low displacement rates. This facilitated the simulation of drained static load testing. The entire carriage can also be displaced through 240 mm vertically and 150 mm horizontally to permit testing at multiple sites if necessary.

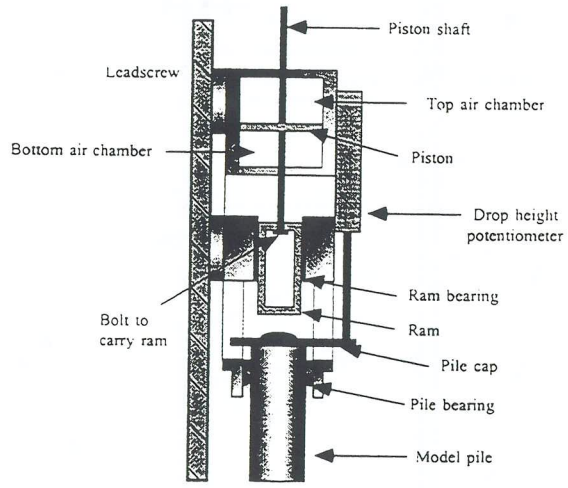

Figure 1 - Working Parts of the Miniature Pile Driving Hammer Carriage

2.2 Model Piles

Figure 2 shows a schematic diagram of the model piles used throughout the centrifuge pile tests. Tests performed with an instrumented pile are denoted IP, and those performed with a less instrumented pile are denoted UP. The instrumented and uninstrumented piles were both fabricated from a thin-walled cylindrical stainless steel section which has had its surface roughened by sand-blasting. In order for the model pile

roughness to correctly scale with the prototype roughness, the ratio of the mean sand particle size, d_{50} and the steel roughness was conserved. By gluing a removable end cap into the toe of the pile a closed-ended pile could also be simulated.

At 100 g the model piles have a prototype diameter, D varying from 0.95 m (UP) to 1.15 m (IP), with a 0.05 m wall thickness and a maximum embedment depth of 20 m.

Varying numbers of strain gauges have been bonded to the model piles in order to measure the axial strain (and hence force) generated during installation and pile loading. In order to protect and seal the gauges from the saturated soil, a thin layer of epoxy resin extends along the shaft of the IP. However, since the volume of soil entering a pipe pile during installation is critically influenced by the ratio of the wall thickness to diameter at the pile toe, the epoxy resin was only extended to the bottom gauge.

The topmost strain gauge was similarly located in both the UP and IP, and remains above the soil surface at all stages of pile installation and testing. This gauge provides a measure of the gross pile behaviour. Additional strain gauges placed along the pile shaft allow the local shaft friction profile along the pile shaft to be determined.

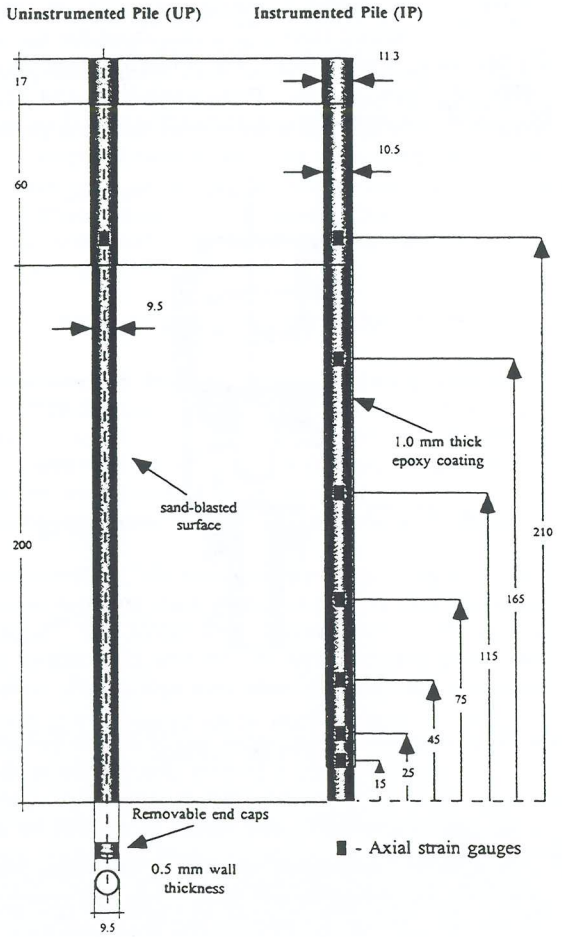

Figure 2 - Model Piles

2.3 Plug Monitoring Device

A displacement transducer is connected to a small 11.9 g aluminium cylinder which is guided along the inside of pile by a high strength kevlar line. The line is passed ov pulley housed within the pile cap and attached to displacement transducer, which resides on the actuator. density of the aluminium cylinder is such that the submerged density is greater than that of water, sufficiently low so that only a light pressure (of around kPa at 100 g) is applied to the internal soil plug.

3. SOIL SAMPLE CONDITIONS

All centrifuge tests were conducted in a saturated fine-grai silica flour (or silt) which has a mean particle size, d_{50} of μm and d_{10} of 9 μm. The well-graded nature of the allows it to be densely compacted, with the potential to at very high strengths.

Maslen (3) conducted a series of constant normal stiffn direct shear tests on silica flour in order to determine frictional and dilatancy characteristics. Based on t conducted at varying vertical effective stresses both constant volume friction angles and dilation angles compa very well with those measured for much coarser silica sar It was concluded that whilst the silica flour had a m particle size an order of magnitude smaller than a field sc sand, it correctly modelled the mechanical properties o field scale silica sand.

3.1 Soil Preparation Techniques

Techniques of sample preparation have been refined to stage where samples with various strength profiles can prepared. A slurry of silica flour and water was initia mixed and de-aired before being transferred into a test container. After allowing sufficient time for the sample consolidate, excess water on the surface of the sample removed, producing a saturated sample with a water cont typically around 25 %. Varying degrees of soil stren could be achieved by vibro-compacting the sample, wh encourages the well-graded silica flour to re-align compact very tightly. A particular sample density could achieved by preparing a known mass of saturated silica fl to a given sample height.

3.2 Soil Characterisation

The cone penetration test, (CPT) is a popular and useful characterisation tool used extensively in geotechnical investigation practice. Within the centrifuge the variation cone tip pressure, q_c with depth was determined using a 7 m diameter model cone penetrometer. A constant profiling o is obtained during a drained installation of the c penetrometer into the silica flour. Figure 3 is a plot of q_c w depth for several different centrifuge tests. It can be seen t values of q_c as high as 80 MPa have been measured, whic representative of soil conditions experienced in offsh conditions, particularly in the North Sea.

4. PILE TESTING PROCEDURE

The standard testing container used on the centrifuge is aluminium segmented box, with internal dimensions 390 m

wide by 650 mm long and 325 mm high. Up to seven pile tests were conducted along the centreline of any one sample. This ensured that each pile test was separated from the others by a minimum of 7 D. Tests were also a minimum of 13 D and 7 D from the nearest horizontal and vertical boundary respectively. In many instances the separations exceeded these distances.

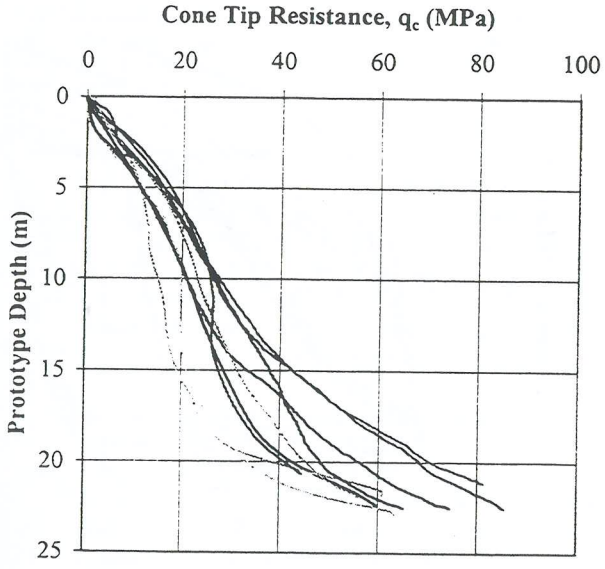

Figure 3 - Cone Penetration Tests

The model piles were installed with the miniature pile driving actuator, which delivered the ram mass with fixed prototype drop heights varying between 1.0 m and 1.7 m. Upon attaining the desired penetration depth, dynamic and static tests were performed on the pile. Dynamic tests involved striking the pile with the ram mass and measuring the transient force and velocity data. Static tests involved driving the entire carriage assembly down (or up) in order to compress (or extend) the pile. Displacement rates used during static tests ensured that drained conditions were maintained throughout the tests. The procedure of driving the pile and then performing static and dynamic tests was repeated at the same testing site for different depths of penetration. Due to the extensive nature of both testing regimes only the static pile tests will be discussed in this paper.

5. PILE TEST RESULTS

5.1 Comparison between IP and UP Static Tests

The size of the instrumentation is relatively large compared to the geometry of the model piles and consequently affects the behaviour of the pile under loading. The first component of the centrifuge testing programme was aimed at quantifying the degree to which the instrumentation affected the loading behaviour. This was achieved by performing identical pile tests using both the UP and IP. The data shown in Figure 4 were derived from a static pile test performed on a pile embedded to a prototype depth of 12.65 metres. The loading path indicated by arrows shows that the compression test preceded the tension test in both cases. The gross load - displacement behaviour for both the UP and IP is superimposed in order to demonstrate the disparity in magnitude of the prototype pile load at similar pile head displacements.

Traditionally, the static pile capacity is taken at a reference pile head displacement equal to 10 % of the pile diameter (or w/D = 0.1). At this reference pile head displacement, the IP mobilised 30 % more soil resistance in compression and 15 % more resistance in tension. The epoxy resin provides an additional 47 % of cross-sectional area and 21 % of surface area to the IP, which perhaps explains why the IP mobilises more soil resistance than the smaller UP. Constant normal stiffness direct shear tests conducted by Maslen, (3) have shown that the interface friction angles of the steel/silica flour and epoxy/silica flour are 29.6°and 31.5° respectively.

A higher frictional angle, in conjunction with greater surface area, would result in higher shaft friction along the IP than the UP.

5.2 Soil Plug Formation During Pile Installation

It is particularly interesting to note the degree to which the instrumentation influenced the formation of the soil plug during installation of the pile. Figure 5 shows the formation of the soil column (or soil plug) for both the UP and IP. The dashed line represents the length of the soil plug if the soil was entering the pile at the same rate as the pile embedment. It is clear that the plug height for both the IP and UP is always less than the embedment depth of the pile. However, the rate of advance of the soil plug in the UP can be seen to approach the rate of pile embedment with increasing pile penetration. In distinct contrast, the rate of advance of the soil plug in the IP is consistently less than the rate of embedment, even though the installation procedures for the UP and IP are similar.

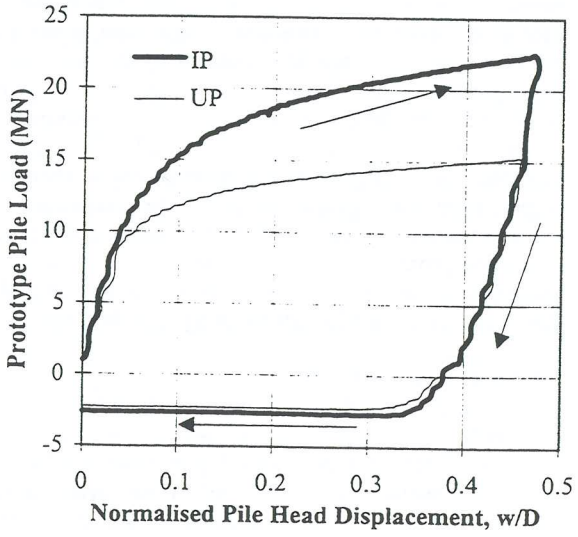

Figure 4 - Typical Pile Static Test

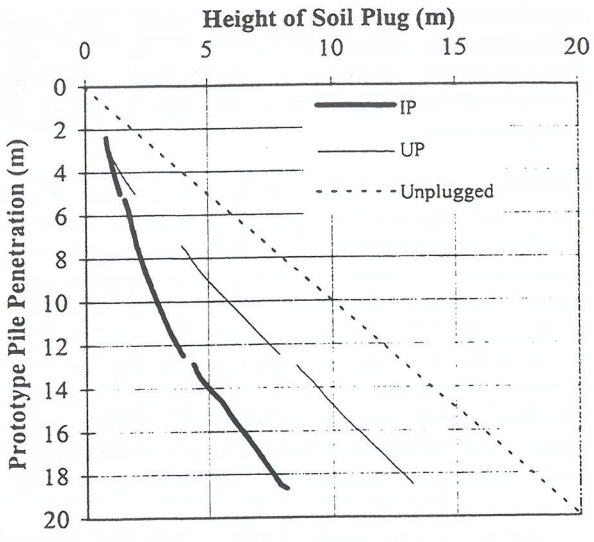

Figure 5 - Formation of the Soil Plug during Pile Installation

This trend was consistently demonstrated by numerous other centrifuge pile tests and suggests that the instrumentation on the IP affects the progression of the plug within the pile, even though it is located a minimum distance of 1.5 D from the pile toe. Perhaps, the larger IP would displace and hence densify a larger volume of soil around the pile tip than the UP. An increase in relative density of the soil would reduce the amount of soil entering the pile toe and consequently reduce the plug height which forms during installation.

It must be noted that while the soil plug continued to form within the open-ended piles during driving, it did not advance during static loading.

5.3 Instrumented Pile

The additional instrumentation located on the IP provides information regarding the distribution of axial load along the length of the pile. The axial load distribution can then be used to calculate more meaningful data such as shaft friction profiles along the embedded portion of the pile, as well as base pressure. In Figure 6, the data from Figure 4 is combined with data generated from the performance of a second static test. The data from all seven gauges are included. As in Figure 4, the topmost curve represents the output from the topmost gauge. The magnitudes of the curves measured by each of the other six gauges reduce with increasing proximity to the pile toe. The outputs of the two gauges near the top of the pile have similar values because they were not embedded during this particular static load test.

5.4 Shaft Friction Profile

In order to estimate the distribution of shaft friction along the pile shaft, the difference in axial load between each gauge has been calculated at a normalised pile head displacement of 0.05. The resultant is then divided by the surface area of the pile between the respective gauges, giving an indication of the local shaft friction acting between the gauges. On the other hand, the local shaft friction acting below the bottom gauge is calculated from the peak value of shaft resistance obtained from gauge 1. A normalised pile head displacement of 0.05 was generally sufficient to mobilise the peak sh friction in both compression and tension static tests.

Figure 7 shows the shaft friction profiles deduced from t first compression-tension cycle shown in Figure 6. A close ended static pile test performed at the same penetration dep is included for comparison.

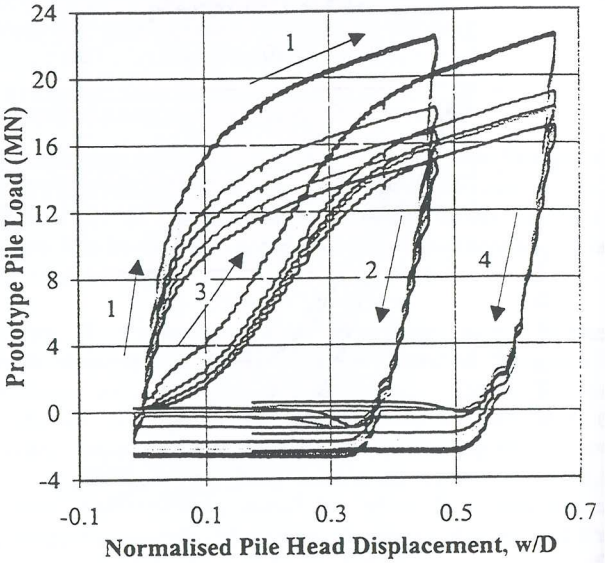

Figure 6 - Typical Static Pile Test (IP)

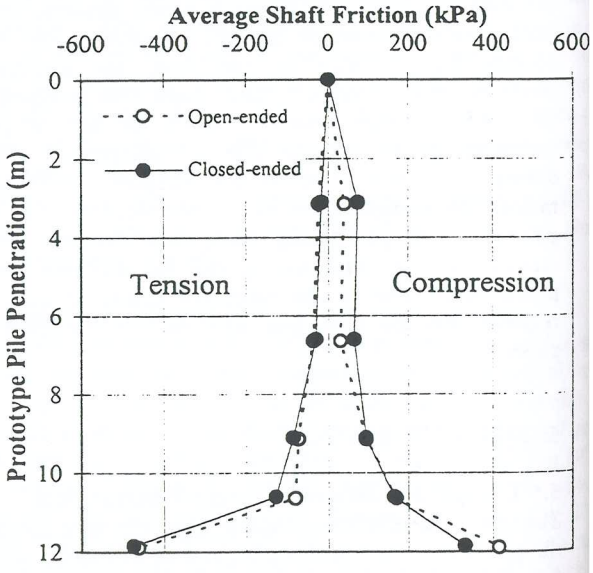

Figure 7 - Typical Shaft Friction Profiles (at a Normalised Pile Head Displacement of 0.05)

A sharp increase in the local shaft friction typically occurr 2-3 D from the pile toe, indicating that most of the sh

friction was mobilised in this region. In sands, the majority of soil resistance is typically mobilised at the pile toe due to the combination of high end-bearing resistance and high localised shaft friction, which is demonstrated in these centrifuge tests.

A general trend arising from the pile tests is that the closed-ended piles exhibit around 10 % higher average shaft friction compared to the open-ended piles. This can be attributed to greater soil displacement during installation and loading, compared to open-ended piles, which allow the soil to form inside the pile.

5.5 End-Bearing Resistance

The end-bearing resistance can be estimated from the gauge readings closest to the pile toe. An over-estimation of the base pressure, q_b is made if the axial load, obtained from gauge 1, is simply divided by the cross-sectional area. This includes the contribution of the shaft friction acting below gauge 1, which can cause an overestimation in q_b by up to 10 %.

To overcome this, an alternative approach was implemented. This involved determining the degradation in shaft friction between gauge 2 and gauge 1, and using it to estimate the degradation in shaft friction between gauge 1 and the pile toe. In accounting for the shaft friction mobilised near the pile toe, this approach provided suitably accurate estimates of q_b. Figure 8 shows a typical plot of q_b, which has been normalised against q_c. The cone tip resistance was averaged over a depth of ± 1.5 D around the pile toe. The normalised base pressure is plotted against the normalised pile toe displacement rather than the pile head displacement. The pile toe displacement can be determined by subtracting the elastic compression of the pile, due to the axial load, from the pile head displacement.

The base capacity of the open-ended pile was less than the closed-ended pile due to elastic compression of the soil plug during static loading. At a normalised pile toe displacement of 0.1 the general trend was for the closed-ended piles to exhibit around 30 % more end bearing resistance than the open-ended piles. However, the increased stress associated with larger pile displacements may be expected to fully compress the soil plug, producing base capacities similar to those of closed-ended piles.

The ratio of q_b/q_c was observed to reduce with increasing overburden stress. The ratio reduced from around 0.6 at a prototype depth of 5 m to as low as 0.18 at 20 m at a normalised pile toe displacement of 0.1. This trend is consistent with tests conducted by de Nicola (2).

6. CONCLUSIONS

The apparatus and testing techniques adopted in the pile tests, conducted at the centrifuge facility at the University of Western Australia, have been outlined. Results from a typical pile test demonstrate the usefulness of the centrifuge as a modelling tool, in as far as plausible results can be readily obtained. The use of instrumented model piles provides qualitatively consistent trends for the mobilisation of shaft friction and end bearing resistance. In addition, the formation of the soil plug during driving and static loading can also be examined.

However, as with all reduced-scale models, the presence of the instrumentation required to monitor the pile behaviour modifies its behaviour to some degree. Quantifying the effect of instrumentation on the behaviour of model piles is thus central to the correct interpretation of results obtained from any heavily instrumented pile. The need to account for this influence becomes critical when extrapolating to field scale, particularly when postulating new design criteria.

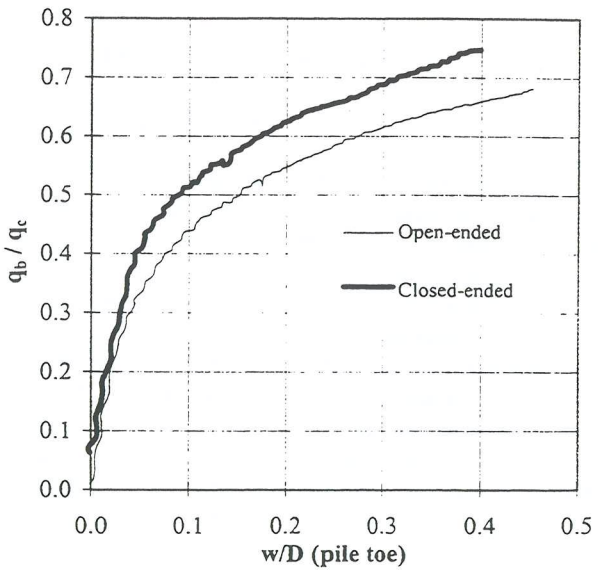

Figure 8 - Base Pressure Normalised with Cone Tip Resistance

7. REFERENCES

1. RANDOLPH, M.F., JEWELL, R.J., STONE, K.J.L. and BROWN, T.A. (1991). "Establishing a new centrifuge facility." Proc. Int. Conf. on Centrifuge Modeling - Centrifuge 91, Boulder, Colorado, 39-9.

2. DE NICOLA, A. (1996). "The performance of pipe piles in sand." Ph.D. Thesis, University of Western Australia, Nedlands 6907, Australia.

3. MASLEN, C. J. (1997). "Constant normal stiffness testing of silica sands." Undergraduate Honours Project, University of Western Australia, Nedlands 6907, Australia.

Case History of an Unusual Embankment Failure

Andrew Campbell, Maunsell Pty Ltd

Summary: The partial failure of a 7.5m high surcharged embankment constructed over soft clay and peat is described. Extensive instrumentation within the embankment and its foundation gave only partial warning of the impending failure. Failure occurred during the final lift of surcharge and resulted in a 0.6m wide tension crack approximately 100m long down the centre line of the embankment. Unusual features included the fill material, lack of pore pressure dissipation during construction despite installation of wick drains, limited lateral deflection prior to failure, near perfect symmetry of the failure and the remedial measures implemented.

1 INTRODUCTION

This paper describes some of the problems encountered and remedial measures implemented during construction of a 7.5m high surcharged section of embankment forming part of the 18km long A16 Spalding to Sutterton Improvement Scheme in the Fenlands of eastern England, 160km north of London, refer Figure 1. Embankments up to 6m high were necessary to cross the River Welland north and south of Spalding. Construction of the southern crossing took place over approximately 10m of soft to very soft silty clay and a thin layer of peat. The ground conditions necessitated the use of wick drains and surcharging to accelerate pore pressure dissipation and settlement. Instrumentation was installed within the embankment and its foundation to monitor stability during construction; it comprised hydraulic piezometers, inclinometers, magnetic extensometers, hydrostatic profile gauges and settlement plates. The failure occurred during the final lift of surcharge at the southern crossing, however the full extent of cracking did not become apparent until removal of the surcharge 12 months later. Remedial measures included backfilling the crack with foam concrete and substantially increasing the amount of reinforcement in the concrete roadbase along that section of embankment.

2 PROJECT DESCRIPTION

2.1 Scope of Works

The A16 Spalding to Sutterton Improvement Scheme involved construction of a single carriageway highway across 10km of green field site to the east of Spalding, followed by 8km north along a disused railway embankment to Sutterton. Embankments were generally constructed less than 1.5m high for reasons of aesthetics, settlements, land-take and construction volumes. However, on the approaches to the River Welland and across the flood detention basin of Cowbit Wash, it was necessary to construct embankments up to six metres high. The project chainage ran from Ch 400 in the south to Ch 18,500 at the north end. The area of interest lies between Ch 1100 and 1250.

2.2 Site Description

Spalding is located in the Fens, a low lying region of peat bogs, estuarine mud flats and salt marshes located in eastern England. The Fens cover an area of approximately 4000 square kilometres and have been reclaimed by construction of seawalls and drainage channels since Roman times, however

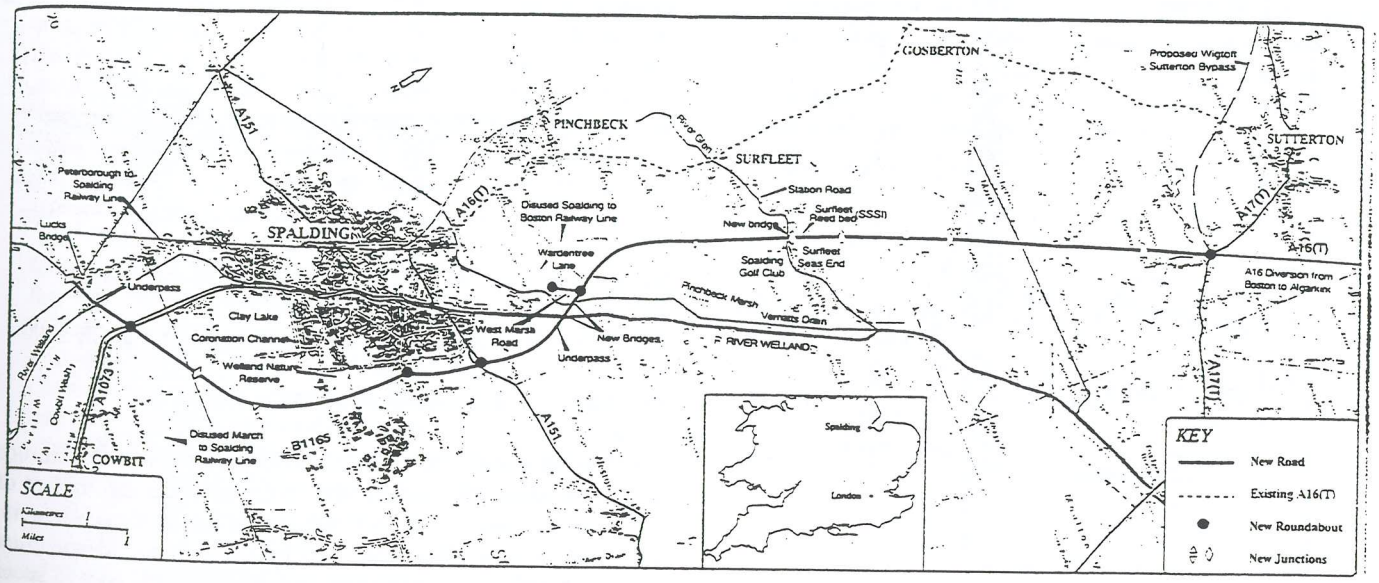

Figure 1: Site Location Plan

most activity has occurred over the past 300 years. The region is typically between 0 – 5m above sea level.

2.3 Geology

The solid geology underlying the Scheme comprises Oxford Clay, a very stiff to hard silty clay of middle Jurassic age. During the Quaternary, the area was subjected to as many as four episodes of glaciation, the last occurring in the Devensian Stage between 70,000 and 10,000 years ago. This resulted in deposition of the Chalky Boulder Clay, a lodgement till comprising a stiff silty clay matrix with gravel sized clasts of chalk and limestone. The Fen deposits overlie the Boulder Clay and comprise peat, clay, silty sand and sandy gravels according to the environment of deposition. The peat beds under the Scheme were up to 1m thick and formed in a freshwater or brackish environment. The silty sands were deposited under marine conditions whilst the clays are inferred to be of estuarine origin. Fluvioglacial sands and gravels are present under parts of the Scheme and were deposited by melt waters either under the ice sheets or as the ice retreated.

The ground conditions immediately under the failed section of embankment are shown on Figure 2 and comprised a 1m thick desiccated crust of firm silty clay, 5m of soft to very soft silty clay with traces of peat, 1m of soft fibrous peat, 1m of soft to firm silty clay, 6m of stiff Chalky Boulder Clay then Oxford Clay.

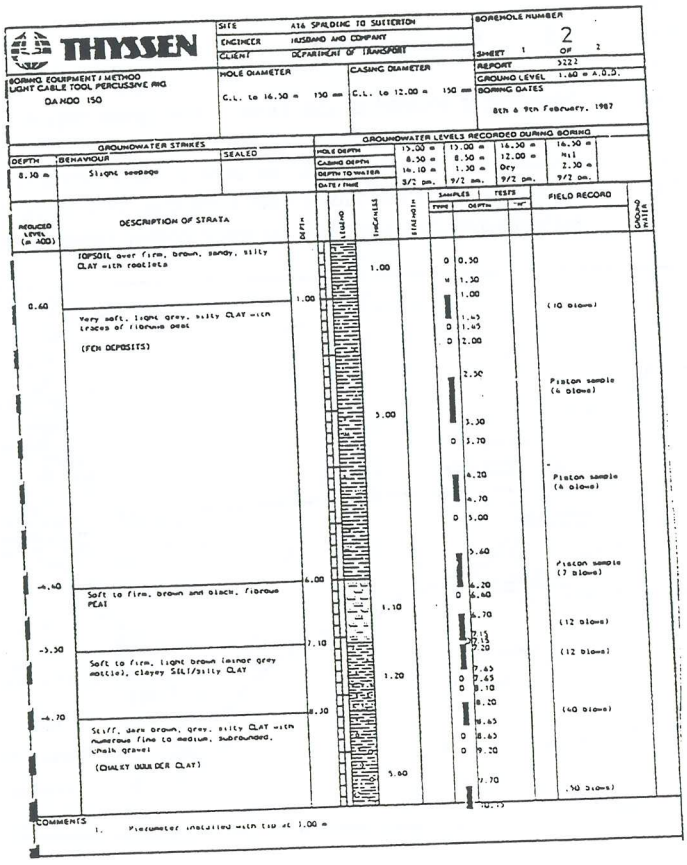

Figure 2: Borehole Log at Ch 1200

2.4 Embankment Design

An embankment height of 6m was required to give clearan across the Welland River. Due to the compressible nature the Fen deposits, a surcharge of 40kPa was required in t form of 2.0m of compacted Class 6F1 sand and gravel. T embankment footprint was 48m wide comprising a formati width of 11.3m and batters set at 1:3. Following topsoil str a drainage blanket-cum-work platform 0.5m thick was plac over a non-woven geotextile and the instruments installe Wick drains were installed at 1.5m centres through t blanket to the base of the Fen deposits, except in t immediate vicinity of the instruments so as not to cau damage. Uniformly graded granular material was specifi for the body of the embankment. The rate of filling w restricted to 0.75m per seven consecutive days.

2.5 Instrumentation

Instrumentation at Ch1200 comprised 24 hydrau piezometers, five magnetic extensometer settlement gaug four inclinometers, one hydrostatic profile gauge and settlement plate. The arrangement of instruments is shown Figure 3. All piezometers were connected to terminals on right hand side of the embankment.

The piezometers, inclinometers and hydrostatic profile gau were read using data loggers which down-loaded directly t PC and onto spreadsheets. The magnetic settlement gaug were read using a manual reed switch probe whilst settlement plates were surveyed; this data was entered o spreadsheets manually.

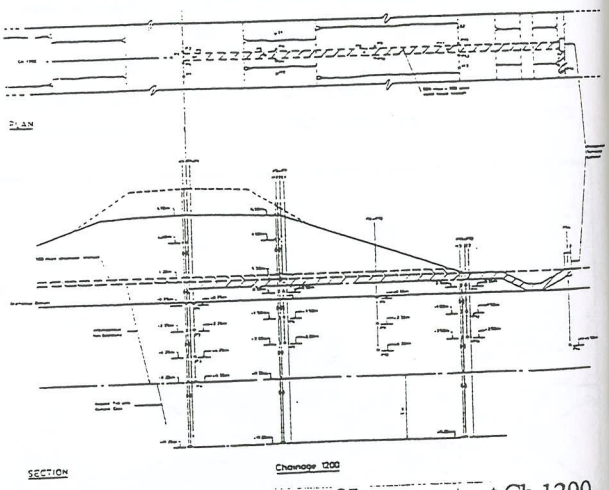

Figure 3: Arrangement of Instruments at Ch 1200

2.6 Embankment Fill Materials

Embankment fill material could not be sourced from bor pits adjacent to the site due to the soft saturated nature of near-surface soils and restrictions on land-take due to area's agricultural use. To enable year-round constructi and hence minimise construction time, material was specif as select granular fill. The Contractor elected to use re bricks from brickworks located 25km south of the site.

material had a bulk density of 1750 kg/m^3 when placed and compacted. The surcharge had a compacted density of 2000 kg/m^3

3 CONSTRUCTION AND MONITORING

3.1 Sequence of Events

Installation and commissioning of instruments was completed at the end of March 1993. The instruments were monitored on a regular basis throughout the construction and surcharge periods. Records for the centreline, right hand verge, shoulder and toe, and fence line piezometers are attached as Figures 4 - 8 respectively. Selected toe inclinometer data is shown on Figures 9 & 10. Centre line and right hand toe extensometer data is shown on Figures 11 & 12. Selected readings from the hydrostatic settlement gauge are shown on Figure 13.

Filling commenced in the first week of April 1993. Pore pressure response to loading was monitored in terms of B-bar, the ratio between incremental pore pressure rise and increase in vertical stress ($B = \Delta u / \Delta\sigma_1$). Filling was halted for 10 days once the embankment had reached a height of 3.0m to observe pore pressure response and settlement. It had been expected that pore pressure would drop by about 0.3 - 0.5m in this time; almost no change was observed despite settlement of approximately 100mm. Lateral deflection at the toes was approximately 25mm in the peat layer but indicated as pinching-in near original ground level (+1.6m AOD).

A further 2m of fill was placed over the next three weeks. This was followed by a six week pause while the Contractor used the area as a preparation platform for adjacent piling works. Reference to Figure 10 indicates that as in the previous pause, settlement was occurring throughout the foundation although almost no pore pressure dissipationwas being recorded by the piezometers. Surface settlement in that period was 150mm. Seepage was observed from the drainage blanket indicating that the wick drains were functioning; hence there was a suspicion that the piezometers, positioned in an area without wick drains, were not accurately reflecting the pore pressures in the rest of the foundation. Filling with Class 6C material re-commenced and was complete by the end of July. A non-woven geotextile was laid to act as a separator between the brick fill and sand surcharge.

Surcharge was placed throughout August. Prior to placing the final lift, inclinometer readings indicated only 50mm lateral movement, concentrated in the peat. Although B-bar was approaching 1.0, it was felt that this was misleading. Continued settlement and limited lateral deflection suggested that the embankment foundation was capable of taking the final lift of material. Placing of the final lift was substantially complete on Friday 10 September. Dramatic pore pressure changes were observed on the following Monday during final trimming: there was a drop of approximately 1m head at the centreline and comparable rises throughout the rest of the foundation, indicating failure. Heave of 200mm was observed in the toe extensometers. The shape of the hydrostatic settlement gauge plot indicates that the embankment had split and rotated although the toe inclinometer readings still showed no lateral movement at ground level and only minor movement in the peat. Small swallow holes appeared in the surface of the surcharge along with a very faint step along the centreline. A trial pit was excavated into the brick fill however no crack was observed. The following day the four inclinometers were unreadable as were four of five extensometers and the hydrostatic profile gauge. A metre of surcharge was removed over a 150m length in a bid to prevent complete collapse. Over the following weeks, the centreline extensometer kinked and became unreadable. New inclinometers were installed at the toes.

The embankment was left for eight months to settle and gain strength prior to a second attempt to reach the full surcharge height. During this time, piezometers on the left hand side of the embankment began to fail, probably due to pulling of the tubing and consequent breaches of the bentonite seals. However, the toe extensometers could be read intermittently suggesting that the embankment blocks were settling back towards the centreline. It should be noted that the replacement inclinometers did not indicate such movements.

The metre of surcharge was reinstated over a period of four weeks in a series of 250mm lifts. Surcharge was placed over the 25m length of the embankment straddling the instruments. The foundation reaction was observed for two full days. Material was placed over the rest of the embankment if it was felt that there had been no adverse reaction to loading. The last lift induced pore pressure rises equivalent to B-bar = 1.0 and it was decided not to place any additional material. The embankment remained in surcharge for a further four months.

During removal of the surcharge, the geotextile separator placed on the surface of the brick fill was torn, revealing the suspected crack. The crack, located along the centreline of the embankment, was 100m long by 0.6m wide and extended to the base of the fill where clay could be seen. It confirmed that a brittle tensile failure had occurred. Trenches were excavated across the embankment to establish the longitudinal and lateral extent of the crack.

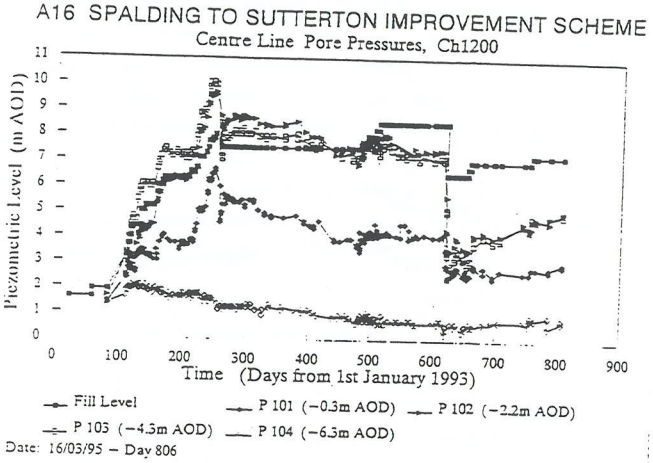

Figure 4: Centre line piezometer readings

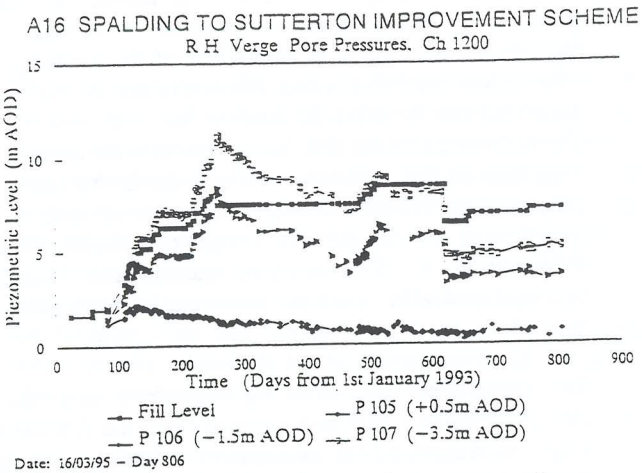

Figure 5: Right hand verge piezometer readings

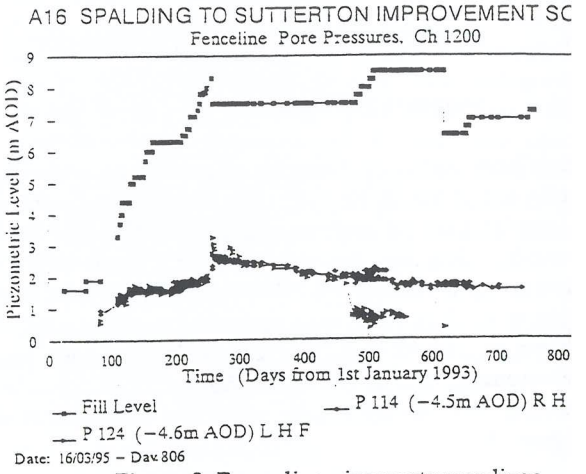

Figure 8: Fence line piezometer readings

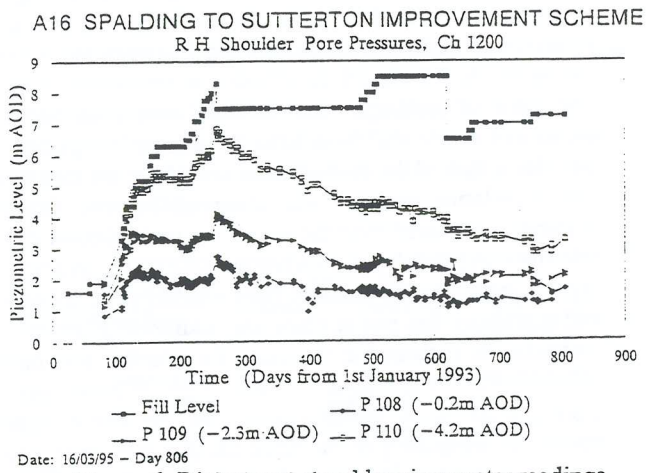

Figure 6: Right hand shoulder piezometer readings

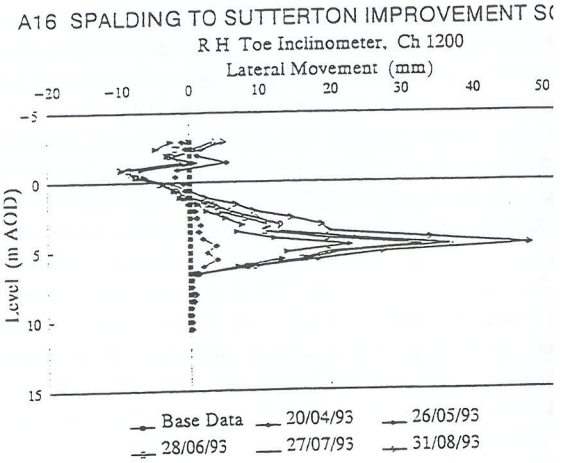

Figure 9: Right hand toe inclinometer reading

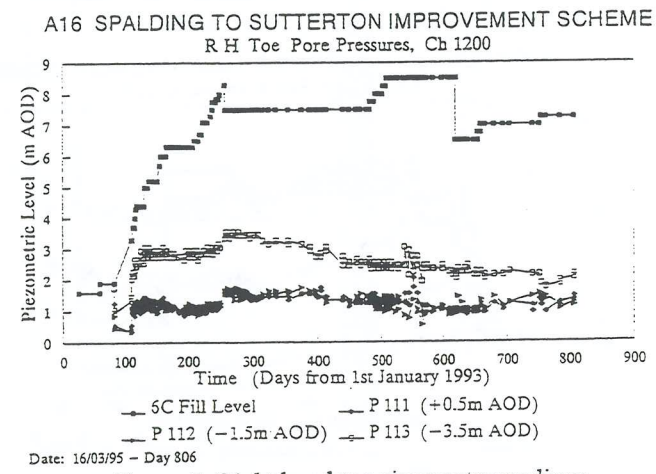

Figure 7: Right hand toe piezometer readings

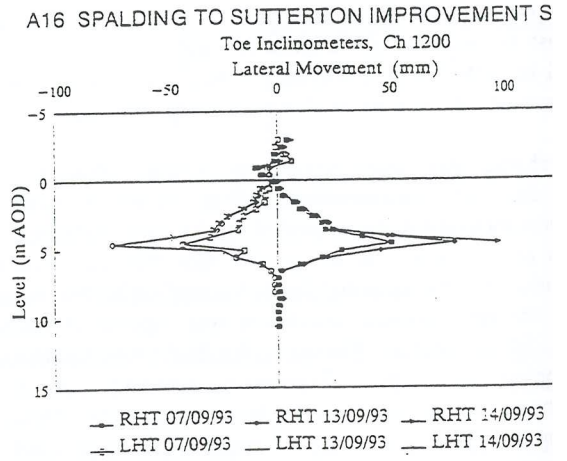

Figure 10: Left and right toe inclinometer readi

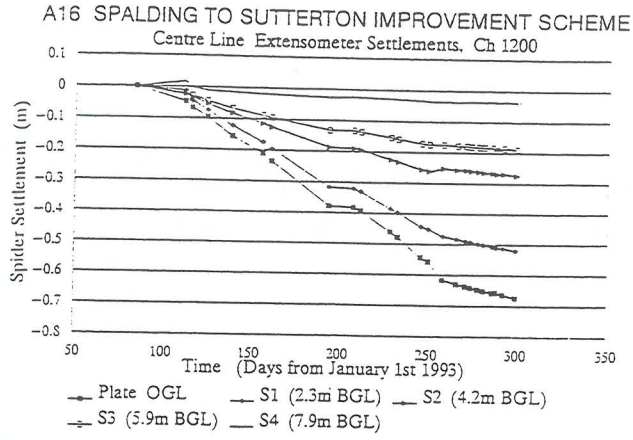

Figure 11: Centre line extensometer readings

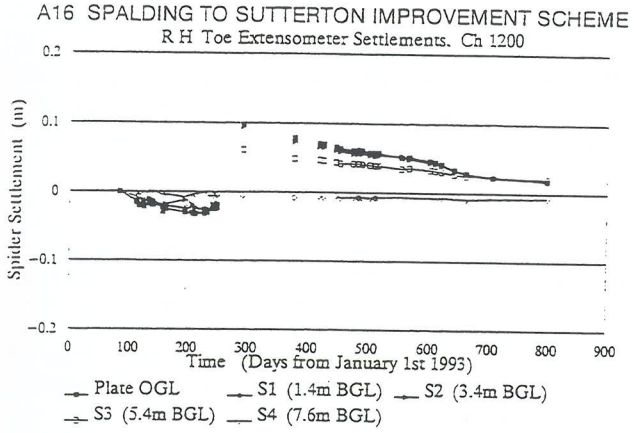

Figure 12: Right hand toe extensometer readings

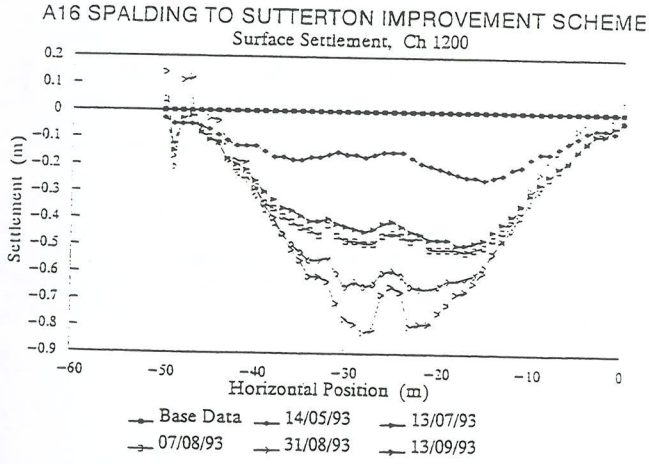

Figure 13: Hydrostatic profile gauge readings

3.2 Remedial Measures

Future stability of the embankment was considered when formulating the remedial measures. Two options were considered: complete removal and reconstruction of the embankment; and grouting of the crack. The choice of solution depended upon the response of the foundation and embankment to the second episode of surcharging.

A review of the data indicated that the embankment had not spread or rotated during the second surcharging. The main evidence for this came from the pore pressure response. During the original failure, sharp rises in pore pressure were observed throughout the foundation from the verge to the fence lines in response to lateral squeezing of the soil; no comparable behaviour was observed during the second episode of surcharging. Readings from the toe extensometers indicated that the blocks had steadily settled 50mm since the original movement. The replacement inclinometers installed at the toes had indicated only slight movement.

On the basis of the above assessment, remedial measures comprised:

- Grouting of the crack with free-flowing low density foam concrete;
- heavy compaction of the surface;
- laying of a woven polyester structural geotextile; and
- additional transverse steel in the continuously reinforced concrete roadbase.

4 CONCLUSIONS

Instrumentation is vital in controlling construction of embankments on soft clay however it is not without problems. During construction, seemingly contradictory data was being provided by the instruments leading to uncertainty about which ones to believe, although in hindsight all of the warning signs of impending failure were there. Consolidation was occurring, as evidenced by settlement throughout the foundation and seepage of water from the drainage blanket, however there was no concomitant reduction in pore pressure. The lack of pore pressure dissipation suggested that the piezometers were not functioning correctly and therefore greater emphasis was placed on ground movements, in particular inclinometer readings. In hindsight, the piezometers were more reliable indicators of impending failure.

- The non-structural geotextile placed at original ground level, coupled with the brick fill material, created a rigid embankment which suffered a brittle failure.
- Incremental pore pressure response to loading should be taken as the key indicator of foundation stability.
- A lack of ground movement in response to loading should not be used to infer ongoing stability.
- The instrument readings at the time of failure gave enough warning for emergency steps to be taken.
- Removal of the metre of surcharge probably saved the embankment from complete collapse.
- The instrument data enabled design of suitable repairs to the embankment.

5. ACKNOWLEDGEMENTS

Grateful acknowledgment is made to Mott MacDonald Group for permission to write this paper and for assistance during the works described, in particular to Ron Williams and Bill Sim.

Trials to Determine the Usefulness of Vibro Stone Columns in the Prevention of Liquefaction of Silty Sands

Sharon Cassidy, BE
Geotechnical Engineer, Arup Geotechnics Pty Ltd, formerly Ove Arup & Partners UK

Summary A proposed Liquefied Natural Gas (LNG) plant in the south of Trinidad involved the foundation design of two 74.4 m diameter, 30 m high, concrete outer wall, LNG tanks. The site is located 1 km from an active fault. The proposed foundation system was steel tubular driven piles. Vibro stone columns were proposed to densify the silty sand layers above the founding stratum in order to minimise the number and size of piles required. This paper presents the results of trials carried out on the top feed vibro replacement wet method of stone column installation, including CPTs before and after installation. These trials showed the method to be unsuccessful in densifying all the silty sand layers. Hence these silty sands fall into an intermediate category of a material which can liquefy under earthquake conditions, but cannot be densified using this method of stone column installation.

1 INTRODUCTION

A liquefied natural gas (LNG) plant is being constructed by Bechtel for ALNG in the south of Trinidad. The plant has two 74.4 m diameter, 30 m high LNG tanks, Tank A and Tank B, which are being constructed by Whessoe Projects Limited. The site was located 1 km from an active fault. The stratigraphy comprised approximately 10 m of Fill and Marine Deposits overlying a hard clay or silt. The Fill and Marine Deposits contained silty sands. In order to prevent liquefaction of these sands during an earthquake, it was proposed to install stone columns, using the top feed vibro replacement wet method, through the Fill and Marine Deposits to the top of the hard clay/silt below. The purpose of this was to minimise the number and size of piles required for foundation design. Three vibro stone column tests to establish the effectiveness of the treatment in the silty sands were carried out.

2 GROUND CONDITIONS

2.1 Site Investigation

A site investigation was carried out to establish the bearing capacity of the hard clay/silt for pile design and to assess the composition of the Fill and Marine Deposits. The site investigation was supervised by Ove Arup & Partners UK and comprised fifteen boreholes approximately 30 m deep, with two to 70 m. Fifty-six Cone Penetration Tests (CPTs) were carried out to confirm the composition of the Fill and Marine Deposits at the tank locations.

2.2 Stratigraphy

At the location of Tank A, essentially three strata were encountered. The first stratum was recently-dumped Hydraulic Fill which comprised a mixture of soft to firm clays and loose to medium dense silts and sands. This overlay Marine Deposits which generally comprised loose to medium dense silty sands to sandy silts. This stratum overlay a stiff to hard Grey Clay. Figure 1 shows a section through Tank A.

At the location of Tank B, five strata were encountered. The first and second were the Fill which overlay the Marine Deposits as found in Tank A. Over parts of Tank B this overlay a firm to hard Brown and Grey Clay which overlay the Grey Clay as found in Tank A. For the remainder of Tank B, the Marine Deposits were underlain by a hard or very dense Oily Silt. Figure 2 shows a section through Tank B.

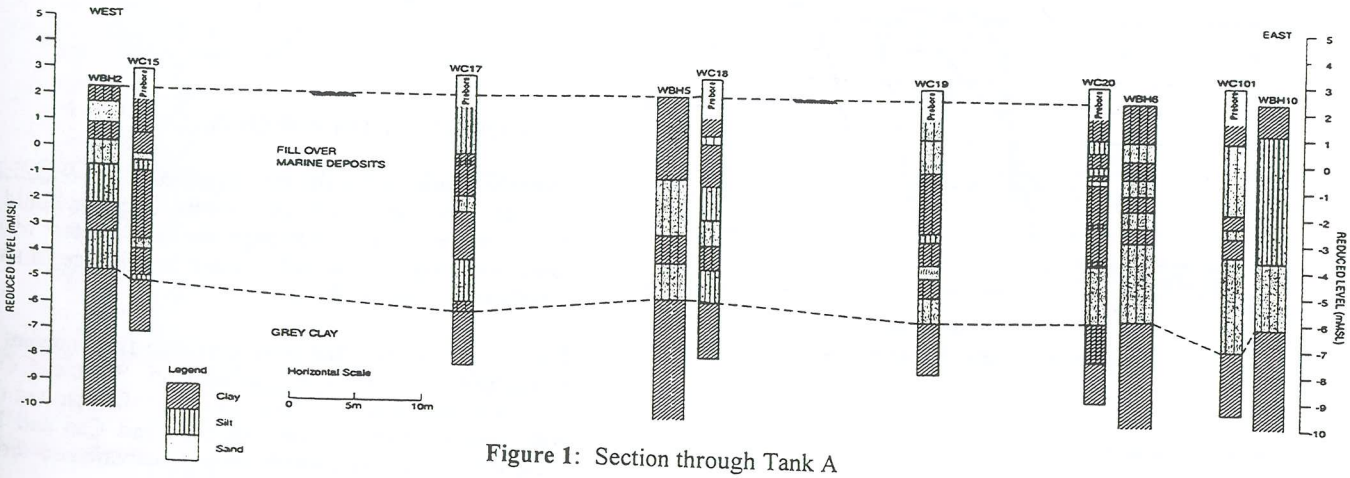

Figure 1: Section through Tank A

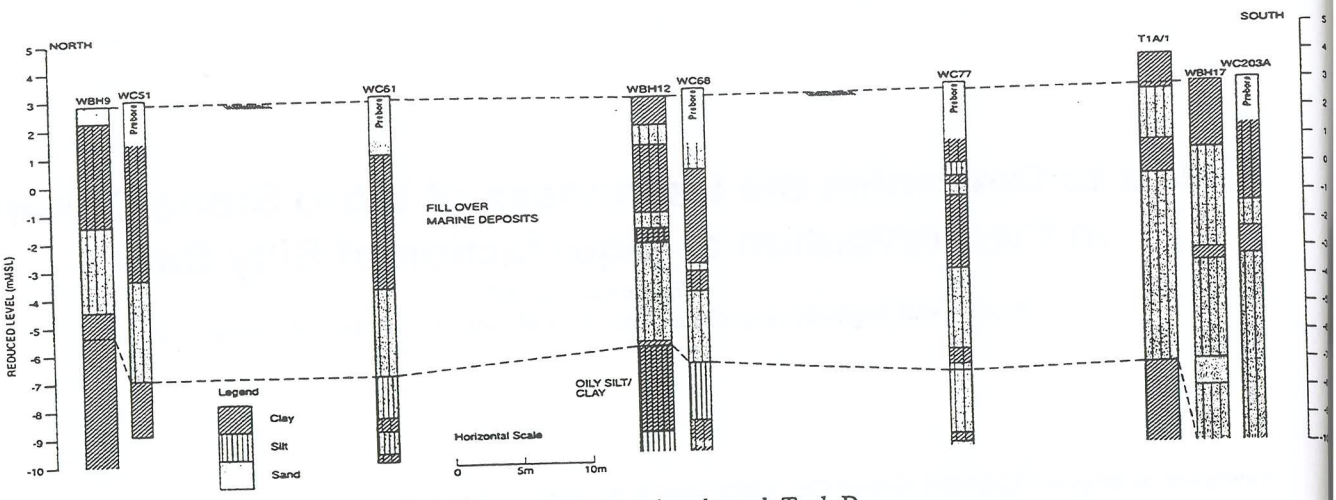

Figure 2: Section through Tank B

2.3 Properties of the Silty Sands

Particle size distribution tests were carried out according to ASTM-D422 for the sand materials in the Fill and Marine Deposits. The distributions are plotted in Figures 3, 4, 5 and 6 and are compared with the boundaries proposed by Tsuchida (1) for most liquefiable and potentially liquefiable soils. The grading curves show the sands to have high fines content generally close to the boundary between most and potentially liquefiable soils*.

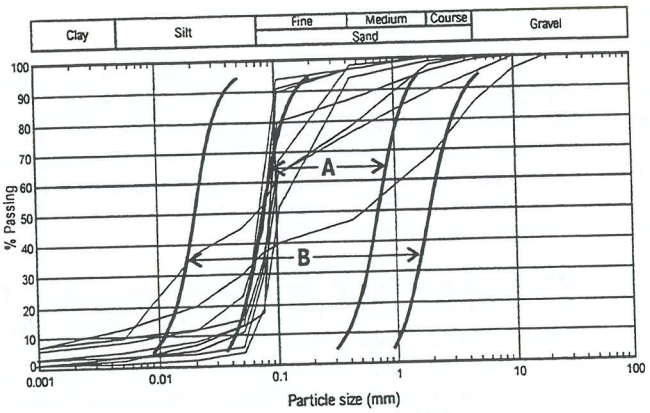

Figure 3*: Tank A Fill

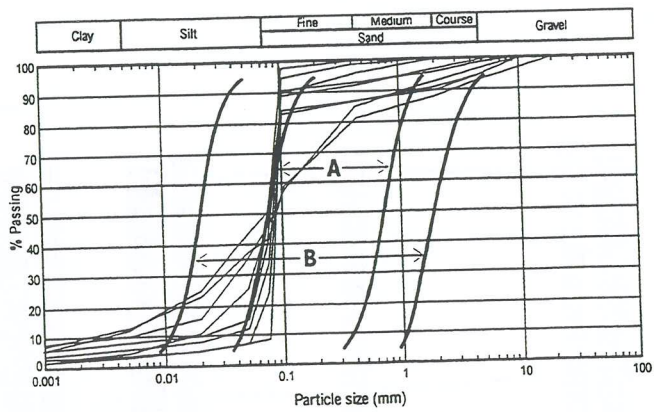

Figure 4*: Tank A Marine Deposits

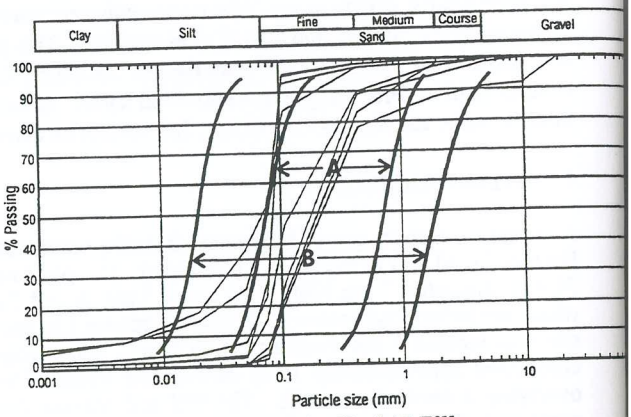

Figure 5*: Tank B Fill

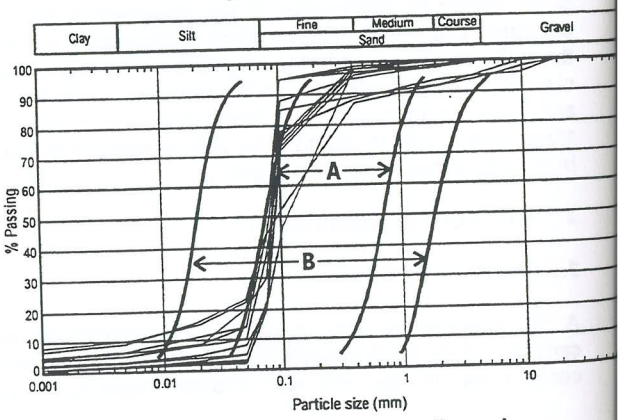

Figure 6*: Tank B Marine Deposits

3 LIQUEFACTION POTENTIAL

From the results of the site investigation, it was established the silty sands in the Fill and Marine Deposits could liq during an earthquake. Although the fines content of the sands were high (up to 40%), there is evidence to show liquefaction could occur.

Figures 3 to 6 show that soils with high fines content ma susceptible to liquefaction. In addition, Stark and Olse compiled case histories which show liquefaction had occ with fines content in excess of 50% and Cao and Law compiled case histories which show liquefaction occurring clay contents of up to 12%.

* For Figures 3, 4, 5 and 6
A = Most liquefiable soils, B = Potentially liquefiable soils

4 STONE COLUMN TRIALS

Initially two trials had been planned but this was extended in scope following the first two trials. The stone columns were installed using the top feed vibro replacement method which involves vibrating the vibro-flot, which has a water jet, into the ground to the required depth. The vibro-flot is then partially withdrawn and stone fed from the top and the vibro-flot reintroduced into the ground. This continues until a column of the required size has been formed. The three trials carried out were as follows:

Trial 1: Tank A - 600 mm Columns
Trial 2: Tank B - 600 mm Columns
Trial 3: Tank B - 1200 mm Columns

The trials comprised at least sixteen columns at 2 m square grid spacing. The trials were located close to boreholes considered to be representative of the ground conditions at the tank locations.

5 ACCEPTANCE CRITERIA

The CPTs carried out as part of the site investigation were correlated with the boreholes in order to be able to accurately identify the presence and consistency of sands and silty sands. Therefore CPTs were carried out between the stone columns before and after the vibro trials to identify the strata and assess the effectiveness of the treatment. The acceptance criteria against liquefaction were calculated based on a method devised by Seed et al (4) which determines the liquefaction potential based on the N-value from a standard penetration test. The relationship is between stress ratio $\frac{(\tau_{av})}{(\sigma_{v'})}$, N value and percentage of Fines. Figure 7 is an extract from the Seed et al (4) paper.

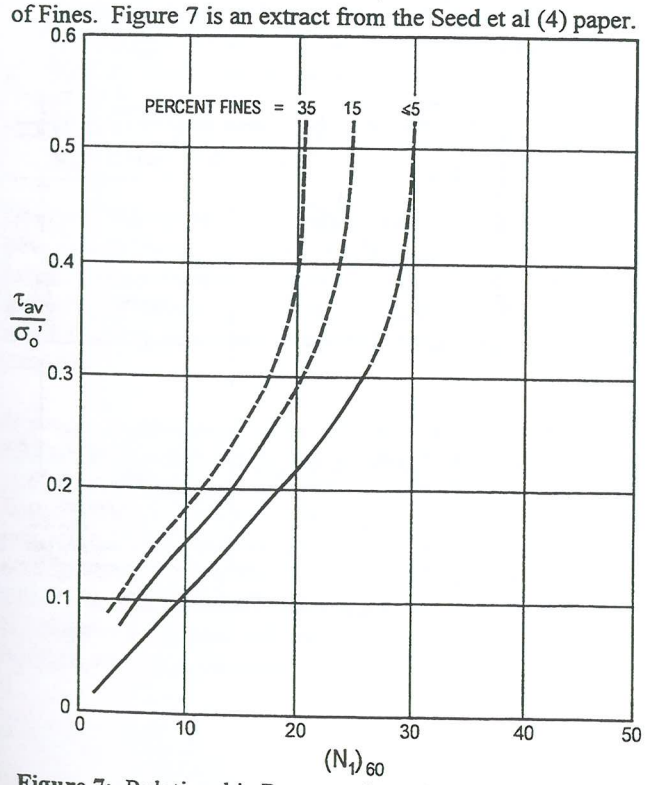

Figure 7: Relationship Between Stress Ratio, SPT N Value and Fines Content (after Seed et al, 1986)

The equation for $\frac{(\tau_{av})}{(\sigma_{v'})}$ is:

$$\frac{\tau_{av}}{\sigma_{v'}} = 0.65 \cdot \frac{a_{max}}{g} \cdot \frac{\sigma_v}{\sigma_{v'}} \cdot r_d \cdot M_F$$

where a_{max} = peak horizontal ground acceleration

r_d = stress reduction factor - varies from 1 to 0.9 from surface depth to 10 m depth

M_F = Modification Factor due to earthquake magnitude (assumed = 1.0 for magnitude of 7.5).

The CPT cone resistance, q_c, values are converted to SPT N-values using a relationship proposed by Stark and Olsen (2). Figure 8 is an extract from the Stark and Olsen paper (2) showing conversion factors for different fines contents.

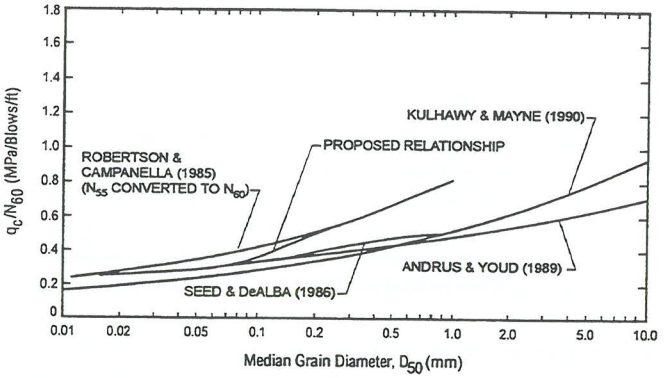

Figure 8: Conversion of CPT q_c Values to SPT N Values Using Median Grain Diameter (after Stark and Olsen, 1995)

There are two design earthquake cases, the Operating Base Earthquake (OBE) where the plant should be operational following an Earthquake, and Safe Shutdown Earthquake (SSE) where the structure must remain intact to allow safe disposal of the contained LNG. The design earthquake magnitude is 7.5. The horizontal ground acceleration for the OBE is 0.3g and for the SSE is 0.55g.

Figure 9 shows the calculated CPT acceptance criteria plotted against liquefaction for 25 % fines content.

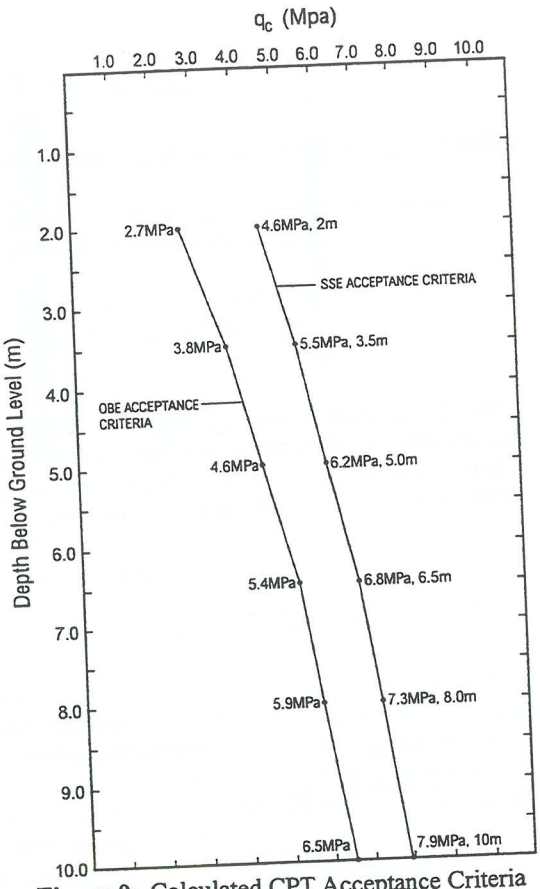

Figure 9: Calculated CPT Acceptance Criteria

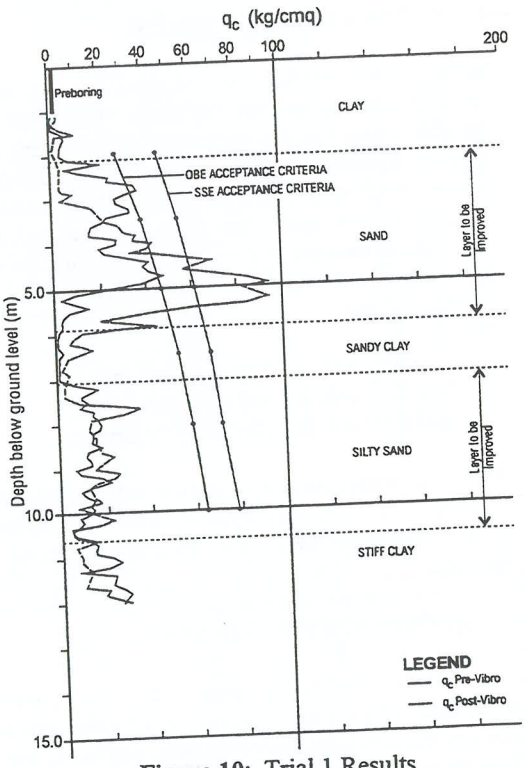

Figure 10: Trial 1 Results

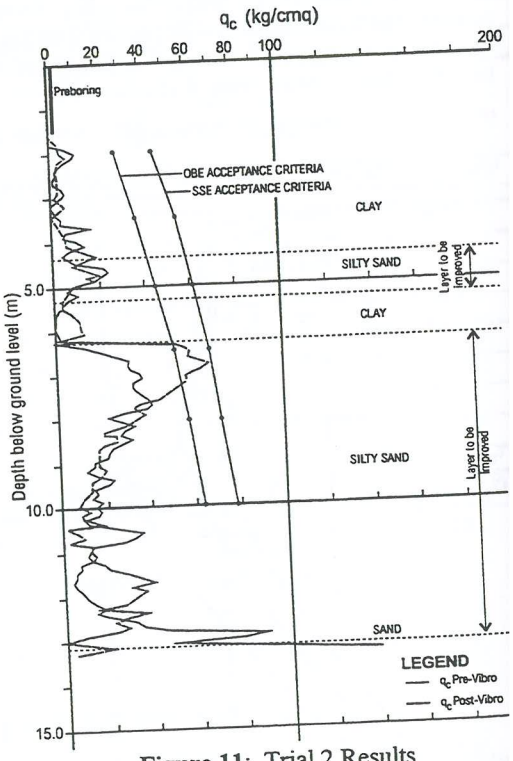

Figure 11: Trial 2 Results

6 RESULTS

Before and after results of trials 1, 2 and 3 are presented in Figures 10, 11 and 12 respectively and are described below.

Trial 1: Tank A 600mm columns
There was an improvement in the sand layers above 5 m depth in five of the nine post-vibro CPTs. However, in the silty sand layer between 7 m and 10 m, there was little or no improvement. Figure 10 shows the improvement in one of the CPTs.

Trial 2: Tank B 600mm columns
There was an improvement in the upper part of the sand layer between 6 m and 10 m. However, little or no improvement occurred below this. Figure 11 shows the improvement in one of the CPTs.

Trial 3: Tank B 1200mm columns
As per trial 2, there was an improvement of part of the sand layer below 6 m but not over the entire layer. Figure 12 shows the improvement in one of the CPTs.

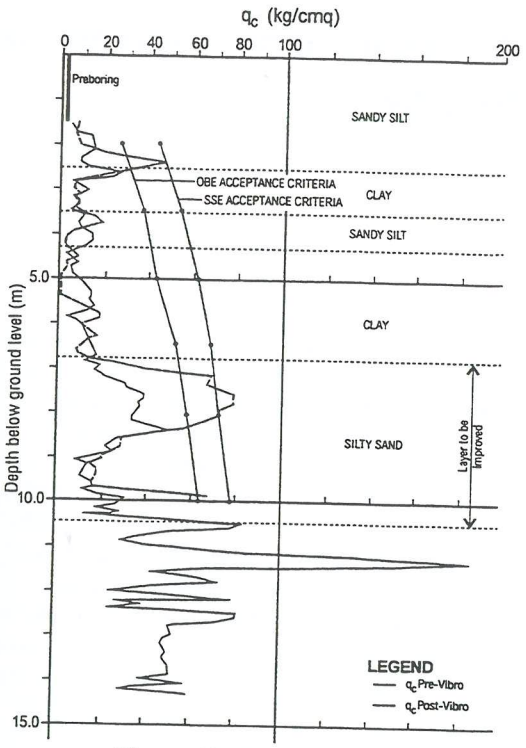

Figure 12: Trial 3 Results

7 DISCUSSION

From the results of the trials, a number of observations can be made.

- The wet method was successful in densifying the sand layers at shallow depths. The improvement in trial 3 was more marked than in trial 2, probably due to the larger diameter stone columns used in trial 3.

- There was little improvement of the silty sand layers at depth in any of the trials.

Therefore, the top feed vibro replacement wet method of stone column installation was not successful at improving all the sand layers, in particular the silty sand layers below about 7 m. There is a potential reason for this: due to the high fines content, the vibrations may have been dampened, preventing densification occurring.

However, as discussed above, although the gradings and the CPTs indicate a high percentage of fines, there is a good deal of published information showing liquefaction can occur with large fines content. Therefore although this high fines content prevents the vibro treatment from improving the silty sand, this does not mean it would not liquefy under earthquake conditions. Therefore, as it had been shown that the vibro stone columns did not improve the ground sufficiently, the piles were designed to resist forces due to liquefaction.

8 REFERENCES

1 Tsuchida H., "Prediction and Countermeasures against liquefaction in sand deposits", Abstract of the seminar in the Port and Harbour Research Institute pp 3.1-3.33 (in Japanese).

2 Stark T.D. and Olsen S.M., "Liquefaction resistance using CPT and field case histories", Journal of Geotechnical Engineering, December 1995.

3 Cao Y.L and Law K.T., "Energy approach for liquefaction of sandy and clayey silts", Second International Conference on Recent Advances in Geotechnical Earthquake Engineering and Soil Dynamics, Missouri March 1991.

4 Seed H.B, Tokimatsu K, Harder L.F and Chung R.M., "Influence of SPT procedures in soil liquefaction evaluations", ASCE Journal of Geotechnical Engineering Vol III No 12 1985, pp 1425-1445.

8 ACKNOWLEDGEMENTS

Whessoe Projects Limited were contracted by the Atlantic LNG Company of Trinidad and Tobago to construct the LNG tanks. Ove Arup & Partners were Whessoe's design subcontractors. I would like to thank Whessoe Projects Ltd for allowing the information in this paper to be published. I would also like to thank David Clare of Ove Arup & Partners who was responsible for the geotechnical design of this project and Tony Phillips of Arup Geotechnics Pty Ltd for his advice on the writing of this paper.

.-.-.-.-.-.-.-.-.-.

Third A-NZ Young Geotechnical Professionals Conference, Cameron, Collingwood & Slatter (eds), Feb. 1998, Melbourne, Australia.

Borehole Roughness: A Key Parameter in Predicting Rock Socket Side Resistance

B. Collingwood
B.E., Grad IEAust.
Postgraduate Student, Department of Civil Engineering, Monash University. Australia

SUMMARY Predicting the performance of rock socketed bored piles has traditionally been a difficult task. The results given by conventional methods of predicting shaft resistance, based on empirical correlations with intact rock strength, have proven to be poor when used outside the specific data set for which they were developed. Researchers have long recognised that socket roughness is an important parameter. However, attempts to incorporate roughness parameters as an integral part of design have been unsuccessful. Recent advances at Monash University have led to a wholly theoretical design method which incorporates roughness as a key parameter. The Monash method is broadly applicable, but its use requires a prediction of socket roughness to be made. At present, rock socket roughness is poorly understood. A better understanding of socket roughness production across a variety of drilling conditions is crucial for the full potential of this new approach to be realised. Using the Monash method, historical load test data has been re-analysed to evaluate the contribution of socket roughness to pile capacity. The results of the study suggest upper and lower bounds on socket roughness, and confirm that roughness variations are particularly significant in low to medium strength rock. A borehole profiler is being developed which will be used in an imminent field investigation of socket roughness. The aim of this investigation will be to develop socket roughness guidelines for use in design.

1.0 INTRODUCTION

Rock socketed bored piles are a common foundation solution for large concentrated loads. They derive their load bearing capacity from both shaft and base resistance components. Figure 1 shows a typical load settlement response for a rock socketed pile. The base resistance component can contribute significantly to the ultimate capacity of the pile. However, as shown in Figure 1, shaft resistance is typically mobilised at considerably smaller pile settlements than that of the base. Ensuring the reliability of base response requires a construction and inspection technique which leaves the socket free of debris. This may be difficult and costly to achieve, particularly in deep sockets which are often drilled under water or drilling mud. As a consequence of these factors, shaft resistance generally dominates pile performance at working loads. Efforts to improve prediction of rock socketed pile performance are therefore primarily concerned with the complex mechanisms of shaft resistance development. Shaft resistance only is considered in this paper.

The paper outlines the limitations of conventional methods of shaft resistance prediction, and introduces the Monash rational approach which incorporates socket roughness as a key parameter. The wide applicability of this new approach is currently restricted by insufficient information relating to socket roughness characteristics in the field. A method of estimating socket roughness by back-analysis of historical data from rock socket load tests is described. The application of this method to a database of 137 pile load tests has provided insight into typical levels of field socket roughness. Selected results from this study are presented and a future field investigation of socket roughness is outlined.

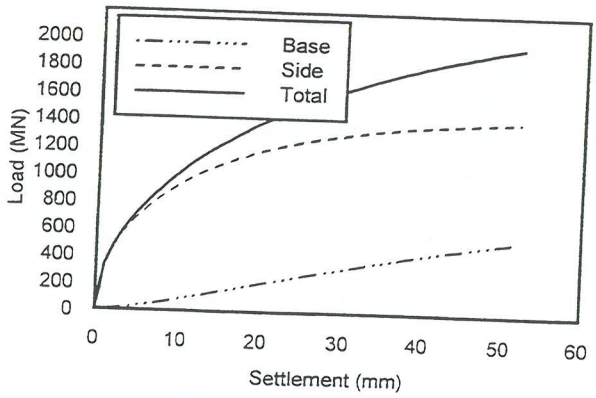

FIGURE 1. Typical load settlement response of a rock socketed pile (Rocket Prediction).

1.1 Conventional design of pile shafts in rock

Detailed discussions of the limitations of traditional methods for predicting rock socket side resistance have been previously published (Seidel and Haberfield, 1994; Seidel et al., 1996). The summary provided in this section draws heavily upon these accounts.

Traditional methods for design of piles socketed into rock have been based on the results of full scale load tests, from which empirical correlations and locally applicable guidelines have been derived (Seidel and Haberfield, 1994). Numerous correlations have been proposed which relate the unit side resistance of the socket to the uniaxial compressive

strength of the surrounding rock. These empirical models generally take the form:

$$f_{su} = \alpha q_u^{\beta} \qquad (1)$$

where f_{su} is the ultimate socket shaft resistance, q_u is the uniaxial compressive strength of the weaker material (in most cases rock), and α and β are empirically determined from load test results.

Many empirical relationships in the form of Equation 1 have been formulated which correlate well with the specific data sets from which they were derived. However, there is no single correlation which can be applied universally to the design of bored piles. O'Neill et al (1995) undertook a comparison of 9 previously proposed empirical correlations based on Equation 1 with an international database of pile load tests in intermediate strength rock. Their database was sufficiently large to include pile sockets of varying geometry, drilled by different methods, at many sites and in a range of rock types. They concluded that none of the methods could be considered an accurate predictor across the range of tests contained in the database. The limitations of the traditional empirical approach are similarly illustrated in the results of two other major database studies (Rowe and Armitage, 1984; Kulhawy and Phoon, 1993).

TABLE 1. Roughness classification (after Pells et al 1980)

Roughness Class	Description
R1	Straight, smooth-sided socket, grooves or indentations less than 1 mm deep.
R2	Grooves of depth 1--4 mm, width greater than 2 mm, at spacing 50 mm to 200 mm.
R3	Grooves of depth 4-10 mm, width greater than 5 mm, at spacing 50 mm to 200 mm.
R4	Grooves or undulations of depth > 10 mm, width > 10 mm at spacing 50 mm to 200 mm.

The empirical correlations proposed by Rowe and Armitage (1984) are shown in Figure 2. They recognised the significance of socket roughness and attempted to incorporate this variable in their study. Correlations were proposed for data obtained from sockets exhibiting roughness levels of R1 to R3 (as defined in Table 1), and for those with roughness R4. Considerable scatter around the proposed correlations is evident.

A similar study was undertaken by Kulhawy and Phoon (1993), who investigated the side resistance of a large number of full-scale load tests in material ranging from firm soil to hard rock. Trend lines were identified for piles in both soil and rock, however, considerable scatter remained. The extent of the scatter is reflected in the correlations they proposed. These were of the general form:

$$\alpha = \Psi (q_u / 2p_a)^{-0.5} \qquad (2)$$

with a constant of proportionality to the outcome, ψ, bei 0.5 for piles in soil, but varying between 1.0 and 3.0 with average of 2.0 for piles in rock. Importantly, Kulhawy a Phoon noted that sockets in soil are generally very smoo whereas sockets in rock exhibit larger variations roughness.

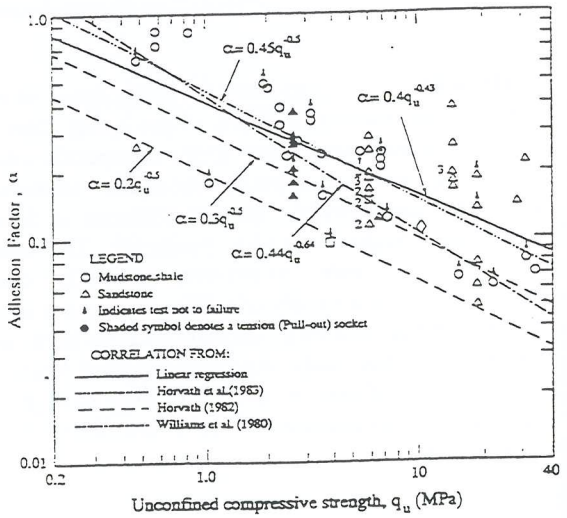

FIGURE 2. Socket resistance correlations for Pe Roughness R1 to R3 (after Rowe & Armitage, 1984)

Seidel et al. (1996) concluded that all three ma investigations have shown that the reliability of curre available empirical design methods for predicting r socket shaft resistance is questionable, because they do address a sufficiently broad range of parameters to acco for the many variables which come into play.

1.2 Socket Roughness

The importance of socket roughness on shaft resistance been recognised by numerous researchers for a considera time (Horvath et al., 1983; Johnston, 1977; Pells et 1980; Williams, 1980).

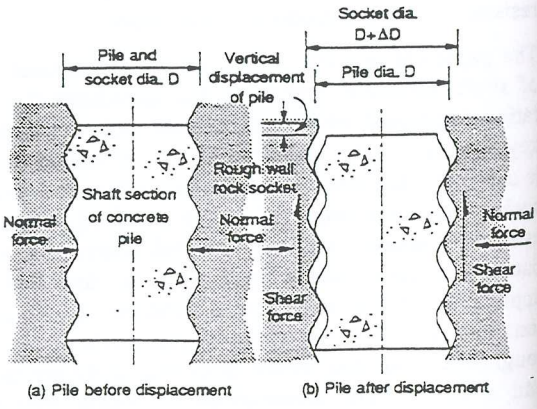

FIGURE 3. Pile rock socket idealisation.

The influence of socket roughness is a consequence of the dilative nature of a rough concrete-rock joint and the constant normal stiffness (CNS) boundary condition which governs interface normal stress. Figure 3 shows a schematic representation of a rock socket in cross-section. The concrete of the pile is initially in contact with the rock socket against which it has been cast (Figure 3(a)). When a load is first applied, elastic deformation of the pile-rock system will occur without any slippage of the pile relative to the rock.

Eventually, a critical load will be reached at which slip commences at the pile-rock interface. As interface is non-planar, this shear displacement must be accompanied by dilation as illustrated in Figure 3 (b). The corresponding radial enlargement of the borehole is resisted by the surrounding rock, resulting in an increase in normal stress at the pile-rock interface. The increase in normal stress will be governed by the radial stiffness of the borehole. This normal stiffness, K, is approximately constant and is given by:

$$K = \frac{E_m}{(1+\nu_m).r_s} \qquad (3)$$

where E_m is rock mass modulus, ν_m is the Poisson's ratio, and r_s is the pile radius. K is known as the constant normal stiffness (CNS).

The mechanisms of sliding and shearing at the pile rock interface are complex. In general, however, the rougher the interface the greater dilation and corresponding normal stress which will result for any given axial displacement of the pile-rock joint. This increased normal stress increases the frictional resistance between pile and rock.

From Equation 3, the change in normal stress, $\Delta\sigma_n$, for a given interface dilation, Δr_s, is:

$$\Delta\sigma_n = K\Delta r_s = \frac{E_m \Delta r_s}{(1+\upsilon_m) r_s} \qquad (4).$$

It is evident in Equation 4 that the increase in normal stress is proportional to the ratio of interface dilation to socket radius. Consequently, for a measure of roughness to be useful in comparing the behaviour of various piles, it must be normalised against socket radius or diameter.

Several researchers have proposed empirical correlations for predicting side resistance which incorporate socket roughness (Pells, 1980; Williams, 1980; Horvath, 1983; Rowe and Armitage, 1984). However, perhaps the greatest obstacle in this pursuit has been the absence of a reliable and sufficiently rigorous method of roughness quantification.

The roughness classification system devised by Pells and his co-workers (Table 1) is often used in Australia for specifying minimum roughness requirements for the purposes of visual rock socket inspections. Although useful in this context, the classification system is open to considerable subjective interpretation, which limits its applicability as a quantitative tool. Both Williams (1980) and Horvath (1983) proposed quantitative methods of evaluating socket roughness, which involved recording and analysing the geometry of measured profiles. However, both roughness models proved to be sometimes ambiguous and open to theoretical criticism (Seidel, 1993, Seidel et al., 1996). Their widespread use has also been hindered by the difficulties associated with measuring roughness profiles in the field.

The lack of a reliable method of roughness quantification and the shortage of measured roughness data have long served as an impediment to the incorporation of socket roughness in routine design.

2.0 RECENT ADVANCES IN UNDERSTANDING ROCK SOCKET BEHAVIOUR

A large fundamental research program into the behaviour of rock-socketed piles has been carried out at Monash University since the early 1980's. This program has been based upon large scale direct shear testing of concrete-rock joints, under CNS conditions. Physically-based analytical models of the observed responses have been formulated, which allow the complex mechanisms of side resistance development to be numerically reproduced (Seidel, 1993). Rather than adopting an empirical approach, Monash researchers have aimed to produce a widely applicable rational design method, based on fundamental rock mechanics principles. Their work has culminated in a development of a computer program named *ROCKET*, which embodies the Monash design approach. The theory behind the *ROCKET* program has been widely published (Seidel, 1993; Seidel and Haberfield, 1994; Seidel and Haberfield, 1995).

It has been shown that pile shaft resistance is a function of the following parameters (Seidel et al., 1996):

- rock strength (drained intact and residual strength parameters are used);
- rock mass modulus (and Poisson's ratio);
- socket roughness;
- socket diameter;
- hydrostatic pressure of concrete at the socket wall; and
- construction practices.

ROCKET accounts for all of the above parameters, with the exception of the last which is currently being investigated. The program predicts the complete shear-displacement (t-z) response of a rock socket.

2.1 The Monash Roughness Model

A major obstacle in the pursuit of a more rational method of side resistance prediction was overcome when Seidel (1993) developed the Monash roughness model. Seidel proposed that a two dimensional roughness profile can be characterised by a series of interconnected line segments or chords of a constant length as shown in Figure 4. The slope of each chord can be determined and a frequency distribution of chord angles produced.

As is the case with natural rock joints, rock socket roughness has been found to produce a normal distribution

of chord angles. Using the Monash model, the mean height of the asperities which comprise the profile can be evaluated at any particular chord length. This is known as the *mean roughness height*, $\overline{\Delta r}$.

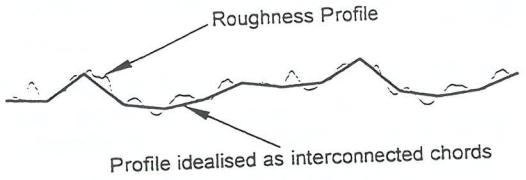

FIGURE 4. Roughness profile idealised as a series of interconnected chords (after Seidel, 1993).

The roughness of a socket profile can be approximated using a range of chord lengths. The shorter the chord length used, the greater the level of detail captured. Small scale roughness will influence socket side resistance at small displacements, while side resistance at large pile settlements is affected by roughness at a larger scale. Mean roughness height can be calculated for any chord length from the standard deviation of chord angles. Ultimate shaft resistance has been shown to be dependent on the maximum mean roughness height which is present in a socket (Seidel et al., 1996)

3.0 THE SOCKET RESISTANCE COEFFICIENT

On the basis of a parametric study using the *ROCKET* program, Seidel et al. (1996) developed a simple method of predicting the peak unit side resistance for a rock socket. They proposed a non-dimensional parameter known as the Shaft Resistance Coefficient, *SRC*.

The *SRC* is computed as follows:

$$SRC = \frac{E_m}{q_u} . \frac{\tan \overline{\alpha} . l_a}{D_s} = n . \frac{\overline{\Delta r}}{D_s} \qquad (5)$$

where n is the modular ratio (E_m/q_u);
$\overline{\Delta r}$ is the mean roughness height; and
D_S is the socket diameter.

The *SRC* factor incorporates all parameters that significantly influence socket resistance. Only the Poisson's ratio and the initial hydrostatic concrete stress are not incorporated, however, these parameters have been found to have a secondary influence on shaft resistance (Seidel et al., 1996).

Seidel and his co-workers conducted a parametric study using *ROCKET* to develop a shaft resistance design chart which allows preliminary estimation of shaft resistance over a wide range of rock strengths. Figure 5 shows the *SRC* design chart. They demonstrated that the adhesion factors predicted using the *SRC* design chart, are in good general agreement with international databases of rock socket load tests.

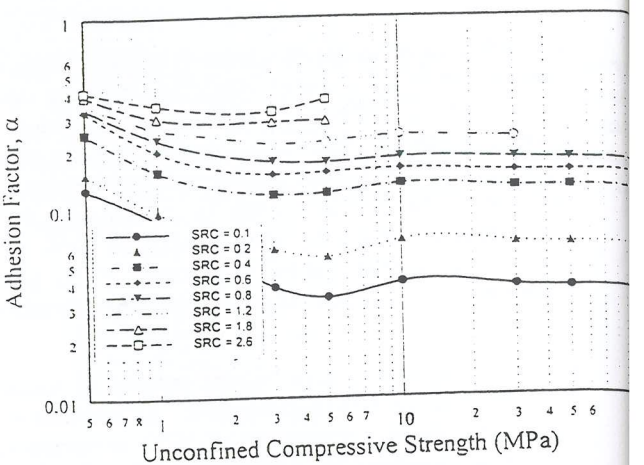

FIGURE 5. Effect of *SRC* on socket adhesion factor (Seid et al., 1996)

4.0 DEVELOPMENT OF A SOCKET ROUGHNESS DATABASE

Application of the *SRC* method or *ROCKET* in desi requires estimation of likely socket roughness heig Despite widespread recognition of its significance, f studies have addressed the production of socket roughn during construction. Although a great many rock soc load test results have been published, few accounts inclu sufficient information relating to borehole roughness allow meaningful interpretation of their results.

The *SRC* provides a simple means of re-analysing load t results in consideration of all major parameters. When parameters E, q_u, D, and α are reported or can reasonably estimated, the mean roughness height, $\overline{\Delta r}$, be evaluated.

Using the *SRC* Design Chart shown in Figure 5, from th value observed in a load test and a representative value uniaxial compressive strength, q_u, the *SRC* which apparent for the socket can be evaluated. From Equatio the effective roughness height can then be calculated as:

$$\overline{\Delta r}_e = \frac{SRC \times D_s}{n} \qquad (6)$$

This allows a quantitative assessment of the contributio socket wall conditions to be made from existing load results, for which socket roughness observations were recorded.

It is necessary to make the distinction between meas socket roughness, and back-calculated values that reflect other factors, such a socket cleanliness, which influence pile response. Consequently, the term *effe roughness height*, $\overline{\Delta r_e}$, is introduced for back-calcul values of $\overline{\Delta r}$.

As part of research into the effect of construction prac on the capacity of rock socketed piles at Monash Unive a load test database has been compiled. Unlike databases previously published such as Rowe and Arm (1984) and Kulhawy and Phoon (1993) which are prim

concerned with side resistance as a function of rock strength, the Monash study aims to consider the full range of parameters which influence shaft resistance. Consequently, the database contains all available details of rock properties, construction techniques, socket roughness and cleanliness, and load test results.

The database currently contains 137 records of load tests carried out worldwide, many of which were addressed in previous empirically based studies. Piles constructed in a variety of rock types are represented, including shale, mudstone, sandstone, chalk, limestone, and schist. The database includes sockets constructed under bentonite, as well as artificially roughened sockets. However, only the results from 93 load tests on unroughened sockets drilled without the aid of a slurry are presented herein. These will be referred to as *conventional* sockets.

The development of the *SRC* design method has allowed the re-analysis of these load tests, in consideration of all relevant parameters. Using the method detailed in this section, the effective roughness height apparent in each load test was able to be back-calculated, and a database of effective socket roughness has been compiled.

4.1 Back-calculated Effective Socket Roughness

Figure 6 shows normalised effective roughness heights back-calculated from the 93 load tests on conventional rock socketed piles. Data points shown as triangles represent load tests in which failure was not achieved. The effective roughness height active in these sockets is therefore greater than or equal to the value plotted.

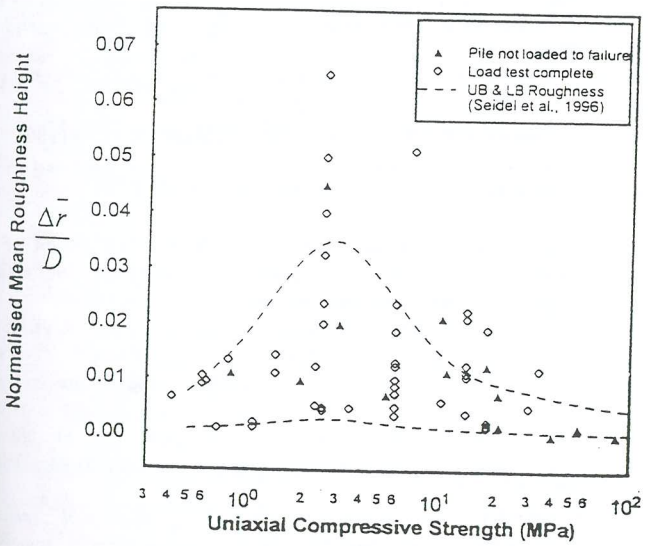

FIGURE 6. Back-calculated effective roughness height versus rock strength

The data shown in Figure 6, supports the observations of Kulhawy and Phoon (1993), and roughness recommendations made by Pells et al. (1980) and Kodikara et al. (1992), that sockets in low strength and high strength materials generally exhibit low roughness, while in intermediate strength rock roughness varies widely. Based on such observations, Seidel et al. (1996) proposed upper and lower socket roughness bounds prior to this study. These are also shown in Figure 6. The proposed bounds have been normalised against the range of socket diameters used in the study, and are in reasonably good agreement with the back-calculated data.

A number of data points in Figure 6 indicate extremely high levels of normalised roughness (ie. normalised roughness greater than 0.04). Examination of the source of these points shows that they are attributable to sockets which were constructed using manual excavation techniques or in extremely jointed rock (Webb and Davies, 1980; Williams and Ervin, 1981). Both these factors would be expected to produce extremely rough sockets. These outliers therefore support the validity of the method of analysis used.

The size of the database is not currently sufficient to properly assess the influence of factors such excavation technique and rock fabric on roughness production. This may be possible once additional historical data is incorporated. However, the records of many load tests do not include enough information concerning construction methods and geology to allow meaningful interpretation.

4.2 Comparison with Measured Roughness Data

Figure 7 shows measured roughness from a number of sockets varying from 300 to 1500 mm in diameter, along with the proposed roughness bounds of Seidel et al. (1996).

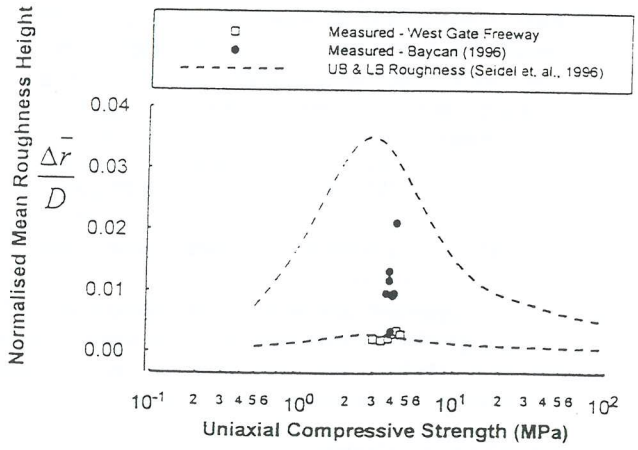

FIGURE 7. Measured socket roughness.

The measured data is limited to argillaceous rock of 3 to 5 MPa uniaxial compressive strength. However, this is within the range of rock strengths at which roughness has been observed to be most variable. The spread of the measured data is similar to that apparent in the back-calculated data of Figure 6, providing further support for the validity of back-analysis using the *SRC* method and Seidel's proposed roughness bounds.

4.3 Discussion

The level of roughness variation shown in Figures 6 & 7 is significant in terms of its influence on available side resistance across the entire rock strength range, but this particularly so between 2 MPa and 12 MPa uniaxial compressive strength. The implication of this finding is underlined when it is considered that the majority of sockets are installed in rock of low to medium strength, due to its drillability and generally good load bearing capacity (O'Neill et al. 1995). This may be particularly true in the U.S.A., where a strong market for bored piles exists (Ibid). Therefore, the benefits of understanding socket roughness production are significant, and justify considerable research effort.

The upper and lower bound roughness guidelines proposed by Seidel et al. (1996) are currently used with *ROCKET* in commercial practice, to evaluate the likely range of side resistance response. For piles in formations where sufficient roughness data has been collected, for example Melbourne mudstone, reliable *ROCKET* predictions can be made. However, there remains considerable scope for improved socket roughness guidelines covering a range of geological conditions and construction techniques.

5.0 FIELD INVESTIGATION OF SOCKET ROUGHNESS

Monash researchers have developed a socket profiler to remotely measure the roughness of rock socket sidewalls in the field. Known as the *Socket-Pro*, the device is capable of accurately profiling sockets in the dry or under water and drilling mud. It is operable in sockets of 600 to 1800 mm diameter, and to depths of up to 60 metres. The *Socket-Pro* incorporates a fully automated down-hole profiler, which is serviced from trailer mounted winching, control and data acquisition equipment at the surface. During measurement, roughness data is relayed in real time to logging equipment at the surface.

The *Socket-Pro* will be deployed on construction projects to take direct measurements of field socket roughness. Geological conditions and relevant construction practices such as drilling technique will be recorded, and correlated with the measured roughness. The results will be used to develop roughness guidelines for use in design. The *Socket-Pro* can also be used to verify design assumptions after construction commences.

6.0 CONCLUSIONS

In order to significantly reduce the need for conservatism in rock socket design, a design approach must be adopted which takes all influential parameters into account. *ROCKET* incorporates such an approach, but its ability to enhance predictions is limited by the quality of input parameters.

To maximise the potential of *ROCKET* as a design tool, a sound understanding of socket roughness is required. If design certainty is to be significantly improved, designers must be able to reasonably predict roughness from a knowledge of site geology and construction method. present, insufficient roughness data is available to pr more than approximate guidance.

The *SRC* design method provides a simple means of b calculating effective socket roughness from pile load results. This has allowed more meaningful interpretatic historical data. The back-calculated roughness presented in this paper has quantitatively confir previous observations of socket roughness, and highli the need for better understanding.

Socket roughness has been shown to be particularly vari in low to medium strength rock. As a large proportio rock sockets are installed in formations falling into category, the benefits of understanding socket roughness expected to be significant and wide reaching.

Monash researchers will shortly commence a fi investigation using the *Socket-Pro*, aimed at compilin comprehensive socket roughness database. The results the study are expected to make a significant contributio enhancing rock socketed pile efficiency.

7.0 REFERENCES

Horvath, R.G., Kenney, T.C. and Kozicki, P. (1983). *Meth for Improving the Performance of Drilled Piers in Weak R* Can. Geot. Jnl. Vol. 20, 1983 : 758-772.

Johnston I.W. (1977). *Rock-socketing down-under.* Cont Journ. 279 : 50 -53.

Kodikara J.K., Johnston I.W. and Haberfield C.M. (19 Analytical predictions for side resistance of piles in r Proceeding 6th ANZ Conf. on Geomechanics, 1992.

Kulhawy F.H. and Phoon K.K. (1993). *Drilled shaft resistance in clay soil to rock.* Proc. Conf. on design performance of deep foundations: piles and piers in soil and rock. Geotechnical special publication No. 38, ASCE: 172 - 18

O'Neill M.W., Townsend F.C., Hassan K.M., Buller A. and C P.S. (1995). *Load transfer for drilled shafts in Intermedi Geomaterials.* U.S. Department of Transportation, FHWA-R 95-XXX Draft report, January, 1995.

Pells P.J.N., Rowe R.K. and Turner R.M. (1980). *experimental investigation into side shear for socketed piles sandstone.* Proc. Int. Conf. on Struct. Founds on Rock, Sydn 1980.

Rowe R.K. and Armitage H.H. (1984). *The design of p socketed into weak rock.* Report GEOT-11-84, University Western Ontario, London, Canada.

Seidel J.P. (1993). *The analysis and design of pile shafts in w rock.* PhD Dissertation. Dept. of Civil Engg., Monash Universit

Seidel J.P. and Haberfield C.M. (1994). *A new approach to prediction of drilled pier performance in rock.* Proceedings of U.S. FHWA "International Conference on Design Construction of Deep Foundations", December 1994, Orlan Florida.

Seidel J.P. and Haberfield C.M. (1995). *The axial capacity pile sockets in rocks and hard soils.* Ground Engineering, Ma 1995.

Seidel J.P, Gu, XF; Haberfield C.M. (1996). *A new factor the improved prediction of the resistance of pile shafts in rock.* ANZ Conference on Geomechanics. *Adelaide, July, 1996.*

Williams A.F.. (1980). The design and performance piles socketed into weak rock. PhD Dissertation. Dept Civil Engg., Monash University.

AUTOMATION OF TRADITIONAL GEOTECHNICAL INSTRUMENTATION

M.W.Crawford
Geotechnical Systems Australia Pty. Ltd., Bayswater, Vic., Australia

SUMMARY : The rapid growth in automation of traditional Geotechnical Instrumentation is causing new technologies to be used in conjunction with standard traditional applications. Instant access to information about a particular monitored site makes automation an attractive proposition.

In order to understand the developments of instrument automation, the paper will discuss automation generically and then focus on how existing probe extensometers were automated to a user's specifications. The development of Geotechnical Systems Australia Pty.Ltd.'s AMEC (Automatic Magnetic Extensometer Controller) system illustrates a working example of a traditional instrument, in this case a probe extensometer, undergoing the metamorphosis of automation.

1 GEOTECHNICAL INSTRUMENTATION

The need, use and application of Geotechnical Instrumentation has created a highly specialised field of its own within the broad spectrum of Geotechnical Engineering. In order to gain a better understanding of the behaviour and conditions of a particular field site, engineers employ the appropriate instrumentation.

A Geotechnical Instrument can be defined as a device that measures and monitors geotechnical parameters, in the field, relative to the initial reading upon installation. Typically the parameters are displacement, pressure and temperature which can be redefined from an engineering perspective, as stress, strain and shear. To measure these parameters instruments rely on various types of optical, mechanical, hydraulic, pneumatic and electrical transducers.

The most attractive feature of Geotechnical Instrumentation is that it monitors what is actually happening on site. It is therefore extremely important that an instrument be reliable in producing an output of high repeatability and resolution. The vital information provided by these instruments can be interpreted in many ways, ultimately assisting in project design, management and safety.

Instrumentation, however, is only of benefit if the user is clear about the instrument's application. Selection of suitable instrumentation requires that the user :

- Knows geotechnically what is trying to be achieved.
- Knows which geotechnical parameters are to be assessed.
- Can roughly predict the magnitude of change in relation to the operating range of the instrument.
- Pre-determines the location of the instrument taking into consideration existing and future hazards.
- Is aware of installation procedures.
- Is aware of instrument's limitations.

2 DEVELOPMENTS IN INSTRUMENTATION

The development of Geotechnical Instrumentation is an ongoing process. Although the basic operating and measurement principles of the instruments have not changed with time, the applications and variety have.

Initially instruments were simple in operation and application. They were very expensive, sporadically reliable, were of poor resolution and from a reading perspective were manually exhaustive. These instruments also required well-trained technicians to operate the systems to obtain a reading. To some users these apparent deficiencies are only of minor concern. To the greater majority they are totally unacceptable.

The market demands instruments to be of a high quality. As such, users play a significant role in the development of Geotechnical Instrumentation. Often products custom built by a manufacturer to meet a client's particular specifications have been further developed to the point

where the once state-of –the-art instrument has now become a standard off-the-shelf item. Since the user constantly wants instruments that are better, easier to use and cheaper, it is up to the manufacturer to supply. A healthy, cooperative relationship between user and manufacturer is vital to the development of new instruments.

Without doubt the advent of computer technology and complex electronics have made the largest impact on Geotechnical Instrumentation. Instrumentation parameters are being constantly stretched, even redefined, with most instruments now being able to provide an electronic output. Where instruments once had to be read with dial gauges, they can now be accurately read with electronic readout devices.

The most useful contribution associated with computer technology has been the introduction of data acquisition systems. These systems automate instrumentation allowing vast quantities of instrument data to be monitored, logged, analysed and finally presented in an easy to understand format. Geotechnical Instrumentation is finding itself immersed in a new frontier that is being driven by the user demands of wanting more but physically doing less.

3 AUTOMATED GEOTECHNICAL INSTRUMENTATION

3.1 Datalogging

The automation of Geotechnical Instrumentation is steadily creating an environment where users will have full access to all on-site information at their fingertips. To be able to have vast quantities of data displayed in a graphical form at the press of a button is highly attractive to any user.

In the most straightforward cases, instrument automation consists of an instrument with an electronic output capacity connected, usually by hardwiring, to a datalogger. It is the datalogger that allows intelligent automation to take place. In the last 10 years dataloggers have progressed enormously. They are capable of monitoring all types of sensors associated with temperature, frequency, pressure, period, flow, voltage, strain, current and resistance, as well as digital functions outputs. Depending upon sensor types, a datalogger can typically monitor 10 sensors, but can be expanded to cater for 100 sensors. The actual storage capacity of some dataloggers is 30 000 individual readings that can be further increased to 1 000 000 readings if used in conjunction with a memory expansion data card. The data from all dataloggers is readily downloaded into a spreadsheet format, where it can then be more closely scrutinised and manipulated.

3.2 Datalogger Software

The various software packages associated with dataloggers have been constantly revised in order to make a product more user friendly. The improvements in both dataloggers and software have created systems capable of performing functions of higher complexity than just simply recording data to memory.

Many sensors require calibration and scale factors to b applied to the raw data output in order to obtain readings i engineering units. Software allows these factors to b applied automatically and can also allow the user to appl various statistical evaluation techniques to the data; fo example calculating and displaying the average of th output readings. The most powerful feature associated wit the software is being able to raise event-triggered alarms These allow the logger to make logical decisions based o whether a particular event is true or false. The alarm ca then be implemented to initiate functions such as increasin the logging rate, read a second instrument or even activat another system (e.g. pump system).

Graphical or virtual interface software is starting to replac the traditional line command software. In the past lin command software meant that a whole new language had t be learned prior to programming a datalogger. Learning th system software was very time consuming and even writin a simple program proved to be an arduous task. However the introduction of graphical software allows new users t use and configure dataloggers more easily, quickly an confidently.

3.3 Remote Automation

The greatest time and cost savings associated with automating instrumentation is that a remote site many kilometres away can be easily and quickly accessed. In many cases Geotechnical Instrumentation is located in very difficult to physically access regions, or a vast quantity of instruments to be monitored are spread over a large area. Using a remote automation system means that all instruments can be read, or recorded data downloaded, at one conveniently accessed location.

The simplest way to network instruments is to hardwire them all at a central location to a datalogger. Understandably not all sites allow hardwiring of instruments. In many cases the distance between instrument and datalogger makes hardwiring not feasible. To counter this radio and telephone modems provide a more than suitable alternative.

Telemetry automation of Geotechnical Instrumentation is a popular alternative. A fully automated telemetry system can be configured so that a particular event (e.g. flooding in a monitored flood plain) triggers a message is sent via modem to a designated number, to confirm the event occurrence. By using a telemetry system such as this an event hundreds of kilometers away can be almost instantly accessed and assessed by personal computer.

3.4 Advantages and Disadvantages

The advantages and disadvantages of automating geotechnical instrumentation are summarised below.

Advantages.

- Fast and easy to use with almost instant access.
- Reduces the need for manual reading therefore saving time and money.
- Gives an option to increase frequency of data collection.
- Can be left alone and read/downloaded as required.
- Can monitor instruments in regions of difficult access.
- Can monitor a large number of instruments over a large area in a short time.
- Easily networked.
- Easily powered including solar power option.
- Can be set to trigger other electronic systems.
- Reduces reading discrepancies associated with individual user collections of data.
- Easily adapted to suit previously existing electronic instrumentation that was manually read.

Disadvantages.

- Initially very expensive.
- Difficult to set up, usually requiring experienced personnel to install.
- Requires user to be fully familiar with system.
- Reduces user awareness, such that an instrument may be faulty for months without being noticed until downloaded.
- Reduces physical inspection of site conditions.
- Can be prone to total data loss.

4 EXTENSOMETER APPLICATION AND BACKGROUND

4.1 Extensometer types

The generic term extensometer covers a broad range of geotechnical instruments. Essentially an extensometer can be simply defined as being an instrument that measures and monitors differential movement between a minimum of two points. The applications of the various extensometers and their hybrids are enormous. Although in some applications highly complex instruments are utilised, the basic operation concept still remains. Extensometers can be easily categorized into three groups, they being : surface extensometers, borehole extensometers and probe extensometers.

4.2 Surface Extensometers

Surface extensometers as the name implies, measure the change in movement between two points on a given surface, such as ground surface or even the surface of a particular structure or excavation. Surface extensometers once were further divided into two categories; crack monitors and convergence monitors. Logically a crack monitor measures the expansion between two fixed points as opposed to a convergence monitor that measures contraction between the points. However, the development of extensometers has meant that many instruments are quite capable of performing the dual role of a crack and convergence monitor. An excellent example of a surface extensometer is a tape extensometer.

In many cases surface extensometers can be easily automated by linking to a data logger providing the instrument is capable of producing an electronic output. In general surface extensometers are relatively cheap, easy to install and are quite often reusable.

4.3 Borehole Extensometers

Borehole extensometers consist of steel rods or wires, which are anchored at specific levels within a borehole. As movement occurs within the borehole, the relative positions of the rods/wires change. The changes are determined with respect to the instrument's collar head, which is used as a datum. The physical measurement changes can be measured manually using calipers or an electronic readout provided the extensometer head is designed by the manufacturer to provide a suitable output. Once an extensometer has an electronic output capability it can easily be automated by linking it to a data logger.

The maximum number of anchor points to be measured is dependent upon the length and diameter of the borehole in which the instrument is to be inserted. In most cases anchor capacity is restricted by the particular instrument manufacturer's extensometer specifications.

The difference in operation between the wire and rod extensometers is that wire extensometers operate on the basis of measuring axial movement within the borehole using either springs or complex pulley systems to keep the wire between the anchor and head in tension. The rod extensometers rely on the tensile spring nature of the steel rods to maintain tension between the anchors and head. Each of the extensometers has their own advantages and disadvantages. Rod extensometers have been used to measure over 200m with a rod extension range of 0-150mm. They are easily installed and transported and can also be installed horizontally and vertically inverted if desired. Rod extensometers usually have a monitoring capacity of 6 anchors and over long depths have a very limited ability to accurately monitor borehole settlement. Wire borehole extensometers can measure over 500m with an extension range of up to 4m and can monitor up to 20 anchors. Since wire extensometers employ complex wire tensioning techniques they are quite expensive and require extreme care when installing. In most cases installation by the manufacturer is recommended. Both borehole extensometers can readily be automated.

4.4 Probe Extensometers

Probe extensometers operate by allowing anchors to slide along a central access tube, loosely sheathed in a collapsible outer tube, within a borehole. The anchors which are usually spring loaded are placed at the critical points to be monitored within the borehole. The anchors are free to move with the vertical settlement or heave associated with the adjacent-to-the-borehole soils. Once the anchors, access tube and collapsible outer tube are placed, a probe with an attached tape is fed down the central access tube. Each anchor consists of a material that triggers an audible alarm within the probe. If a magnetic sensing reed switch is used the triggering anchors will contain magnets but if an inductance type probe is used the triggering anchors will contain stainless steel rings. To use the magnetic probe as an example, once the magnetic sensitive probe enters the magnetic field produced by the target, the audible alarm is triggered and the corresponding depth is read from the tape. It is extremely important that this depth is referenced to a surveyed datum.

The advantages of probe extensometers are their relatively low cost, ability to monitor an infinite number of anchors, easy to install and are capable of monitoring up to 2m of anchor displacement in either direction (settlement or heave). Although the depth range of a probe extensometer is about 100m, the real disadvantages are associated with the precision in readings due to the instrument being quite labor intensive.

The need to automate probe extensometers in an effort to increase precision and repeatability and eliminate the manual operation became apparent. However, a reliable instrument to perform this task has not yet been available.

5 HONG KONG APPLICATION

5.1 Brief history and site overview

Hong Kong's Kai Tak Airport currently deals with 28 million passengers a year and as a result suffers from an overburden on existing services. In order to satisfy Hong Kong's extreme air traffic congestion and maintain its status as the pivotal trade focus in Asia, Kai Tak Airport will make way for a new airport at Chek Lap Kok island which is 25kms west of Hong Kong's Central Business District. The Airport Authority of Hong Kong (AAHK) oversees the current construction of the new airport, which is considered to be one of the largest construction projects worldwide.

The airport platform was created by removing the top off Chek Lap Kok island, reclaiming 75% of the platform mostly from the sea and capping the entire area with a 2 metre layer of compacted sand or completely decomposed granite and in effect joining the island of Chek Lap Kok with Lam Chau island (see Figure 1.). The airport occupies 1248 hectares. Prior to any filling taking place it was necessary to dredge the soft marine muds from the site in order to reduce settlement. The dredge level of the mud had to satisfy a minimum cone resistance (q_c) of 500 KPa, equivalent to an undrained shear strength of about 25Kpa. The reclaimed part of the site consists of a combination of the mined Chep Lap Kok and Lam Chau islands, importe rock and marine sands obtained from nearby contracts an marine sands obtained from nearby designated borro areas. The remaining 25% of the platform lies on th levelled granitic base of the original islands of Chep La Kok and Lam Chau. The reclamation is protected by a se wall consisting of up to 5 tonne in mass of Chek Lap Ko blasted rock. The compacted sand/decomposed granite ca is separated from the fill material using a geotexti separator.

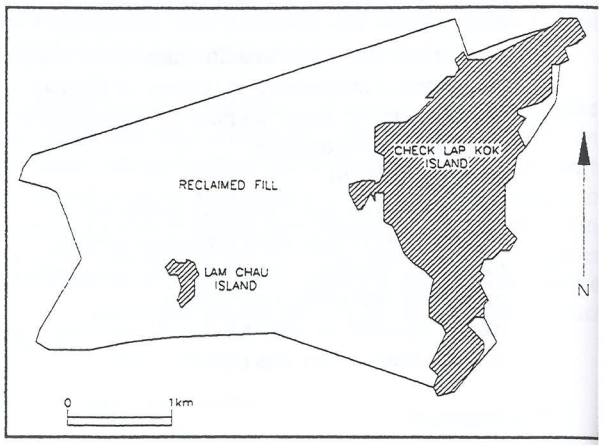

(Figure 1. Hong Kong Airport Platform)

5.2 Settlement

Settlement with respect to the reclaimed platform is a issue of much debate. Initially settlement estimates, base upon an analytical evaluation of the platform, wer between 1-1.5metres. As construction has progresse settlement predictions have been monitored to check th settlement predictions.

As outlined earlier, the platform comprises of various fill and existing material. These vary from solid rock to up t 20 metres of reclaimed fill overlaying 30 metre beds o lightly overconsolidated alluvial sediments. In some regions of the platform bedrock is at depths of up to 6 metres. Understandably the various fills during the completion of construction phases have been placed a different times. As a result different stages of settlement are experienced on the platform at any given time. This i compounded by the fact that the various fill material type will also have differing stiffnesses further affectin consolidation, compression, creep and ultimatel settlement.

5.3 Instrumentation

AAHK's observational approach to settlement meant tha instrumentation was to play a leading role in understandin the issues regarding the settlement of the platform. To gai a clear insight of the total settlement profile, subsurface instrument clusters and surface monitoring points have been used. The clusters were placed specifically, takin into account geology, settlement prediction and the planne positions of temporary and permanent structures. Eac cluster typically comprises of a Sondex (inductance extensometer and to a lesser extent magnetic extensometer

together with a combination of pneumatic, vibrating wire or Casagrande piezometers. The settlement rate, particularly of the alluvial deposits, can be measured taking into account excess pore pressure and pore pressure dissipation rates determined by the piezometers and comparing these with the settlements obtained from the extensometers.

The data obtained from the instrumentation is placed into a spreadsheet program where it is appropriately 'massaged' and stored. Of the 60 existing instrument clusters it is anticipated that 20-25 of these will be retained. Ideally these retained clusters are to be automated in order to provide and create a unique database showing the settlement behaviour of the reclamation fill materials within the platform.

5.4 Existing Magnetic Extensometer System

Each cluster is arranged so that the Sondex extensometer acts as the central instrument surrounded by three to four piezometers within a 20 metre radius. About half of the clusters include a magnetic extensometer placed next to the central Sondex extensometer. On average a space of 400-500 metres exists between the clusters. In regions where greatest settlement is envisaged the cluster spacing is reduced to about 200-250 metres.

The operation of magnetic extensometers is relatively simple. The ring magnets slide along a central access tube (ϕ70mm O.D., ABS) and within a collapsible outer tube. The magnets act as targets and are fixed within the borehole, using spring supports, at locations where expected movement is to be monitored. The central access tube, collapsible outer tube and targets are all installed then backfilled with a bentonite/cement grout and gravel fill. During installation all extensometers had a datum target placed at a minimum of 2 metres into Grade III rock. The extensometer boreholes are up to 90 metres deep with up to 11 target points. The location of the targets is determined by using a magnetic probe, connected to a tape, which is then lowered through the central access tube. Each magnetic target triggers an audible probe signal whereby the depth of the target can be measured from the tape relative to the top of the extensometer central access tube.

The readings are taken manually and are then placed in a spreadsheet format. Data and data plots are then presented in the following ways :

- Accumulated settlement against depth for all survey dates.
- Accumulated settlement for all targets against time.
- Absolute settlement of any one target against time.
- The distance between any two targets plotted against time.

5.5 Automation of Magnetic Extensometer

It has been AAHK's plan to continue monitoring well into the operational phase of the Airport. Understandably the access to the instrumentation clusters would be extremely limited given the obvious frequency of aircraft activity expected within the settlement monitored region. To address this problem it has been proposed to employ an automated settlement monitoring system. However, of all the instrumentation in current use, only the vibrating wire piezometers can be readily adapted to remote automation. Historically there has been no evidence of a fully functioning magnetic extensometer with automative capabilities.

6 AMEC SYSTEM

6.1 Description

The Automatic Magnetic Extensometer Controller (AMEC) is, as the name implies, an automated magnetic extensometer. Currently conventional magnetic extensometers operate by manually lowering a calibrated sensor and cable assembly down a borehole to detect magnetic targets positioned at various depths. To enable regular and repeatable long term measurements, at a site with limited accessibility, an alternative to manual measurement had to be found. Therefore, an automated magnetic extensometer was developed to meet the perceived needs of long term, repeatable and high resolution measurement.

The new airport being built in Hong Kong was the catalyst in creating AMEC. With many manual magnetic extensometers already in operation, the need to automate for the future was apparent. AAHK wanted to make use of the existing boreholes with magnetic targets, therefore a system had to be designed to conform with and utilise what was already in place. As no such automated system existed, the challenge, to create a state-of-the-art automated magnetic extensometer, evolved. It was an Australian company, Geotechnical Systems Australia Pty. Ltd., that designed a system satisfying AAHK's requirements.

6.2 Development

AMEC took 6 months to design. The initial design parameters were emphasised by AAHK and as a result, it was important that AMEC satisfied the following criteria.

- Make use of the existing magnetic extensometer installations.
- Be fully automated.
- Have a remote power supply.
- Able to be controlled and monitored via a personal computer.
- Output to be expressed in text file format to be easily imported into a spreadsheet file.

6.3 Finished Product

AMEC consists of four distinct parts; sensor assembly, measurement assembly, enclosure and power module (see Figure 2.).

The sensor assembly allows a maximum of 8 sensors to be suspended in close proximity to specific targets. During the measurement cycle, sensor outputs are continuously interrogated and each of their trigger points is logged against the vertical displacement of the head assembly.

The measurement assembly's on-board microprocessor manages all measurement, control and data storage processes. These include sensor monitoring, displacement, log time intervals, data storage, data retrieval and transmission, programmable functions, power optimisation and self-diagnostic checking.

The controller is housed inside a cylindrical stainless steel enclosure that is hermetically sealed to IP68 waterproof standard. The enclosure provides access to power and RS232 communication links.

The power module is housed in a powder coated aluminium case sealed to IP68. Powering can be from mains power, D.C. power or internal battery with solar charger.

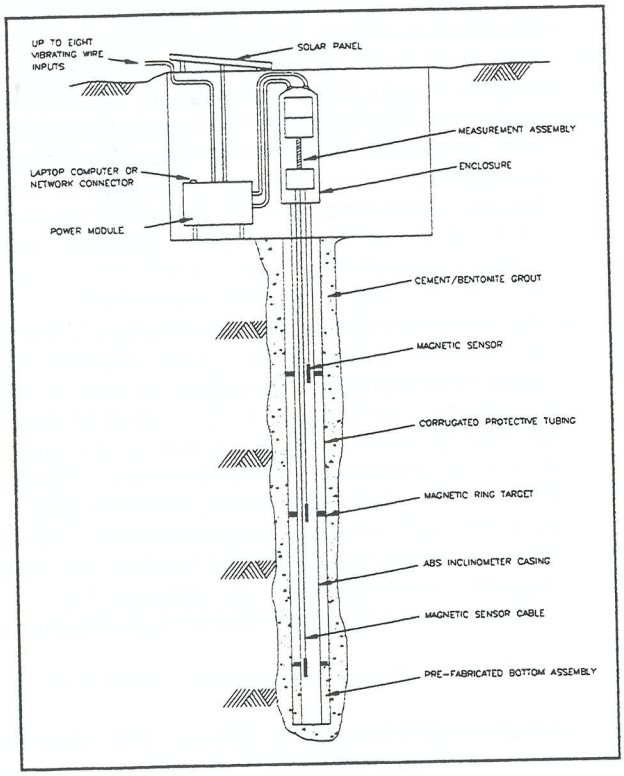

(Figure 2. AMEC Profile)

6.4 Operation

Once fully installed, AMEC is programmed to take readings at a fixed time interval. When operating, the stepper motor, via a threaded drive shaft, slowly raises all 8 sensors at the same time. Each of the sensors contains a reed switch that closes once in contact with the magnetic field created by the magnetic targets within the borehole. The vertical position of the sensor is recorded once the reed switch has initiated a closed circuit (see Figure 3.). The sensor positions, which are measured only during the raising of the sensors, are referenced to the bottom anchor, which is positioned in rock. Once the threaded drive shaft is fully extended, the stepper motor reverses and lowers all 8 sensors back to their initial pre-scanning positions. The sensors are not read during the lowering cycle. If a particular sensor indicates no reading, it means that the amount of either settlement or possibly heave has exceeded the drive shaft's full extension range of 200mm during scanning. Where excessive settlement has occurred, either the borehole casing collar on which AMEC is housed can be cut lower, or new sensors with longer cables may be fitted. For excessive heave sensor cables may be shortened to bring the sensors back into the magnetic field range of the targets.

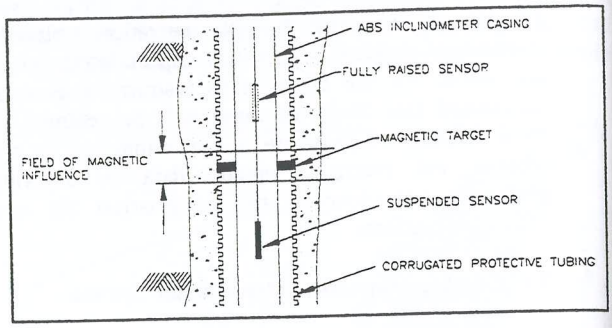

(Figure 3. Operation detail)

6.5 Features

The features of AMEC are:

- It is a stand-alone measurement system.
- Monitors up to 8 targets.
- Has high resolution readings.
- Has non-volatile data storage.
- Can be removed for manual reading.
- Waterproofed to IP68.
- Microprocessor controlled.

The following tables (see Table 1. & Table 2.) detail the physical and electrical specifications of AMEC.

6.6 Installation

The installation of AMEC is a relatively simple process. Prior to installation the depth of the borehole and anchor positions must be known. The sensor cables are cut to the appropriate depth and fixed with locking ferrules to the head assembly. The wires of the cables are stripped and attached to terminals. Once the cables with sensors have been fed down the hole, the enclosure is placed over the head assembly and locked into position. The power module is then fixed into position and communication cables are attached. The system is checked with a personal computer running AMEC through several scans to make sure that a full set of repeatable readings is obtained.

Since AMEC is a new product, installation by the manufacturer is recommended. However, detailed installation and operation manuals accompany each unit.

PHYSICAL SPECIFICATIONS	
Controller:	
Size:	800mm long×ϕ150mm
Weight:	17kg
Material:	Stainless Steel
Sealing:	IP68
Power Module:	
Size:	350mm long×160mm wide×100mm high
Weight:	8kg
Sealing:	IP68
Sensor Cable:	
Size:	ϕ5.1mm
Material:	Polyethylene with nylon jacket
Construction:	4 core, jelly filled
Weight:	2.9kg/100m
Sensors:	
Size:	200mm long×ϕ19mm
Material:	Stainless Steel
Weight:	450gm
Accuracy:	± 0.1mm

(Table 1.Physical Specifications)

6.7 Software

It was important to create a user-friendly software that can be quickly learnt. To achieve this AMEC was designed to work in conjunction with a Windows 95 based custom software interface. With this software the user controls how often and at what time scanning will occur. Each scan is recorded with the corresponding date and time, with displacement relative to the vertical displacement of the head expressed in millimetres. The scanned data can then be downloaded into a spreadsheet file for further analysis. Other software specifications are listed in Table 2., under datalogging and communications.

7 CONCLUSION

The automation of traditional Geotechnical Instrumentation is steadily increasing in popularity amongst users. With the barriers to what can and cannot be automated eroding, the application for instrument automation have been dramatically enhanced.

The development of AMEC has shown the evolution of an automated probe extensometer from conceptual origins to a fully functional system. For AMEC to be an advantageous benefit, cooperation between user and manufacturer (AAHK and Geotechnical Systems Australia Pty. Ltd.) was vital. The result is a state-of-the-art instrument available to the global geotechnical industry.

8 ACKNOWLEDGEMENTS

The author wishes to acknowledge Geotechnical Systems Australia Pty. Ltd. and Cadeanco Pty. Ltd. for their active participation and contribution to this paper.

ELECTRICAL SPECIFICATIONS	
Controller:	
Inputs:	Up to a maximum of 8
Index Accuracy:	± 0.1mm
Index Repeatability:	± 0.1mm
Index Resolution:	0.014mm
System Accuracy:	± 0.5mm
Power Module:	
Mains:	240V, 120V, 50-60Hz, 50Watts Peak (optional)
Battery , D.C. Supply:	Sealed lead acid, 10W Solar charger
Backup:	2 × Sealed lead acid, 12V, 1.2Ah
Data Logging :	
Storage Capacity:	500 measurements of 8 inputs (Inc. Date, Time & Status information)
Data backup:	10 years without primary power
Logger Timing:	Real-time clock, non-volatile operation, 10 year count without primary power
Scanning Intervals:	Choice of scanning intervals from 1hour to daily
Communications:	
Baud Rate:	9600 Baud, 8data, 1 start, 1 stop, no parity
Data Format:	8 Data points, Time, Status data
Data Separator:	Tab separated columns, text format
Data Recovery:	Customized WIN95 Interface Software
Networking:	Optional linking of up to 10 sites for data. Recovery from a single access point

(Table 2.Electrical Specifications)

9 REFERENCES

Dunnicliff, J. (1988), "Geotechnical Instrumentation for Monitoring Field Performance." John Wiley and Sons Inc. New York.

Dunnicliff, J. (1995), "The Practical Use Of Geotechnical Instrumentation : Some Problems and Solutions." Proc. 4th International Symposium on Field Measurements in Geomechanics, Bergamo Italy. 239-256.

Hanna, T.H. (1985), "Field Instrumentation in Geotechnical Engineering." Trans Tech Publications. Clausthal-Zellerfield. Germany.

Ground Engineering/AAHK Chek Lap Kok Supplement (December 1996), Published by Emap Construct. London.

Third A-NZ Young Geotechnical Professionals Conference, Cameron, Collingwood & Slatter (eds), Feb. 1998, Melbourne, Australia.

Case Studies in the Assessment of Rock Mass Criteria

Kurt J. Douglas
Department of Geotechnical Engineering, The University of New South Wales

Summary Various rock mass failure criteria are being validated against field performance as part of a large research program into the geotechnical risk of concrete gravity dams. The project has sought rock structures which may contribute to providing either upper or lower bounds to various failure criteria. The emphasis therefore has been on finding sites with high quality field and laboratory data. This paper summarises the analysis and results of a large pit slope at Kidston Gold Mine, together with a summary of other previously reported cases. The results from the studies allow the field stresses and strengths to be compared with the commonly used Hoek-Brown empirical rock mass failure criterion. As expected, the bounds on the various failure criteria are very broad and care must be taken when placing any reliance on any particular criterion.

1 INTRODUCTION

The author is currently involved with a research project into the risk assessment of concrete dams. A major component of this project is to attempt to validate various rock mass failure criteria against field performance. An extensive literature review has shown that almost all the data supporting the published criteria are laboratory test results from intact specimens, with, in general, very little and often no field validation. Rock mass strength is clearly scale dependent and thus laboratory testing alone cannot be expected to have captured important field characteristics.

The most commonly used strength criterion is the Hoek-Brown empirical rock mass failure criterion. The most general form of which is given in Equation (1). This criterion was developed by Hoek and Brown (1) due to the lack of any available empirical strength criterion. The equation which has subsequently been updated by Hoek and Brown (2) and Hoek et. al. (3) was based on correlations between brittle fracture of intact rock cores and the original Griffith theory (4). The only 'rock mass' tested and used in the development of the Hoek-Brown criterion was 152mm core samples of Panguna Andesite from Bougainville in Papua New Guinea (1). Brown and Hoek (5) later noted that it was likely this material was in fact 'disturbed'. The validation of the updates of the Hoek-Brown criterion have been based on experience gained whilst using this criterion. It is unfortunate however, that to the authors knowledge the data supporting this experience has not been published.

$$\sigma_1' = \sigma_3' + \sigma_c \left(m_b \frac{\sigma_3'}{\sigma_c} + s \right)^a \qquad (1)$$

Due to the difficulty with assessing the parameters in the Hoek-Brown criterion correlations with rock mass rating parameters were developed. The most current of these is the Geological Strength Index (GSI) (6) which is a variation on the rock mass rating (RMR) of Bieniawski (7 and 8) and the tunneling quality index (Q) of Barton et al. (9). These are shown in Table 1. The parameters m_i and m_b are intact and mass material constants; a and s are constants that depend on the rock mass characteristics; σ_c is the uniaxial compressive strength of the intact rock; and σ_1' and σ_3' are the major and minor principal stresses respectively.

	GSI<25	GSI>25
$\frac{m_b}{m_i}$	$\exp\left(\frac{GSI-100}{28}\right)$	$\exp\left(\frac{GSI-100}{28}\right)$
s	0	$\exp\left(\frac{GSI-100}{9}\right)$
a	$a = 0.65 - \frac{GSI}{200}$	0.5

Table 1: Hoek-Brown GSI Strength Parameters

This paper describes some of the authors work in attempting to correlate field data to the Hoek-Brown criterion. Results from several case studies are shown.

2 KIDSTON GOLD MINE

The footwall of the Wises Hill pit, located at Kidston Gold Mine, Queensland, is approximately 240m high. The average slope angle is approximately 48° with a maximum bench height and slope of approximately 36m and 73° respectively. The pit has been successfully mined with no overall stability problems. The pit was chosen for analysis due to its highly

stressed nature. An analysis using the stability program *Slope/W* has been performed and the stresses obtained compared with those output from the Hoek-Brown criterion.

2.1 Rock Parameters

The major rock type in the slope is a very high strength granodiorite breccia. Rock mass parameters were obtained from Coffey Partners International Pty Ltd (10) and line mapping histograms created by Pells Sullivan Meynink Pty Ltd (PSM). Estimates of GSI were derived using RMR_{76}, Q, Table 8.4 in Hoek et. al. (11) and Figure 1 in Hoek (12). The value of m_i for granodiorite was taken from Hoek et. al. (11). The Hoek-Brown parameters are shown in Table 2. Three estimates were made: LB being the lower bound; BE being the best estimate; and UB being the upper bound.

Parameter	LB	BE	UB
GSI (RMR_{76})	77	82	92
GSI (Q)	72	72	73
GSI (Table 8.4)	70	70	85
GSI (Figure 1)	60	65	75
UCS	100	100	120
m_i	30	30	30
a	0.5	0.5	0.5

Table 2: Hoek Parameters for Kidston

As can be seen in Table 2 the value of GSI varies considerably depending on the method used to derive it. The latest approach by Hoek (12) gives the lowest estimate. Indeed, an inspection of this method shows that the highest possible GSI is 80 for a 'blocky structure' with 'very good surface conditions'. Due to this variation it is suggested that those using the criterion make sure they are using the latest update for the estimation of GSI and the Hoek-Brown criterion.

2.3 Slope Stability Analysis

The stability program *Slope/W* was used for the analysis with both Bishop and Morgenstern & Price analyses. The parameters used are shown in Table 3. They were obtained using the Hoek-Brown strength criterion and the solutions derived by Balmer (13) with a linear interpolation of the points in the stress region of interest.

Parameter	GSI=60	GSI=70	GSI=92
m_b	7.2	10.3	22.5
ϕ (°)	67	68	68
c (MPa)	1.2	1.9	6.7

Table 3: Results of Hoek-Brown Analysis (σ_n= 0.8MPa)

It should be noted that the suggested values of minimum principle stress, σ_3, given by Hoek et. al. (11) for use in their spreadsheet are applicable more to highly stressed underground workings than slopes. The high cohesions of rock masses result in negative σ_3 being required to obtain low σ_n on potential failure planes. Users should use stress which yield normal stresses, σ_n, applicable to their proble The values for the cohesion, c, and angle of friction, ϕ, Table 3 assume a normal stress of 0.8MPa. This norm stress was determined iteratively using the slice base norm forces output from *Slope/W* and adjusting the paramete accordingly.

Both a deep failure surface and a shallower failure surfa incorporating only the steeper section of the pit we analysed. For the deep failure surface the slope was modell as three material types with the least stressed upper a lower materials given a slightly lower strength (σ_n= 0.8M used) compared to that of the middle layer (σ_n=1.2MPa).

A further analysis was carried out to assess the effect a joi would have if it occurred at the toe of the slope. This w justified from the line mapping results by PSM whic showed the presence of long joints (5-10% greater than 50m in the region of the toe. To carry out the analysis a zone material with joint strength properties was added in t location of the toe of the shallow failure slip surface. T joint strength properties, of zero cohesion and an angle friction, ϕ, of 40°, were taken from Coffey Partne International (10). The weak 'joint' material was stopp short of the face due to the presence of rock bolting in t face at Kidston.

Tension cracks were added for all analyses at the top of t failure surfaces to limit tension.

2.4 Results

Figures 1, 2 and 3 show the failure surfaces for the dee shallow and joint material analyses respectively. T analyses through the rock masses gave a FOS approximately 6.5. The analysis where the joint region w included yielded a FOS of 4.9. Lower factors of safety we obtained for other surfaces but were rejected due to th shallow nature or excessive tensile stresses between slices.

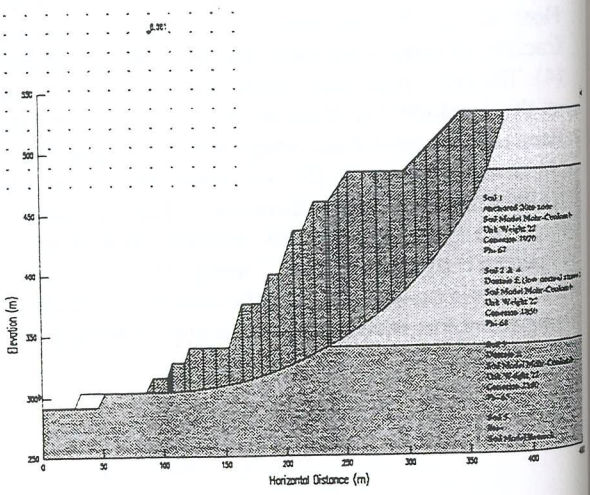

Figure 1: Deep Seated Failure - Kidston Mine

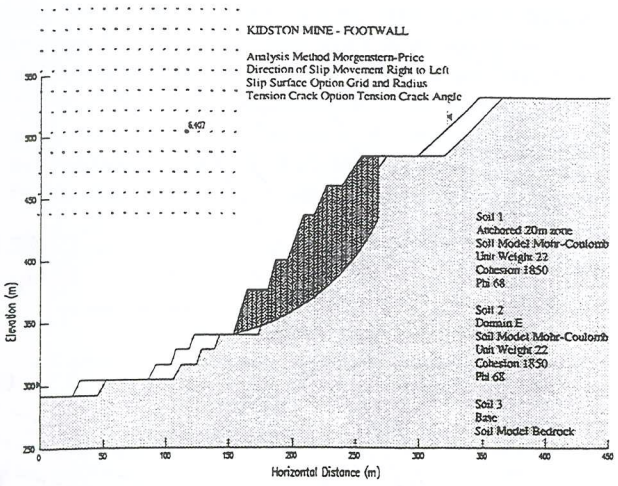

Figure 2: Shallow Failure Surface - Kidston Mine

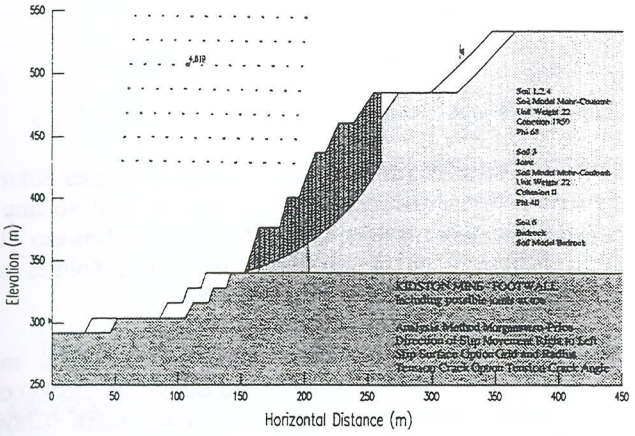

Figure 3: Failure Through Joint Region - Kidston Mine

The slice base normal and shear stresses are plotted on Figure 4 together with the Hoek-Brown criterion curves for the lower bound, best estimate and upper bound GSI values (60, 70 and 92 respectively). Figure 4 shows that although the slope appears highly stressed it does not appear to be a very good bound for rock mass strength.

It is difficult to imagine rock mass behaviour leading to failure for slopes with a high GSI rock mass. Using the best estimate rock mass strengths output by the Hoek-Brown criterion for Kidston a quick analysis with *Slope/W* showed a 70° slope could be over 5000m high without inducing failure.

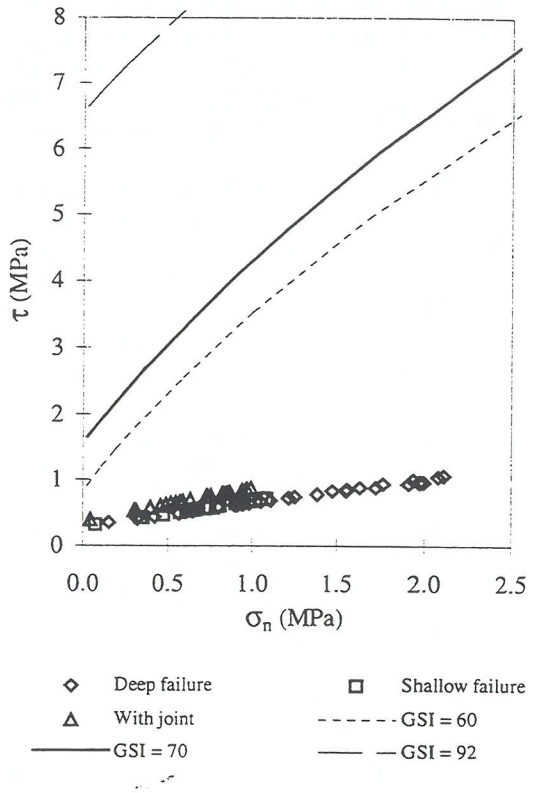

Figure 4: Hoek-Brown vs Stresses for Kidston

3.0 OTHER CASE STUDIES

3.1 Aviemore Dam

Aviemore Dam, a 57m high concrete dam constructed between 1963 and 1968, is located on the Waitaki River, 185km south west of Christchurch, New Zealand. During construction eight large scale in-situ shear tests were carried out on the foundation in order to determine the strength of the concrete/rock interface for stresses relevant to those induced by the proposed dam.

The in-situ tests were carried out on a greywacke rock mass which was closely jointed, veined, and often crushed and sheared. All tests failed through the rock mass, approximately 50-100mm below the rock-concrete contact, involving failure of several defects.

During the tests both the test and reaction blocks failed. Foster and Fairless (14) re-analysed the test results and adjusted the vertical stresses on the test and reaction blocks assuming that vertical forces were transferred from the reaction block to the test block due to differential displacement. The values were adjusted to yield similar τ/σ_n ratios for the reaction and the test blocks. Their results have been adopted as a best estimate of the true failure stresses. By using *UDEC* Helgstedt et. al. (15) found it was possible to validate the assumptions made by Foster and Fairless (14) and thus provide a greater confidence in their results.

The test results are presented in Figure 5 together with the estimated Hoek-Brown envelopes. As can be seen the best estimate Hoek-Brown criterion gave a higher estimate of the rock mass strength compared with the adjusted test values. The failure stresses appear to correspond reasonably to the lower bound estimated Hoek-Brown envelope.

The Hoek-Brown curves derived using the chart in Hoek (6) give a lower estimate of the rock mass strength. The Hoek-Brown curves derived using Barton's Q system give higher estimates than those from Bieniawski's RMR_{89} and the Hoek-Brown chart in Hoek et. al. (11). It appears from the results that the curves derived from the Hoek-Brown chart give the best estimate of the rock mass strength.

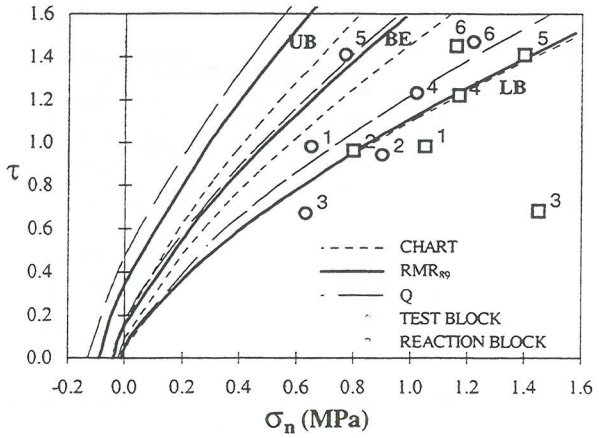

Figure 5: Aviemore In-Situ Shear Test Results

3.2 Chichester Dam

Chichester Dam is a 41m high concrete gravity dam located on the Chichester River, 80km north of Newcastle, NSW. The dam has been heavily investigated with approximately 150 boreholes drilled between 1950 and 1980. As a result of these investigations, the dam was post tensioned to provide additional security against extreme hydrological events.

The parameters used in the analysis are described in detail in Mostyn et. al. (16). The dam foundation was modelled using UDEC. The results from the analysis are shown in Figure 6.

The results from the analysis indicated that a planar wedge failure was the likely failure mode and hence the Hoek-Brown criterion was not applicable. The analysis also showed that the low stresses beneath a dam of this size are not conducive to placing tight bounds on rock mass strength criteria.

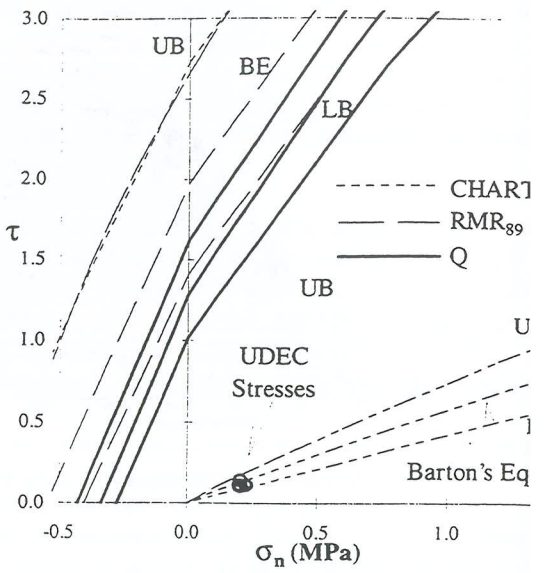

Figure 6: Chichester Dam Results

3.3 Nattai North

The Nattai North escarpment failure is located 80k west of Sydney. The failure, with a total volum million cubic meters and height ranging between 300m, is one of the largest rock mass failures occurred in Australia in modern times.

The conditions at Nattai North are such that competent rock (Scarborough and Bulgo Sandstones) weaker, more fractured strata (Wombarra Cla Together with this, the bedding planes tend to dip slope, resulting in large pillars that are prevente sliding or toppling. These pillars are then supported highly stressed weaker Wombarra Claystone. conditions are believed to be sufficient to cause s through the claystone and failure of the escarpmer believed that the failure was induced by mining of coa beneath the escarpment.

The modelling of the failure was performed using Two series of runs were made, with and without mi described in Mostyn et. al. (16). The GSI was es using the two modified Hoek-Brown criterion classi systems, RMR_{89}, Q and the Hoek-Brown chart given i (6).

The results of the analysis using *UDEC* correlated w the assumed failure mode. In Figure 7 the stresses p at failure by *UDEC* have been compared to those fr Hoek-Brown criteria. It is seen that the Hoek-Brown c gives a higher estimate of the rock mass strength. The stresses appear to correspond reasonably to the lowe estimated Hoek-Brown envelope.

The shear plane for the mining case showed failure both through the area of fictitious joints in the toe of the slope and through the coal seam. As the coal seam would have a different GSI to that estimated the stresses along both zones have been plotted separately. A Hoek-Brown envelope corresponding to a GSI of 25 for a crushed rock mass with fair to poor joint conditions has been plotted (the lowest curve on Figure 7). This envelope appears to correspond reasonably to the failure stresses obtained along the coal seam.

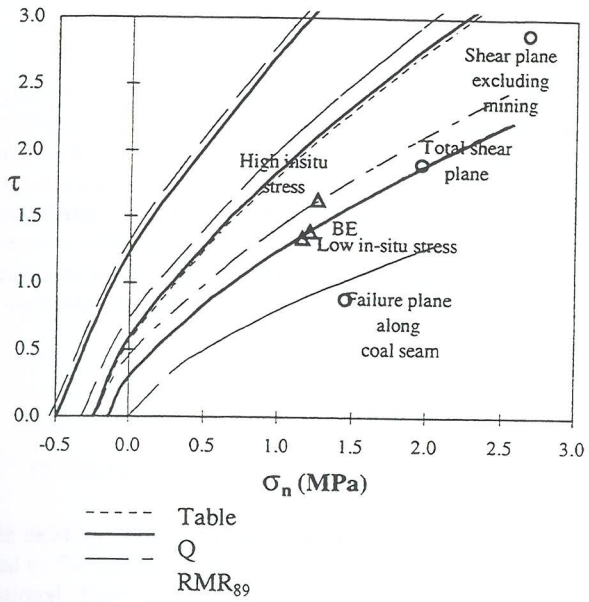

Figure 7: Hoek-Brown vs Estimated Stresses for Nattai

4.0 CONCLUSION

The case studies presented within this paper provide a first step towards a better understanding of the Hoek-Brown failure criterion. Further case studies are currently being analysed and results and conclusions will be presented as they become available. The authors are also involved in investigating the large scale in-situ shear strength of discontinuities. Due to the difficulty of obtaining good case studies on large scale discontinuity failures, only one defect case study has been attempted.

As has been shown in the case of Kidston Mine it is difficult to locate slopes that have failed through rock mass. This is particularly true for rock masses with a reasonably high GSI and/or intact rock strength.

The author would be grateful for any qualitative performance and rock mass characterisation data on rock masses that have failed or are near failure (both mass or defect controlled). If any reader is aware of such information do not hesitate to contact the author.

5.0 ACKNOWLEDGEMENTS

This paper was written as part of a research project into the risk assessment of concrete dams. The project has been supported (both financially and in access to data) by the following sponsors: Australian Water Technologies; Dept. of Land and Water Conservation; NSW Dept. of Public Works and Services; SA Water Corp.; ACTEW; Hydro-Electric Commission; Dams Safety Committee of NSW; Dept. of Land and Water Conservation; SMEC; Dept. of Natural Resources; Rural Water Corp./Goulburn Murray Water; GHD; Melbourne Water; Pacific Power; Water Authority of WA; ECNZ; and the Snowy Mountains Hydro-Electric Authority.

Access to information on mine pit slopes has been provided various mine owners and Pells, Sullivan, Meynink Pty Ltd.

The author was also supported by the Australian Research Council and the Faculty of Engineering at UNSW. The research into rock mass strength is being led by Mr Garry Mostyn. Assistance on the project by Marcus Helgstedt is acknowledged and appreciated.

3.6 References

1. Hoek, E. and Brown, E.T. "Empirical strength criterion for rock masses", J. of the Geotech. Engng Div., ASCE,, Vol 106, No. GT9, 1980, 1013-1035.
2. Hoek, E. and Brown, E.T. "The Hoek-Brown failure criterion - a 1988 update", Proc. Of the 15th Canadian Rock Mech. Symp., Toronto, 1988, 31-38.
3. Hoek, E., Wood, D. and Shah, S. "A modified Hoek-Brown failure criterion for jointed rock masses", Eurock '92, 1992, 209-214.
4. Griffith, A.A. "Theory of rupture", Proc. 1st Congr. Applied Mechanics, Delft, 1924, 55-63.
5. Brown, E.T. and Hoek, E. "Discussion on paper no. 20431 by R. Ucar, entitled: Determination of shear failure envelope in rock masses", J. of the Geotech. Engng Div., ASCE,, Vol 114 No. 3, 1988, 371-373.
6. Hoek, E. "Strength of rock and rock masses", Int. Soc. for Rock Mech. News Journal, Vol 2 No. 2, 1994, 4-16.
7. Bieniawski, Z.T. "The geomechanics classification in rock engineering applications" Proc. 4th Congr. Int. Soc. Rock Mech., Montreux, Vol 2, 1979, 41-48.
8. Bieniawski, Z.T. Engineering Rock Mass Classifications, New York, Wiley, 1989.
9. Barton, N.R., Lien, R. and Lunde, J. "Engineering classification of rock masses for the design of tunnel support", Rock Mech. Vol 6, No. 4, 189-236.
10. Coffey Partners International Pty Ltd, Wises Hill Pit Geotechnical and Hydrogeological Study - Phase II, Report No. Z105/2-AF, 23 April, 1991.
11. Hoek, E., Kaiser, P.K. and Bawden, W.F. Support of Underground Excavations in Hard Rock, A.A.Balkema, 1995, 84-98.
12. Hoek, E. Technical Note: Reliability of Hoek-Brown estimates of rock mass properties and their impact on

design, submitted to the Int. J. Rock Mech. & Min. Sci, 1997.

13. Balmer, G. A general analytical solution for Mohr's envelope, Am. Soc. Test. Mat., Vol 52, 1952, 1260-1271.
14. Foster, P.F. and Fairless, G.J. Waitaki Dam - Review of Aviemore rock strength. (unpublished) ID: 9W551.BO, 1994, Power Engineering Office Works Consultancy Service Ltd (Wellington, N.Z.).
15. Helgstedt, M.D., Douglas, K.J. and Mostyn, G. " evaluation of in-situ direct shear tests Aviemore New Zealand", Australian Geomechanics, No. 37, 1997, 56-65.
16. Mostyn, G., Helgstedt, M.D. and Douglas, K.J. "To field bounds on rock mass failure criteria", Int. J. Mech. & Min. Sci., Vol 34, No.3-4, Paper No. 208, 1

Blanchetown Bridge Geotechnical Investigation

M.L. DUTHY, BE(Hons), PhD, MIEAust, CPEng
Geotechnical Engineer, PPK Environment & Infrastructure Pty Ltd

Summary: A geotechnical investigation for a proposed replacement bridge at Blanchetown, South Australia was carried out. The investigation comprised drilling, coring, field and laboratory testing, analysis, pile testing and reporting. The background to the geotechnical investigation, the investigation methodology and the investigation results are briefly outlined, and a model of the geotechnical profile along the proposed bridge alignment is presented. The main geotechnical issues for the design and construction of the proposed bridge are then discussed. These comprise design and constructability of the bridge pier and abutment footings; slope stability and excavatability of the western bridge approach cutting; use of the excavated material as fill; settlement performance of the eastern bridge approach embankment; and design or construction techniques to minimise the effects of embankment settlement.

1. INTRODUCTION

The existing bridge at Blanchetown, South Australia, carries road traffic across the River Murray. The bridge is located on National Highway 20, about 130 km north-east of Adelaide, South Australia. However, the existing bridge is unable to carry the predicted future traffic loadings and so a replacement bridge is being constructed nearby. Rust PPK Pty Ltd (now PPK Environment & Infrastructure Pty Ltd) were commissioned by the Department of Transport (now Transport SA) to undertake a detailed geotechnical investigation for the proposed new bridge, which comprised drilling, coring, field and laboratory testing, analysis, pile testing and reporting. The background to the geotechnical investigation, the investigation methodology and the investigation results are briefly outlined, and a model of the geotechnical profile along the proposed bridge alignment is presented. The main geotechnical issues for the design and construction of the proposed bridge are then discussed. These comprise design and constructability of the bridge pier and abutment footings; slope stability and excavatability of the western bridge approach cutting; the use of the excavated material as fill; settlement performance of the eastern bridge approach embankment; and design or construction techniques to minimise the effects of embankment settlement.

2. GEOLOGY OF THE AREA

Published information (Geological Survey of South Australia (1), (2)) shows that the site lies within the Murray Basin, which was formed at the beginning of the Tertiary. The oldest geological unit of interest is the Lower Miocene Mannum Formation. This unit is a marl (calcareous shelly sandstone of marine origin) that is expected to be present as a continuous layer at depth across the site area. The marl is massive, fossiliferous and of low strength, and is expected to be over 30 m thick. The marl is overlain by the Lower Miocene Morgan Limestone geological unit. This is a sandy limestone/calcareous sandstone that is also of marine origin, massive, fossiliferous, and of low strength and significant thickness (>15 m).

In areas not subjected to significant erosion, the sandy limestone is expected to be overlain by the Pliocene Norwest Bend Formation, which contains fossiliferous sandstone, limestone, calcareous sand and oyster beds. This formation is in turn overlain by Pleistocene Bakara Soil, which is a soil containing moderately hard, massive sheet or nodular calcrete and fossils. Recent aeolian sands are expected to cover the Bakara Soil and form the existing ground surface west of the cliff tops present on the western side of the River Murray in the general area.

Over the course of many years the River Murray has cut through the Morgan Limestone and into the marl for a depth of tens of metres, and this has resulted in the exposure of these rock strata on the face of the steep cliff that is present on the western (Adelaide) side of the river in the general area.

The relatively flat marl surface that resulted from the previous river scouring was then overlain by more recent sands. This material is likely to represent drift sands deposited by wind and then reworked by river flow. The sands belong to the Recent Monoman Formation. They are present east of the western cliff face to thicknesses of the order of 15 m, though over the existing river width some reduction in thickness due to river erosion is likely. The

sands are fine to coarse grained and relatively loose in general.

Organic clays, silts, sands and muds several metres thick are expected to overlie the riverine Monoman Formation sands and form the surface strata for that part of the river bed within 100-150 m of the western bank. These soils are soft and loose, compressible and saturated and represent the riverine Coonambidgal Formation.

The land beyond the eastern river bank is low lying for a significant distance eastwards and contains a number of lagoons. The Recent surficial soils in this area are also expected to contain several metres of Coonambidgal Formation soils.

Geotechnical information obtained by the Department of Transport (DoT) from the borehole drilling for the original bridge at Blanchetown, though not discussed in this paper, was consistent with the foregoing published information.

3. PROPOSED CONSTRUCTION

The proposed development comprises the provision of a new bridge and associated infrastructure over the River Murray at Blanchetown to replace the existing bridge. The new bridge and associated infrastructure will be similar to the existing bridge and associated infrastructure in its geometry, form and construction, and will be located slightly upstream (20-30 m) of the existing bridge. The proposed development will comprise the following elements:

(1) Western Approach

The western (Adelaide) approach road to the proposed bridge will be cut into the existing land from within about 500 m west of the proposed western abutment. The depth of the proposed limestone rock cutting will be similar to the existing cutting (approximately 9 m maximum depth) but the new north batter slope will be only about 1 vertical : 2 horizontal, instead of up to 1 vertical : 1 horizontal as for the existing cutting.

(2) Western Abutment

The western (Adelaide) abutment of the new bridge will comprise a shallow spread footing founded on the weathered limestone rock near the top of the 20 m high cliff that is present at this location.

(3) Bridge

The new bridge will span 407 m between abutments, and will be made up of end spans of 32 m and 25 m for the western and eastern ends respectively, and seven internal spans of 50 m. The two lane road carriageway will be supported by a post tensioned concrete box girder and 8 concrete piers, each of which are in turn supported by a pile cap and pile group. The piles are to be precast prestressed octagonal concrete piles driven to the marl. The elevation of the proposed b and its longitudinal gradient will correspond to that c existing bridge. The alignment of the proposed bric nearly parallel to that of the existing bridge. The bridg be incrementally launched from the embankment o eastern side of the river.

(4) Eastern Abutment

The eastern (Waikerie) abutment of the proposed bridg comprise a cellular raft retaining structure and piled foo the end of the eastern embankment, the piles of which be founded below the relatively weak surface soils ar the marl at depth.

(5) Eastern Approach

The eastern (Waikerie) approach road to the proposed will be supported by an embankment along its entire The height of the proposed embankment will be simila to 1 m higher than the existing embankment (approxim m maximum height) though the new north batter slope only about 1 vertical : 3 horizontal instead of up to 1 v 2 horizontal as for the existing embankment. Th embankment will traverse low lying ground and the e two lagoon pools along its length.

4. OUTLINE OF INVESTIGATION

The objectives of the investigation were to:

- identify the general sub-surface geological profi site;
- determine the strength parameters for the various
- develop a geological model for the site, based field work and the results of previous investigati
- define appropriate footing solutions for the p bridge piers and abutments, and exami constructability of the various footing options;
- assess the stability and excavation methodolog proposed cutting on the western approach, suitability of excavated material for genera pavement use;
- assess the expected performance of the embankment on the eastern approach, in t settlement potential for various design construction scenarios.

The fieldwork was carried out in March 1996 unde time supervision of experienced geotechnical engine test location plan for the fieldwork is given in Fig total of 7 land based boreholes and 6 over-water were drilled to depths between 5.8 m and 25.55 m. based boreholes were drilled by a truck mounted ri over-water boreholes were drilled by mounting th onto a floating steel pontoon assembly. The boreh positioned at each of the proposed pier and locations for the new bridge, as well as along th approach.

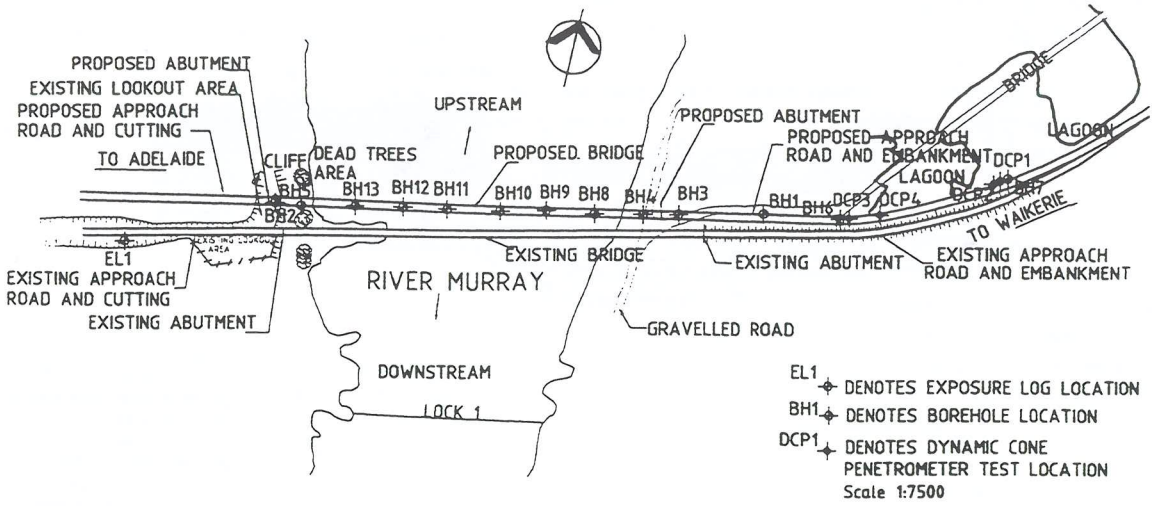

Figure 1: Test Location Plan

In general, each land based borehole was drilled using the hollow spiral auger technique with split spoon sampling at regular intervals initially, and then wash boring. For the over-water boreholes, wash boring was generally used for approximately the uppermost 10 m, before diamond coring was adopted for the weathered marl rock that comprised the remainder of each borehole.

The soil and rock samples recovered from the drilling were logged by the visual manual method cited in AS1726-1993 "Geotechnical Site Investigations", with hand held Geotester readings taken in all cohesive strata in order to estimate their consistency. Selected thin walled push tube samples were taken of the soft compressible clay soils encountered in the boreholes located along the proposed eastern approach embankment of the new bridge, in order to obtain hand held Geotester readings of the clay in an undisturbed state and hence more accurately estimate the in situ consistency of the clays. Standard Penetration Tests (SPTs) were also carried out in the granular soil layers in each borehole in accordance with AS1289 test 6.3.1, in order to determine the relative densities of the sand and gravel soil strata encountered in the drilling. SPTs were also completed in the weathered marl rock strata that were encountered, though only when wash boring was used as the drilling technique.

Oedometer testing in accordance with AS1289 test 6.6.1 was undertaken for three thin walled push tube (undisturbed) samples of the soft clay soils encountered in the Waikerie embankment boreholes, in order to determine the consolidation properties of these soils. Point load strength index testing ($I_s(50)$) of rock specimens from all boreholes where diamond coring was used was also undertaken in accordance with International Society for Rock Mechanics (ISRM) standards (3).

The exposed face of the existing Adelaide approach cutting was logged using the visual manual method cited in AS1726-1993 "Geotechnical Site Investigations", in order to provide information about the expected subsurface profile along the alignment of the proposed Adelaide cutting. The existing cutting was logged at the approximate location where the cutting depth was greatest. Samples of the soil and rock materials exposed along the depth of the cut face at this location were collected for Estimated CBR testing in accordance with the Department of Road Transport test method DRT-MAT-TP133. The purpose of this testing was to determine the utility of the cutting material as general fill or pavement fill for the proposed Waikerie embankment.

5. RESULTS OF INVESTIGATION

The stratigraphy of the subsurface strata encountered along the alignment of the proposed replacement bridge confined the published information and the results of the drilling for the original bridge. Sands, clayey sands and some clay layers were encountered across the river and the land to the east, from the ground surface to depths between 7.6 m and 15.7 m. These deposits principally comprised sand layers, but some surface or near surface clays were present within the shallow, western-most 100-150 m width of the river and within the land east of the river. The upper clay layers were generally very soft in consistency over water, and firm to stiff in consistency over land. The lower sand layers were generally medium dense over dense. The marl stratum that underlay the river soil deposits was very similar in appearance and properties across the site, and the marl horizon showed only a slight dip to the west. The marl was found to generally be a very low strength rock, and equivalent to a dense gravelly sand in strength. The surface of the marl rises steeply at the western bank of the river, so that the thickness of overlying riverine deposits is significantly reduced. Weathered limestone of low strength directly overlay the marl on the western bank of the river and formed the nearby steep cliff.

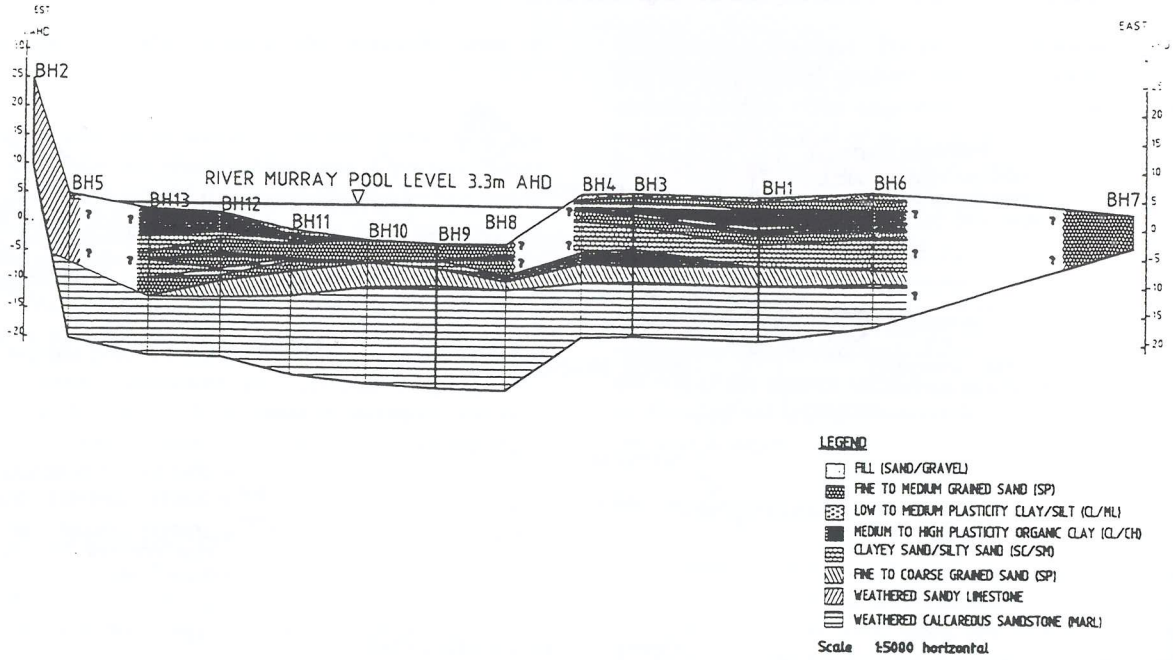

Figure 2: Inferred Geological Transect Along Bridge Alignment.

Figure 2 summarises the results of the soil drilling and rock coring in an inferred geological transect along the alignment of the bridge.

The results of the oedometer testing indicated that all three clay samples were actually heavily over-consolidated, with over-consolidation ratios of the order of 15 due to periodic dessication. The coefficient of consolidation was found to be around 10 m^2/yr and the coefficient of volume change was found to be around $1x10^{-4}m^2/kN$ over the stress range of interest.

The exposure log of the existing cutting confined the published geology. Assessment of the true nature of the exposed strata was made difficult by the fact that the cut face has been exposed for about 30 years and therefore has been subjected to appreciable weathering. However, the limestone material appeared massive and without obvious discontinuities. The strength of the material was judged to be very low to low. SPT testing at the proposed western abutment showed that the weathered limestone was equivalent to a very dense sand in general. Diamond coring and point load strength index testing of the weathered limestone below 5 m at this location confirmed that the rock strength was very low to low in general.

Prior to particle size distribution and Atterberg Limits testing, each sample of the approach cutting material received a set amount of mechanical energy to try to break up the larger sized fragments. This was done to simulate the fracturing of the cut face materials that would occur upon excavation and subsequent placement and compaction as fill.

The results of the testing indicated that all samples were s not sufficiently fine sized for Estimated CBR testing, desp the pre-test mechanical energy treatment. This implied t the Estimated CBRs of the tested material exceeded 20. T test results indicated that the weathered limestone degraded a gravelly silty sand material under moderate mechani effort, and therefore was of low strength at most.

6. DEVELOPMENT OF GEOTECHNICAL MODEL

Based upon the published geological information for the ar and the investigation for the proposed bridge, an idealis geotechnical model along the alignment of the propos bridge and approaches was developed. This geotechnic model was used as a basis for the geotechnical desi recommendations and construction advice for the project t are discussed in Section 7 of this paper.

6.1 Western Bridge Abutment

The conceptual geotechnical model for this location (on t of western cliff) comprised very dense sand represent weathered limestone to 5 m depth, and limestone rock bel 5 m.

6.2 Bridge Pier 1

The conceptual geotechnical model for this location (western river bank at base of cliff) comprised loose grave sand to 2 m depth, over firm clay/silt to 5 m, over medi dense gravelly sand to 12 m depth, over marl.

6-3 Bridge Piers 2-4

The conceptual geotechnical model for these locations (over western part of River Murray, and encompassing the shallow portion of the river) comprised 3 m thickness of soft clay, over 1 m thickness of clayey sand, over 3 m thickness of medium dense sand, over 2 m thickness of clayey silt, over 3 m thickness of medium dense sand, over 2 m thickness of coarse grained dense sand, over marl.

6.4 Bridge Piers 5-7

The conceptual geological model for this location (over eastern part of River Murray, encompassing the deeper portion of the river bed) comprised 4 m of medium dense sand, over 1 m of clayey sand, over 3 m of coarse grained, dense sand over marl.

6.5 Bridge Pier 8 and Eastern Bridge Abutment

The conceptual geological model for this location (on eastern river bank) comprised 1 m of loose gravelly sand, over 2 m of stiff clay, over 2 m of medium dense sand, over 4 m of medium dense clayey sand, over 3 m of stiff clay, over 3 m of medium dense coarse grained sand, over marl.

6.6 Eastern Approach Embankment

The conceptual geological model for this location (land to east of River Murray) comprised 2 m of medium dense gravelly sand, over 4 m of stiff clay, over 2 m of medium dense sand, over 5 m of medium dense clayey sand, over 3 m of medium dense coarse sand, over marl.

7. DISCUSSION OF GEOTECHNICAL ISSUES

7.1 Western Approach Cutting

Geotechnical issues for the western approach cutting comprised slope stability, excavatability and use of excavated material as fill. The faces of the existing cutting have slopes of up to 1 vertical to 1 horizontal (1V:1H). Though the existing cutting was approximately 30 years old, it appeared to be performing satisfactorily apart from some apparent weathering and erosion of the exposed cut face that would have resulted in periodic minor sloughing and slumping of surficial material. It was very likely that the new cutting would be excavated in soil and weathered rock that was similar to the material excavated for the existing cutting. Since the proposed cutting slope was approximately 1V:2H, the western approach cutting could clearly be constructed without an unacceptable risk of slope instability failure (an approximate factor of safety of 2.0 results if a friction angle of 45° is assumed for the weathered limestone), provided that the proposed cut face is suitably protected from erosion due to water.

It was expected that the new cutting would be able to be excavated by a combination of digging and ripping. This was confirmed through use of a Franklin (Franklin et al (3)) chart, which relates excavatability of rock to the point load index strength and fracture spacing. An average point load index strength of 0.1 MPa (very low to low strength rock) was assumed for the material to be excavated, based on observation of the rock material exposed in the existing cutting, and the field and laboratory test results associated with the borehole drilled at the proposed western bridge abutment location. Although the limestone rock was massive, it was easily fractured. Adopting an average fracture frequency of 10 fractures per lineal metre based on Rock Quality Designation values from the cored rock samples, the Franklin chart showed that the limestone rock could still be ripped with a Cat D9 equivalent dozer.

Most of the material to be excavated from the proposed cutting was weathered limestone, that is equivalent to a gravelly silty sand when broken down. Based on the results of the Estimated CBR testing, the weathered limestone rock from the cutting was expected to break down under the mechanical energy of excavation and then placement and compaction, to form sand to gravel sized particles. Based on the foregoing qualities, the material that was excavated from the proposed cutting was expected to be suitable for pavement fill, as well as for general fill. A CBR value of 20 for excavated material comprising a sand/gravel mixture was suggested for preliminary pavement design purposes. A later compaction trial performed by DOT confirmed the foregoing recommendations, and also showed that the bulking factor for the material was 0.87.

7.2 Western Abutment

Geotechnical issues for the western abutment comprised excavatability, vertical bearing capacity and slope stability. Excavatability of the weathered limestone rock was discussed in Section 7.1 of this paper, and it was expected that the cliff top material above the abutment footing would be able to be excavated by a combination of digging and ripping.

An allowable bearing capacity of 500 kPa was recommended for a spread footing founded in the weathered limestone material. This was obtained by equating allowable bearing capacity to 0.3 times unconfined compression strength (correlated from a mean point load index test result of 0.164 MPa) and then selecting approximately half this value to allow for rock weathering and proximity to the cliff face.

The proposed spread footing to support the Adelaide abutment was to be located close to the top edge of the steep cliff face that was present in the area. The existing cliff face appeared to be stable, although there was evidence of shallow surface sloughing and slumping due to weathering and erosion. Based on the survey information provided by the DOT, the cliff height was approximately 20 m and the average cliff slope was about 45°. The centerline of the

proposed abutment was approximately 5 m west of the edge of the cliff.

The slope stability of the cliff was analysed using Bishop's simplified method of slices as implemented in computer program XSLOPE (University of Sydney, 1986). Provided that the foundation material for the abutment was no weaker then very dense sand or very weak to weak limestone, as encountered in the borehole at this location, an adequate factor of safety against slope instability of 1.6 was indicated by the computer analysis, assuming that the foundation soils and cliff face are protected from softening and erosion due to water.

7.3 Bridge Piers

The geotechnical issues for the proposed bridge piers 1-8 included the capacity of the footings and how this varied with founding material, depth, footing type and footing size; and the proposed construction technique for the footings. A deep footing must be used to support the bridge piers both on land and over-water, as the near surface soils were not sufficiently strong to support the loads from the bridge superstructure if a spread footing was used. Driven preformed piles were considered to be the most appropriate pile type for the proposed bridge in terms of constructability and performance, given the need to install piles over water and through weak ground with a high water table. A number of different driven preformed pile types were available, though it was considered that precast prestressed concrete piles or steel tube piles were most likely to be used. A nominal 450 mm size pile was expected.

The piles would generally have to be driven so as to penetrate or at least reach the very low to low strength weathered marl rock that underlay the sand and clay soils across the extent of the bridge site. In areas where the marl strength is relatively high and significant driving resistance of the piles in this stratum is achieved, little penetration of the marl is then needed and the axial pile capacity will be mainly from toe bearing. However, for lower strength marl, significant penetration of the pile into the marl stratum may be required to develop the required pile set. In this case, a greater proportion of the pile axial capacity would develop from shaft friction. Significant toe and shaft capacities may also develop in the dense, fine to coarse grained gravelly sand that overlay the marl in some locations (bridge piers 5-7 for example).

The predicted ultimate pile capacities for vertical compressive loading were about 2000-2500 kN (depending on the depth of overburden) for 450 mm size piles founded on the marl surface when the simple calculation methods and parameter values presented in Appendix A of AS2159-1978 "SAA Piling Code" were used. The marl was considered as equivalent to a dense sand with N_q value of 180 for the toe capacity calculations. However back-calculated ultimate compressive capacities from the driving records of the existing bridge piles, using wave equation analyses, were 4800-5000 kN for a 400 mm dimension octagonal concrete pile founded near the marl surface. Therefore, the theoreti pile capacities were less than half the back-calcula capacities. There were a number of possible reas suggested for this. Firstly, the maximum values for sh friction and toe bearing suggested by the "limiting dep concept in AS2159-1978 may be unnecessarily conservati The magnitude of shaft friction and toe bearing are sensiti to the value of limiting depth, and therefore the actual valu could be significantly higher than those suggested by t theoretical design. Secondly, the nature of the subsurf soils may be such that the soil strength after pile drivi decreases with time. This is because for founding str equivalent to dense sands, dilatant soil behaviour could expected when the in situ soils are disturbed by pile drivi leading to temporary negative pore pressures. If t foundation soils were dilatant, the pile capacities ba calculated from the pile driving records would be up bounds to the true in service pile capacities.

For detailed pile design, it was recommended that t minimum ultimate bearing capacity of a 450 mm diame pile be taken as 2000 kN for a pile bearing on the surface the marl, based on a static analysis and the minimum depth soil overburden to the marl. A simple elastic analysis gav predicted pile settlement of around 5 mm under corresponding working load of 800 kN.

However, due to the uncertainty associated with the predic pile bearing capacity, it was recommended that a pile driv test be undertaken prior to construction piling.

A 400 mm diameter steel tube test pile was therefore dri initially open ended, and then with a gravel toe plug, in low lying land adjacent to the proposed location of eastern abutment of the replacement bridge.

The dynamic load test including CAPWAP analysis indica that an ultimate geotechnical strength for a 450 mm diam pile driven closed ended was at least 2580 kN for a 5 penetration into the marl. A design geotechnical strengt 2000 kN was recommended to be adopted for the bri design.

The pile test indicated that any hollow pile to be used for bridge must be driven closed ended, as a pipe pile dri open ended could not be expected to form an adequate p plug at the site.

The pile test also indicated that pile "set up" could anticipated at the site and that the measured resistance a time of driving will be the lowest achieved stre throughout the life of the pile. Since the restrike resistan the pile was found to be higher than the end of dri resistance at this site, this finding was contrary to ea predictions. An explanation could be related to the natu the medium dense sand and marl occurring at depth. T materials were highly calcareous with a high proportio shell particles, so that their behaviour would be differe that previously observed on mainly quartzitic sands.

The test result provided site specific data for a back analysed wave equation analysis of a 450 mm closed ended pile. For a pile driven to the interface of the medium dense sand and marl at the site of the eastern abutment, at an ultimate resistance of 2580 kN, a set of 5 mm per blow was expected for the pile driving equipment that was likely to be used.

It was recommended that the piling specification for the project states a target depth to which each pile is to be driven but that the contractor ensures that the ultimate geotechnical capacity of each pile is to be at least 2500 kN (2000/0.8), and the contractor provides site sets and necessary calculations to verify the required capacity of every pile installed.

7.4 Eastern Embankment

The geotechnical issues for the proposed eastern embankment included the magnitude and time of settlement of the foundation strata under the embankment surcharge, and construction techniques for the embankment. Based upon the results of oedometer tests for the alluvial clays along the proposed embankment alignment, and the idealised geotechnical model presented in Section 6 of this paper, a consolidation settlement of 110 mm over 150 days was calculated for the maximum height of embankment (10 m). An immediate settlement of 140 mm was also estimated from simple elastic theory, based on elastic moduli values for the foundation strata that were derived from approximate correlations with SPT N values, and conceptualising the embankment foundation surface as a flexible rectangular loaded area. Thus, a maximum total settlement of 250 mm was suggested for the embankment construction. It was recommended to construct the embankment a suitable time period (say several months) prior to the start of bridge construction, such that the calculated remaining consolidation settlement at the end of that time period could be accommodated by the bridge construction activities. Thus, ground improvement techniques such as provision of drains to the consolidating strata and/or placement of large additional fill surcharge were not considered necessary.

The proposed embankment should be constructed using a clean gravelly material similar to a quarry waste, that would be strong, relatively incompressible and erosion resistant. The material to be excavated from the western approach cutting was considered suitable for this purpose. Placement and compaction of the embankment fill material in layers to achieve a specified compaction performance was recommended. The proposed embankment side slopes of 1 vertical to 3 horizontal were expected to have an acceptably low risk of slope instability if the foregoing procedures were followed, since for a friction angle of only 35°, the approximate factor of safety is still 2.1.

7.5 Eastern Abutment

The geotechnical issues for the proposed eastern abutment were the type of footing and abutment, the means of carrying the applied vertical and lateral loads, and the interaction between the abutment and embankment. The eastern abutment will be the launching abutment during bridge construction and the fixed abutment in the final structure. This abutment must therefore be able to carry the vertical loads from the end bridge span during launching and after construction, as well as longitudinal launching reactions and longitudinal forces due to earthquake effects.

A cellular raft supported by piles founded on the weathered marl was considered to be the most appropriate abutment configuration for the site conditions. Piles were required to support the cellular raft base, due to the low strength and relatively high compressibility of the near surface clay soils in the area of the abutment. Driven preformed piles, as per the proposed internal bridge pier footings, were considered to be the most suitable pile type. The piles would carry a portion of the lateral loading applied to the abutment as well as vertical loads, and for this reason they were to be raked. Due to the large size and mass of a cellular raft, abutment stability against lateral forces could be at least partly achieved by gravity retaining action. For horizontal forces from the bridge acting eastwards, the passive pressure mobilised in the embankment fill behind the abutment, as a result of lateral deflection of the cellular raft, would also contribute to lateral abutment capacity. For horizontal forces from the bridge or the embankment fill that act westwards, "dead man" anchors connected to the cellular raft would increase the lateral capacity over that offered by gravity retaining wall action and lateral pile capacity alone.

The load actions and magnitudes of loading that will act on the proposed piled cellular raft abutment will depend, among other factors, on the interaction between the abutment and the adjoining embankment. The interaction, in turn, depends on the relative sequence of construction for the abutment and embankment. Of particular concern is any part of the abutment footings or superstructure that is constructed prior to the completion of consolidation settlement of the foundation soils under embankment surcharge. Such elements must then be designed for additional horizontal forces due to lateral spreading of the embankment fill and foundation soils as a result of vertical settlement and self weight of the fill, as well as vertical drag down forces due to vertical settlement of the embankment fill and foundation soils. The solution adopted in the detailed bridge design was to construct the fill embankment, then at the appropriate construction stage, locally excavate at the proposed abutment location in order to allow the piles to be driven and the abutment to be built, before backfilling around the abutment.

8. CONCLUSIONS AND RECOMMENDATIONS

A geotechnical investigation for a proposed replacement bridge at Blanchetown was undertaken. The investigation involved a review of the geology of the area, a program of soil drilling, rock coring, field and laboratory testing, the development of a geotechnical model for the site, a pile test, and geotechnical design recommendations and construction advice for the bridge approaches, abutments and internal

piers. The key conclusions and recommendations based on the results of the geotechnical investigation were as follows:

- The limestone at the location of the proposed western approach cutting was expected to be rippable by dozer, and suitable for use as fill for the proposed eastern approach embankment.
- A spread footing founded near the top of the weathered limestone cliff was appropriate for the proposed western abutment, with the slope stability of the nearby cliff face expected to be adequate despite the abutment surcharge.
- Driven preformed piles founded on or within the weak marl rock at depth were required for the pier footings, with a design geotechnical strength of 2000 kN suggested for a 450 mm size pile driven to the marl surface.
- The maximum total settlement of the foundation strata to the proposed eastern approach embankment was calculated as 250 mm, with a maximum time period for practical consolidation of 150 days. This settlement behaviour was expected to be accommodated by constructing the embankment sufficiently early in relation to the bridge construction, to allow for most or all of the predicted settlement to occur prior to bridge construction.
- A piled cellular raft with "dead man" anchors extending back into the approach embankment fill was recommended for the eastern bridge abutment, to carry all of the vertical and horizontal loads imposed during and after bridge construction. The interaction between the abutment and embankment will determine some of the loads that the abutment will carry, with the nature of the interaction being in turn dependent on the relative construction sequence for abutment and embankment.

9. ACKNOWLEDGMENTS

The author gratefully acknowledges the permission of then South Australian Department of Transport to publish paper, and in particular wishes to thank project personnel Richard Herraman, Geotechnical Engineer, and Mr Ror Washyn, Project Manager. The views expressed in this pa are those of the author and PPK Environment Infrastructure Pty Ltd, and do not necessarily reflect views of the Department. Professor Ian Donald, and Dr P Mitchell of PPK, are thanked for their review of the paper.

10. REFERENCES

1. Geological Survey of South Australia. "Renma Sheet SI 54-10, Department of Mines, 1971.

2. Geological Survey of South Australia (LW Parkin, "Handbook of South Australian Geology". Departm of Mines, 1969.

3. International Society for Rock Mechanics (ISR Commission on Testing Methods. "Sugges Methodfor Determining Point Load Strength", Int Rock Mech. Min. Sci & Geomech. Abstr., Vol 22, N pp 51-60.

4. Franklin JA, Broch E and Walton G. "Logging Mechanical Character of Rock". Transactions of Institution of Mining and Metallurgy, Volume Section A, pages A1-A9, 1971.

Obtaining Cyclic Load-Transfer Curves

Mr. G. J. Dyson: Research Student, The University of Western Australia

Summary: Load-transfer curves are commonly used in the design of piled foundations subjected to substantial lateral loads. There currently exists a need to develop a database of this information for the calcareous sediments present on the North West Shelf of Australia. In particular, the behavior of piles subjected to cyclic loading in these soils needs to be understood and quantified.

A geotechnical centrifuge can be used to experimentally determine load-transfer curves. Instrumented model piles have been tested at high acceleration levels to simulate prototype conditions. In order to model cyclic conditions accurately, the pile has to be loaded at high frequencies. This necessitates a suite of pile loading hardware as well as an automated load control system.

The necessary rate of pile lateral loading creates a requirement for data acquisition at frequencies higher than 10 kHz. In order to accommodate this, and other data logging requirements, a 32 channel data acquisition system has been developed and installed in the geotechnical centrifuge facility at the University of Western Australia.

Post processing of the experimental data involves curve fitting bending moment data followed by numerical differentiation and integration to obtain profiles of deflected shape and pile force per unit length. These results can be combined to form load-transfer curves for piles subjected to monotonic and cyclic loading conditions.

1 NOTATION

CPT = Cone Penetrometer Test
d = pile diameter
g = acceleration due to gravity = 9.81 ms^{-2}
H = shear force
ℓ = Pile length
M = pile internal moment
N = number of equivalent earth gravities
P = force per unit length
p = lateral pressure
r = radius
t = pile wall thickness
ω = angular velocity
y = pile lateral deflection
z = depth
z_o = unit depth

2 INTRODUCTION

In recent years there has been substantial development of the hydrocarbon fields present in the North West Shelf of Australia. The weather conditions in this region are considered to be extreme due to the prevalence of cyclones in the summer months. Consequently, the design of offshore structures needs to consider the effects of cyclic loading due to wave action.

Piled foundations are commonly used for offshore structures to provide the necessary vertical and horizontal resistance. Although extensive studies have been carried out to determine the axial capacity of piles in calcareous soils, there is a paucity of data covering the lateral response. Due to the unique nature of these soils and the problems which have been associated with platform installation in the past, it is necessary to develop a more complete understanding of the soil behaviour.

The most popular approach for the design of piled foundation systems subjected to lateral loading utilises load-transfer curves. Load-transfer or "P-y" curves idealise the soil as a set of non-linear independent springs which describe the relationship between force per unit length and lateral displacement at a prescribed depth. Once the nature of these curves is known it is relatively easy to implement them in a beam-column style analysis to determine the response to applied loads.

P-y curves can be obtained experimentally using small models in a geotechnical centrifuge. In order to determine these curves for monotonic and cyclic loading conditions, it is necessary to develop a range of software and hardware to control the experiments and convert the results to a usable form.

This paper describes how cyclic P-y curves can be obtained using the geotechnical centrifuge at the University of Western Australia. The hardware, software and analytical methods, which have application in other fields of research, will also be described.

3 CENTRIFUGE TESTING

The Geomechanics Group at the University of Western Australia currently operate two centrifuges, a "Fixed Beam" and a "Drum". A fixed beam centrifuge operates by rotating a package which contains soil, model equipment and

instrumentation about an axis (Figure 1). A drum centrifuge rotates a ring of soil about an axis. The fixed beam centrifuge was used for the pile lateral loading and further details regarding this facility can be found in Randolph *et. al.* (1).

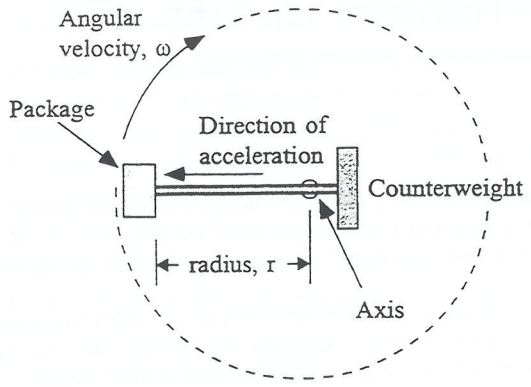

Figure 1. A basic fixed beam centrifuge.

The rationale behind testing small models in a centrifuge to represent full scale conditions has been explained by Schofield (2). The fundamental advantage is that it is possible to use small manageable models to represent prototype events in a cheaper, quicker and simpler manner than would be required for full scale tests.

The scaling effects associated with using a centrifuge are a function of the radial acceleration generated by the rotation of a package about a fixed axis. This rotation results in an acceleration (Ng) being applied to the package, the magnitude being dependent on the radius (r) and angular velocity (ω) as described in (1) below.

$$Ng = \omega^2 r \qquad (1)$$

The effect of this acceleration is for the stress gradient in the package to be the same as that of a prototype with length dimensions N greater. Further scaling relationships also exist as outlined by Schofield (2).

3.1 Model Pile Testing

For this research, a closed-ended model pile of dimensions d = 13 mm, and ℓ = 340 mm is being used. This pile is tested at an acceleration of 160 g to represent a prototype with dimensions d = 2.08 m and ℓ = 54.4 m.

The model pile is made of 12 mm diameter by 1 mm thick aluminium alloy tube to which thirteen levels of strain gauges calibrated for bending moment are attached. A 0.5 mm thick coating of epoxy is also applied in order to protect the gauges. This model pile has a bending stiffness of 3×10^8 Nmm^2 based on the combined EI of the aluminum wall and epoxy coating. The corresponding prototype stiffness for this model is 26.7×10^3 MNm^2. A typical steel pile used in offshore conditions has a d/t ratio of approximately 30 with a corresponding stiffness of 44.5×10^3 MNm^2. It is assumed that differences in pile stiffness would have little load-transfer curves.

The model pile used in this testing was closed-ended to protect the internal wiring of the bending momen Offshore piles are typically open-ended but recent (Dyson & Randolph (3)) has shown that, for calcareo at least, pile tip conditions have very little effect or lateral behaviour.

The model pile is installed by either jacking or driv strongbox with internal dimensions of 650 long × 39 325 deep (mm). The soil depth is typically 270 mm in a prototype pile embedment depth of 43.2 m.

During a monotonic test, the pile is loaded later constant rate until a prescribed load limit is achieve testing involves displacing the pile laterally betwe load limits at a specified frequency for a defined n cycles.

4 PILE LATERAL LOADING

When designing offshore foundation systems th design case relates to storm loading. Consequen foundation systems need to be designed to considerable cycling due to wind and wave action.

Whilst axial and lateral loads are often combin prototype conditions it is assumed that the late transfer characteristics of soil are virtually independ axial behaviour. For this reason, pile model testing restricted to purely lateral loading. In order to unde testing, considerable specialist equipment and sc required.

4.1 Pile Lateral Loading Hardware

Experimental P - y curves can be generated by in the results of laterally displaced model piles. Th moment profile, as obtained from the gauges duri can be used to determine pile lateral force per unit and lateral deflection (3).

$$\frac{d^2M}{dz^2} = P$$

$$\int\left(\int\frac{M}{EI}dz\right)dz = y$$

The pile is loaded laterally using a combination o purpose loading leg and a general purpose act author has designed two loading legs: the first whic pile head rotation and the second which allows rotation. Each load leg is instrumented with strain measure lateral load and, in the case of the restrain loading leg, pile head moment. The two loadin illustrated in Figure 2.

There are two general purpose actuators use centrifuge. The "Cone" actuator, typically used f soil characterisation tests, can drive laterally at

ranging from 0.0025 mm/s to 3.14 mm/s. This actuator has been used for slow, drained, monotonic testing. The "Footing" actuator is more powerful in the lateral direction and has the capacity to load at rates ranging from 0.4 mm/s up to 80 mm/s. This actuator is used for fast cyclic work.

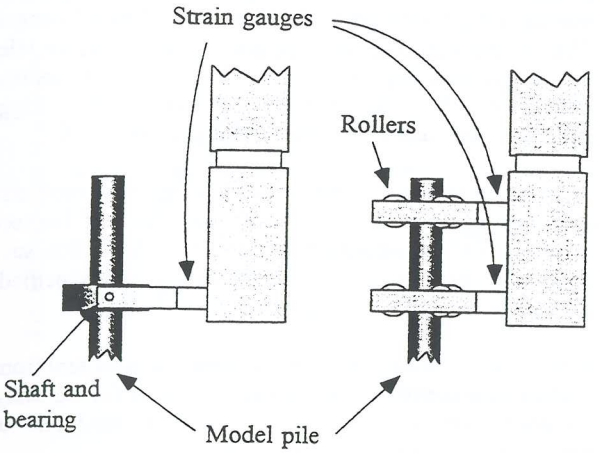

Figure 2. Pile head loading apparatus

Typical prototype wave loading conditions correspond to a loading frequency of approximately 0.1 Hz. The degree of drainage during loading strongly affects the lateral behaviour of a pile. Consequently, the pile needs to be loaded at a rate which replicates the prototype drainage conditions. Consolidation events in the centrifuge scale with N^2 so at a test g level of N = 160 the model loading rate would need to be 160^2 x 0.1 = 2560 Hz. This is unachievable with the existing equipment over the desired load limits. This frequency can be lowered however, by modifying the viscosity of the pore fluid. In this instance, silicon oil with a viscosity 100 times greater than water is used, reducing the required loading frequency by a factor of 100 to 25.6 Hz.

The footing actuator, using the software which has been developed by the author, is capable of cycling at 25 Hz for small displacements and at rates up to 9 Hz for displacements of +/- 3 mm. This corresponds to a pile lateral displacement of +/-25 % of the diameter. A typical cycle, at this rate, is over in nearly 0.1 s. As a consequence of the time scale in which these events occur, it is necessary to control the actuator with an automated system.

4.2 Automated Load Control System

The actuator control system is a combination of a series of computers and interface systems which are located within the centrifuge and in an external control room.

Whilst the centrifuge is in operation, all changes made to the package and equipment are controlled or triggered externally via slip rings. These changes are made in the control room where the test is monitored. The control computer "CPU2" is linked to the centrifuge via the COMS port and then through a slip ring to the "Flight1" computer. On CPU2 there resides a number of programs designed for controlling various actuators and other equipment.

The programs, which the author has developed specifically for laterally loading piles, contain a number of routines. It is possible to maneuver the pile head through 2 dimensions in real time or cycle the pile head between load or displacement limits. Cycling can be either frequency controlled or velocity controlled for a specified number of cycles.

Once the desired mode of pile head loading has been selected, the data is sent via the COMS port to the Flight1 computer situated on the centrifuge turret. This computer has a program which accepts the data from the control room and interprets the desired mode of loading. The Flight1 program then sends commands to the actuator controlling the rate, direction and duration of loading. For the manual movement modes, the Flight1 program sends a constant stream of data via the COMS port back to CPU2 so that the status of critical instrumentation is known. For the cyclic modes of operation, the Flight1 program is self contained and does not send any information back to the control room until the loading package is complete. This is designed to maximise the responsiveness of the load and displacement control.

The cyclic loading routine is designed to achieve the desired velocity of loading without exceeding the target loads or displacements. This is achieved using an algorithm that ensures that the speed of the actuator is proportional to the square root of the difference between the target load limit and the current load (Equation (4)).

$$\text{Velocity} = \frac{\text{Maximum velocity}.\sqrt{\text{load} - \text{limit load}}}{\sqrt{\text{Soil stiffness constant}}} \qquad (4)$$

In theory the actuator would never reach the load limit as the velocity would be zero. In reality, the momentum developed by the entire system ensures that the actuator reaches the limits.

Figure (3) shows the effect of this algorithm on the relationship between pile head displacement and load with time.

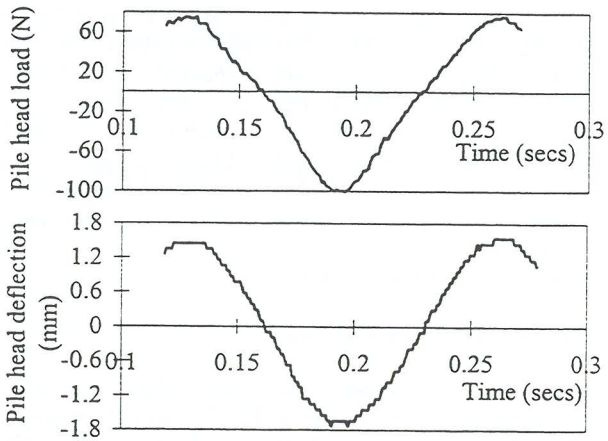

Figure 3. Relationship between displacement and pile head load with time for cyclic loading.

It can be seen that there is a sinusoidal response of the pile head during cycling as the actuator accelerates and decelerates about the load limits.

During a typical cyclic package, in calcareous sediments, the stiffness of the soil changes quite dramatically. The cyclic loading routine has been designed to maintain a constant frequency by modifying the soil stiffness constant after each loading cycle. If the previous cycle was too slow, corresponding to a softening of the soil and increased lateral displacement, the soil stiffness constant is decreased. If the previous cycle is too fast, corresponding to a stiffer sample, the constant is increased.

5 HIGH SPEED DATA ACQUISITION

Cyclic events in the centrifuge occur over a very short space of time. As a consequence of this, it is necessary to record a large amount of data very rapidly. For this case of cyclic loading of a pile, there are 19 channels of data which need to be recorded: 13 bending moment gauges, 2 laser displacement transducers, 2 load cells and 2 actuator displacement transducers.

Within a typical cycle of loading it is desirable to have at least 100 sets of data points for analysis. Cycling at 9 Hz means 900 sets of data or 900 x 19 = 17100 data points are required per second, corresponding to a data acquisition rate of 17.1 kHz. Cycling at higher frequencies or sampling a larger number of instruments would obviously increase the demands on a data acquisition system.

In order to satisfy these and other fast data acquisition requirements on the centrifuge, a high speed data acquisition system was developed by the author. This system has the ability to log 32 channels of information at a frequency of 6.25 kHz, 2 channels at 100 kHz or, for the lateral loading instance, 19 channels at 20 kHz.

5.1 Data Acquisition Hardware

The core components of the fast data acquisition system are two new computers situated on the centrifuge turret; "Flight2" and "Flight3". These machines are dedicated to data acquisition and contain ComputerBoards DAS16Jr cards. Each of these cards can log one channel at up to 100 kHz or 16 channels at 6.25 kHz. The two computers are connected with the Flight1 computer and a separate computer "Control" in the control room via an Ethernet connection through a slip ring. Data acquisition is triggered manually from the control room or independently via the Flight1 computer. Data is streamed directly to RAM disks, then to the hard disks on the Flight2 and Flight3 computers and finally, after the test is complete, through the Ethernet connection out to the hard disk on the Control computer.

5.2 Data Acquisition Software

A number of different programs, and components of programs are used to control the acquisition of data. In the centrifuge there is the "Streamer" program from Keithley Metrabyte which controls the DAS16Jr cards. This program is triggered either manually from the Control computer via the Ethernet or via a rising digital trigger from the DAS8 Flight1 computer.

The Flight1 computer has the data acquisition triggerin incorporated in the load control routines. The last step program prior to commencing lateral loading in sending a digital trigger to the Flight2 and Flight3 com This remote triggering ensures that all data from the r test is recorded, regardless of how quickly an event The two data acquisition computers are tri simultaneously and stream data independently.

From the control room, the two data acquisition compu the centrifuge can be accessed via the Ethernet conn This enables characteristics of the data acquisition s number of channels and rate of acquisition to be specif changed whilst the centrifuge is in flight.

After a cyclic loading test is completed, the data sent fi centrifuge is converted from binary to ASCII format us Streamer software so that it can be analysed preconstructed spreadsheet templates.

6 CONSTRUCTION OF LOAD-TRANSFER CU

Once a test is complete it is necessary to convert t experimental data into P - y curves. The first stage process is to separate the data into individual cycles. each cycle it is then possible to develop a set of P - y c

Once a cycle has been isolated, discrete events dur cycle need to be separated. This results in a se "snapshots" of the bending moments, pile head displacements and rotations at a particular instant.

Each of the sets of bending moment data need to be co into a polynomial form in order to facilitate differe and integration using equations (2) and (3). This is a using a spreadsheet which splices three curves tog linear function and two 4th order polynomials) as illust Figure 4. These curves are spliced together using b conditions of continuity of the first and second der (shear force and pile force per unit length) as well as z tip moment.

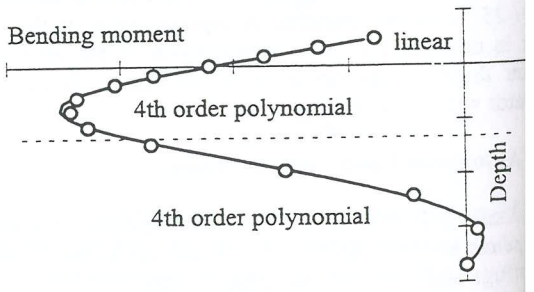

Figure 4. Curve fitting of bending moment data

Once the polynomial forms of the bending momen are quantified, they are differentiated and integrated give the pile force per unit length and the lateral de Boundary conditions of pile head rotation and defle measured during the test, are used in the integr determine the pile shape.

The shape and pile lateral force per unit length relationships for each selected cycle are then combined to form load-transfer curves at specific depths. Figure 5 shows typical drained monotonic load-transfer curves for a sample of calcareous sand (Dyson & Randolph (4)).

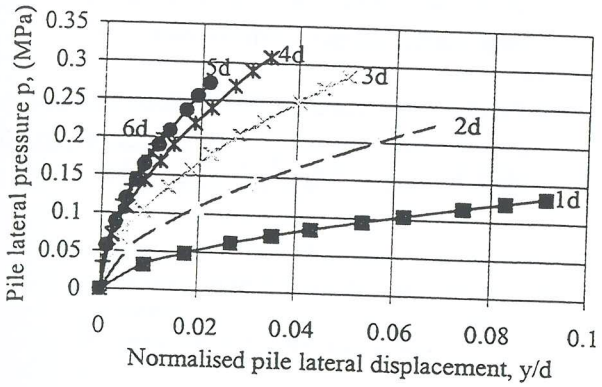

Figure 5. Monotonic drained P - y curves for calcareous sand

This drained behaviour can be compared to Figure 6 which shows an example of undrained load-transfer curves for a calcareous sand after 11 cycles at 9 Hz.

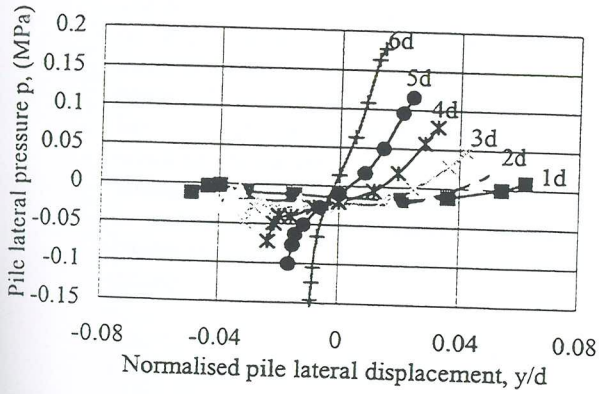

Figure 6. P - y curves for calcareous sand after 11 cycles

It is immediately obvious that there is a significant difference in behaviour. The cyclic curves display far less strength at all deflections and have a different shape in general.

It can be seen that after only 11 cycles the near surface soils have virtually zero strength. This indicates that gapping or fluidisation of the soil is occurring at these depths. It is only at the extremes of the lateral displacements that the pressures start to increase.

This transition in soil strength with progressive cycling can be seen in Figure 7. This shows, at a depth of 2 diameters, the change in lateral load-transfer behaviour. The soil stiffness reduces steadily with cumulative cycles and appears to exhibit gapping or very low strength behaviour after 6 cycles tending, to equilibrium after 9 cycles. The load-transfer relationships tend to be exhibit a substantial change in gradient towards the end of each curve, suggesting a sharp increase in soil stiffness either side of the gap.

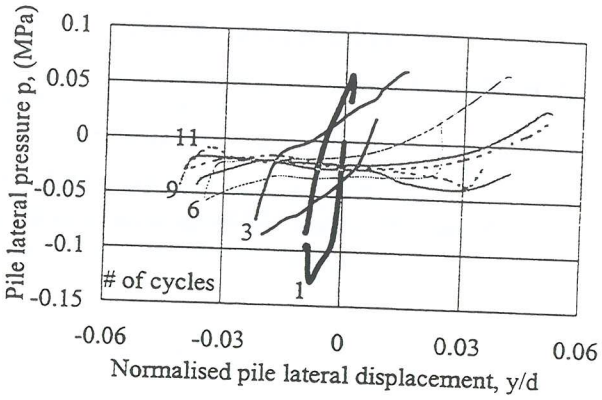

Figure 7. Cyclic P - y curves for calcareous sand at 2 d

Whilst these are only preliminary results, the consequences for design are numerous. Further testing is required to expand this database of load-transfer data.

7 CONCLUSION

Geotechnical centrifuges are a very useful tool for experimental research in designing offshore foundation systems, and many other areas related to soil mechanics.

The centrifuge and associated equipment and software at the UWA Geomechanics Group is capable of applying cyclic loads to a variety of different foundation types. The data acquisition system has the capacity to either manually or automatically record data at rates of up to 100 kHz, and record information from as many as 32 channels.

A framework has been developed, using the data obtained from experimental testing, to determine P - y curves for laterally loaded piles in any soil. This methodology has been shown to provide accurate results in previous studies investigating monotonic drained loading conditions (Dyson and Randolph (4)) and also in preliminary tests undertaken for this research.

As expected, initial results indicate that the cyclic undrained behaviour of calcareous sand is far different from the drained monotonic results obtained previously. Further testing using the equipment and software developed should provide an extended database of cyclic load-transfer curves for calcareous sand and silt.

8 ACKNOWLEDGEMENTS

The work conducted here has been funded through a joint industry project, supported by the Minerals and Energy Institute of Western Australia, the West. Australian Petroleum Company and Woodside Offshore Petroleum. The project forms part of the activities of the Special Research Centre for Offshore Foundation Systems, funded through the Australian Research Councils Research Centre's program. The author is supported by an Australian Postgraduate Award. Special thanks are due to the workshop and centrifuge staff at UWA without whose excellent technical support the equipment

development and experimental research would not have been possible.

9 REFERENCES

1. Randolph M. F., Jewell R. J., Stone K. J. L. and Brown T. A., "Establishing a new centrifuge facility", (1991), Proc. Int. Conf. on Centrifuge Modelling - Centrifuge 91, 3 - 9.

2. Schofield A. N., "Cambridge University geotech centrifuge operations", (1980), Geotechnique **30**(3), - 268.

3. Dyson G.J. and Randolph M.F., "Installation effect lateral load-transfer curves in calcareous sand", Proc Conf. Centrifuge 98, (submitted Nov. 1997).

4. Dyson G.J. and Randolph M.F., "Load transfer curve piles in calcareous sand", (1997), Proc. 8th Int. Con the Behaviour of Offshore Structures, 245 - 258.

Low Permeability Liner Construction Difficulties

Andrew Green - Golder Associates Pty Ltd (Melbourne)

Summary During construction of low permeability liners at various sites within Victoria and South Australia a number of construction difficulties have been observed by the author. Various constraints on the projects included physical restrictions, climatic conditions and material properties.

The aim of this paper is to outline several difficulties encountered during construction of low permeability liners and provide case study examples of some practical solutions.

The emphasis will be on three commonly used liner materials - clay, geomembrane and slimes. In several cases the issues were site specific relating to physical conditions encountered. However, the majority of construction problems encountered could be traced back to problems associated with moisture level, bearing capacity, subgrade strength and material properties.

1. INTRODUCTION

Low permeability liners are constructed for a variety of different uses and are generally designed to either contain material within a storage area and prevent migration beyond the site boundary, or as a capping layer to isolate the storage area and prevent water infiltration through the liner. Low permeability liners are commonly used in landfills and by mines and heavy industry which generate waste product requiring temporary or permanent storage. Storage facilities are typically lined and capped to prevent the migration of potentially contaminated soil, liquid or gases beyond the storage area.

The type of liner used varies according to the characteristics of the site, climate, location, materials available, level of liner permeability required, site specific uses, and ultimately the cost to construct. The three most commonly used liner materials are clay, geomembrane and slimes. Composite liners combining different materials are also in use.

Some sites have adequate supplies of clay or slimes are available as a by-product from an extraction process. However, some sites may require a geomembrane liner due to a lack of suitable alternative material or because of the level of permeability required.

Clay liner construction difficulties are generally associated with either;

1. moisture loss resulting in cracking of the clay,
2. damage to the clay by construction traffic,
3. material properties which lead to problems achieving compaction and/or permeability of the liner,
4. shear failure of the clay, and
5. the strength of the underlying subgrade.

The problems in installing geomembrane liners are usually associated with weather conditions and the strength and finish of the underlying subgrade layer.

Slimes are a saturated fine grained soil, generally clay, silt and sometimes with sand, which can be used for the construction of a low permeability liner. Slime liners provide construction difficulties due to a low shear strength and moisture loss causing settlement.

Construction difficulties encountered with clay, geomembrane and slimes low permeability liners are discussed in more detail in the following sections.

2. CLAY LINER CONSTRUCTION

The specification of clay liners varies depending upon the specifics of the particular project. A typical landfill site in Victoria requires a liner with a coefficient of permeability of about 1×10^{-9} m/s. This can generally be achieved by compacting a predominantly clayey material to achieve a minimum dry density ratio (AS 1289.5.4.1) of 95% Standard, moisture conditioned within the range of 0% to +3% of the Standard Optimum Moisture Content (SOMC) in accordance with AS1289.2.1.1.

To achieve the permeability requirements of the clay liner typically the clay needs to be moisture conditioned to be wet of SOMC. Subsequently, depending upon the material properties, the reconditioned clay generally has a higher moisture content than its natural moisture level and has a lower strength than when compacted dry of SOMC.

Several construction difficulties emerge when handling clay soils which require re-conditioning to be wet of SOMC. In dry, hard clay soils, particularly high plasticity clays which have a natural moisture content very much lower than SOMC (as is typical of much of the arid clays found in South Australia), the action of moisture conditioning clays becomes difficult. The clay tends to break into 'clods' which become saturated on the surface but the water does not immediately penetrate to provide the even moisture profile required. As a result the clay becomes extremely slippery and can become unworkable for normal construction plant. Subsequent compaction of such a clay layer may appear sufficient on the surface of the layer. However, inspection of the layer can often reveal a matrix of clods of dry, low density clay which have not been sufficiently remoulded resulting in a high permeability layer. Reworking the material can be a time-consuming and costly exercise.

Alternatively once clay has been adequately remoulded to wet of the SOMC any significant drying of the clays results in typical shrinkage cracking of the surface.

Construction traffic can cause problems with clay soils which have been remoulded to a moisture content wet of SOMC. Clay liners generally require several layers of compacted clay to complete the liner. In large scale production the liner material is bulk hauled with heavy machinery requiring fully laden highway trucks, dump trucks, scrapers or similar to travel over the preceding layer in order to place the material for the next layer. The results of continuous trafficking over clay liners is that pore water pressures can develop and the clay liner can deform and fail in bearing capacity and shear failure.

The author has observed several examples of shear failure of clay liners particularly in high plasticity clays located in South Australia. Shear failures were observed in the clay on either side of the wheel ruts observed on haul roads. The ruts were created by dump trucks travelling over clay which had been compacted to a minimum dry density ratio of 95% Standard at moisture contents wet of SOMC. Attempts were made to restore the affected areas by compaction with pad foot rollers. The top 100mm of the layer had been remoulded sufficiently within the 'footprint' of the 'pads' of the pad foot roller and testing proved that the density and moisture content limits had been achieved throughout the full layer. However, close inspection of the clay revealed shear failure planes throughout the underlying bottom half of the layer. Large sections of the clay could be peeled off to reveal slickensided semi circular shaped clay faces showing clear evidence of widespread shear failure of the clay. Despite the surface appearing suitable and the density testing meeting the technical specification the clay layer was rejected due to the potential for the shear planes to act as high permeability faults within the liner.

Another common problem is the effect the quality of the subgrade or underlying layer has on the construction of clay liners. Low strength subgrades typically result in difficulty in reaching the compaction levels required. If the subgrade does not offer sufficient resistance then no amount of compactive effort will achieve the required density levels in the clay liner. If the clay liner is overworked the potential for contaminating the clay liner by 'pumping' the subgrade material into the uncompacted clay is also significant, particularly if the subgrade is saturated. Various methods for treating subgrades include removal of isolated trouble spots, bridging the subgrade with an intermediate soil layer and various forms of geotextile which act to stabilise the subgrade.

The author has observed various examples of unstable subgrades generally associated with highly compressible and/or saturated soils, such as water courses which have been diverted, and compaction over fill material.

Examples include landfill sites where the compacted wastes were particularly spongy and uneven and required a clay capping layer. An example of a poor subgrade which comprised highly compressible wood shavings is discussed in more detail in Section 5 - Case Studies.

3. GEOMEMBRANE LINER CONSTRUCTION

Geomembrane liners are becoming increasingly popular in areas where there is a shortage of suitable clay deposits to construct clay liners. Geomembrane liners have various forms. However, for the purposes of this paper the discussion will be limited to one of the most commonly used forms of membrane, the High Density Poly Ethylene (HDPE) liner.

HDPE liner used in construction observed by the author is generally 1.5mm thick although different thicknesses are available. During construction of the geomembrane liner, panels of HDPE are spread over the subgrade and subsequently welded together with specialised equipment to provide a seam which is stronger than the parent material. The panels typically come in large rolls approximately 6 to 7 metres wide and 110 metres long.

Changes in ambient temperatures can cause the HDPE panels to expand or contract considerably over such a long section of panel. As a result wrinkles can easily develop in the panels and cause problems during welding of the seams. For example, if two panels are welded together where one panel is at a different temperature to another (say for example if a recently rolled panel is sitting adjacent to a panel which has been out in the heat all day) then once the panel temperature stabilises the two panels expand or contract by different amounts. Hence, stresses build up along the weld seam which can affect the soundness of the liner. Typically when this occurs one panel will appear even and well constructed while the adjoining panel will have a series of wrinkles emanating from the weld seam as the panel wants to expand to its original shape, but is restricted by the weld.

Expansion and contraction of the HDPE can also produce problems with the final liner if temperatures during construction are very much higher than normal operating temperatures for the HDPE liner. In such cases the liner contracts as temperatures drop and creates tension stresses within the liner. The author has observed an HDPE liner constructed within a lagoon with a flat base and edge walls sloping at 1V:3H with liner extending to the crest of the wall. Temperatures during construction of the liner were generally above 30 degrees C in the day during welding. Panels were secured at both ends in trenches and left overnight. During the night the temperature fell dramatically, causing the HDPE liner to contract by at least 1 to 2 metres laterally across the lagoon, causing the HDPE liner to lift away from the edge wall under the tension and create an air void at the base of the lagoon walls between the liner and the underlying subgrade. If left unchecked the liner would have sustained high tensile stresses once filled.

Another problem encountered with HDPE liner construction is the influence of wind displacing panels during construction and blowing dust over the panels. Dust can interfere with the welding process and create potential faults in the welds. Wind blowing over the top of a fully constructed liner can also cause an uplift effect which has been known to lift the HDPE liner off its subgrade and create large wrinkles across the liner.

Where significant, wrinkles in the liner must be removed so that the HDPE remains flat when loaded under working conditions. If left unchecked the wrinkle may fold on itself and create a crease in the HDPE and potentially weaken the liner.

The quality of the subgrade is another problem associated with the construction of HDPE liners. The surface needs to provide a firm unyielding foundation for the geomembrane with no sudden sharp or abrupt changes or break in grade, free of sharp objects, rocks, hollows, sticks, roots or debris of any kind. If any of these defects are found on the subgrade surface they have the potential to tear or rub the HDPE panels. This problem is particularly significant during construction and any unloaded phases of use when the liner is free to expand and contract with daily temperature changes. The panels are likely to move continuously over the debris causing higher potential for failure of the liner. An example of a problem with the subgrade surface quality and a practical solution is discussed further in Section 5 - Case Studies.

Heavy machinery used to place HDPE panels can often cause rutting in the subgrade surface. Ruts and wheel marks create sharp edges with the potential to deform the HDPE liner once loaded. Hence, particular care is required to maintain a smooth surface. Often the geomembrane is part of a composite system and is laid over the top of a clay liner. In these cases the subgrade is particularly susceptible to

damage by machinery moving panels into position due to the high moisture content and low strength of the liner as previously discussed. As a result panels are quite often rolled out by hand to avoid these difficulties.

4. SLIMES LINER CONSTRUCTION

Slimes are saturated fine grained soils, (clays or silts, sometimes with fine sands or combinations of all three) produced as a by-product during wet processing from metallurgical or extraction industries. For example, the extraction of minerals from an ore body often creates vast quantities of saturated clay and silt which is generally spread out to facilitate evaporation of the liquor, leaving a highly compressible, high moisture content slimes.

Use of slimes in liner construction generally occurs where there is a significant cost advantage due to the availability of this material on or near the construction site. Due to a typically high moisture content and low strength, slimes are generally pumped or carted into position and then require a period of time to consolidate and allow excess liquid to evaporate.

Construction difficulties arise with slimes liners when the time for consolidation and evaporation of each layer is too long for suitable construction times. If layers are added without adequate time for consolidation then the potential for settlement problems is high.

Loads applied to slimes liners are also a major problem during construction. The slimes may have a sufficiently low permeability but also exhibit a low shear strength and bearing capacity and are unable to support the weight of product to be stored over the slimes liner or the live loads of construction vehicles. Further examples are discussed in Section 5 - Case Studies.

5. CASE STUDIES

5.1 Composite Clay / Geomembrane liner, South Australia

A composite clay / geomembrane liner was constructed in an arid area of South Australia. The construction process consisted of subgrade preparation, placing and compaction of a minimum 0.5m thick clay liner capable of achieving a coefficient of permeability of 1 x 10^{-9} m/s, overlain by a HDPE geomembrane 1.5mm thick. Construction occurred during extended periods of windy, hot weather with temperatures ranging up to 40 degrees C but typically 25 degrees C during the day and generally falling to 5 to 10 degrees overnight. The lagoon was designed to contain highly acidic liquor.

During construction of the clay liner particular care was needed to ensure that only non-calcareous clays were used for the liner. Calcareous clays containing calcium carbonate were found in abundance at the clay source. If a leak were to occur and acid came in contact with calcareous soils the carbonates would potentially react with the acid to form an acid-base reaction giving off gas and water as per the following equation:

$$(1)\ CO_3^- + 2H^+ \longrightarrow CO_2 + H_2O$$

If such a reaction were to occur the permeability of the clay liner would increase dramatically as the carbonates are converted to carbon dioxide and water, leaving voids in the liner. In addition, a build up of gas from acid attack of calcareous clays would be trapped beneath the HDPE liner and create a gas bubble underneath the liner. Hence, only non-calcareous clays were used during construction of the clay liner.

Due to the high rates of evaporation in the arid construction area there was a constant threat of water loss from the clay liner. The specification required a minimum dry density ratio of 95% Standard, moisture conditioned within the range of 0% to +3% of SOMC.

The Contractor used an RS500 rotary mixing machine to moisture condition and break down the dry, hard, high plasticity clays to ensure a homogenous clay layer was produced. The RS500 was observed to produce a remoulded clay layer without the problem of dry 'clods' of high permeability clay as discussed previously in Section 2 - Clay Liner Construction. The RS500 was also used to prevent desiccation and cracking of the clay liner due to moisture loss. After a layer was completed the following layer would be placed and conditioned including the top 50mm depth of the previous layer. Hence, the RS500 was able to remove any surface laminations, desiccated or dry soil which may have been on the surface of the first layer. After compacting

the second layer testing was then undertaken on the first layer. Once passed, the process continued thereby ensuring that the clay met the specifications. The final layer was placed to a level approximately 150mm above the finished surface and cut back to level just prior to laying the HDPE geomembrane liner on top, thereby maintaining the integrity of the clay liner.

Another problem arose during construction due to the heavy traffic of fully laden dump trucks carting clay over conditioned clay layers. Shear failure of the wet clays (as discussed previously in Section 2 - Clay Liner Construction) was apparent particularly along the haul routes. Sections of clay were able to be peeled back to reveal slickensided shear faces which provide high permeability fault lines through the clay liner. As a result affected areas were reworked with the RS500 mixing machine and haul routes were built up above the height of the liner to span the clay and prevent further damage to the liner.

The author noticed that the bearing strength of the reconditioned clay appeared to increase with time particularly, when left without traffic loads. Testing of the layers showed no apparent drying out of the clay. It therefore is surmised that pore pressures generated during compaction had dissipated with time resulting in higher strength. Clay layers left for several days appeared to sustain traffic for longer periods without damage in comparison with conditioned layers which were covered immediately with another layer.

During construction of the HDPE geomembrane liner ruts and wheel marks caused by construction vehicles placing HDPE panels in position were constantly occurring. Wherever possible panels were pulled out by hand or with light weight vehicles.

Gypsum crystals were found throughout the clay liner. The sharp edges of the gypsum crystals would tear the HDPE and fail the liner if left unchecked. Hence, to avoid this problem the clay, which comprised a high plasticity clay in a very dry state, was sifted to remove all large crystals and hard, dry clay lumps. The resulting non-calcareous clay 'dust' was spread over the top of the clay liner to provide a smooth surface for the geomembrane, free of protrusions and sharp or uneven grades.

Wrinkles in the geomembrane were also observed as discussed in Section 3 - Geomembrane Liner Construction. This problem was overcome by only welding panels at night in the cool temperatures so that induced stresses in the panels were avoided during welding.

Wind continued to be a problem during the course of construction so sandbags were used to hold the liner in position. The sand bags were only finally removed once filling of the lagoon with liquor had commenced.

5.2 Landfill, Eastern Victoria

A landfill constructed in a high rainfall area located in eastern Victoria required a low permeability capping layer to prevent infiltration of rainwater into the landfill and thereby minimise the generation of leachate. The landfill product consisted predominantly of wood shavings of many tens of metres depth. The wood shavings provided a very 'spongy' subgrade which was highly compressible and was also observed to rebound as loads were removed. Sections of the landfill were poorly drained resulting in 'sink holes' of saturated wood shavings with very low bearing capacity. Areas were also observed where constant trafficking was 'pumping' water up through the fill from lower perched water areas located throughout the landfill.

Initial compactive efforts failed to meet the specified density (minimum dry density ratio of 95% Standard) due to the 'spongy nature' of the waste material which was acting as the subgrade for a low permeability clay liner. A field capping trial was conducted to assess the suitability of on-site materials and to confirm that adequate compaction and permeability could be achieved.

Various different layer thicknesses, roller types, compaction methods and materials (ranging from sandy clay to clayey sand and silty clay) were trialed. No amount of compactive effort could provide a suitably solid subgrade due to the spongy nature of the wood shavings. Landfill waste was observed to have been pumped into the first layer of clay when it was over compacted.

The trial indicated that the landfill waste could not be adequately prepared as a subgrade for construction of the capping layer, so a bridging

layer was required between the subgrade and the clay liner. The most effective and efficient bridging layer available on site was a clayey sand material. The clayey sand was observed to work best when placed in a 150 mm thick layer, conditioned to near the SOMC. Considerable heaving of the layer occurred when rolled, whereby the material deflected downwards under load then rebounded to above its original level before stabilising. However, it provided a more stable base than a layer of conditioned clay liner. The author believes this may be due to the increased sand content helping to bind the layer together.

The clay liner was then able to be adequately compacted on this bridging layer to achieve the required coefficient of permeability of 5 x 10^{-9} m/s in the trials. Although the density requirements were not always met the permeability requirement, which controlled the specification, was achieved allowing full scale production to begin. Isolated soft spots of saturated wood shavings needed to be partially removed and back filled to subgrade level.

5.3 Landfill, Eastern Suburbs Melbourne

A landfill, located in the eastern suburbs of Melbourne in a relatively high rainfall area, required a side liner to prevent leachate migration beyond the site boundary. A large supply of slimes consisting of silt, sand and clay deposits in a saturated condition was being used to create the low permeability side liner. The original design called for the slimes to be supported externally by the rock face of an old quarry and internally by solid inert waste bales in turn supported by continuous landfill operations.

The slimes were pumped in thin layers and allowed to consolidate and dry through evaporation to provide a low permeability layer prior to a further layer being added. The slimes wall was expected to have sufficient strength to be constructed parallel to the perimeter walls at batter angles between 60 to 80 degrees to horizontal with internal support and landfill wastes eventually being placed on top of previous slimes layers to minimise the loss of airspace in the landfill. However, due to time restrictions and inclement weather conditions, layers had inadequate time to consolidate or dry to achieve the desired bearing capacity.

The solution to this construction problem was achieved by introducing solid inert rubble consisting of material greater than cobble size particles which contained no voids or sections capable of creating air voids in the liner. The rubble was immersed in the saturated slimes wall creating a slimes / rock matrix. Filling continued until the rock was just below the surface of the slimes liner. Piezometers were installed throughout the trial area to monitor the performance of the slimes by performing falling head tests to estimate the permeability of the slimes wall. A constant head of slimes was maintained above the layer of rubble to ensure that any consolidation and loss of water from the slimes / rock matrix was continuously replaced to minimise the risk of air voids forming. The rock / slimes matrix was then capable of achieving the required bearing strength. Ongoing monitoring of the slimes wall is continuing.

6. CONCLUSION

During the construction phase of low permeability liners including clay, geomembrane and slimes liners a variety of problems have been observed by the author. Climatic conditions and site specific conditions are often encountered.

Clay liners are particularly sensitive to moisture variation, material properties, subgrade strength and composition, rutting and shear failure of wet clay due to construction traffic. HDPE geomembrane liners are susceptible to the weather conditions and the strength and finish of the subgrade. Slimes liners can be disrupted by inclement weather conditions and material properties.

Practical solutions vary from site to site but can generally be associated with preventative measures which minimise expenses and avoid time delays caused by disruption to the construction process.

7. REFERENCES

1. Australian Standard AS1289, Methods of testing soils for engineering purposes.

Third A-NZ Young Geotechnical Professionals Conference, Cameron, Collingwood & Slatter (eds), Feb. 1998, Melbourne, Australia.

Issues for consideration with arid soils in South Australia

Andrew Haynes - Golder Associates Pty Ltd (Melbourne)

Summary This paper presents some issues that may require consideration during site investigations in arid portions of South Australia. Issues identified include moisture content and strength, the presence of duricrusts and cementation, the potential for collapse settlements and expansive movements, and a few aspects relating to the chemical composition of these soils. The aim of this paper is not to provide a detailed discussion of any of the areas identified. Rather the paper is intended to highlight some important characteristics that may not be considered by practitioners familiar with investigations in wetter climates.

Many of these issues are no more complicated than those addressed by investigations in wetter areas. However, in many cases the issues are less well understood, possibly because the typical remoteness and lower populations of many areas containing arid soils means that fewer investigations are performed and hence practitioners are given less exposure to these soils.

The properties of sand dunes which occur over much of the arid areas of South Australia have not been addressed by this paper as they are considered to be a separate topic.

1. INTRODUCTION

Arid and semi arid soils are defined as those soils which have developed in a climate that has a net moisture deficit, meaning that the annual evaporation exceeds the annual precipitation (Atkinson, 1994). The distinction between arid and semi-arid soils is based on the extent by which evaporation exceeds precipitation. These conditions occur over almost all of South Australia. Most of South Australia possesses a significant depth of soil cover and hence a large quantity of arid or semi arid soils would be expected.

These soils often present a different range of challenges to the geotechnical practitioner. Issues such as bearing capacity, consolidation settlement and liquefaction potential are often of lower significance than for soil profiles that have developed in wetter environments. Arid soils are typically of high strength, reaching that of weak rocks at times. In some situations these factors make the design of footings founded on arid soils a relatively straightforward task. However, dismissing these soils as unworthy of thorough investigation may invite problems from a number of other factors that may not be considered in wetter climates.

Typical characteristics of arid soils include low moisture content, high strength and high salinity, cementation of the soil, the presence of duricrusts, and the potential for collapse settlements or expansive movements. These characteristics are discussed in more detail in the following sections.

2. MOISTURE CONTENT

As evaporation exceeds rainfall in an arid environment, and groundwater is at a significant depth below ground surface over much of the state, soil moisture contents are typically low. The soils are often described as dry in accordance with Australian Standard AS1726, with clayey soils often being at a moisture content well below their plastic limit.

The significance of this factor is clearly evident during earthworks. The soils will often be much drier than the Optimum Moisture Content (OMC) for either Standard or Modified compactive effort, and it is therefore often necessary to increase the moisture content of the soil significantly to enable efficient compaction.

With fine grained soils, particularly of high plasticity, the exercise of moisture conditioning is often extremely time consuming. Achieving an even distribution of moisture throughout previously dry soils is often difficult to achieve with techniques that are successful in moist soils. If inappropriate techniques are adopted it is common to encounter clods of soil with a wet, slippery periphery and a dry core. When this situation occurs further moisture conditioning is often impossible due to the reduced traction available to the conditioning equipment.

The low moisture content often results in high soil suctions. Soil suction may be defined as the ability of a soil to draw moisture from a source and comprises two components, matrix suction and solute suction. Matrix suction is a pressure resulting from the capillary forces acting in the pore spaces of a soil. The capillary forces are strongest in soils with small pore spaces, such as in fine grained soils. Solute suction is the osmotic pressure generated as water attempts to move from areas of low salt concentration to areas of higher salt concentration in order to equalise the concentrations. Where soils contain large proportions of soluble salts the solute suction component becomes large.

In general, soils with a high moisture content have a low soil suction, and soils with a low moisture content will have a high soil suction. Dry, fine grained, saline arid soils will therefore generally have a high ability to draw moisture into their matrix.

The typically low moisture contents and high soil suctions influence many other characteristics of arid soils, including several that are discussed in the following sections.

3. STRENGTH

The high strength and stiffness of many cohesive arid soils often leads to predictions of comparatively higher maximum allowable bearing pressures and lower settlements than would normally be expected from soils of similar composition in wetter climates.

It is noted that where relatively impermeable membranes such as concrete slabs are built over dry arid soils, the high soil suction may draw moisture from any nearby sources. As losses of moisture to evaporation are prevented this may result in the long term wetting up of the soil and a reduction in strength. The strength measured during an investigation of an undeveloped site may therefore be higher than the strength that may occur in the long term after construction.

The high strength of arid soils may also result in high excavation resistance, and hence influence the choice of excavation method and machinery.

4. SOIL CHEMISTRY

Due to the lack of moisture to act as a leaching agent, arid soils will often contain high salt concentrations. Two of the more common salts that influence the engineering characteristics of arid soils are calcium carbonate ($CaCO_3$) and calcium sulphate ($CaSO_4$).

Two examples of the significance of soil chemistry on the material characteristics include gypsiferous soils and the susceptibility of some soils to acid attack.

4.1 Gypsiferous Soils

The presence of calcium sulphate as gypsum ($CaSO_4.2H_2O$) in soils may be significant to the soil properties. Gypsum typically appears as elongated, translucent crystals, which may be present individually but will more commonly appear as aggregations of nested crystals. These aggregations may be quite extensive, with nests of tens of metres in diameter having been reported. Excavation of such materials may be very difficult, even with large excavation machinery. The excavation spoil of such materials may contain sharp particles which may cause damage to elements that are placed in contact with the spoil.

Gypsum contains water of hydration which can be removed from the crystalline lattice by heat. This characteristic must be considered whenever changing the moisture state of such soils, and especially when oven drying the materials. Australian Standard AS1289.2.2.1 provides guidance on the use of low temperature ovens to avoid erroneous measurements of moisture content due to the removal of water of crystallisation from the soil.

4.2 Acid Attack

The presence of carbonates (specifically calcium carbonat may also be significant to many aspects of the soils behaviou One such area is the attack of soils by acids.

The containment of acids is notoriously difficult and spillag or leakages easily occur if stringent handling practices are n maintained. Such problems may occur in areas of ac production, storage, distribution or disposal. When aci contact soils containing carbonates the following reacti occurs :

$$CO_3^- + 2H^+ \rightarrow CO_2 + H_2O$$

Acid attack products are also formed. The composition of t attack products will depend on the type of acid and the salts the soil, for example :

1. Calcium carbonate and sulphuric acid

   $CaCO_3 + H_2SO_4 \rightarrow CaSO_4 + CO_2 + H_2O$

2. Calcium carbonate and hydrochloric acid

   $CaCO_3 + 2HCl \rightarrow CaCl_2 + CO_2 + H_2O$

In the above examples the attack products are calciu sulphate and calcium chloride.

Despite the loss of mass due to the formation of carbo dioxide (CO_2) gas, the production of the acid attack produc may cause a net volume increase, leading to the generation swelling pressures (Wrench and Geldenhuis, 1992). In light loaded areas these swelling pressures may result in significa heave. The author has observed heave of up to about 100 m resulting from acid attack.

If the attacked soil is subsequently subjected to water t attack products may be leached from the soil causing lar settlements.

The heave and subsequent settlement movements may cau distress to supported structures. In the case where tho structures form part of the acid handling process, t movements may accentuate existing leaks or create n sources for leakages to occur, leading to ongoing movemen

The design of structures where acid is involved sho carefully consider the consequences of acid coming i contact with underlying soils, and minimise the risk of t occurrence wherever possible.

4.3 Other Soil Chemistry Issues

The possibility of sulphate attack of concrete structu constructed within gypsiferous soils should be considered.

If water enters a soil containing soluble salts a saline leach is likely to result, which may cause corrosive conditions structures founded in the soil.

5. CEMENTATION

A common characteristic of arid soils is the presence of cementation, consisting of chemical bonds between soil particles. These bonds may significantly increase the dry strength of the soil, sometimes up to that of weak rock, and hence are a key factor in the engineering behaviour of the material.

The chemical composition of the cementing agents may be highly variable, with calcium carbonate being most common. The various cementing agents each have varying solubilities. Where the cementing agents are soluble in water, substantial variations in the engineering characteristics of the materials are likely to occur with variations in the moisture content of the materials. If the chemical bonds are dissolved a loss of shear strength usually occurs. The extent of the changes in strength with moisture content variations is often more dramatic than for uncemented soils.

It is not uncommon for cemented sands containing relatively few fines to be capable of standing in unsupported vertical faces of significant height when in a dry state. In Port Lincoln, on the Eyre Peninsula, near vertical cliffs of weakly cemented sand up to about 100 m in height can be observed. However, rapid instability of these materials may occur following the ingress of water. The instability is often due to the removal of the cementation rather than a build up of excess pore pressures.

6. DURICRUSTS

Duricrusts are defined as hard crusts that form in the upper portion of a soil profile in a semi arid environment. In South Australia they are usually formed from calcium carbonate (calcrete) or silicon oxide (silcrete). Iron oxide (ferricrete) duricrusts also occur.

Calcrete is understood to form by the leaching of wind blown calcium carbonate ($CaCO_3$) down through a soil profile. The calcium carbonate then precipitates from solution, commonly around a lime rich particle. Continuing precipitation on the periphery of the particle will cause growth of a calcrete nodule.

The presence of calcrete is widespread throughout South Australia, usually occurring as gravel sized nodules within the top 1 m to 3 m of the soil profile, but sometimes forming larger aggregations. The nodular calcrete may grow to reach cobble and boulder sizes or may form continuous sheets, generally parallel to the ground surface. These sheets may be massive and contain few defects. The thickness of these sheets may vary considerably, with layers of up to about 1 m thickness being common. Considerably thicker layers may also occur. Calcrete is generally of medium rock strength, but high rock strength materials are not uncommon.

Zones of loose weakly cemented material are common immediately below the base of sheet calcrete. These zones are easily overlooked during site investigations, and careful logging is essential as they may be very significant to the engineering performance of the soil.

Silcretes form by crystallisation of silicon oxide (SiO_2) and may occur as gravel but, in the author's experience, cobbles, boulders and sheet rock are more common. The rock is typically of high to extremely high strength. The occurrence of silcrete in South Australia is less common than calcrete, and is most common in the far north of the state.

Duricrusts typically present higher excavation resistance than their parent soils, particularly when present as sheet rock. The excavation resistance of calcrete may range from low to high, depending on the strength of the rock substance and the presence and orientation of defects. Due to its high to extremely high substance strength silcrete will generally present high resistance to excavation.

7. COLLAPSE OF SOILS

The potential for soils to undergo collapse settlements is widely known, but, in general, poorly understood. Collapse is defined as large settlements that occur when certain soils subsequently become wet. Collapse is most common in low density, wind blown sands or silts, but may also occur in clay soils if the induced stresses are high.

Soils with a high potential for collapse are relatively common in arid environments, probably due to the fact that many of the arid soils are formed at least in part by aeolian deposition. These sediments are often deposited at a low density and, in an arid environment, may not have been subjected to significant quantities of water. Should wetting up of such a soil occur, realignment of the particles to a more dense state may result in large, rapid, settlements.

Collapse settlements are particularly relevant to cemented soils where the cementing agent is soluble in water. Due to their typically high dry strength, cemented soils may initially appear to provide a competent founding medium. However, to limit the assessment of these materials to consideration of the properties at the field moisture state may seriously overestimate the ability of the materials to support applied loads over time. In particular the likely settlements may be grossly underestimated.

Such settlements are usually observed below structures, suggesting that the applied load is responsible for the collapse, however several occurrences of collapse have been observed in domestic residences with low applied bearing stresses. In these instances it is often possible to associate the settlement with the presence of water. It is therefore considered that the movements are initiated by the increased moisture content even at low applied stresses. In some situations collapse of soils under only the overburden pressure may be possible.

The methods of assessment of the collapse are also generally poorly understood. Methods include laboratory oedometer testing, where samples are loaded to a stress state representative of the anticipated loading conditions, and then saturated. Large scale field wetting tests may also be used. Such tests typically involve introducing water into a loaded soil profile and measuring the resulting settlement. These tests may provide high quality information on the large scale behaviour of collapsing soils, but unfortunately such tests are often impractical for an initial site investigation. Other methods of assessment may involve the comparison of the in-situ density with the remoulded density obtained from compaction tests.

The increase in dry strength due to cementation often leads to higher penetration resistance than would be expected for uncemented soils of the same density. Therefore correlations of in-situ density with penetration resistance, either by Electric Friction/Cone Penetrometer Tests (CPT), Standard Penetration Tests (SPT) or Dynamic Cone Penetrometer (DCP) tests are often of limited value for cemented soils. Such tests are therefore generally not appropriate for the assessment of the density or collapse potential of cemented soils during site investigations.

It is therefore extremely important for the field engineer or geologist to identify potentially collapsible soils during the field investigation by careful observation and logging. Further testing is then required, either by field wetting tests or laboratory tests to quantify the likely extent of collapse settlements that may be anticipated.

8. EXPANSIVE MOVEMENTS

The potential for clayey soils to undergo large volumetric changes as a result of variations in moisture content and soil suction is well documented.

The resulting vertical movements are commonly predicted using the following (Australian Standard AS2870) :

$$\Delta H = \Delta\mu \times I_{pt} \times h$$

Where ΔH = predicted movement (mm)
$\Delta\mu$ = change in soil suction (pF)
I_{pt} = Instability Index
h = thickness of layer (mm)

Expansive movements are equally relevant to arid climates but accurate prediction of the movements in remote arid areas is often limited by the lack of information on the seasonal suction changes.

Soils in arid climates typically possess extremely high soil suctions, often above the measurable range for common equipment. Due to the extremely low annual rainfall, the majority of which often occurs at the time of highest evaporation, the seasonal variations in soil suction may not be as large as in areas of higher rainfall. Seasonal movements may therefore be limited by the seasonal suction change rather than the soil reactivity.

Highly reactive soils will however be susceptible to sw as a result of increased soil moisture from other sources, as leaking services or pooled water due to poor site drai Swelling may also result from the wetting of soils b barriers to evaporation such as buildings, as described e in this paper.

The specified moisture content range for compactic clayey materials should be carefully considered, taking account the required density, permeability and the exp equilibrium moisture regime. Careful selection of specified moisture content will optimise the long performance of the compacted material by minimising potential for shrinkage or swelling of the placed materia

9. CONCLUSION

Site investigations in areas containing arid soils often ne address different issues to those in areas containing formed in wetter environments. As with every investigation the relevant issues must be identified a planning stage of the investigation, so that suffi information is recovered during the fieldwork. Diff investigation techniques are often necessary as the typi high strength materials that are typically encountered render conventional sampling and testing met ineffective. The likely long term moisture conditions sh be considered when assessing the characteristics of mate during investigations of undeveloped sites.

The issues involved with arid soils are often no r complex than for other materials, but they are probably well understood due to the fact that most site investiga are performed in the most highly habited areas, which typically the least arid.

10. REFERENCES

1. Atkinson, J.H. "General report : Classification of soils for engineering purposes", Enginee Characteristics of Arid Soils, Balkema, 1994, pp 57 t

2. Australian Standard AS1726 - 1993, Site Investiga Code.

3. Wrench, B.P. and Geldenhuis, S.J.J. (1992) "Heave settlement of soils due to acid attack" proceedings o 7th International Conference on Expansive Soils. AS Dallas, Texas.

4. Australian Standard AS1289, Methods of testing soil engineering purposes.

5. Australian Standard AS2870 - 1996, Residential s and footings.

Development of a Pavement Management Strategy for Tomago Aluminium Smelter

Jason Lee, BE(Hon) ,Grad IE Aust, P Eng

Summary: This paper outlines the development of a site specific Pavement Management Strategy for Tomago Aluminium Company Pty. Ltd. (TAC). Existing pavement management strategies were found to be too general and more suited to public road systems, with TAC requiring an individually tailored, site specific study to be carried out. As a result the Pavement Evaluation Study incorporated new technologies adapted to the geotechnical field, such as Ground Penetrating Radar together with more common, standard geotechnical practices. Factual data obtained during the study was reported in a simplified format summarising existing road condition to aid TAC staff in prioritising areas requiring remedial work, based not only on existing pavement condition, but also dependant on the roads usage as part of the smelter operations. The majority of site roads within the smelter road network were found to be structurally sound, with poor road pavement conditions generally associated with ride comfort, roughness and road serviceability.

1 INTRODUCTION

This paper outlines the development of a site specific Pavement Management Strategy for Tomago Aluminium Company Pty. Ltd. (TAC) at the Tomago Aluminium Smelter Plant Site located just north of Newcastle, N.S.W. The study covered a road network of approximately 15 kilometres within the smelter. Site roads are trafficked by standard highway type vehicles, as well as primary production vehicles with solid rubber tyres and non standard axle and load configurations. These vehicles are used for transporting raw materials, molten metal and finished metal products. The study included a re-assessment of traffic patterns and volumes on the smelter road network, provided estimates of remaining road pavement life and presented recommendations on a Pavement Management Strategy over a five year period.

2 BACKGROUND INFORMATION

2.1 Design Vehicles

The majority of TAC bulk material handling is by means of wheeled vehicles. These vehicles transport raw materials, molten metal, potline consumables, waste and by-products and carry finished metal product off site. The main contributor to pavement distress appeared to be

- Molten metal tankers travelling between the potlines and the casthouse (See Figure 1).
- Anode transporters carrying fresh and spent anodes to and from the potlines.
- Potshell transporter (Scheuerle).
- Forklifts for loading and unloading semi trailers, servicing casthouse and product storage areas.
- Special permit vehicles and semi trailers for transportation of raw materials and finished metal products on and off site.

Details of axle loads and axle configurations were obtained for all design vehicles on site.

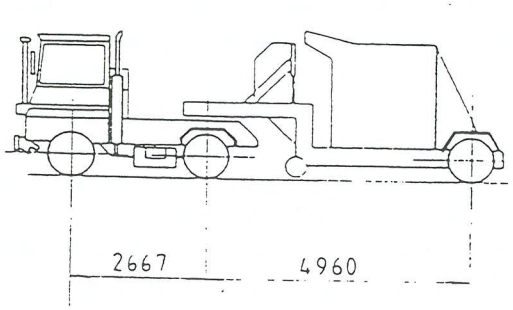

Figure 1 – Hot Metal Transport Vehicle

2.2 Traffic Data

Traffic patterns had recently been altered as a result of additions to the plant, but it was expected that existing patterns would remain stable in the medium term (3 to 5 years). Traffic patterns for all site vehicles involved in smelter operations were provided by the client.

Traffic density figures were collated from smelter production records, with figures generally indicating the number of trips per day for that activity. Trip numbers were projected for the full production rate of the smelter in the medium term.

2.3 Pavement Types

Generally roads within the smelter are comprised of flexible pavements constructed from crushed rock basecourse and sub-base with an asphaltic concrete, (AC) wearing course.

Pavement materials generally consisted of unbound material except for a number of areas across the site, where sections of road had been reconstructed using crushed and granulated slag.

Roads from the initial construction stages were approaching about 15 years of age for an initial design life of 20 years. Significant reconstruction and overlay works had taken place to extend the life and improve serviceability of some of the more heavily trafficked sections of these roads.

Roads associated with recent additions to the plant site also consisted of flexible pavements constructed from unbounded fine crushed rock basecourse and sub-base with an A.C wearing course. These roads were about 5 years old and were generally in good condition.

As built records of pavement types and records of subsequent reconstruction and overlay were available for a number of site roads, however additional geotechnical testing of questionable areas would be required to verify pavement profiles and subgrade conditions.

The as built records indicated pavement thicknesses of existing roads to vary from about 300mm to 500mm, with an AC wearing course typically in the order of about 50mm. Subgrade soils across the site generally comprised of sand.

3 SCOPE OF WORK – FIELD TESTING

3.1 Initial Condition Survey

A road pavement condition survey was carried out in order to identify:-

- Areas of rutting.
- Areas of potholing and cracking.
- Areas of poor surface texture and skid resistance.
- Poor vertical and horizontal cross-geometry or site intersections.

The visual survey was generally undertaken in ac with NAASRA (Ref 1). The observations made walkover assessment of the road system were rec pro-forma sheets, coded in accordance with ter suggested by NAASRA and related to road reference chainage and lane.

In addition to the visual assessment, selected smelt were tested for roughness using a multi-laser profi measuring roughness in NAASRA counts/km to ai assessment of pavement serviceability conditions.

Roughness results varied from values ranging from counts/km for road sections in good condition, t ranging from 200 to 400 counts/km for poor road Based on these results, road sections were graded or of low to high road roughness, with low roughness b values of less than 75 counts/km, grading to high ro for values of greater than 125 counts/km.

3.2 Road Serviceability Study

Ride comfort of the operator was one of the most in factors with regard to pavement serviceability at the Aluminium Smelter. This was particularly the case pavements which were utilised by non sprung vehic solid rubber tyres (anode transporters, hot metal tanke

Road serviceability and ride comfort was assesse interviews with road transport staff, and test riding in vehicles operating around the site. The results were co with road roughness testing carried out in the initial co survey. The results of the study were used to set gui for acceptable roughness condition for the roads desig be trafficked by these specialised vehicles.

Good correlations were obtained between areas identi transport staff as having poor ride comfort and obser from the visual condition assessment and roughness tes

3.3 Load Deflection Testing

Load deflection testing was carried out on the smelt network using a "Dynatest 8000" Falling

Deflectometer (FWD). The FWD uses a falling mass to generate a load pulse of similar magnitude and duration as that of an Equivalent Standard Axle (ESA) travelling at normal road speeds. Geophones placed on the pavement at set intervals from the single stationary load point measures the resultant velocity, enabling deflection to be calculated at each geophone location. The basic output consists of a deflection bowl providing maximum deflection and curvature functions which can be further processed to provide stiffnesses of the various pavement layers including the subgrade.

The characteristics of the deflection bowl can be used to provide a prediction of the pavements future performance. The assessment procedures outlined in AUSTROADS (Ref 2) consist of two values used in the structural evaluation of pavement condition as shown in figure 2.

- maximum deflection (d_o)
- curvature ($d_0 - d_{200}$),

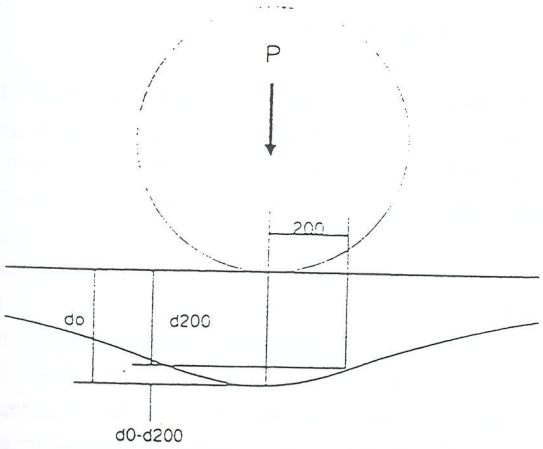

Figure 2 – Deflection bowl of a pavement under a wheel load

The data collected during testing was used to divide the smelter road network into relatively homogenous sections with similar characteristic values for deflection and curvature. An assessment of remaining pavement life was then made for each section.

Maximum deflections are mainly influenced by pavement thickness and are closely related to subgrade vertical compressive strain. Maximum deflections are used to predict the number of cycles (ESA's) to cause a certain increase in surface rutting. Very high deflections (greater than 1.5mm) usually indicate weak subgrade conditions. The test results indicated all site roads to have characteristic maximum deflections of less than 1.0mm, with the majority of road sections typically in the range of 0.2mm to 0.6mm.

Curvature is influenced mainly by basecoarse stiffness and is related to the strain in the AC wearing course. It can be used to estimate the number of cycles (ESA's) to induce fatigue failure. As a general guide, high curvatures of >0.3mm may indicate a weak or thin pavement lacking stiffness, or a pavement with cracked wearing coarse. Characteristic curvature values for the site roads tested were all less than 0.3mm, with the majority of road sections typically in the order of about 0.1mm.

3.4 Pavement Profiles

Pavement profiles were assessed using Ground Penetrating Radar (GPR) calibrated with pavement profiles obtained from a number of boreholes drilled through the road pavements at selected locations.

GPR has been trailed by several road authorities with mixed success. It was judged that GPR would be particularly useful on this site due to the expected relatively consistent pavement and subgrade conditions. GPR offered the opportunity of quick conformation of pavement depths and a reduction in required subsurface investigations across the site.

GPR works on the same principle as navigational radar used by ships and planes. A pulse of high frequency electromagnetic energy is transmitted into the ground and reflections of the pulse from buried objects are received and recorded. The GPR reflections are caused by changes in the electromagnetic character of the material. The GPR response for a particular pavement type has a general character which is related to the pavement structure and the type of construction material used. GPR profiles were recorded using the SIR-2 GPR system. The testing comprised of dragging the recording unit equipped with a 500MHz and 900MHz antenna on a sleigh behind a station wagon containing the recording software and computer.

At this site, GPR was used to give an indication of variations within the wearing course, basecourse and subgrade and to identify possible weak zones or anomalies within the pavement or underlying subgrade. Estimates of layer depths were made from the unprocessed recorded time sections, an example of which is shown in figure 3.

The time to a particular anomaly on the time sections is the time for the radar pulse to travel to the anomaly and return to the antenna and is usually called the two way travel time. The depth estimate is calculated from the two way travel time and the velocity of the pulse in the material(s) through which it passes. The GPR anomalies which are considered to represent the pavement layer interfaces are selected from time sections which have been digitally processed to subdue the appearance of spurious events such as multiple reflections in the time sections and to enhance the appearance of the reflections from the interfaces of these layers.

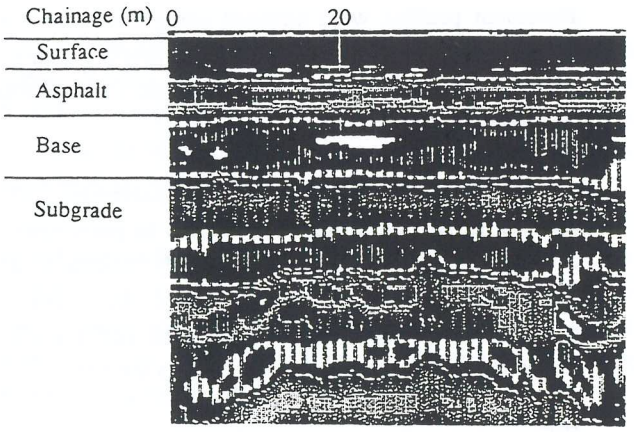

Figure 3 – Unprocessed time section

The GPR testing showed relatively few major anomalies which were usually of limited extent. The regions which exhibited major GPR anomalies generally correlated with high FWD deflection results.

The use of GPR testing allowed a large volume of data relating to pavement and subgrade profiles to be collected over the entire smelter road network in a relatively short period of time. At the same time the testing methods provided minimum disturbance to on going smelter operations. The information collected was used to identify areas of different pavement construction and helped to target areas where subsurface investigations to assess pavement and subgrade profiles would be most suitable.

3.5 Subsurface Investigations

Based on FWD and GPR test results, twelve locati selected where subsurface investigations would b out. These were selected to confirm general paveme and also target anomalies identified by th Investigations comprised the drilling and sam boreholes using a trailer mounted drilling rig to a quality, thickness, moisture and material types pavement construction and the underlying subgrade s

The results of the subsurface investigations were provide correlations with the GPR testing and to su known data previously collected. The extent of s investigations was minimized to limit any disturbances to ongoing smelter operations.

The results of the investigations generally confi pavement types as outlined in Section 2 3.

4.0 RESULTS AND INTERPRETATION

4.1 Vehicle Loadings

The majority of Tomago Aluminium Smelter's bulk handling is by means of wheeled vehicles with var load and axle configurations for the range of vehic site roads.

Details of vehicle load configurations for "normal" vehicles were used to determine the number of E Standard Axle (ESA) repetitions to produce the same as one pass of the axle group. The number of produce equivalent damage to a pavement layer given vehicle were assessed using the axle group equ relationships outlined in AUSTROADS (Ref 2).

As previously discussed, a number of design vehicle differed considerably from common axle confi associated with "normal" highway type vehicles and of standard load equivalency techniques were not ap For these vehicles, an assessment of the number of E each vehicle to produce equivalent damage to a p layer were calculated using finite layer elastic analy CIRCLY (Ref 3) software.

The following table presents a brief summary of the of ESAs produced per vehicle for a selection of vehi on site

Vehicle Type	Equivalent Damage To Layer (ESAs)	
	Asphalt	Subgrade
Tri-axle type trailer	3	4
Forklift (16 tonne)	8	20
Alumina Tanker	4	244
Potshell Transporter	3	423

4.2 Remaining Theoretical Life

An evaluation of remaining pavement life in terms of ESA's was made using the results of the FWD load deflection testing and adopting the criteria outlined in AUSTROADS (Ref 2). Traffic patterns and traffic count data for each site vehicle were used to assess equivalent number of ESA's per day for each road section, allowing an assessment of remaining road pavement life in terms of years.

Remaining road pavement life assessment was made for both structural integrity of the base and subgrade layers and the fatigue performance of the asphalt wearing course.

Traffic patterns indicated site roads to be subject to total traffic loadings per year in the range of $1x10^3$ to $9x10^6$ ESA's.

Results of the deflection testing indicated the road pavements to have theoretical remaining structural life varying from $5x10^5$ to greater than $1x10^8$ ESAs.

4.3 Pavement Management Strategy

Based on the data accumulated during the study, recommendations for a Pavement Management Strategy over a five year period were presented, with the format of the final report a result of consultation with TAC engineering staff to allow presentation of the data in the most effective way.

The information for each road section was presented in a spreadsheet, summarising the following:-

- Road section reference number
- ESAs per year
- Remaining structural life
- Remaining asphalt life
- Roughness and road serviceability
- Visual condition assessment
- Comments on remedial works recommended

The majority of site roads were found to be structurally sound, with poor road pavement conditions on site generally found to be associated with ride comfort, roughness and road serviceability. As a result, recommendations for remedial work typically comprised of milling and resurfacing of the asphalt wearing surface to provide improved road serviceability. Full reconstruction was only recommended for a few selected road sections.

The simplified table summarising all of the factual data collected, allowed quick and easy assessment of each road sections condition and highlighted any areas of potential concern.

The format of the data collected allowed TAC staff to be able to prioritise road sections requiring remedial work not only based on existing pavement condition, but also dependant on the roads usage as part of the smelters operations.

An ongoing program of maintenance, inspection and testing to assess changing traffic patterns and monitor road condition and serviceability was provided for future works.

5.0 CONCLUSIONS

The Pavement Evaluation Study demonstrated how new technologies could be incorporated and adopted to the geotechnical field, together with more common, standard geotechnical practices.

Due to the unique work environment and site conditions at the TAC Smelter, innovative and alternative methods for assessing road pavement condition were utilised. These methods included relatively standard techniques such as borehole investigations and deflection testing, as well as new technologies such as the GPR testing, with the factual data obtained used to formulate a Pavement Management Strategy tailored to meet the clients specific requirements.

GPR was found to be useful at this site as it allowed a large volume of data on road pavement profiles to be collected in a relatively short period of time, while causing minimal disruption to ongoing plant site operations.

The suitability of GPR on similar type projects is likely to be site specific, limited to sites where consistent pavement and subgrade conditions are expected, with different material properties allowing accurate delineation of pavement layers.

REFERENCES

Ref 1. NAASRA, A Guide To The Visual Assessment of Pavements, National Association of State Road Authorities, 1987.

Ref 2. AUSTROADS, Pavement Design. A Guide To The Structural Design of Road Pavements, 1992.

Ref 3. CIRCLY, Version 3.0h, MINCAD Systems Pty. Ltd. 1997.

Third A-NZ Young Geotechnical Professionals Conference, Cameron, Collingwood & Slatter (eds), Feb. 1998, Melbourne, Australia.

The Albany Regional Centre Development

A J Linton
Foundation Engineering Limited, Auckland, New Zealand

SUMMARY

The Albany Regional Development is located in Albany, about ten minutes north of Auckland City on Auckland's North Shore. Some 200 hectares are being developed for a combination of residential, commercial and industrial uses. Development has been underway since 1994 with completion of the project expected to take another four to five years. Three stages have been completed to date, with Stage 4 to begin in the 1997/98 earthworks season. The site straddles quite different geological terrain with variable earthworks characteristics requiring detailed monitoring during fill placement. One area of the development was found to contain old timber treatment chemical contaminated filling which had to be removed and dealt with under strict health and safety guidelines. Several gullies have, or are to be filled to depths of up to 18 metres requiring detailed subsoil drainage specification, stability and settlement analysis. The site illustrates several problems encountered in undertaking earthworks on what is essentially "soft rock" terrain.

1.0 Geology

The Albany Regional Centre site comprises two distinct geological formations.

The east of the site is characterised by rolling hills and incised gully features being deeply weathered Miocene Age Waitemata Group deposits. The Waitemata Group is a flysch or flysch-like deposit dominated by interbedded mudstones and poorly graded sandstones. Weathering of these deposits tends to produce sandy silts and silty clays.

Much of this material on site consists of pink silts which tend to be volcanogenic in nature, have high water contents and are moderately sensitive to disturbance. This has implications for earthworks control, the soils being quite difficult to earthwork unless within a few % of optimum water content.

To the west of the site, the geology is characterised by relatively gentle gradients and shallow gullies. This area consists of Pleistocene Alluvium unconformably overlying Waitemata Group deposits. In Pliocene times the area was below sea level, resulting in deep embayment of the Waitemata Group. A depositional basin was then created with the infilling of Pleistocene sediments. As the alluvium in this area of the site is basically eroded Waitemata Group material the upper weathered profile is relatively similar to that in the east. This profile typically comprises mixtures of orange/ brown/ light grey clays, silts and sands, with some organic inclusions and pumiceous silts.

Development earthworks generally consist of cutting down the hills in the east and filling over the alluvium in the west. Apart from the pink silts mentioned above, other earthworks challenges include obtaining suitable fills from variable and variably mixed residual and alluvial soils as well as settlement considerations given the depths of filling anticipated.

2.0 Site Investigation

Site investigations are an extremely important part of any major development. Knowledge of the prevailing ground conditions is necessary to enable cut/fill designs to be evaluated and changed if necessary. Several different methods of site investigation have been employed on this development.

For the most part site investigations for the Albany Regional Centre have involved hand auger boreholes and machine boreholes. A total of 132 hand auger boreholes and thirty machine boreholes have been drilled to date to depths of up to 5.2 metres and 25 metres respectively.

Hand auger boreholes are very useful when investigating the upper 5 to 6 metres of any given profile. They provide a rapid economical investigation technique for either smaller jobs or where coverage is required over a large area. Information such as the insitu shear strength, remoulded strength, detailed descriptions and depths of strata can all be obtained. During drilling shear vane readings are taken in the undisturbed soil at the base of the hole using a Pilcon hand shear vane. If ground water is encountered the standing groundwater level is recorded following drilling completion.

Disturbed samples can be taken to ascertain water content, liquid limit, plastic limit, allophane contents, Casagrande classification and associated parameters.

Machine boreholes allow the gathering of detailed information about the soil profile to greater depths than is possible with hand augers and trial pits. The changing strata, from weathered residual soils, through transition materials, and the underlying bedrock can all be examined in detail. Samples from the core, as well as undisturbed samples from the upper soil profile, can be taken for laboratory testing at a later date. Samples of the underlying bedrock can be used for triaxial testing. Consolidation tests are often performed on samples of the residual materials likely to be used as fill so as to provide estimates of likely settlements within the fill.

Within the underlying natural ground in areas to be filled, consolidation tests can be performed to estimate settlements due to fill placement. Joints and defects within the underlying strata can often be identified through inspection of the core recovered from machine boreholes. Closer examination can be carried out on samples brought back to the laboratory.

When slope stability is likely to be of importance, laboratory tests on samples taken from machine borehole core can give parameters, such as cohesion and friction angles, for design of final contours and any retaining structures to be constructed.

Another method of investigation used on this site was the excavation of trial pits. This method of investigation was used only in the area of the Western Entry as old filling containing timber treatment chemical contaminated waste and other assorted waste including bricks, glass, car parts and timber mixed with clayfill, topsoil and hardfill was found.

Trial pits are usually excavated with a 12 to 20 tonne tracked excavator and enable an accurate description of strata encountered, generally in the top 5 to 7 metres. Provided strict health and safety guidelines are followed, it is possible to descend into the pit for detailed inspection of the material encountered. It is often possible to examine slip faces and joint defects insitu, thus enabling accurate descriptions of dips and strikes. A potential disadvantage is the disturbance caused by the excavation. The trial pits excavated in the Western Entry allowed estimates of volumes of the various old fill types.

3.0 Laboratory Testing

Laboratory testing has been an integral part of our investigations on this site. Given the differing geology across the site, it was essential that testing was undertaken to evaluate the differences in the materials encountered. Water contents, plastic and liquid limits, Casagrande classifications, shrinkage potential, allophane contents, cohesion, friction angles and settlement parameters were all evaluated from borehole samples taken during the site investigation phase.

Water contents across the site ranged from 20% up to 67%. Within the clayey alluvial materials, water contents tended to be lower, while water contents within the more silty, weathered Waitemata Group were a lot higher. These high water contents have caused minor difficulties when this silty material was used for filling, as laboratory testing has shown optimum water contents to be in the vicinity of 25% to 35%, and within the weathered Waitemata Group the average water content was 42%.

Figure 1 shows results from several compaction tests in and around the Albany area in similar geological terrain to the residual weathered Waitemata Group deposits on this site, which gave an optimum water content and dry density for fill material.

As can be seen in Figure 1., the weathered Waitemata Group deposits have an optimum water content between 25% and 35%.

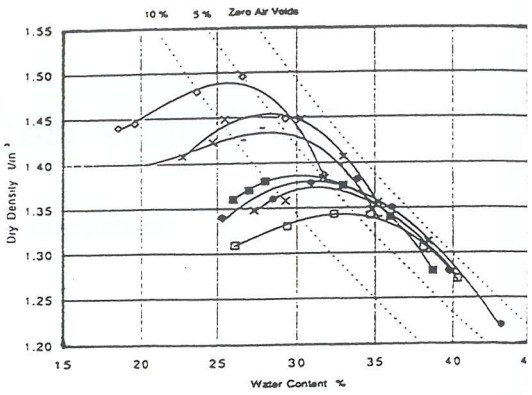

Figure 1. Optimum Water Content Within Waitemata G Deposits

On this site, within the weathered Waitemata Group, showed the material to be generally an inorganic silt, within the Pleistocene alluvium, testing showed this m to be generally an inorganic clay. Figure 2 Casagrande Classifications for samples taken fro different geological terrain present on the Albany Re Centre site.

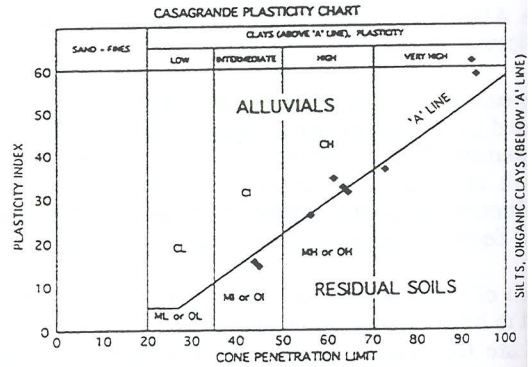

Figure 2. Casagrande Classification Results

The liquidity index is a measure of the proximity natural water content to the liquid and plastic limit. the weathered Waitemata Group soils, the samples test values around 1, indicating high compressibilit sensitivity. Within the alluvials, values obtained testing were around zero, indicating highly over-consol soils.

The results from our tests showed the subsoils moderately to highly expansive. This is a phenor common to both Pleistocene alluvial and Waitemata subsoils throughout many parts of the Auckland Area. implications of moderately to highly expansive soils brittle building construction on shallow founda However, provided adequate drainage is installed pr developments occurring, problems can be avoided quite

The allophane content is an indication of the amou allophanic clay minerals in the soil. Allophanic soils marked irreversible changes in their physical properties dried below the natural water content.

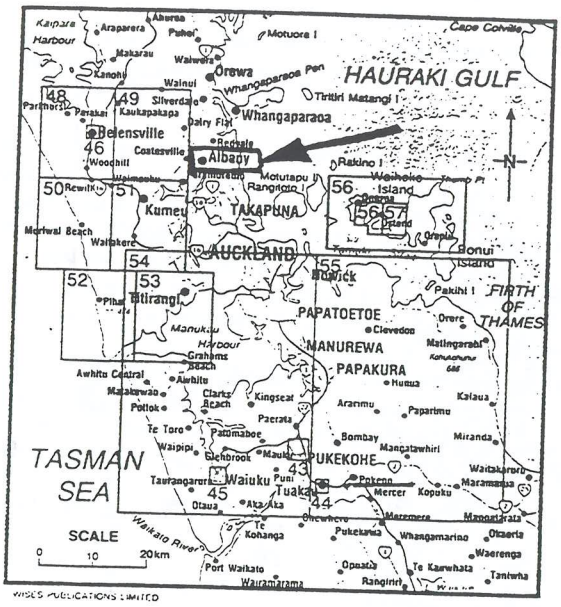

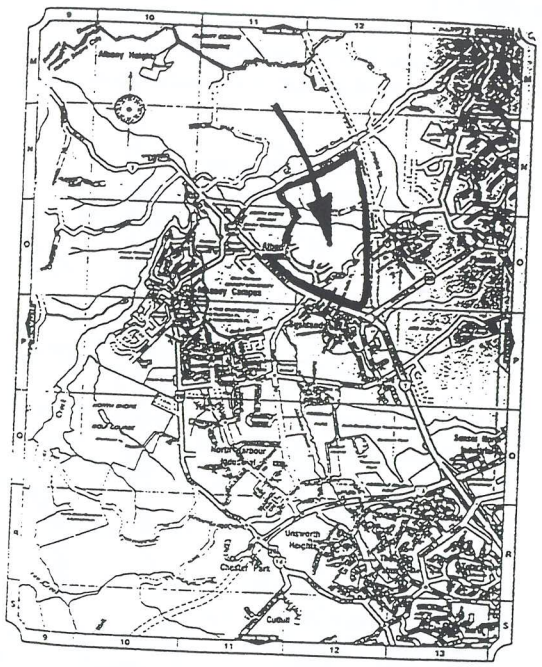

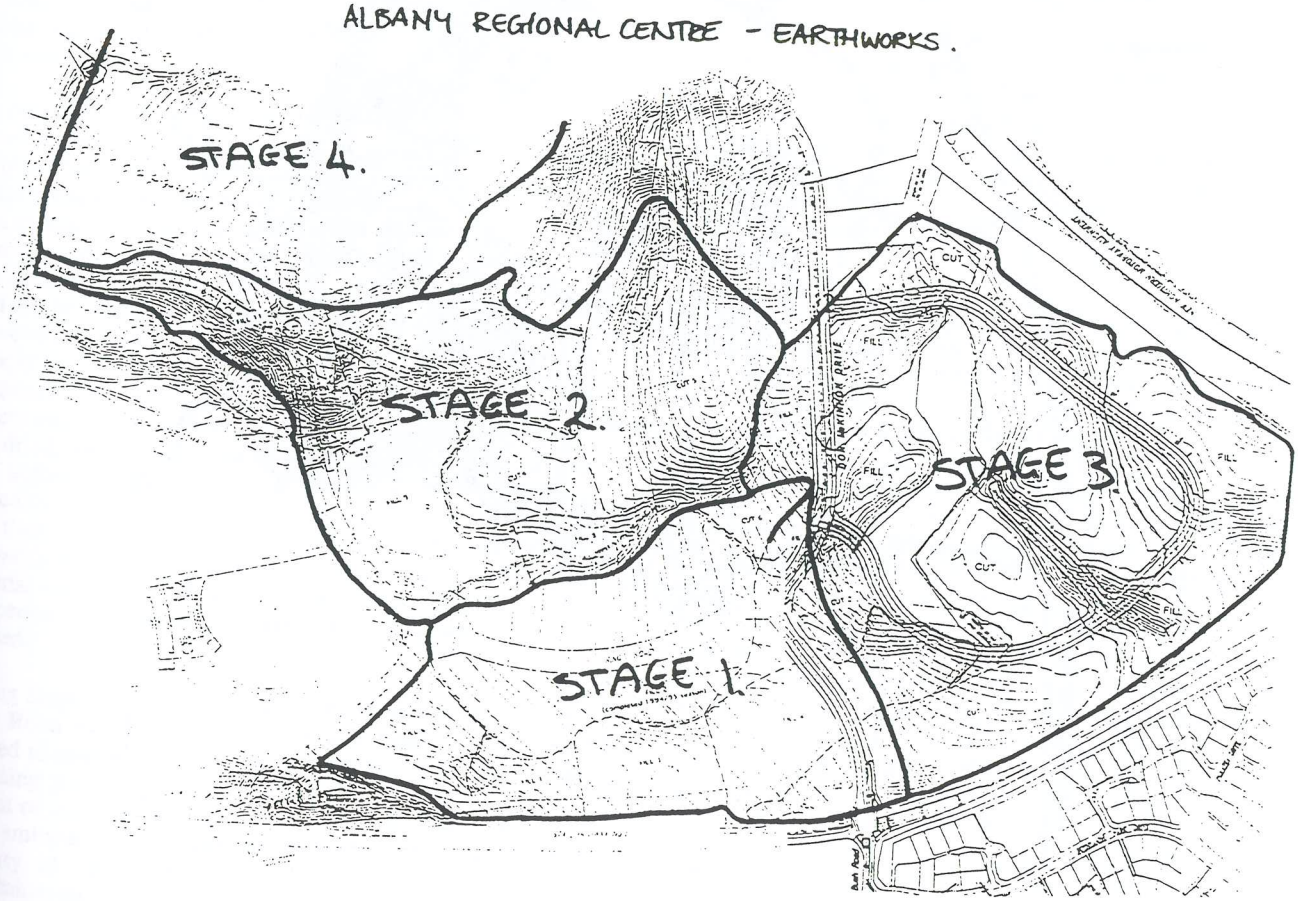

Figure 3. Site Location and Earthworks Stages

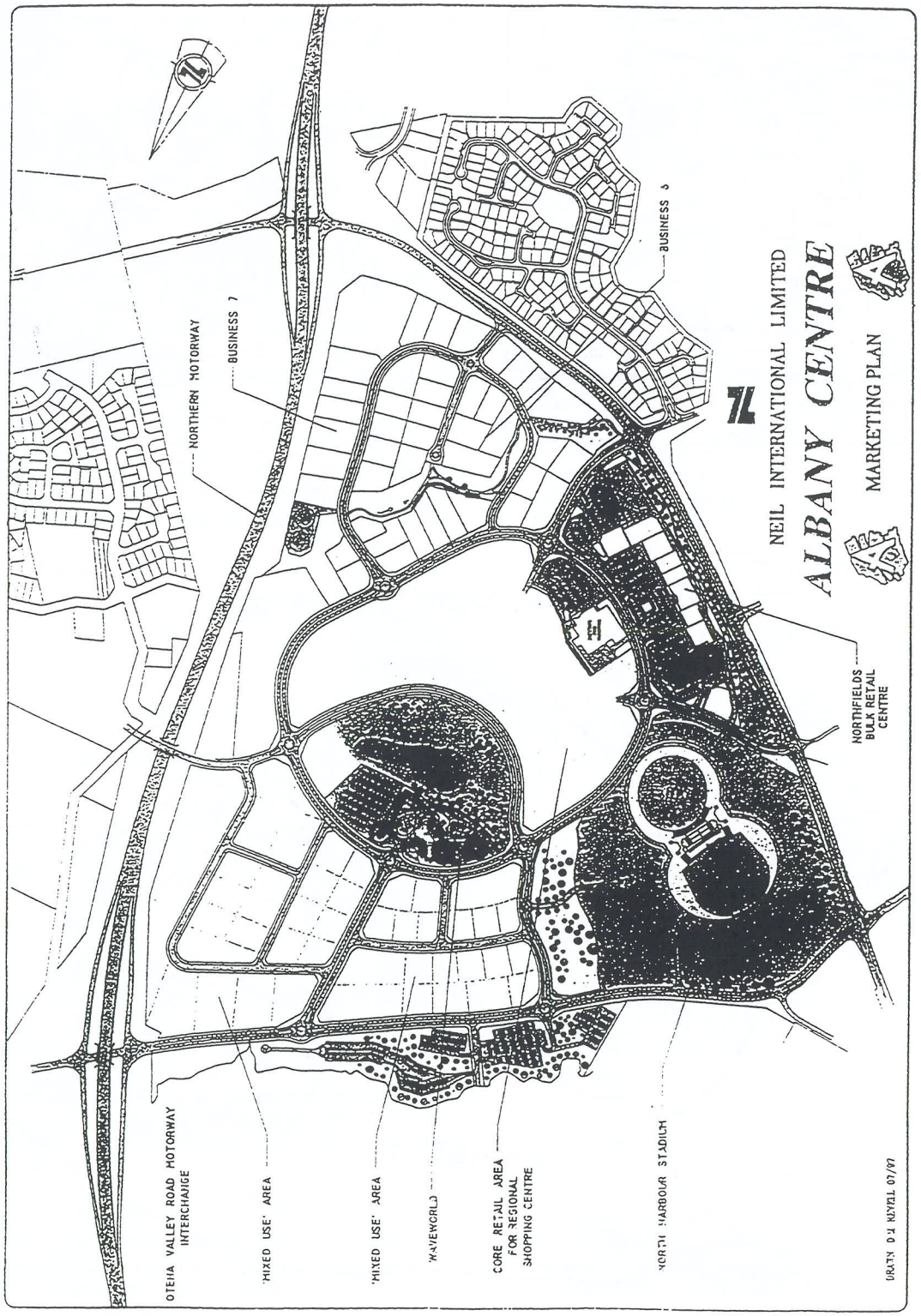

Figure 4. Marketing Plan for the Albany Regional Centre

Our testing within the Waitemata Group soils showed allophane contents of less than 5% and within the alluvial soils allophane contents were between 5% and 7%. Provided care is taken when working with higher allophane content soils, any difficulties should be minor.

Coefficients of compressibility and consolidation have also been established. The compressibility of the soils across the site lie in the low to medium range. The coefficients of consolidation calculated over appropriate loading ranges showed that any settlements that do occur as a result of the fill loading are likely to be at a moderate rate, 90% being likely to have occurred within the first year.

As development of any single site is likely to occur outside of this time frame, and with associated post-construction swelling of the fill likely to negate any settlement effects, no problems are envisaged.

4.0 Earthworks

4.1 Stages 1 to 3

Stage 1 of the Albany Regional Centre development commenced in the 1994/95 earthworks season. (See Figure 3 for site location and earthworks stages). This stage essentially involved the filling of a gully adjacent to State Highway 1. Following mucking out of the gully, suitable drainage was placed and filling began. Figure 4 shows the marketing plan for the site when all works have been completed.

In subsequent earthworks seasons, Stages 2 and 3 commenced. These areas are adjacent to Stage 1 and involved the filling of gullies and levelling off of hillsides. These areas were chosen to be worked initially to give a large area available for early development of the commercial area. During the early stages of each earthworks season there were few difficulties as the upper profile of the Waitemata Group tends to be slightly more clayey than the material at depth. However, once this has been used up, siltier, wetter material is exposed. This material requires drying before it can be adequately compacted. This resulted in contractors discing the cut areas prior to cutting, laying the cut out to be disced and dried, and then discing the material once it was in the fill, before compaction could occur. To add to the difficulties experienced with this material, if it became too dry then air voids within the fill would be above the allowable limits. To get around this problem, as silty, wet material was uncovered in a cut area, another cut area would be opened up so a mixture of clayey and silty materials could be used.

During Stage 3 operations we were informed that part of the Ring Road extension through the site needed to be fast tracked to enable access to the North Shore Stadium, on an adjoining property. This involved mucking out up to 4 metres of mullock and unsuitables and then filling for the road embankment. The final depth of fill was in the vicinity of 18 metres. At the time that work was undertaken on the Ring Road Extension, there was very little clayey material left in the open cut areas. This meant that as filling was progressing rapidly in this small area almost constant supervision of the filling operations was necessary to ensure water contents, air voids and shear strengths were at acceptable levels.

Late in the season part of Stages 1 and 2 was sold for commercial development. To facilitate the completion of these areas in what was becoming very inclement weather the cut area was limed to assist drying prior to placement in the fill.

To check the assumptions made during laboratory testing as to any likely settlements, settlement markers were placed following the completion of filling in Stage 2.

Results showed virtually zero settlement occurred over several months, which appeared to validate our initial assumptions.

4.2 Stage 4.

At present the geotechnical investigation has been undertaken in the Stage 4 area. Earthworks are expected to commence during the 1997/98 earthworks season.

4.3 Western Entry

The site for the Western Entry had in the past had several different owners. Initially the site was used as a timber mill between 1950 and 1978. The owner of the site claimed that no treatment had occurred on the site during his occupation, and from the remaining facilities on site it was assumed that there would be no contaminated material found.

Following its use as a timber mill the site had been used for boat building, pole storage and as a car wreckers. However, following site investigations in this area, large amounts of old, contaminated filling were found. Environmental and Earth Sciences were contracted to undertake a detailed environmental investigation of this area. Several trial pits were excavated under Environmental and Earth Sciences' supervision to ascertain just what exactly had been dumped in this area.

In the top two to four metres, unsuitable filling comprised varying amounts of refuse, steel offcuts, timber, brick rubble, tyres, old batteries, car parts and glass, mixed in with topsoil, clay fill and hardfill. Below this material, large volumes of woodwaste from the timber mill were found.

This waste was tested for a wide range of contaminants and it was found that there were large amounts of chromium, copper and arsenic present. The levels of these contaminants were well above both the New Zealand Environmental Protection Agency and Dutch Guideline cleanup levels.

Obviously this material could not be left where it was, so the waste was excavated and removed to approved disposal sites. This operation had to be conducted under stringent Health and Safety controls. This resulted in all those likely to be involved with the operation being taken through an induction course on the removal and handling of contaminated materials. Any person venturing on site during the works had to first be screened by the clerk of works to ensure they knew of, and abided by the health and safety measures. Each truckload of material taken offsite was logged as the woodwaste was being sent to a contaminated material disposal site, whereas the steel, brick and carparts were being sent to a regular landfill site. Each truckload also had to be covered by a tarpaulin to ensure no material was lost in transit.

Following the removal of all contaminated unsuitable fill material, work began on the actual earthworks for the Western Entry. The development proposals for this area included an 8 metre embankment with a road to be constructed across the top of this. To the east of this embankment a stormwater retention pond was to be constructed. Normal earthworks specifications for filling were not acceptable for this area and contractors were informed that specifications had been changed.

The specifications were changed to allow the fill to be placed slightly wet of optimum so as to prohibit the occurrence of high air voids, which could compromise the integrity of the embankment.

As there was a limited amount of clayey fill material available on site it was decided that the siltier fill was to be placed slightly wet of optimum to allow the material to bind adequately.

Discharging into this stormwater retention pond were several subsoil drains. This discharge, combined with the overflow from the pond was directed into a manhole and then into a pipe running through the dam. To prohibit seepage occurring along the line, the pipe was placed in a trench backfilled with vibrated concrete.

Below the downstream face of the dam, a subsoil drain comprising scoria, novacoils and wrapped in a geotextile cloth was constructed to relieve any uplift pressures likely to occur.

5.0 Parallel Developments

The North Shore of Auckland is a rapidly expanding area with more than 90 subdivisions of various sizes on the North Shore City Council's books last season. Adjacent to the Albany Regional Centre development work is almost complete on the North Shore Stadium. This complex contains a state of the art stadium overlooking a full sized cricket pitch/rugby field surrounded by an athletics track. There is also another cricket pitch behind the main stand.

Across State Highway 1 from the Albany development, work is continuing on construction for the Albany campus of Massey University.

To the east of the site, work will soon be commencing on the extension of the northern motorway. This development is included in the development proposals for the Albany Regional Centre.

6.0 Summary

In conclusion, the Albany Regional Centre is a la development incorporating residential, commercial a industrial uses, and is part of a general increase development of the North Shore. The site is situated differing geological terrain, which led to complexity earthworks supervision and has been a very interesting site be involved with.

Acknowledgements

Thanks to Neil Construction Limited for permission publish details on this development.

References

Kermode, L.O. (1992), "Geology of the Auckland Urb Area", sheet R11, 1:50,000. IGNS Limited, Wellingt New Zealand.

Scholfield, J.C. (1967), "Geological Map of New Zeala sheet 3 - Auckland", 1:250,000. DSIR, Wellington.

Foundation Engineering Limited (1991), "Prelimin Geotechnical Report on Albany Sub-Regional Centr reference 5324.

Foundation Engineering Limited (1994), "Geotechni Investigation Report on Albany Commercial Centre, St 1", reference 6599.

Foundation Engineering Limited (1994), "Geotechni Investigation Report on Albany Regional Centre, Stage reference 6921.

Foundation Engineering Limited (1996), "Geotechni Investigation Report on Albany Regional Centre, Stage reference 7361

Foundation Engineering Limited (1996), "Combi Geotechnical and Environmental Investigation report Proposed Western Access", reference 6864.

Foundation Engineering Limited (1997), "Geotechni Investigation report on Albany Regional Centre, Stage reference 7695.

The Seismic Properties of a New Zealand Sand

Steve Marks and Dr T.J. Larkin
Civil and Resource Department, The University of Auckland, New Zealand

Summary: The seismic site response analysis of sand deposits requires an understanding of the dynamic properties of the soils involved. Most of the dynamic soil data currently available in the literature has not been derived for New Zealand sands, and the relevance of this data to New Zealand pumice sands is rather unclear. An extensive experimental investigation of the dynamic response of a pumice sand was therefore undertaken, which investigated the liquefaction response from cyclic triaxial tests and the shear modulus response from bender element and dynamic torsion tests. The liquefaction results indicated that the liquefaction response was similar to that observed in quartz sands. The low strain shear modulus of the pumice sand was found to be significantly lower than that of quartz sands at similar relative densities, and the non linear constitutive relationship was markedly different from other sands, particularly in the mid strain range.

1. INTRODUCTION

A recent study by Holzer [3] stated that approximately 98% of the US $5.9 billion in property damage from the 1989 Loma Prieta earthquake was caused directly by ground shaking. Amplified ground shaking from site effects was responsible for approximately two thirds (US $ 4.1 billion) of that property damage. Another 2% of the damage cost was attributed to permanent ground deformations. It is clear from this that ground shaking characteristics and local site amplification must be considered if realistic structural design loads and hazard mitigation are to be achieved.

Both site amplification and liquefaction behaviour may be included under the general category of site effects. Many recent earthquakes, in addition to Loma Prieta, have graphically demonstrated the results of site effects. Kobe (1995), Northridge (1994), and Mexico City (1985) all exhibited significant ground motion amplifications. Significant liquefaction induced damage was observed during the Kobe (1995) and Edgecumbe (1987) earthquakes. These recent events amongst others have prompted a renewed research interest in the field of liquefaction and site response behaviour.

Earthquake induced liquefaction is a major cause of strength loss in saturated sand deposits, with associated damage often significant. This damage can take the form of foundation bearing capacity failures, large and sometimes differential vertical settlements, lateral spreading and damage to underground services. In recent decades, a tremendous research effort has gone into understanding this behaviour. Nearly all of the work however has been directed towards the behaviour of quartz sands, with very little of the research effort focused on the dynamic and liquefaction behaviour of volcanically derived sands.

The active geologic past of New Zealand has lead to widespread deposits of volcanic soils throughout the country. The Taupo Volcanic Zone (TVZ) in the central region of the North Island (extending east to the Bay of Plenty) in particular has extensive deposits of volcanic ash, clays and pumice sands. The Auckland region also has significant deposits of predominantly ash and tuff from the many small volcanic cones in the area, but few areas of significant volcanic sands.

Problems with sands of volcanic origin have been encountered in the past in some large geotechnical projects in New Zealand. The Edgecumbe earthquake of 1987 exhibited widespread liquefaction of these types of sand. Failures in projects in the hydro development area have also occurred due to the high erodability of pumice sands. These events have highlighted the unique behaviour of some of the sands of volcanic origin in New Zealand and emphasized the need for further experimental study in this area.

This paper presents results from an experimental investigation of the liquefaction and general dynamic properties of a pumice sand taken from the Puni river in the Waikato, known as Puni pumice sand. Stress controlled cyclic triaxial testing of representative loose and dense samples was used to investigate the liquefaction response of the pumice sand. The repeatability of the liquefaction testing and sample preparation methods was investigated. The non linear constitutive response of soils is very important in strong motion numerical dynamic analyses, and results are presented for the constitutive behaviour of the Puni sand. These results were derived from bender element tests, torsion tests and the triaxial tests.

All methods of seismic analyses depend to varying degrees on site specific soil information. In practice there is very often little laboratory or detailed site data available which

leads to a reliance on a number of empirical relationships and correlations for much of the required soil data. It is therefore important to assess the validity of these commonly used empirical correlations for local soils, and these results are also presented for the pumice sand.

2. GENERAL PROPERTIES OF THE PUMICE SAND

2.1 Summary of General Sand Properties

A summary of the general properties of the Puni sand discussed is shown in Table 1. These were determined from a combination of laboratory testing by the authors and the results of a previous study at Auckland University on the same sand [5].

Table 1. Summary of general Puni sand properties

Puni Sand Property	Value
D_{50}	0.76 mm
Uniformity Coefficient (D_{60}/D_{10})	2.64
Apparent solid density	2230 kg/m^3
Appropriate solid density, ρ_s [1]	1770 kg/m^3
ρ_{dry} (maximum)	940 kg/m^3
ρ_{dry} (minimum)	745 kg/m^3
e_{min}	0.88
e_{max}	1.38
ϕ' (dense) [2]	41°
ϕ' (loose) [2]	39°
Permeability range	0.08 to 0.4 cm/s

[1] from reference [5]
[2] in close agreement with [5]

The main factor to note from the above table is the two different values of solid density given. Larkin et al. [5] found that due to the vesicular nature of pumice particles, two values of solid density were required to be determined. The first, which may be termed the apparent solid density, was determined in the standard manner. It was found however that water was infiltrating the solid particles and this was giving an overly high result. For void ratio considerations, only the void areas surrounding the solid particles are relevant and so an "appropriate" solid density had to be determined. A different test procedure therefore had to be used by Larkin et al. to determine the appropriate solid density which didn't allow time for the water to infiltrate the solid particles.

In conclusion two different solid density values had to be used in this study for the calculations required. For void ratio and relative density calculations, ρ_s=1770 kg/m^3 was used. The bulk densities of all samples tested were calculated from ρ_s=2230 kg/m^3 where the absorption of water by the pumice particles had to be accounted for.

2.2 Particle Size Distribution

The particle size distribution of the Puni sand used for all samples reported in this study is shown in Figure 1.

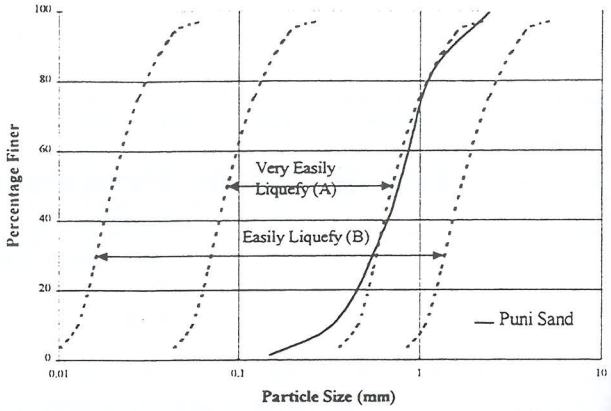

Figure 1 Particle size distribution curve of Puni sand showing the zones of liquefaction susceptibility (from [13])

The sand is classified as a well graded medium to coarse sand, with a small percentage of fines. The particle size ranges for sands that have been shown to be susceptible to liquefaction are also shown on Figure 1. The Puni sand falls within the readily liquefied zone of the graph and is hence a good choice for dynamic liquefaction testing.

3. LIQUEFACTION TEST RESULTS

3.1 Sample Preparation

The main difficulty in the laboratory testing of sands is sample preparation. The Puni sand is free flowing which means all samples were constructed. For the loose test results reported in this paper, all samples were prepared by a dry pluviation method. Larkin et al. [5] investigated a number of sample preparation methods, and concluded this method gave reliable and repeatable results for this sand.

The loose samples had an average relative density of 33% using this method, which was repeatable for each sample to a tolerance of around 10%. Dense samples were formed using the method of vibro-compaction of the sand in the sample former, which yielded consistent dense samples.

Saturated samples were placed in the triaxial cell, flooded with carbon dioxide (CO_2) and de-aired water and left overnight. Saturation tests the next day indicated complete saturation of all samples had been achieved using this method.

3.2 Repeatability of Liquefaction Test Procedure

The repeatability of the sample preparation and testing method is a very important factor to consider when performing laboratory testing, and therefore two different loose samples were tested in the same manner to compare the results. The properties of the two samples (labeled D and E for convenience) are shown in Table 2

Table 2 Material properties of the repeatability testing loose samples

	Sample D	Sample E
Dry Density (kg/m^3)	803.0	797.0
Bulk Density (kg/m^3)	1443.0	1440.0
Relative Density (%)	35.0	32.0

The results in Table 2 indicate that the dry pluviation method produces loose samples of similar density, which is very important in liquefaction testing [9]. Both of these samples were then subjected to the same cyclic load controlled liquefaction test, the results of which are shown in Figures 2 and 3.

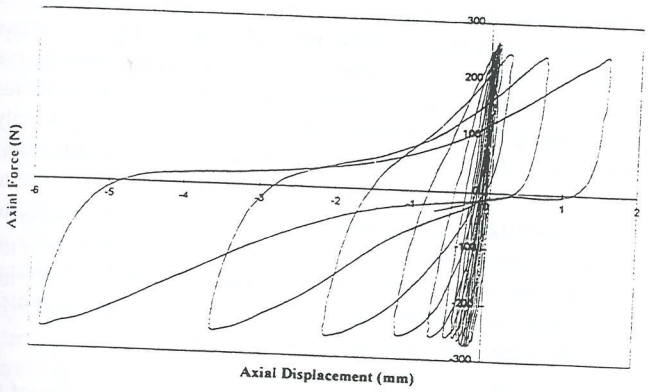

Figure 2 Axial load displacement plot for loose sample D (σ_3'=100kPa)

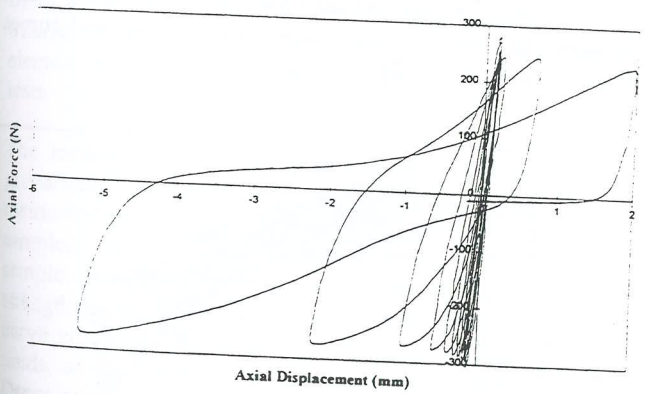

Figure 3 Axial load displacement plot for loose sample E (σ_3'=100kPa)

These two test results show a similar liquefaction response, with sample D experiencing liquefaction in 13.5 completed loading cycles, and sample E in 14.5 cycles. Both failed in the extension phase of loading, hence the extra ½ cycle.

3.3 Loose Sample Liquefaction Results

A number of load controlled tests at a variety of stress ratios were performed to generate a liquefaction strength curve for the loose Puni sand. Figure 4 plots the liquefaction resistance curve of the loose samples.

Figure 4 also shows the liquefaction curve given by DeAlba et al. [2] that is often used to generate the shape of a liquefaction curve in the widely used empirical method of Seed and Idriss [10]. This data shows that the shape of the Puni sand curve is slightly flatter than the overseas data, particularly for the low stress ratio region where the number of cycles to liquefaction are large.

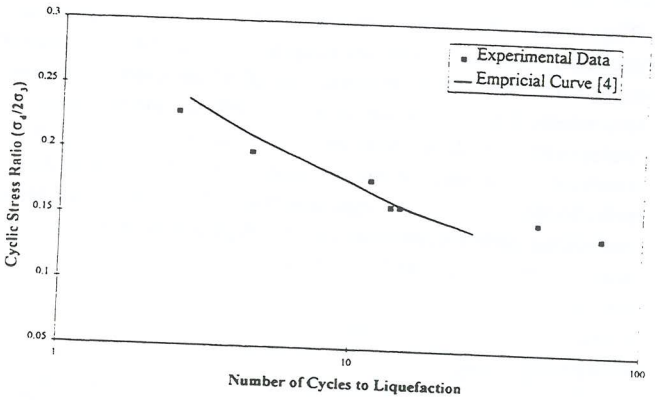

Figure 4 Loose Puni sand liquefaction curve and empirical shape

The normalised increment in pore pressure for all of the loose tests are shown in Figure 5. This shows the steadily increasing residual pore pressure component that is a result of the induced shear and potential volumetric strains. The residual pore pressure curves show very similar behaviour for most of the samples. Figure 5 also shows the upper and lower bounds of the residual pore pressure curve collected by Seed et al. [11] for cyclic triaxial tests, and the Puni sand falls well within these boundaries. This indicates that the pore pressure response of the pumice sand is similar to other sands. This is important in the use of some numerical models in liquefaction analyses [6,8,11].

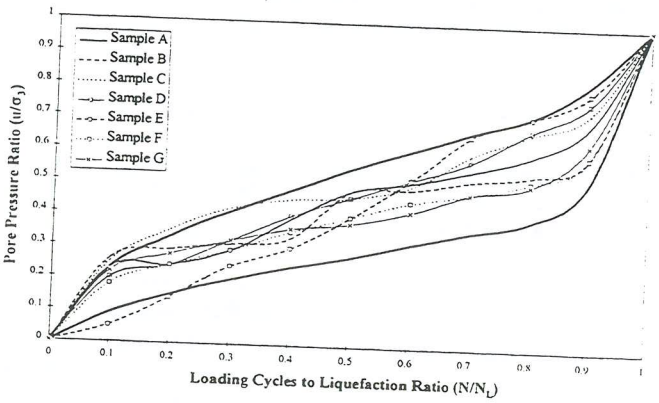

Figure 5 Pore pressure response of all samples

4. LOW STRAIN SHEAR MODULUS PROPERTIES

An accurate assessment of the relationship between low strain shear modulus and confining pressure is very important in seismic site analyses. A number of Puni sand samples were tested in the free vibration torsion test equipped with bender elements to determine the low strain shear modulus and non linear behaviour of the sand. These results are reported elsewhere [7], but some of the more interesting behaviour is presented and extended here.

The relationship between low strain shear modulus and confining pressure was investigated. The best fit power expressions derived from the test results (not shown here) had essentially the same power term for both the loose and dense state, with the difference being confined to a multiplying constant. The multiplying constant is clearly a function of relative density, and the experimental data for both the loose and dense state (represented by an expression known as K_2) may be replotted in the form of Figure 6.

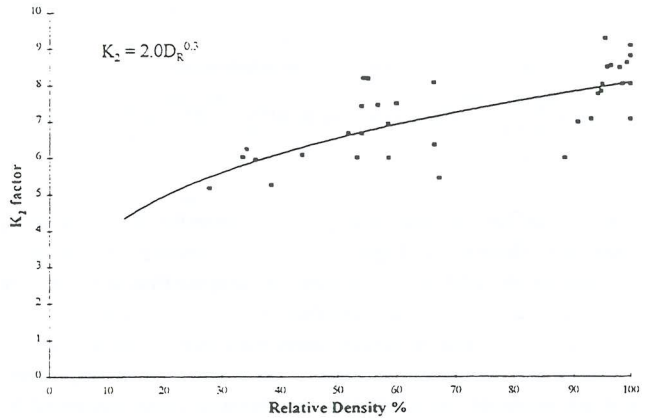

Figure 6 K_2 factor for G_{max} versus density from experimental data

The most commonly used expression relating confining pressure and low strain shear modulus is from Seed et al. [12], which is in the form (in S.I. units)

$$G_{max} = 6945 K_2 (p')^a \qquad 1$$

where G_{max} is in Pa
p' is the effective confining pressure in Pa
a,K_2 are constants

Typically a is taken as 0.5 and K_2 can be related to relative density or SPT blow count. For the Puni sand however, the power term (constant a) was found to be 0.6, and the K_2 term is derived from the best fit line of Figure 6. The full expression for the low strain modulus (D_R>10%) is therefore

$$G_{max} = 6945 * 2.0 (D_R)^{0.3} (p')^{0.6} \qquad 2$$

where D_R is the relative density in % (D_R>10%)
p' is the confining pressure in Pa

In comparison to the expressions derived for quartz sands [12], the pumice sand exhibits significantly lower values of G_{max} for all relative densities. This ranges from 30% to 60% of the G_{max} values of quartz sands at the same relative densities. Ideally the low strain shear modulus should be determined in situ by recording shear wave velocities, but this data is often not available and the practitioner must rely on correlations with penetration resistance or relative density. The above result emphasises that it is important to use appropriate correlations for New Zealand soils where possible.

5. NON LINEAR CONSTITUTIVE PROPERTIES

The constitutive properties of soils are very significant in seismic response computations [4] and requires close consideration. The available dynamic torsion test data on the form of the non linear shear strain versus shear modulus relationship for Puni sand from a previous study [7] only extends to shear strains in the region of 10^{-1}%. Shear strains of this magnitude are likely to be induced in moderate to large earthquakes, and very large earthquakes are likely to induce larger strains in soft ground. Therefore the form of the constitutive relationship of the Puni sand at large strains was determined from the cyclic triaxial test results, which induced shear strains up to 1% in some cases.

The ratio G/G_{max} was determined by dividing the value of G obtained from the cyclic triaxial test results, tested at a confining pressure of 100 kPa, by the value of G_{max} determined from Equation 2. These large strain results were then plotted on the existing data from the torsion tests, which is shown in Figure 7. Also shown are the empirical curves given by Seed et al. [12] for sands.

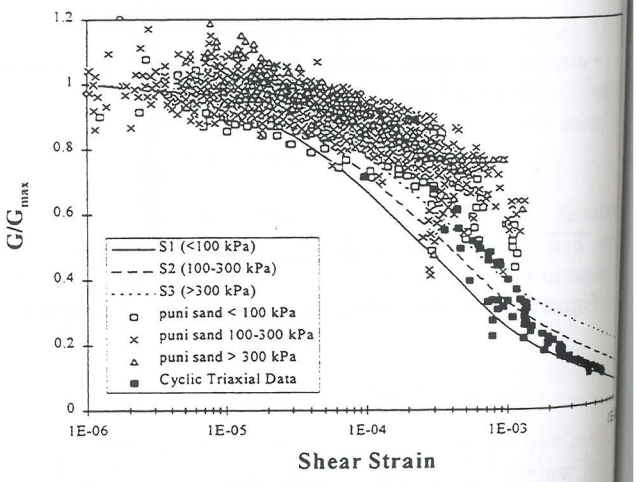

Figure 7 Normalised shear modulus versus shear strain response from all tests

This plot shows the scatter and trends of the constitutive behaviour of the sand. The Puni sand plots significantly above the empirical sand curves in the medium strain range (torsion test results), and then shows a rapid decay of the

curve in the larger strain zone (cyclic triaxial test results). There is the difficulty here of comparing results from two different testing methods, but there appears reasonable agreement where the two sets of results overlap. These results indicate that the pumice sand exhibits more linear less damped behaviour than quartz sands over the medium to low strain range, and tend to behave in a similar manner to quartz sands in the larger strain range.

Torsion test results from volcanic ashes [1] exhibited an extended shear modulus plateau, with a rapid decay after this plateau. The Puni sand shows similar behaviour, but the plateau appears to extend to a higher strain range. Based on this limited data it is not possible to conclude whether this large plateau and rapid decay behaviour is indicative of volcanically derived soils as a whole, but a trend does appear to be emerging. More work is clearly required to conclude a firm trend however.

6. CONCLUSIONS

The aim of this study was to investigate the seismic properties of a New Zealand pumice sand, such as are found extensively in the upper and central North Island. As the literature on dynamic soil properties in dominated by overseas data derived primarily from quartz sands, it was important to investigate the dynamic behaviour of a New Zealand pumice sand. Most seismic design analyses rely to varying degrees on empirical soil relationships, and these therefore must be investigated for New Zealand conditions. An extensive testing programme was undertaken to characterise the dynamic behaviour of the pumice sand, including cyclic triaxial liquefaction tests, free vibration torsion tests, bender element tests and a number of other general soil classification tests.

The repeatability of the dynamic triaxial test and sample preparation techniques was established, indicating that the method of dry pluviation sample construction gave consistent samples. A liquefaction testing programme on Puni sand samples was then undertaken to generate a liquefaction strength curve for the sand at a range of stress ratios. This curve was found to be of a similar shape to that of quartz sands, as were the excess pore pressure generation curves. Dense samples clearly illustrated the expected behaviour of limited strain potential.

No significant grain crushing was detected in any of the samples tested under dynamic conditions, even when the magnitudes of applied loading were significantly in excess of those expected during an earthquake. This finding indicates that one of the characteristic properties of pumice sands can perhaps be disregarded when considering its liquefaction response. This may explain the relatively classical liquefaction behaviour of this sand.

The low strain shear modulus response of a sand is a very important property to consider. A number of free vibration torsion tests and bender element tests were incorporated in this study. These results showed that the shear modulus was proportional to the confining pressure raised to the power 0.6, which is significantly higher than the frequently used 0.5 power term. For similar relative densities, the low strain shear modulus of the pumice sand was found to be significantly lower than that expected of quartz sands. A specific expression was derived for the low strain modulus behaviour of the Puni sand.

The form of the non linear constitutive relationship is very important in numerical seismic analyses, and the free vibration test and cyclic triaxial tests were used in this regard. These results showed that the Puni sand exhibits more linear behaviour over the medium strain range that the literature suggests, with a rapid fall off to strongly non linear behaviour at larger shear strains. A previous study on volcanic ash showed similar trends. Based on the limited available data a trend does appear to be emerging, but clearly more work is required in this area if firmer conclusions are to be drawn.

The largest unknown feature of the behaviour of pumice sand is its response to penetration testing. As most dynamic analyses tend to rely on either SPT or CPT in situ penetration results this is a very important area for further research. At present the University of Auckland is involved in a research project on the penetration resistance of pumice sands, which may help to reduce some of the uncertainty in the seismic analyses of these types of soils in the future.

7. ACKNOWLEDGMENTS

The financial assistance of the Earthquake Commission and the NZNSEE (Postgraduate Scholarship) is gratefully acknowledged. The authors also wish to thank Mr Graham Duske for his assistance with the MTS, and Vaughan Meyer and Jien Ma for their assistance with some of the experimental work.

8. REFERENCES

1. Chan S.Y., "Measurement of Dynamic Properties of Some Volcanic Ash Soils", 1990, M.E. Thesis, University of Auckland.

2. De Alba P., Seed H.B. and Chan C.K., "Sand Liquefaction in Large Scale Simple Shear Tests", 1976, Journal of the Geotechnical Division, Proc. ASCE, Volume 102, p. 909-927.

3. Holzer T.L., "Loma Prieta Damage Largely Attributed to Enhanced Ground Shaking", EOS, Volume 75, No. 26, p. 299-301.

4. Larkin T.J. and Donovan N.C., "Sensitivity of Computed Non Linear Effective Stress Soil Response to Shear Modulus Relationships", 1979, Proceedings of the Second U.S. National Conference on Earthquake Engineering, Stanford, p. 573-582.

5. Larkin T.J., Pranjoto S., Wesley L.D. and Pender M.J., "Engineering Properties of a New Zealand Pumice Sand", Geotechnique, (in review).

6. Marks S. and Larkin T.J., "The Seismic Response of Volcanic Sites", Report Ref. No. 4771.00, Auckland Uniservices Limited, pp. 207.

7. Meyer V.M., Marks S., Larkin T.J., Duske G.C., Wesley L.D. and Pender M.J., "Dynamic Properties of a Pumice Sand", 1997, Technical Conference of the NZNSEE, Wairakei.

8. O'Halloran M., :The Earthquake Stability of Earth Structures", 1986, PhD Thesis, University of Auckland.

9. Seed H.B., "Soil Liquefaction and Cyclic Mobility Evaluation for Level Ground During Earthquakes", 1979, Journal of the Geotechnical Division, Proc. ASCE, Volume 105, p. 201-255.

10. Seed H.B. and Idriss I.M., "Simplified Procedures for Evaluating Soil Liquefaction Potential", 1971, Journal of Soil Mechanics and Foundations Division, Proc. ASCE, Volume 97, p. 1249-1273.

11. Seed H.B., Martin P.P. and Lysmer J., "The Generation and Dissipation of Pore Water Pressures During Soil Liquefaction", 1975, EERC, University of California, Berkeley.

12. Seed H.B., Wong R.T., Idriss I.M. and Tokimatsu K., "Moduli and Damping Factors for Dynamic Analyses of Cohesionless Soils", 1984, Report No. EERC 84-15, University of California, Berkeley, California.

13. Tsuchida H. and Hayashi S., "Estimation of Liquefaction Potential of Sandy Soil", 1971, Proc. 3rd Meeting, U.S. Japan Panel on Wind and Seismic Effects, Tokyo.

Use of Simple Model for Dynamic Foundation Design

Nathan McKenzie, Prof. Michael J. Pender
Civil and Resource Engineering, The University of Auckland, New Zealand

SUMMARY: The dynamic response of a structure can be significantly influenced by the motion of the foundation and the under lying soil, increasing both the flexibility and damping of the system. These additional degrees of freedom can be included into a simple analysis of a structure using widely available stiffness and damping coefficients. This investigation compared the prediction of the response of a structure resting on an elastic soil layer using two models; a simple three degree of freedom model and a more complex finite difference program, using transfer functions as a means of comparison. It was found that the simple model closely predicted the first mode frequency and damping found in the complex model, but did not predict the deviation in response observed in the finite difference program. These differences were more significant for softer soils were the influence of the foundation was greater on the response of the structure. The deviation between the models was attributed to frequency dependence of the foundation coefficients and to the effect of the shallow soil layer causing shear waves to reflect back to the surface from the base rock.

1. INTRODUCTION

This paper presents some of the results of a research project into the influence of soil structure interaction (SSI) on the response of a structure subject to seismic loading. The response of a structure can be significantly altered by the inclusion of additional modes of vibration due to the translation and rotation of the foundation on the underlying soil. This becomes more influential for soft soils and for relatively rigid structures, where the first mode of the system tends to be strongly influenced by foundation modes of vibration.

Modeling of the structure and soil were made using two levels of sophistication. The first used a simple three degree of freedom system to model the structure and foundation. The second model was analysed using the finite difference program FLAC (Fast Lagrangian Analysis of Continua). The soil was modelled as a linear elastic layer with Rayleigh damping resting on a rock base, and the structure as a series of beams.

The aim of the investigation was to compare the simple model of a structure and foundation system with the FLAC model, with the soil remaining linear. The shear modulus of the soil profile was held constant over the depth of the soil layer for simplicity and a range of shear moduli were analysed. This had the effect of altering the relative dominance of the foundation on the response of the structure and altering the site response characteristics of the soil profile. Two aspects of this interaction were investigated; firstly the influence of the structure on the free field site response of the soil layer and secondly the effect of the soil layer on the response of the structure.

2. SIMPLE MODEL

2.1 Introduction

The simple model of the structure and foundation system used for this investigation was one with only three degrees of freedom (3DOF); one for the structure and two for the foundation to model translation and rotation of the foundation on the soil, refer to figure 1. The stiffness and damping coefficients for the foundation were found from solutions for a rigid foundation on an elastic halfspace, and were dependent on the soil shear modulus and Poisson's ratio (Wolff, 1988, Gazetas, 1990). Using these parameters the equations of motion were worked out for the system and the model solved in the time domain for a base acceleration time history. As the system was linear modal superposition could be used to uncouple the equations of motion. Of these uncoupled equations, it was necessary to discard one as its frequency was too high to allow a numerically stable solution to be found. But typically for the situations investigated this mode could be shown to have a negligible contribution to the response due to its low participation factor.

The foundation stiffness and damping parameters used in the analysis were chosen at the static value of the parameter. The foundation stiffness and damping in rotation and translation have been found to vary with the applied frequency of the loading, making it difficult to select the appropriate value of the parameter for use in a time domain analysis. This frequency dependence is further complicated by the presence of a relatively rigid layer at shallow depth by causing waves to reflect back to the structure. Including this frequency dependence is not possible for a solution in the time domain.

2.2 Equations of Motion

The equations of motion were determined for the structure as represented by figure 1. The degrees of freedom for the

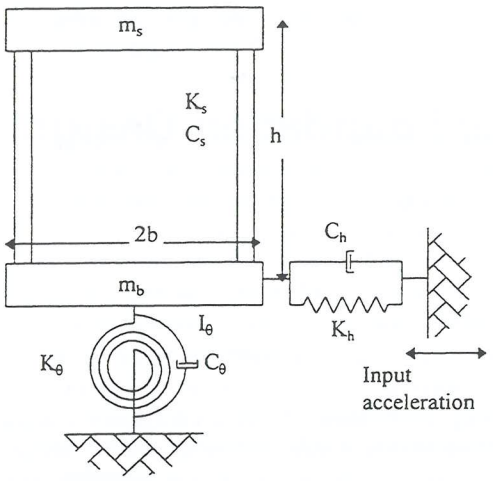

Figure 1. 3DOF model of structure and foundation.

system were the top of the structure relative to the base, and the foundation translation and rotation relative to an at rest position.

$$M_{ssi}\begin{bmatrix}\ddot{u}_s\\ \ddot{u}_b\\ \ddot{\theta}\end{bmatrix}+C_{ssi}\begin{bmatrix}\dot{u}_s\\ \dot{u}_b\\ \dot{\theta}\end{bmatrix}+K_{ssi}\begin{bmatrix}u_s\\ u_b\\ \theta\end{bmatrix}=-M_{load}\ddot{u}_g$$

For convenience the rotational degree of freedom was changed to the equivalent lateral motion of the structure due to rotation at the base. This was a relatively simple modification, but required the alteration of the mass, stiffness and damping matrices to maintain consistency within the model.

$$u_\theta = h\theta$$

The mass matrix for the system, including this change of coordinates, was

$$M_{ssi}=\begin{bmatrix}m_s & m_s & m_s\\ m_s & m_s+m_b & m_s\\ m_s & m_s & \dfrac{I_\theta}{h^2}\end{bmatrix}$$

where m_s was the mass of the structure, m_b was the mass of the base and I_θ was the rotational mass of the whole structure about the centre of the base. The stiffness, damping and loading matrices were as follows

$$K_{ssi}=\begin{bmatrix}K_s & 0 & 0\\ 0 & K_h & 0\\ 0 & 0 & \dfrac{K_\theta}{h^2}\end{bmatrix}$$

$$C_{ssi}=\begin{bmatrix}C_s & 0 & 0\\ 0 & C_h & 0\\ 0 & 0 & \dfrac{C_\theta}{h^2}\end{bmatrix}$$

$$M_{load}=\begin{bmatrix}m_s\\ m_s+m_b\\ m_s\end{bmatrix}$$

The stiffness and damping values used for the translation and rotation of the strip foundation were found using the following formulae, taken from Wolff (1988)

$$K_h = G(1+5\nu^2)$$

$$K_\theta = Gb^2(1.8+5.2\nu^2)$$

$$C_h = (2-2.2\nu)\frac{b}{V_s}K_h$$

$$C_\theta = (0.14-0.24\nu^2)\frac{b}{V_s}K_\theta$$

where G was the soil shear modulus, V_s was the soil shear wave velocity, ν was the soil Poisson's ratio, and b was the semi width of the foundation.

2.3 Modal Response of System

The equations of motion were uncoupled into a set of independent equations of motion using the principal of modal superposition. A requirement of modal superposition was that the coefficients of the mass, stiffness and damping matrices remained constant. This restricted the use of any modification the stiffness and damping values for the foundation to account for frequency dependence. The foundation coefficients used were the static values of stiffness and damping.

The modal frequencies and eigen vectors were determined according to the following equation

$$[K_{ssi}-\omega_j{}^2 M_{ssi}]\phi_j = \tilde{0}$$

where ω_j was the modal frequency and ϕ_j was the eigen vector of that mode. For this system there were three solutions to this equation, of which one had a very high frequency. This high frequency mode had a relatively minor contribution to the response of the system, and was left out of the subsequent analysis. This frequency became higher as I_θ became closer to $m_s h^2$. If I_θ was set to equal $m_s h^2$ this third mode disappeared altogether.

The relative influence of each mode was determined by the modal participation factor, Γ_j

$$\Gamma_j = \frac{\phi_j{}^T M_{load}}{\phi_j{}^T M_{ssi} \phi_j}$$

and the damping ratio, ξ_j, for each mode

$$\xi_j = \frac{1}{2\omega_j} \frac{\phi_j{}^T C_{ssi} \phi_j}{\phi_j{}^T M_{ssi} \phi_j}$$

The response of each mode of the system could then be solved for in the time domain and, using the modal participation factors and the eigen vectors, the response of the system determined.

This system was strongly influenced by the first mode. This mode was one in which all three contributing degrees of freedom were in phase with one another, denoted by the eigen vector components being either all positive or all negative. This dominance of the first mode meant that the influence of the foundation on the response of the system could be illustrated by comparison of the frequency and damping ratio of the structure and of the first mode of the structure and foundation system.

3. FLAC MODEL

The model of the soil and structure in FLAC was composed of a layer of soil overlaying a rigid rock base. For the linear analyses the soil was modelled as linear elastic with Rayleigh damping, centred around the natural frequency of the soil profile. The structure was modelled using beam elements to form a foundation and a structure which would behave as a single degree of freedom (SDOF) oscillator. The structure was comprised of two columns with a connecting beam at the top. The beams and columns were of equal length, and the Young's modulus of the columns was set at one tenth that of the top beam and the foundation, as was the density. This ensured that almost all of the flexure in the structure was in the columns with little rotation at the ends. Making that assumption the equivalent stiffness of this 'column sway' structure could be easily worked out and used in the simple model. Damping was included in the structure again using Rayleigh damping centred at the first mode of the structure.

The spacing of zones (the FLAC equivalent of elements) was set to meet two criteria. The first was to accurately pick up the high frequency components of the earthquake time history. This set the maximum spacing possible for the grid. The other was to model the soil accurately in the region of the foundation, where the gradients of stresses would be expected to be highest and to allow comparison between FLAC results with the formulae used in the 3DOF model for the foundation stiffness and damping values. This region of close spaced zones was set to a depth equal to the foundation width and extending half the foundation width either side. The remaining zones were then progressively scaled, minimising any rapid change in zone size. Care was also taken to keep the aspect ratio of zones within recommended range (less than ten). The model is shown in figure 2.

The analysis was composed of two section; static and dynamic. For the first part the soil zones and structure were allowed to find static equilibrium due to gravity. This was sped up considerably by applying initial internal stresses and boundary stresses to the zones based on the soils self weight, requiring that only the effect of the weight of the structure needed to be solved for.

In the second part of the analysis an earthquake time history was applied at the base. Acceleration time histories were recorded at the base and top of the soil profile and at the base and top of the structure. The acceleration time history at the base of the structure was used as the input to the 3DOF model. From these acceleration time histories the behaviour of the structure was investigated in both the time and frequency domain. By performing a fast Fourier transform (FFT) on the time history the frequency composition of the record could be examined, and transfer functions calculated for the structure. A FFT decomposes the time history into an equivalent series of sinusoidal waves with a magnitude and a phase angle (often as a complex number) over a range of frequencies. A transfer function between two points A and B, (the top and bottom of the structure for example) is the magnitude FFT at B divided by the FFT at A. This produces a curve which is independent of the original time history, and a means of interpretation and comparison of the results. Results in this form were used to compare between the 3DOF and FLAC models.

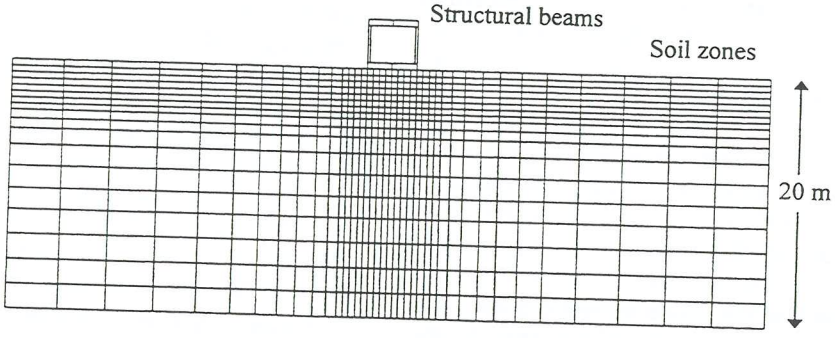

Figure 2. FLAC model of soil and structure

4. COMPARISON OF MODELS

4.1 Introduction

The FLAC model of soil and structure had the following properties:

Soil properties:

Density	$\rho = 2000$ kg m^{-3}
Shear modulus	$G_{max} = 10, 20, 40, 60$ MPa
Poisson's ratio	$\nu = 0.40$

Structure properties:

Frequency	$f_s = 3.883$ Hz
	$\omega_s = 24.398$ rads^{-1}
Width	$2b = 4$ m
Mass	$m_s = 12600$ kg
Mass of base	$m_b = 12600$ kg
Rotational mass	$I_s = 203.6e3$ kg m^2
Foundation contact pressure	$q = 61.8$ kPa

Acceleration time histories were recorded at soil nodes at the bottom of the soil layer and at the top of the soil layer beneath the foundation. The response of the structure was recorded at the centre of the foundation beams and at the centre of the top beam. From these time histories the response of each position was put into the frequency domain using a FFT, and the transfer functions for the site and the structure calculated.

For each linear analysis the soil shear modulus was different. This had two key effects; firstly it changed the response characteristics of the site, changing the magnitude and frequency composition of the excitation into the base of the structure. Secondly the shear modulus changed the dynamic properties of the foundation, which in turn changed the response of the structure. The shear moduli chosen ranged from having a considerable effect upon the behaviour of the structure to only a small influence upon its behaviour. The transfer function for the structure and the site are presented in figures 5, a to d.

For each FLAC analysis a simple 3DOF analysis was performed using the input motion into the structure at the base and the appropriate shear modulus for the determination of the foundation parameters. From this analysis the acceleration time history at the top of the structure was solved for and, using the method outlined earlier, the transfer function for the structure found. This was then compared to that for the FLAC model, also shown in figure 5, a to d.

4.1 Effect of SSI on response of structure

The relative influence of SSI on the response of the structure can be summarised by Table 1. These results were determined from the 3DOF, using modal superposition to solve for the first modes of vibration and the damping ratios of the structure and foundation system. This table shows the decrease to the first mode of the system as the soil softens and the foundation motion becomes more dominant in the vibration of the structure. There was also the expected increase in damping for this first mode.

Table 1. Frequencies and damping ratios of first mode of structure and foundation system for 3DOF model

Shear modulus	First mode frequency, f_1	First mode damping, ξ_1
10 MPa	2.390 Hz	0.0649
20 MPa	2.888 Hz	0.0437
40 MPa	3.282 Hz	0.0298
60 MPa	3.454 Hz	0.0253
Structure	3.883 Hz	0.0211

4.2 Influence of Structure on Site Response

A comparison of the transfer functions of a site with the structure present and of a site with free field conditions is shown in figures 3 and 4 for two shear moduli, G = 10 MPa and 20 MPa. The general trend from these comparisons was of a general lessening in the amplification of the site with the structure present, shown by the reduction in the peaks of the transfer functions where the structure is present. The other main point of interest was the distortion of the transfer curve in the frequency range corresponding to the first mode of the structure and foundation system. This distortion was particularly evident for the G = 10 MPa transfer function. This is discussed further in the following section.

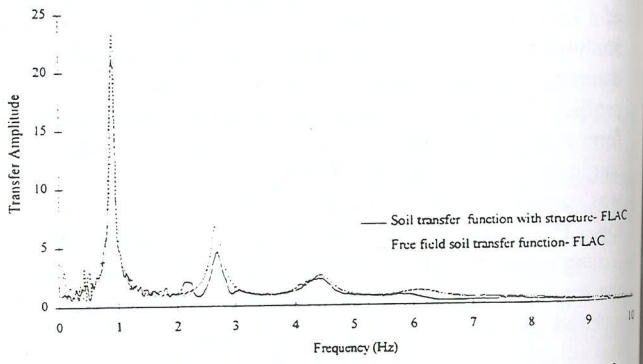

Figure 3. Site response transfer function for free field and with structure, G = 10 MPa.

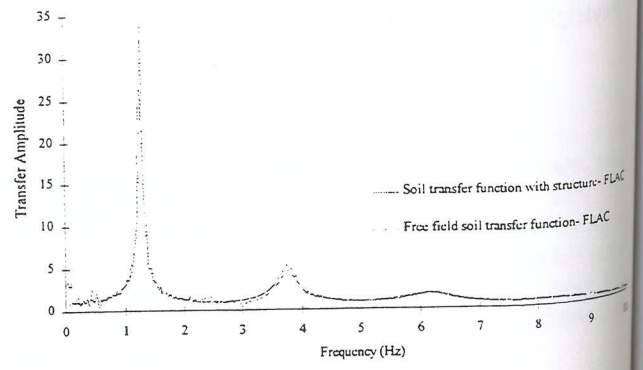

Figure 4. Site response transfer function for free field and with structure, G = 20 MPa.

Both of these effects had an influence on the acceleration time history at the top of the soil layer. This is presented in Table 2. The effect of the structure was most significant for the softest site, with a 24 % drop in the peak ground acceleration at the surface. For the G = 20 MPa site the drop in peak ground acceleration was 7 %. For the stiffer sites the change was less significant. This reduction in response had significance for the use of the 3DOF model. As an alternative to the recorded acceleration time history at the base of the structure, the free field motion could be used, and would usually be conservative.

Table 2. Influence of structure on peak ground acceleration of site.

Peak ground acceleration	G = 10 MPa	G = 20 MPa
Base acceleration	2.174 ms^{-1}	2.174 ms^{-1}
Top acceleration: Free field	4.449 ms^{-1}	3.075 ms^{-1}
Top acceleration: Structure	3.400 ms^{-1}	2.854 ms^{-1}

4.3 Influence of Site on Structural Response

From a comparison of the transfer functions for the structure and the FLAC model a general fit between the two in terms of the frequency and amplitude of the peak response of the structure. The shape of the transfer function for the FLAC structure was not a regular as that predicted by the 3DOF model however. The FLAC transfer function tended to dip more rapidly than the 3DOF model and was generally over predicted by the 3DOF model over a range of frequencies around the peak. This was most evident for the softest site (G_{max} = 10 MPa). As the shear modulus of the site increased the FLAC transfer function became more regular. The difference between the FLAC and the 3DOF models was also very evident in the comparison of the acceleration time histories of the top of the structure. The 3DOF model predicted significantly higher accelerations than were recorded in the FLAC model.

The cause of the difference between the FLAC and the 3DOF models can be strongly linked to frequency dependent factors not incorporated into the 3DOF model. When the site transfer function at each site was looked at for each analysis the was significant distortion of the transfer function in the same region as the FLAC structure transfer function deviating from what was predicted by the 3DOF model. This again was most evident for the softest site. The first mode of the structure and foundation system (2.39 Hz) corresponds roughly to the second mode of the site (2.65 Hz), and the expected peak in the site transfer function was considerable reduced by the influence of the structure. For the stronger sites the influence reduces to only a small deviation in the site transfer function for the stiffest site investigated. Also for the stiffer sites the frequencies of major structural amplification did not coincide with those of the site.

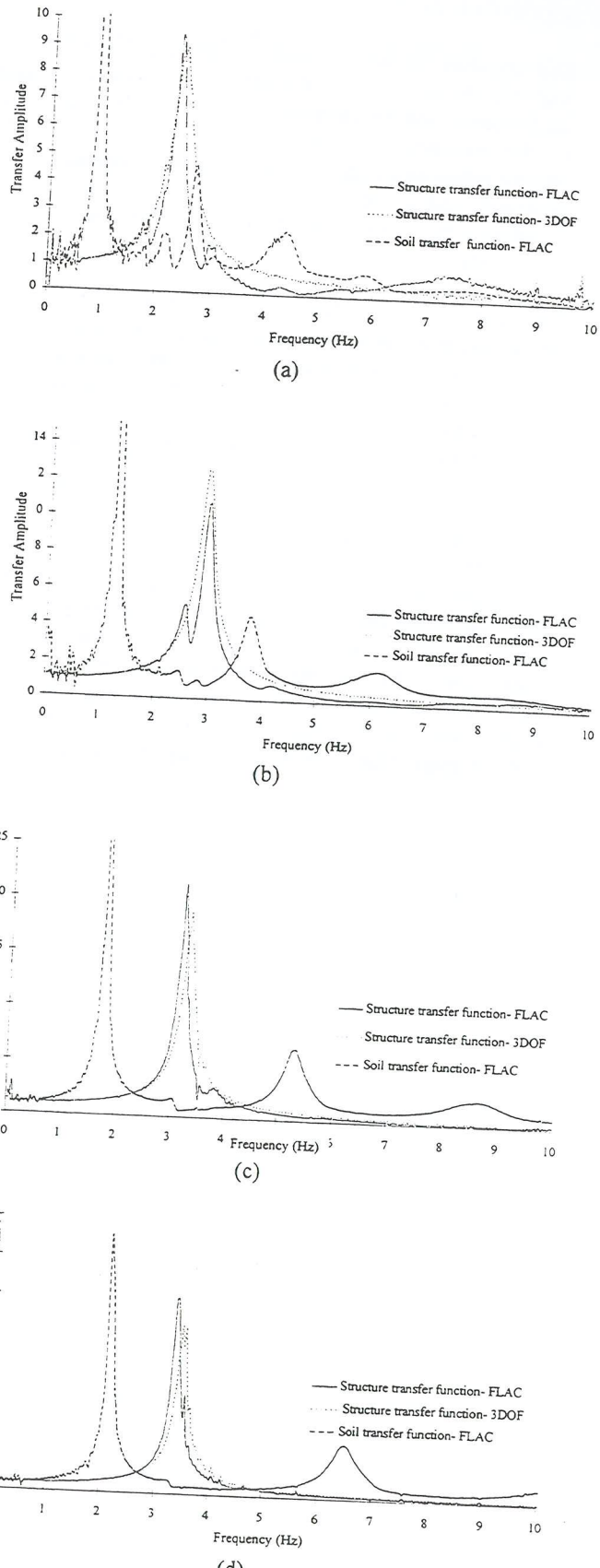

Figure 5. Structural transfer functions for FLAC and 3DOF models; (a) 10 MPa, (b) 20 MPa, (c) 40 MPa and (d) 60 MPa

5. CONCLUSIONS

Soil structure interaction had a significant effect on the response characteristics of the structure, generally increasing the flexibility and the damping of the first mode of the system by the inclusion of additional modes of vibration. The relative influence of SSI on the response increases for stiffer structures, and for structures with little damping, where the foundation may provide the dominant stiffness and damping to the system.

The structure has an influence on the response of the site, and hence the input acceleration it experiences. For the sites investigated the structure reduced the acceleration at the top of the soil profile. This was evident by a reduction in the peak ground acceleration and a general reduction in the transfer function for the site when the structure was present, relative to the free field response.

The response of the structure was reasonably well predicted by the 3DOF model, particularly in the peak amplification of the transfer function at the first mode and the damping at this peak. However, there were significant variations between the two models in the ranges of frequency around the first mode. These were due to the frequency dependence of the foundation stiffness and damping parameters, and due to seismic waves rebounding to the surface from the rock base. Both of these effects were evident by the distortion of the transfer functions for the site and structure for the FLAC model. These frequency dependant effects were most significant for the softest site (G = 10 MPa), and decreased for stiffer sites.

6. ACKNOWLEDGMENTS

The authors would like to acknowledge Dr. T. J. Larkin for his contribution to this paper.

7. REFERENCES

Gazetas, G. (1990). "Foundation Vibrations" in "Foundation engineering handbook, 2nd ed.", Fang, Hsai- Yang Ed. Van Nostrand Reinhold, New York. Chapter 15, p 586

Wolf, John P. (1988). "Soil-structure-interaction in time domain," Prentice Hall, New Jersey, pp. 35- 40.

Wolf, John P. (1994). "Foundation vibration analysis using simple physical models," Prentice Hall, New Jersey, pp. 341-361

Third A-NZ Young Geotechnical Professionals Conference, Cameron, Collingwood & Slatter (eds), Feb. 1998, Melbourne, Australia.

The Bearing Capacity of Strip Footings on Two-Layered Clays

R. S. Merifield

Department of Civil, Surveying and Environmental Engineering University of Newcastle, NSW 2308

ABSTRACT

This paper applies numerical limit analyses to evaluate the undrained bearing capacity of a rigid surface footing resting on a two-layer clay deposit. Rigorous bounds on the ultimate bearing capacity are obtained by employing finite elements in conjunction with the upper and lower bound limit theorems of classical plasticity. Results from the limit theorems typically bracket the true collapse load by approximately twelve per cent, and have been presented in the form of bearing capacity factors based on various layer properties and geometries. A comparison is made between existing limit analysis, empirical and semi-empirical solutions. This indicates that the latter can overestimate or underestimate the bearing capacity by as much as twenty per cent for certain problem geometries.

1. INTRODUCTION

The ultimate bearing capacity of surface strip footings resting on a single layer of homogeneous undrained clay has been studied by numerous investigators with practitioners generally using Terzaghi's (1943) expression to compute ultimate footing loads. In reality, however, soil strength profiles beneath footings are not homogeneous but may increase or decrease with depth or consist of distinct layers having significantly different properties. Whilst the effect of increasing strength with depth on bearing capacity has been addressed by several researchers, notably Davis and Booker (1973), rigorous solutions to the problem of footings resting on layered clays do not appear to exist.

To calculate the ultimate bearing capacity for surface strip footings resting on a horizontally layered clay profile, practitioners commonly use the approximate solutions of Button (1953), Reddy and Srinivasan (1967), Chen (1975), Brown and Meyerhof (1969) and Meyerhof and Hanna (1978). Button (1953) and Chen (1975) calculated upper bound solutions assuming a simple circular failure surface (Figure 2) while Reddy and Srinivasan (1967), assuming the same circular mechanism, obtained results using the method of limiting equilibrium. The solutions of Brown and Meyerhof (1969) and Meyerhof and Hanna (1978) were based upon a series of model footing tests from which empirical and semi-empirical solutions for the bearing capacity factor were derived.

In view of its simplicity, past research into the bearing capacity on layered clays using the limit theorems appears to be restricted exclusively to the upper bound method of analysis. A more desirable solution for engineering practice is a lower bound estimate as it results in a safe design and, if used in conjunction with an upper bound solution, serves to bracket the actual collapse load from above and below.

The purpose of this paper is to take advantage of the ability of the limit theorems to enclose the actual collapse load by computing both types of solution for the bearing capacity of strip footings on a two layered clay profile. These solutions are obtained using the numerical techniques developed by Sloan (1988) and Sloan and Kleeman (1995), which are based upon the limit theorems of classical plasticity and finite elements. The methods assume a perfectly plastic soil model with a Tresca yield criterion and lead to large linear programming problems. The solution to the lower bound optimisation problem defines a statically admissible stress field and gives a rigorous lower bound to the ultimate bearing capacity. The solution to the upper bound optimisation problem defines a kinematically admissible velocity field and hence results in a rigorous upper bound to the ultimate bearing capacity. A statically admissible stress field is one which satisfies equilibrium, the stress boundary conditions and the yield criterion while a kinematically admissible velocity field is one which satisfies compatibility, the flow rule and the velocity boundary conditions.

2. PROBLEM DEFINITION

The plane strain bearing capacity problem to be considered is illustrated in Figure 2. A strip footing of width B rests upon an upper layer of clay with undrained shear strength c_{u1} and thickness H. This is

underlain by a clay layer of undrained shear strength c_{u2} and infinite depth.

The bearing capacity solution to this problem will be a function of the two ratios H/B and c_{u1}/c_{u2}. Past research by Brown and Meyerhof (1969) and Meyerhof and Hanna(1978) indicates that a reduction in bearing capacity for a strong-over-soft clay system may occur up to a depth ratio of $H/B \simeq 2.5$. In this paper solutions have been computed for problems where H/B ranges from 0.125 to 2 and c_{u1}/c_{u2} varies from 0.2 to 5. This should cover most problems of practical interest. Note that $c_{u1}/c_{u2} > 1$ corresponds to the common case of a strong clay layer over a soft clay layer, whilst $c_{u1}/c_{u2} < 1$ corresponds to the reverse.

The bearing capacity of a shallow strip footing on a clay layer can be written in the form

$$q_u = c_u N_c + q \qquad (1)$$

where N_c is a bearing capacity factor and q is a surcharge. For a surface strip footing this equation reduces to

$$q_u = c_u N_c \qquad (2)$$

For the case of a layered soil profile it is convenient to rewrite (2) in the form

$$N_c^* = \frac{q_u}{c_{u1}} \qquad (3)$$

where c_{u1} is the undrained shear strength of the top layer and N_c^* is a modified bearing capacity factor which is a function of both H/B and c_{u1}/c_{u2}. The value of N_c^* will be computed using the results from both upper and lower bound analyses for each ratio of H/B and c_{u1}/c_{u2}. For a homogeneous profile with $c_{u1}=c_{u2}$, N_c^*equals the well known Prantl solution of $(2 + \pi)$. For the range of problem geometries considered, the bound solutions are typically able to bracket the exact bearing capacity factor to within twelve percent or better.

3. FINITE ELEMENT FORMULATION OF LIMIT THEOREMS

The following is only a brief summary of the numerical formulation of the limit theorems and only those aspects specifically related to the current study of bearing capacity are mentioned. Full details of the numerical procedures can be found in Sloan (1988) and Sloan and Kleeman (1995), and will not be repeated here.

Lower bound formulation

The lower bound solution is obtained by modelling a statically admissible stress field using finite elements where stress discontinuities can occur at the interface between adjacent elements. Application of the stress boundary conditions, equilibrium equations and yield criterion leads to an expression of the collapse load which is maximised subject to a set of linear constraints on the stresses.

Unlike the more familiar displacement finite element method, each node is unique to a particular element and therefore any number of nodes may share the same coordinates. This enables a wide range of stress fields to be modelled by permitting statically admissible stress discontinuities at all edges that are shared by adjacent elements, including those edges that are shared by adjacent extension elements.

To furnish a rigorous lower bound solution for the collapse load, it is necessary to ensure the stress field obeys equilibrium, the stress boundary conditions and the yield criterion. Each of these requirements imposes a separate set of constraints on the nodal stresses.

For many plane strain geotechnical problems, we seek a statically admissible stress field which maximises an integral of the normal stress σ_n over some part of the boundary. Denoting the out-of-plane thickness by h, these integrals are typically of the form

$$P = h \int_S \sigma_n \, ds \qquad (4)$$

where P represents the collapse load.

By assembling the various constraints and objective function coefficients for the overall mesh, a statically admissible stress field which maximises the collapse load may be found. A lower bound solution for the footing problem is obtained by maximising the integral of the compressive stress along the soil footing interface.

Upper bound formulation

An upper bound on the exact collapse load can be obtained by modelling a kinematically admissible velocity field. To be kinematically admissible, such a velocity field must satisfy the set of constraints imposed by compatibility, velocity boundary conditions and the flow rule. By prescribing a set of velocities along a specified boundary segment we can equate the power dissipated internally, due to plastic yielding within the soil mass and sliding of the velocity discontinuities, with the power dissipated by the external loads to yield a strict upper bound on the true limit load.

The three noded triangle is again used for the upper bound formulation. Now, however, each node is associated with two unknown velocities and each element has p non-negative plastic multiplier rates (where p is the number of sides in the linearised yield criterion).

To define the objective function, the dissipated power (or some related load parameter) is expressed in terms of the unknown plastic multiplier rates and discontinuity parameters. As the soil deforms, power dissipation may occur in the velocity discontinuities as well as in the triangles.

Once the constraints and the objective function coefficients are assembled, a kinematically velocity field which minimises the internal power dissipation for a specified set of boundary conditions, may be found.

An upper bound solution is obtained by prescribing a unit downward velocity to the nodes directly below the footing along with the additional constraint that the footing cannot move horizontally. After the corresponding optimisation problem is solved for the imposed boundary conditions, the collapse load is found by equating the dissipated power to the power expended by the external forces. The results for the simple case of a surface footing resting on a homogeneous soil profile are shown in Figure 1, where the bearing capacity factor N_c^* was found to equal 5.32 (approximately 3 percent above the exact Prantl solution of $N_c^* = (2 + \pi)$

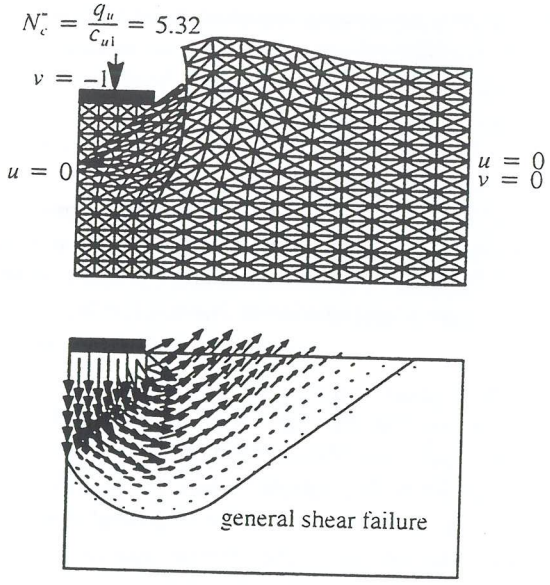

Figure 1 Deflected mesh and velocity diagram for a homogeneous soil profile

4. RESULTS AND DISCUSSION

The computed upper and lower bound estimates of the bearing capacity factor N_c^* for layered clay soils are shown graphically in Figure 3 and Figure 4. These results indicate that, for practical design purposes, sufficiently small error bounds were achieved with the true collapse load typically being bracketed to within 12% or better.

Figure 3 and Figure 4 also compare the numerical bounds and the available upper bound solutions of Chen (1975), the empirical solutions obtained by Brown and Meyerhof (1969), and the semi-empirical solutions of Meyerhof and Hanna (1978).

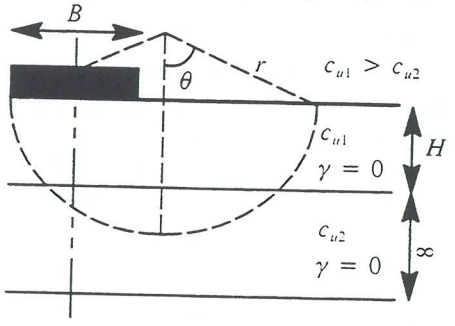

Figure 2 Circular mechanism – Chen

The bearing capacity factors obtained by Chen (1975) were obtained by assuming a circular failure mechanism as shown in Figure 2.

By equating the rate of internal and external work an upper bound expression for the bearing capacity factor can be derived. For a homogeneous soil profile this expression can be solved analytically to give a value of N_c^* =5.53. This is approximately 8 percent above the exact Prantl solution of $N_c^* = (2 + \pi)$.

The ultimate bearing capacity of a footing resting on a strong-over-soft clay deposit, as determined by Meyerhof and Hanna (1978), is based on the assumption that failure occurs by punching shear through the top layer followed by general shear failure of the bottom layer. The ultimate capacity is given by

$$q_u = c_{u2}N_c + 2c_aH/B \qquad (5)$$

where $N_c = 5.14$.

In terms of physical behaviour, the second term in this equation is representative of some type of punching shear through the strong top layer, with the first term reflecting full general shear failure in the bottom layer. The term c_a is defined as the unit adhesion acting on the assumed punching shear plane through the strong top crust and was derived from experimental results. Equation (5) can be rearranged to give the bearing capacity factor N_c^* as

$$N_c^* = \frac{q_u}{c_{u1}} = N_c\left(\frac{c_{u2}}{c_{u1}}\right) + 2\left(\frac{c_a}{c_{u1}}\right)\left(\frac{H}{B}\right) \qquad (6)$$

Brown and Meyerhof (1969) provided charts of the bearing capacity factor N_c^* for both strong-over-soft and soft-over-strong clay profiles based on a series of model laboratory tests. Their results for the soft-over-strong case are reproduced in Figure 3 and Figure 4 for comparison purposes.

Footings on strong clay overlying soft clay

The upper and lower bound results clearly indicate that a complex relationship exists between general, local and punching shear failure and the ratios c_{u1}/c_{u2} and *H/B*. Failure generally occurs by either partial or full punching shear through the top layer followed by yielding of the bottom layer. The distinction between these two failure modes is illustrated in Figure 5. Full punching shear is characterised by a complete vertical separation of the top layer which then effectively acts as a rigid column of soil that punches through to the bottom layer. Conversely, only a small vertical separation of the top layer is evident for partial punching shear (Figure 5(a)), with both local vertical and lateral deformation of the soil column below the footing now apparent. Full punching shear typically occurs for ratios of $H/B \leq 0.5$, regardless of the ratio c_{u1}/c_{u2}, while for $H/B>0.5$ the division between full and partial punching shear occurs at c_{u1}/c_{u2} approximately equal to 2.5. The extent and form of yielding within the bottom layer is dependent on both the depth and strength of the overlying top layer. This is best illustrated by the velocity diagrams shown in Figure 6.

For the case of moderately strong crusts ($c_{u1}/c_{u2} \leq 2.5$), failure is generally caused by partial punching shear. For thin top crusts with $H/B<0.5$, the overall failure mechanism is similar to that depicted in Figure 1. As the depth of the top crust approaches the footing width *B*, upward deformations within the bottom layer become restricted causing an increase in the extent of plastic yielding(see Figure 6)

As the top crust becomes very strong compared to the bottom layer ($c_{u1}/c_{u2} \geq 2.5$) full punching shear through the top layer occurs. The very strong top layer then serves to greatly restrict both lateral and vertical movement of the soil contained in the soft layer below (see Figure 6). This results in the formation of a deep zone of plastic shearing within the bottom layer and, for thicker crusts ($H/B >0.75$), a local elastic zone is formed within the top layer immediately adjacent to the footing.

The limit analysis results indicate that a reduction in bearing capacity for a strong-over-soft clay system occurs up to a depth ratio of $H/B \approx 1.5$ - 2.0. This lower limit is applicable for soil profiles where $c_{u1}/c_{u2} \leq 2.5$, but for profiles that have a very strong top crust with $c_{u1}/c_{u2} \geq 2.5$, punching failure through the top layer is likely to occur up to depth ratio of $H/B=2$. For ratios of $H/B >2$, failure is contained entirely within the top layer and is independent of the ratio c_{u1}/c_{u2}. These results are similar to those predicted by Chen (1975), but are lower than those estimated by Meyerhof and Hanna (1978), who suggest a reduction in bearing capacity may occur up to a depth ratio of $H/B \simeq 2.5$.

The analytical upper bounds obtained by Chen (1975),

who assumed a simple circular failure mechanism, compare favourably with those obtained from the finite element upper bounds for smaller values of H/B but become rather unconservative when $H \geq B$.

For ratios of $H/B \leq 0.5$, the solutions of Chen are less than 5% above the upper bound limit analysis results for all values of c_{u1}/c_{u2}. For larger values of H/B, the solutions of Chen become increasingly inaccurate as c_{u1}/c_{u2} increases, with a maximum error of approximately 15% for H/B=1.5 and c_{u1}/c_{u2}=5. The reason for this is that for larger values of H/B and c_{u1}/c_{u2}, the assumed mechanism of Chen (1975) is no longer a good representation of the true collapse mechanism. The optimal mechanism using a circular failure surface is found to lie almost entirely within the top layer. This is in contrast to the finite element limit analysis results which clearly indicate that the failure mechanism that yields the best upper bound penetrates deeply into the soft bottom layer.

With reference to Figure 3 and Figure 4 it can be seen that for a soil profile having a moderately strong top crust ($c_{u1}/c_{u2} \leq 2.5$) the solutions of Meyerhof and Hanna (1978) typically lie either within or just outside the upper and lower bound solutions. For very strong top crusts ($c_{u1}/c_{u2} > 2.5$), these solutions tend to become over conservative as H/B increases, and lie 12-16% below the lower bound solution. This margin is likely to increase to as much as 20% upon further refinement of the lower bound mesh.

As with the solutions of Chen (1975), the solutions of Meyerhof and Hanna (1978) are limited by their assumption that a single type of failure mechanism exists. Only for the restricted case of thin, moderately strong crusts, where $H/B \leq 0.5$ and $c_{u1}/c_{u2} \leq 2.5$, does the assumption of punching through the crust followed by general shear failure in the bottom layer appear, to some degree, to be valid. This assumption is clearly not correct for larger top crust thicknesses or if the crust is substantially stronger than the bottom layer. For these cases, failure tends to be either a combination of general shear failure through both layers or a deep rotational mechanism, depending on the ratio of the layer strengths c_{u1}/c_{u2}.

Footings on soft clay overlying strong clay

The upper and lower bound results indicate that for ratios of $H/B \leq 0.5$, the bearing capacity increases as the relative strength of the bottom layer rises. For all of these cases the proportion of yielding within the bottom layer decreases as its strength increases. At a limiting ratio of c_{u1}/c_{u2}, no further increase in bearing capacity is achieved as the failure surface becomes fully contained within the top layer. This is represented by the sudden change in the curvature of the plots shown in Figure 3 and Figure 4. As an example, for H/B=0.125 the bearing capacity increases as c_{u1}/c_{u2} decreases until a limiting value of c_{u1}/c_{u2}=0.5 is reached. After this point failure is fully contained within the top layer.

For all values of $H/B > 0.5$, the bound solutions indicate that failure occurs entirely within the top layer and the bearing capacity is independent of the strength of the bottom layer.

The upper bound solutions of Chen (1975) overestimate the bearing capacity factor for all cases where $c_{u1}/c_{u2} < 1$ and are 5-22% above the upper bound finite element solutions. The overestimate is greatest for small top layer thicknesses where $H/B \leq 0.375$. The reason for this is that the optimal slip circle determined by Chen (1975) penetrates deeper into the underlying strong layer than the mechanism predicted by the finite element solution. When the failure mechanism is contained within the thin top layer, failure is by lateral squeezing and local failure at the footing edge and is therefore not accurately modelled by a circular slip mechanism.

As H/B increases above 0.375, the accuracy of the Chen (1975) solutions improves and typically lies 3-7% above the upper bound finite element solutions. This is because the majority of yielding occurs within the top layer and the actual failure mode can now be adequately modelled by a rotational failure mechanism. For $H/B \geq 0.75$ failure occurs entirely within the top layer and the exact solution for these cases will be $N_c^* = 5.14$, the Prandtl solution. This implies that the error in the upper bound finite element solutions is $\approx$3%, while the error in the Chen (1975) solutions is $\approx$6-7%.

The empirical results given by Brown and Meyerhof (1969) are limited to c_{u1}/c_{u2} ratios between 1 and 0.5. For relatively thin top layers with $H/B \leq 0.5$, the solutions of Brown and Meyerhof typically lie near the lower bound finite element solutions. As the top layer thickness increases above $H/B > 0.5$, failure becomes contained within it and the Brown and Meyerhof

(1969) solution lies central to both upper and lower bound finite element solutions.

5. CONCLUSIONS

The undrained bearing capacity of a surface strip footing resting on a layered clay profile has been investigated. Using recent numerical formulations of the upper and lower bound limit theorems, rigorous bounds on the bearing capacity for a wide range of problem geometries have been obtained, with the exact collapse load typically being bracketed to within 12%. The results obtained have been presented in terms of a modified bearing capacity factor N_c^* in both graphical and tabular form to facilitate their use in solving practical design problems.

The following conclusions can be made based on the limit analysis results :

- For a strong-over-soft clay profile a number of different failure mechanisms exist that are functions of both the crust thickness and its strength relative to the underlying weaker layer. For this reason, existing upper bound and semi-empirical solutions that are based on a single assumed failure surface are unable to model the likely failure mode over a large range of problem geometries.
- Existing upper bound,empirical and semi-empirical solutions can differ from the bound solutions by up to $\pm 20\%$. The existing solutions are in greatest error when the top layer is very strong compared to the bottom layer ($c_{u1}/c_{u2} > 2.5$) and/or its depth is greater than half the footing width ($H/B > 0.5$).
- A reduction in bearing capacity for a strong-over-soft clay system occurs up to a depth ratio of $H/B \approx 1.5$ - 2.0, where the lower limit is applicable for soil profiles with $c_{u1}/c_{u2} \leq 2.5$. For depth ratios of $H/B > 2$, failure is likely to be fully contained within the top layer and the bearing capacity is given by the Prandtl solution $N_c^* = 2 + \pi$.
- For a soft-over-strong clay system where $H/B \leq 0.5$, the bearing capacity is likely to increase as the relative strength of the bottom layer rises. For thicker top layers where $H/B > 0.75$, failure occurs entirely within the top layer and the bearing capacity is given by the Prandtl solution $N_c^* = 2 + \pi$.

REFERENCES

1. Brown, J. D., and Meyerhof, G.G. (1969). Experimental study of bearing capacity in layered clays. *Proceedings, 7th International Conference on Soil Mechanics and Foundation Engineering, Mexico, vol.* 2, pp. 45-51.
2. Button, S.J. (1953). The bearing capacity of footings on a two-layer cohesive subsoil. *Proceedings, 7th International Conference on Soil Mechanics and Foundation Engineering, Zurich, vol1*, pp. 332-335.
3. Chen, W. F. (1975). *Limit Analysis and Soil Plasticity*. Elsevier, Amsterdam.
4. Meyerhof, G.G, and Hanna, A.M. (1978). Ultimate bearing capacity of foundations on layered soils under inclined load. *Canadian Geotechnical Journal*, 15, pp. 565-572.
5. Reddy, A.S. and Srinivasan, R.J., (1967). Bearing capacity of footings on layered clays. *Journal of the Soil Mechanics and Foundations Division, ASCE*, 93, SM2, 83-99.
6. Sloan, S. W., (1988). Lower bound limit analysis using finite elements and linear programming. *International Journal for Numerical and Analytical Methods in Geomechanics*, 12, pp. 61-67.
7. Sloan, S. W., and Kleeman P. W. (1995). Upper bound limit analysis using discontinuous velocity fields. *Computer Methods in Applied Mechanics and Engineering*, 127, pp. 293-314

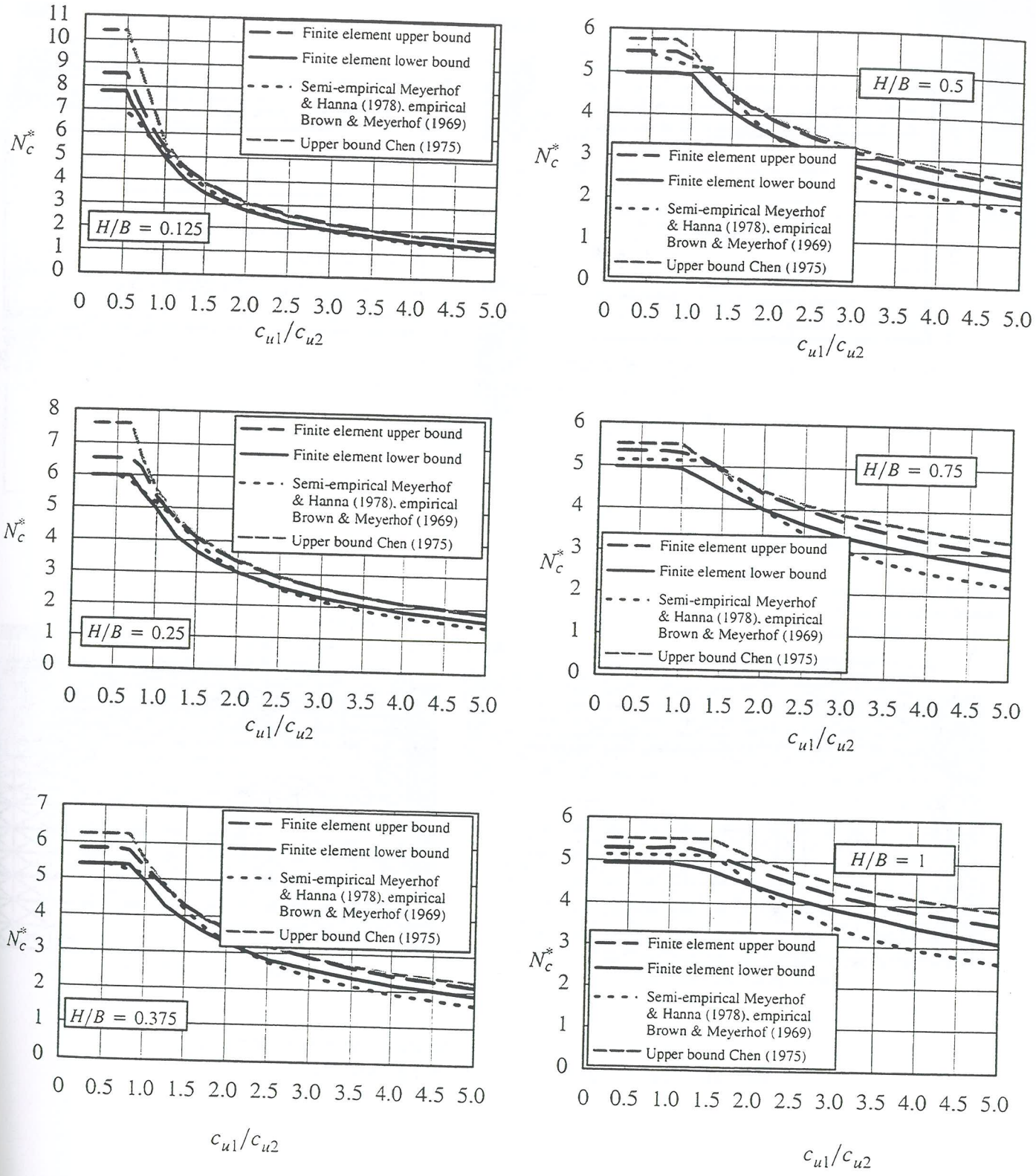

Figure 3 Variation of bearing capacity factor N_c^* (H/B=0.125 to H/B=1.0)

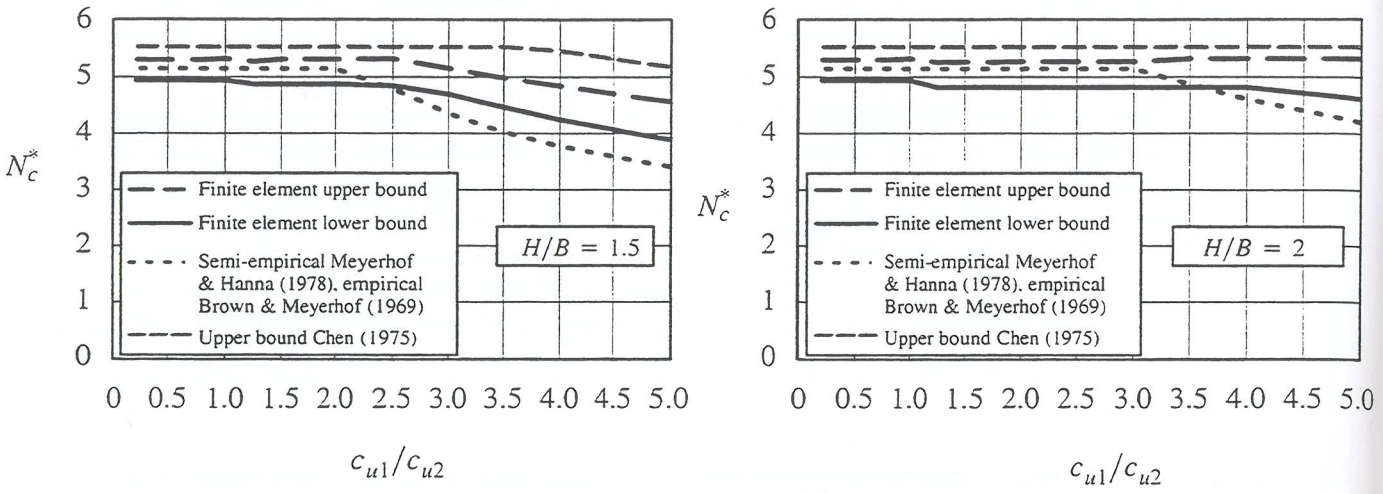

Figure 4 Variation of bearing capacity factor N_c^* (H/B=1.5 and H/B=2)

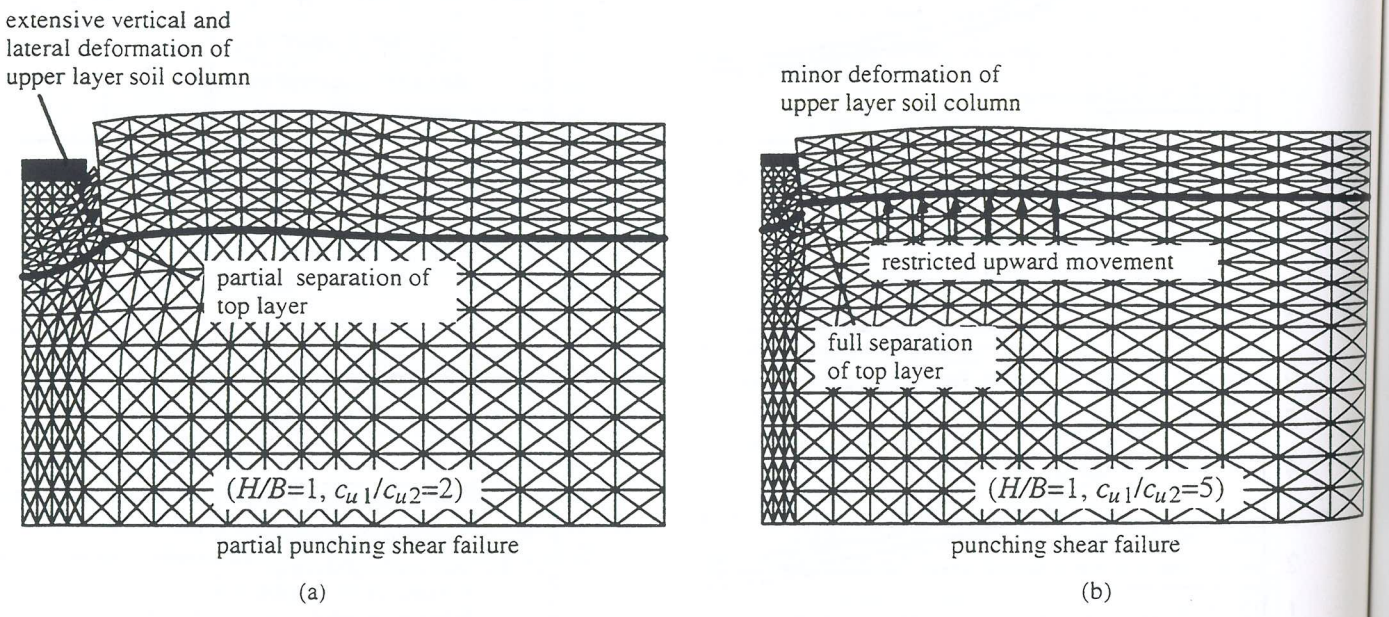

Figure 5 Deflected mesh and zone of plastic yielding for partial punching shear failure and full punching shear failure.

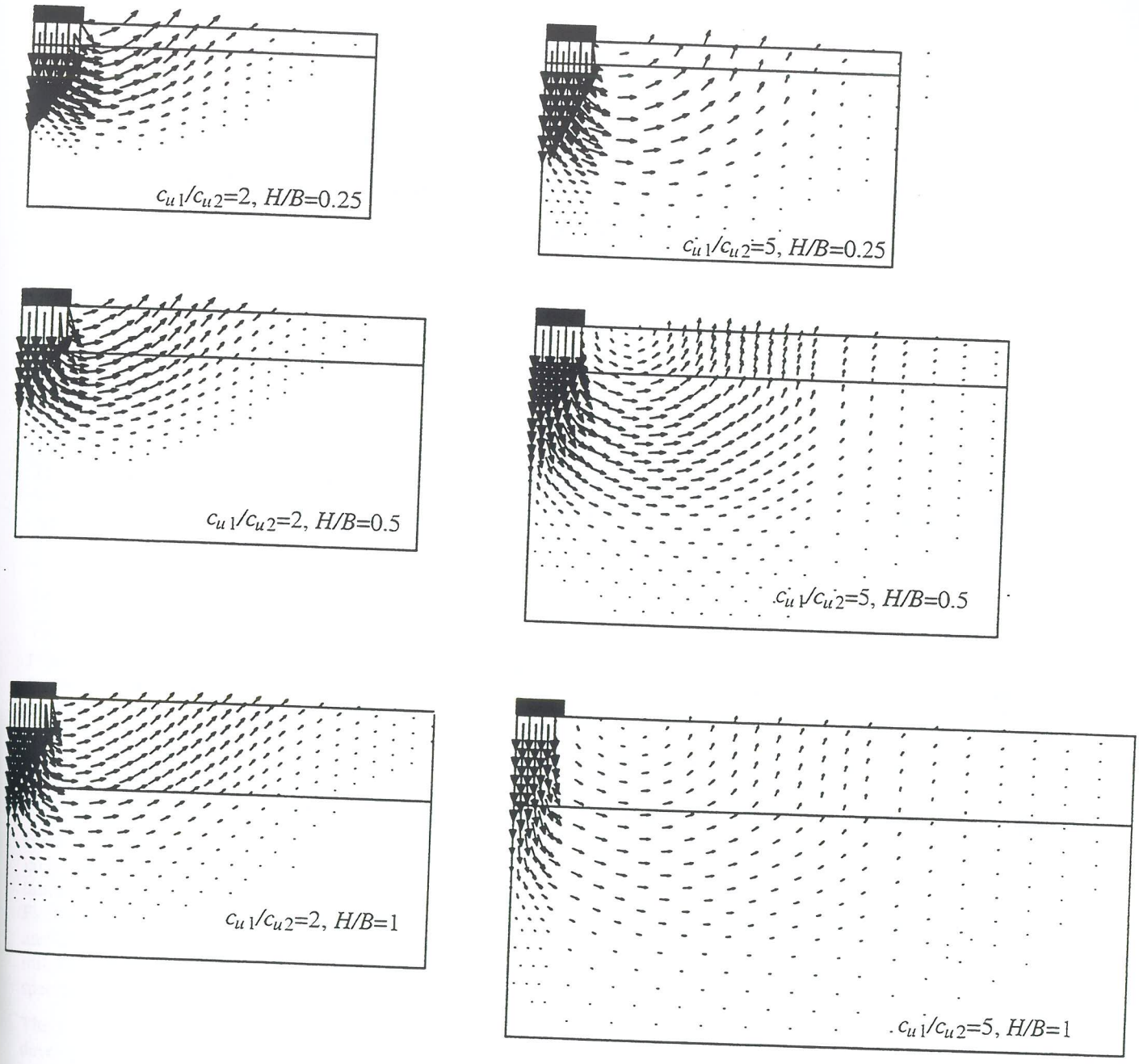

Figure 6 Velocity diagrams for strong-over-soft layers
(c_{u1}/c_{u2}=2,5 and H/B=0.25,0.5)

A Brief Overview of the Development of a Landslide Prediction and Management System for the East-West Highway, Malaysia

Stephen Newman
AGC Woodward-Clyde Pty Ltd
Melbourne, Australia

Summary

This paper presents a brief overview of the development of a landslide prediction and slope management system for the East-West Highway in northern Peninsular Malaysia. The collection and effective utilisation of large amounts of data is discussed along with the development of landslide hazard and risk ratings for over 1,000 embankments and cuttings along the highway.

1.0 INTRODUCTION

The East-West Highway is located in the northern states of peninsular Malaysia and forms the only significant transport link between the east and west coasts in the northern section of the country. The highway is 112.6 km long and was opened in 1982 after a construction period of twelve years. The highway traverses the rugged Main Range mountains which, in the past, have formed a barrier to cross peninsular communications and commerce.

Even prior to opening, the highway had been affected by large landslides. This instability has continued with some landslides requiring road closures of up to a week. Fatalities due to landslides have occurred. Between 1982 and 1995 approximately 521 million Ringgit (roughly 250 million AUD at 1995 exchange rates) had been spent specifically on landslide remedial works on the highway.

There are several contributing factors that have lead to the development of widespread slope instability on the highway. These include:

- the rugged nature of the terrain (steepness, dense primary jungle);
- high rainfall;
- deep residual soil profiles; and
- an active communist insurgency during construction. Guerrilla activities resulted in the adoption of high embankments and steep cuts to avoid the sabotage of tunnels and bridges. The unrest also put a premium on speed and resulted in minimal forward planning i.e. selection of the best corridor. In addition construction was under armed guard and the surrounding jungle was mined.

In an effort to reduce its long term expenditure on landslide remediation, the Government of Malaysia commissioned the *"East-West Highway Long Term Preventive Measures and Stability Study"* to provide a rational basis for the allocation of funds for landslide prevention, remediation and slope maintenance works along the highway. The team for this project was comprised of the Government of Malaysia, Perunding Zaaba (Malaysia), Soil and Rock Engineering (Malaysia), the University of Bristol and the University of Strathclyde.

The three year study was completed in September 1996 and resulted in delivery to the Malaysian Public Works Department of a prioritised listing of the risk of landsliding for all the slopes (1,123 slopes comprising 464 cuts, 577 embankments and 82 natural slopes) along the highway. This risk rating was then used to prioritise landslide prevention works. In addition a computerised database with a facility to allow updating of the conditions and the risk rating at each slope was handed over to Public Works Department.

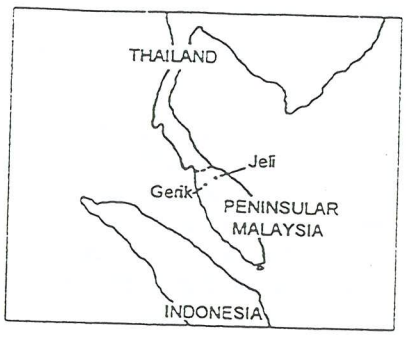

Figure 1: East-West Highway Location

2.0 STUDY METHODOLOGY

The steps involved in producing the prioritised list of landslide risk ratings was:

1. Data collection and database development;
2. Development of a hazard rating for each slope; and
3. Converting the hazard rating of each slope into a risk rating.

Each of these steps are briefly discussed in the following sections.

3.0 DATA COLLECTION AND DATABASE DEVELOPMENT

Initially the data collection phase of the project involved obtaining, reviewing and cataloguing all previous documentation relating to the highway. The documents included site investigation reports remedial works reports and drawings, monitoring data (rainfall, piezometer, inclinometer etc) and other miscellaneous references. Note that no design drawings or completion reports were made during the original construction of the highway.

A six month field data collection programme collected slope specific data for all 1,123 slopes along the highway and involved up to four teams of geologists, geotechnical engineers and geomorphologists. A standard proforma was developed to capture what were considered to be potentially critical parameters influencing the stability of the slopes. The proforma required collection of up to 600 parameters under 13 main groupings. These groupings were:

1. Location;
2. Geometry;
3. Cover;
4. Pavement;
5. Geology;
6. Artificial Drainage;
7. Natural Drainage;
8. Erosion;
9. Side Slopes;
10. Instrumentation;
11. Current Stability
12. Comments; and
13. Sketches

Figure 2 shows one page from the seven page data collection proforma.

The data collected was entered directly into a computer database via the use of laptop computers in the field. This involved developing a set of protocols to ensure that the data was entered accurately and that the data was sensible. This was accomplished by a set of standard queries and alarms in the database package to ensure that extreme or unlikely values were not entered e.g. excessively high slopes, slope angles greater than 90 degrees, etc.). In addition cross referencing to other sources of information was undertaken where possible.

EAST-WEST HIGHWAY LONG TERM PREVENTATIVE MEASURES AND STABILITY STUDY
Field Data Collection Proforma: EMBANKMENTS, CUTS, GRADES, NATURAL SLOPES

Feature Number	157	Feature Type	1
Primary or Secondary Feature	1	Age	3
Logged by	SJN/AJ	Date	29/03/94

NOTE: Some data will be better estimated from desk studies (eg: aerial photos etc). Enter a field estimate with a ? and modify in the office if necessary.

1) LOCATION

Position: Left/Right side of road	2			Up/downslope of road	2
Chainage: Start	25.520			Finish	25.610
Reduced Level	453.56				
Associated Primary Feature No.s	293	295	292	296	

2) GEOMETRY

Recorded Configuration	1				
Slope height	14	Slope type	2	Feature area	2500
Feature aspect	130	Slope angle	28		
Number of benches	1	Bench width	2.5	Batter height	7
Slope cross section	4	Slope plan profile	2		
Ratio of crest length to edge length	0.9	Distance to ridge/gully	0		
Distance from centreline of highway to toe of slope/crest of embankment	10				

For cuts only: Relationship between road cutting and topography 9999

Is there a secondary feature above/below the feature being logged? Y/N? N. If no, ignore the contents of this box. If yes, complete additional NATURAL SLOPE, CUT, EMBANKMENT, or GRADE proforma as required. Enter reference number of Data Sheet following 9999 (enter feature number prefixed C for cut, E for embankment, etc.). In addition the following data should be recorded for upslope features:

Upslope catchment area: 0

Is there structural works at the slope? Y/N? N If no ignore the contents of this box. If yes complete STRUCTURAL SUPPORT proforma reference S 9999 (enter feature number).

3) COVER

Feature Uncovered (%)	0	Main Cover Type	3
Vegetation cover (%)	100	Vegetation cover treed (%)	100
Artificial cover (%)	0	Condition of artificial cover	9999
Weepholes in artificial cover	9999	Weephole Flow	9999
Logging on feature?	9999	Distance to tree line (m)	9999

FOR CALCULATION PURPOSES ONLY:

	1	2	3	4	5	6	7	8	9	10	11	12	13
Batter height(m)	6	8											
Bench width(m)	2.5												

Figure 2: Field Data Collection Proforma

Running simultaneously with the slope data collection programme was a survey of the entire highway length including a minimum 300 metre corridor on either side of the highway. Note that the only existing survey of the highway comprised 1:50,000 topographical maps which were of limited use. The survey was completed using an Airborne Laser Survey which utilises a laser pulsating 2000 times per second from a helicopter platform to penetrate dense foliage and return true ground data. The helicopter is located in real time by continuous reference to GPS earth stations established prior to flying. The helicopter flew flight lines at 40 metres separation over a minimum 600 metre wide corridor. Vertical and spatial accuracies were within one metre. An additional benefit of the laser survey was to provide coordinated and elevated video images of the entire highway length.

4.0 THE DEVELOPMENT OF HAZARD RATINGS FOR EACH SLOPE

For the East-West Highway project hazard was defined as the probability of slope instability during the lifetime of the highway. Note that this definition contains no reference to the size of the failure.

The full dataset of 1,123 slopes was split into two subsets, embankments and cuts. natural slopes were included in the cuts subset.

In addition the data set was subdivided into "environments" where slopes considered to be similar were grouped for analysis. Environments were created based on geology, elevation and terrain units.

A total of six different predictive slope stability models were used to derive a hazard rating for each slope with two of these methods giving the best results. These two methods were:

1. A statistical Discriminant Analysis; and
2. A Factor Overlay Analysis.

These two methods are discussed in the following sections.

4.1 Discriminant Analysis

Discriminant analysis is a statistical method of representing the separation between two or more groups of data belonging to a common set of variables. For the purposes of this study the Discriminant Analysis may be used to categorise the slopes into stable and failed groups by producing a discriminant function that models the data set. This model is of the form:

$$Y = a_1X_1 + a_2X_2 + \ldots + a_n X_n + b$$

where, a and b = constants; and

X = variables (e.g. slope height etc.)

Variables considered statistically insignificant when discriminating between failed and stable slopes were excluded by the SPSS software package used for this analysis. The stability of a new slope can be evaluated by substituting the appropriate variables into the model function and determining its discriminant score Y_1. If Y_1 is greater than the mean discriminant score the slope is classed as potentially unstable. These scores can be interpreted as the probability of a slope failing and therefore can be ranked and a relative hazard rating assigned.

A stepwise Discriminant Analysis was performed on the data set to rank the variables in terms of their statistical ability to discriminate between failed and stable slopes. Tables 1 and 2 show variables from this analysis ranked in terms of their statistical ability to predict failures for geological environments.

The results in Tables 1 and 2 indicate that:

- Erosion is a key indicator of potential instability. Note that for the results to be meaningful it is essential that the field recording programme differentiates between failure caused by erosion and failure causing disruption to drainage which then results in erosion;

  There are a number of apparent contradictions with the variables in these lists. For example the number of drains variable for embankments (NO_DRAIN) suggests that as more drains are placed on the slope, the more likely it is to fail. What must be kept in mind is that the Discriminant Analysis is selecting these variables purely on a statistical basis. With the NO_DRAIN variable an increased probability of failure may reflect that the drains are blocking orbreaking and thereby introducing water to the slope. Alternatively, the NO_DRAIN variable may have been selected by the Discriminant Analysis in combination with all the other variables as a good discriminator between stable and failed slopes i.e. on a purely statistical basis and not on the number of drains on the slope;

Table 1: Significant Variables - Cuts

GEOLOGICAL ENVIRONMENT		
Granites	**Metasediments**	**Sediments**
Erosion	Erosion	Slope height
Bench drains	Number of water courses adjacent to the slope	Erosion
Relationship between the cutting and topography	Distance to ridge behind the slope	Distance to tree line behind the slope
Distance to ridge behind the slope	Plan profile of the slope	Relationship between the cutting and topography
Elevation	Batter height	Culverts
Vegetation cover	Rock Condition profile	Horizontal Drains
	Slope angle	Slope angle
	Slope height	

Table 2: Significant variables - Embankments

GEOLOGICAL ENVIRONMENT		
Granites	**Metasediments**	**Sediments**
Erosion	Erosion	Erosion
Vegetation cover	Age	Vegetation cover
Age	Number of water courses adjacent to the slope	Slope height
Slope height	Distance to ridge behind slope	Slope cross section
Horizontal drains	Batter height	Number of drains
Bench drains	Bench Drains	Upslope catchment area
Number of water courses adjacent to the slope	Slope height	Feature area
Culverts	Number of benches	
Elevation	Culverts	
Slope area	Vegetation cover	
Distance to ridge behind the slope	Ratio of crest length to edge length	
Number of drains on slope		

- For cuts, variables reflecting external influences such as erosion are dominant with variables reflecting slope geometry (eg. slope height) also significant; and
- For embankments, variables reflecting external influences such as erosion are dominant with variables reflecting material properties also significant. Material properties are reflected through the AGE variable which is the years since construction of the embankment. Embankments that have been reconstructed since the highway opening in 1982 (due to road realignments or landslides) were generally constructed to higher standards than the original embankments. This reflects the difficulties experienced during the initial construction of the highway.

There is some overlap in the variables listed in the Tables 1 and 2. For example, the material properties will influence the susceptibility to erosion hence the high ranking of the erosion variable may be at least partially influenced by the material properties.

4.2 Factor Overlay Analysis

To derive a hazard rating for the slopes, the Factor Overlay Analysis method involved the following steps:

1. Selection of significant parameters believed to contribute to instability. These were selected based on the ranking of variables that the Discriminant Analysis determined were statistically the best indicators of instability.
2. A maximum weighting of 2.0 and a minimum weighting of 0.1 was assigned to each parameter.
3. The parameters were subdivided and each division was assigned a weighting based on the number of known failures. An example of this process is shown on Figure 3.
4. For any slope a hazard value is then calculated by summing the sub-parameter values. These were converted to hazard ratings of very high, high, moderate, low and very low based on a linear split of the maximum and minimum hazard values.

Various methods of selecting parameters and assigned weightings were trialed in an attempt to refine the Factor Overlay Analysis method to produce the best results.

4.3 Other Methods of Determining Hazard Ratings

Several other methods of determining hazard ratings for the slopes were trialed in the project. These included a method proposed by the Geotechnical Control Office of Hong Kong. This method was modified slightly for the conditions on the East-West Highway and involved a process similar to the Factor Overlay Analysis method except that the significant parameters were as used in Hong Kong, as was the sub-parameter weightings.

An Applied Engineering Judgement method was utilised where the project team selected what they considered to be the most significant parameters causing instability based on their understanding of the conditions on the highway. Sub-parameter weightings were then selected between the

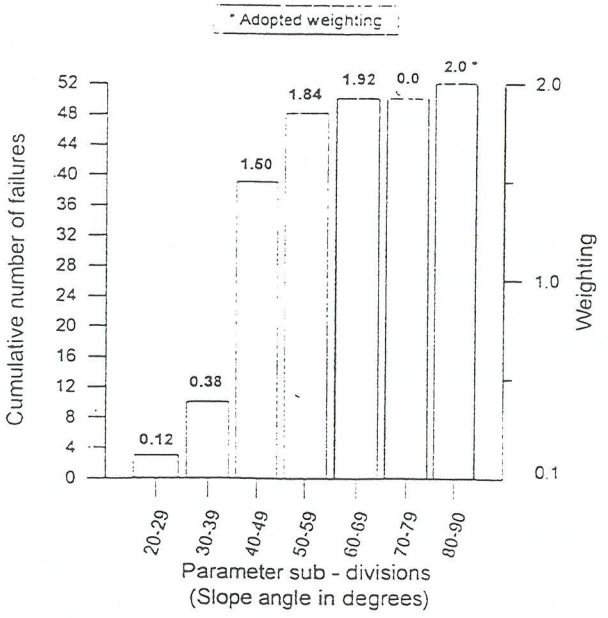

Figure 3: Factor Overlay Sub-Parameter Weighting

ranges of 0.1 to 1.0 or 0.1 to 2.0 dependent on how influential that parameter was thought to be. In addition, some multipliers were utilised to allow for parameters that could not be applied to all the slopes. For example, if the presence of a black shale was observed in a cutting the hazard value would be multiplied by 1.5.

4.4 Selection of Hazard Rating Method

A method to compare landslide hazard maps produced by different assessment methods was proposed by Gee (1992). The method involved comparing different hazard rating classes (very low to very high) within each method. The method that gives a good separation between the high and low hazard classes, with the majority of the known failures in the high class, being the best method.

This method was adapted to the East-West highway project to compare the various hazard rating models.

Under the method proposed by Gee the statistical Discriminant Analysis method was the best performing hazard rating model and the results of this method were used to derive the final hazard ratings. The Factor Overlay Analysis method was the next best performing method although it should be noted that the Factor Overlay Analysis method in part used the Discriminant Analysis result to select significant parameters. Note that the methods based on engineering judgement performed least well.

5.0 RISK RATING

For the East-West Highway project risk was defined as the probability of failure multiplied by the consequences of failure. The probability of failure is obtained directly from the hazard rating as described in Section 4.0. The consequence of failure was calculated as follows:

For embankments $= S + V + R;$

For cuts $= S + P + R;$

where, S = size of failure;

R = time required to re-route the road;

V = vulnerability (a measure of the degree to which the expected failure would affect the road eg. a slip affecting one lane of a four lane highway would pose less of a problem than a slip affecting one lane of a two lane highway; and

P = proximity of the cutting to the road.

A numerical weighting was applied to each of these parameters (S, V, R and P) and a consequence of failure calculated. An example of the weightings for the re-routing parameter is shown are Table 3. From these weightings a final risk value was obtained by multiplying the consequence value by the hazard value. These risk values were then rated as very high, high, moderate, low and very low on a linear split between the highest and lowest values. Plans showing the risk rating of each slope on the highway were then produced and an example of one of these maps is shown on Figure 4.

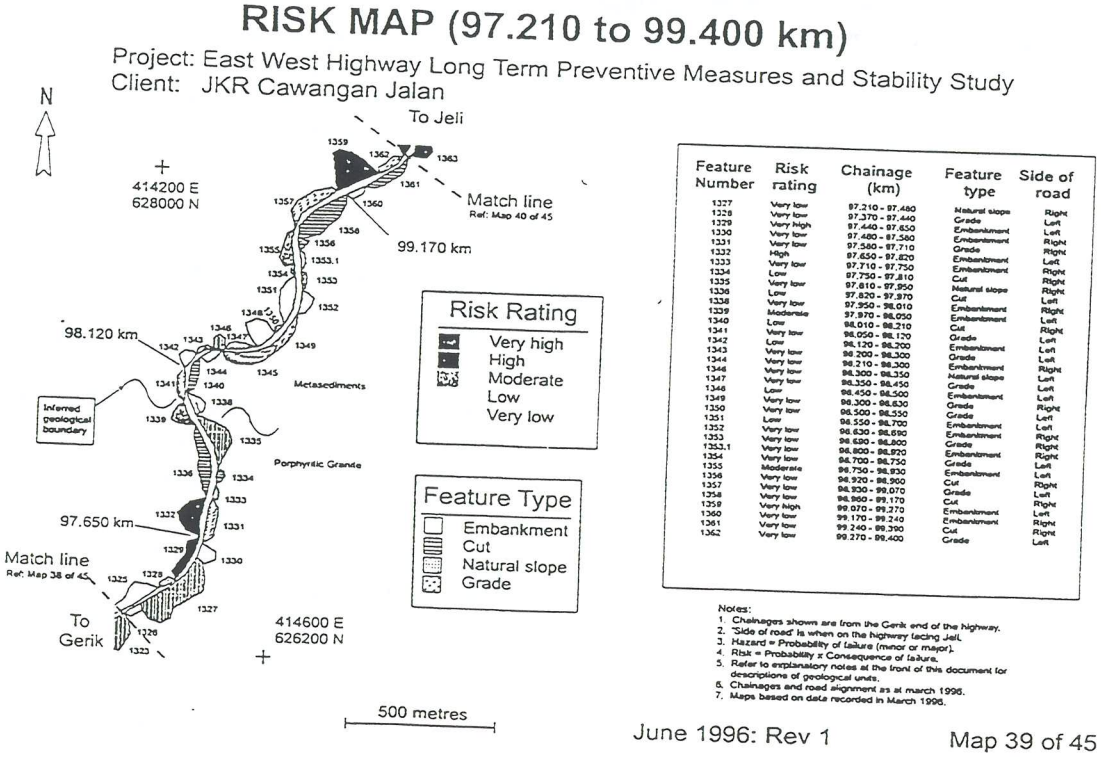

Feature Number	Risk rating	Chainage (km)	Feature type	Side of road
1327	Very low	97.210 - 97.480	Natural slope	Right
1328	Very low	97.370 - 97.440	Grade	Left
1329	Very high	97.440 - 97.550	Embankment	Left
1330	Very low	97.480 - 97.580	Embankment	Right
1331	Very low	97.580 - 97.710	Embankment	Right
1332	High	97.650 - 97.820	Grade	Right
1333	Very low	97.710 - 97.750	Embankment	Left
1334	Low	97.730 - 97.810	Embankment	Right
1335	Very low	97.810 - 97.950	Cut	Right
1336	Low	97.820 - 97.870	Natural slope	Right
1338	Very low	97.950 - 98.010	Cut	Left
1339	Moderate	97.970 - 98.050	Embankment	Right
1340	Low	98.010 - 98.210	Embankment	Left
1341	Very low	98.050 - 98.120	Cut	Right
1342	Low	98.120 - 98.200	Grade	Left
1343	Very low	98.200 - 98.300	Embankment	Left
1344	Very low	98.210 - 98.300	Grade	Left
1346	Very low	98.300 - 98.350	Embankment	Right
1347	Very low	98.350 - 98.450	Natural slope	Left
1348	Low	98.450 - 98.500	Grade	Left
1349	Very low	98.300 - 98.630	Embankment	Left
1350	Very low	98.500 - 98.550	Grade	Right
1351	Low	98.550 - 98.700	Grade	Left
1352	Very low	98.630 - 98.690	Embankment	Left
1353	Very low	98.690 - 98.800	Embankment	Right
1353.1	Very low	98.800 - 98.920	Grade	Right
1354	Very low	98.700 - 98.750	Embankment	Right
1355	Moderate	98.730 - 98.930	Grade	Left
1356	Very low	98.920 - 98.960	Embankment	Left
1357	Very low	98.930 - 99.070	Cut	Right
1358	Very low	98.960 - 99.170	Grade	Left
1359	Very high	99.070 - 99.270	Cut	Right
1360	Very low	99.170 - 99.240	Embankment	Left
1361	Very low	99.240 - 99.390	Embankment	Right
1362	Very low	99.270 - 99.400	Cut	Right
			Grade	Left

Figure 4: **Example Risk Rating Map**

Table 3: Numerical Weighting for Re-routing

Days to Re-route	Numerical Weighting
4 days or more	4
3 days	3
2 days	2
1 day or less	1

6.0 CONCLUSIONS

The methodology developed for the East-West Highway Long Term Preventive Measures and Stability Study Project provides a rational basis for evaluating the risk of landsliding along the Highway. The method does not rely on subjective assessments of the probability of landsliding and the methodology could equally be applied to landsliding anywhere, including Australia.

One of the key findings of the study was that a statistical approach can be effective in identifying instability provided that data of sufficient quality and quantity can be collected and that careful selection of data subsets is undertaken. In addition, the dataset must continually be updated if it is to continue providing a useful tool in evaluate the risk of landsliding.

7.0 ACKNOWLEDGMENTS

The data presented in this paper was obtained whilst the Author was in the employ of Soil and Rock Engineering (Malaysia) and the contributions of my former colleagues is gratefully acknowledged, in particular Mr Geoff Hurley and Mr Denis Smith.

Third A-NZ Young Geotechnical Professionals Conference, Cameron, Collingwood & Slatter (eds), Feb. 1998, Melbourne, Australia.

The Construction of a Zoned Embankment Dam in Indonesia

C.D. NOSKE
Grad IEAust
MPA Williams and Associates, Melbourne, Australia

Summary This paper documents the construction of a 30m high water storage dam at the Bukit Sentul Project in West Java, Indonesia. The author was extensively involved in the design phase of Dam L2 and spent a subsequent six month period in Indonesia for the construction of the embankment. This paper discusses the major technical and engineering issues which arose, as well as focusing on the more practical aspects of living, working and managing a project in a foreign country.

1. INTRODUCTION

Dam L2 is an "off-stream" storage, and carries a curved road alignment on its crest, which dictated the final dam location. The L2 embankment was designed as a zoned earth/soft rockfill embankment with a central clay core. Geotechnical investigation and design were carried out through the latter part of 1994, with construction taking place from April to December 1995.

During the design phase the author undertook stability, seepage and seismic risk analysis, before travelling to Indonesia to take up the position of Laboratory Manager late in June 1995. This position provided much experience in construction supervision, and in September a reduction in site personnel resulted in the author's duties being extended to include the role of Site Engineer.

The specific aspects of engineering supervision included the excavation of foundations which exhibited unusually rapid deterioration upon exposure, the construction and placement of the extensive filter/seepage collection system and the quality control of material selection, compaction and testing for the ten separate zones incorporated into the embankment.

Some of the more practical issues encountered centred on the problems inherent with understanding and adapting to a different culture and working environment, such as the initial training of laboratory staff, the establishment of satisfactory standards and practices, and the continual liaison with the client and contractors.

2. PROJECT BACKGROUND

The Bukit Sentul Project is a US$500M privately funded residential and resort development situated 40 km south of Jakarta in the hills surrounding the city of Bogor. Bukit Sentul could be described as a "satellite city" for affluent Indonesians, a development trend popular at the moment in South-East Asian countries with rapidly emerging economies.

The project contains a number of housing precincts, a hotel complex, high quality golf course and country club, as well as associated water supply, sewerage and transport infrastructure.

Major components of the water supply infrastructure include pumping stations set up on the nearby Citereup River, two water storage dams; L1 and L2, and a treatment plant. The original intention was to construct the two dams simultaneously, but project finances and other constraints did not allow this to occur. Dam L2 is the slightly smaller of the two, with a capacity of 400 megalitres and a maximum crest hight of almost 30 metres. Its design function was to store water for golf course irrigation and to provide a temporary supply for potable water treatment.

The road on the crest and the proximity of residential subdivisions to both abutments meant that conventional spillways could not be used, so a "glory-hole" type spillway tower and outlet culvert was incorporated into the design, together with an increased freeboard. The General Arrangement of Dam L2 is depicted in Figure 1.

To this day, construction of Dam L1 has not been completed. Its original purpose was to store water for supply to a treatment plant located over the downstream toe of the embankment. This plant was, at the time urgently required, and the author was subsequently involved in the construction of the downstream toe and treatment plant platform immediately after completion of Dam L2. This work took a further two months.

2.1 Site Topography

The Dam L2 site is located within the prestigious 'Northridge' subdivision area, in a relatively narrow "V" shaped valley. Prior to clearing the area was covered with low trees and dense undergrowth. There were signs of previous cultivation in small alluvial flats adjacent to the water course. Both abutments are located on relatively steep slopes, as is the rim of virtually the entire impounded area.

2.2 Site Geology

The site is underlain by the Tertiary Jatilihur Formation, comprising marl, claystone and clay shale, with quartz sandstone intercalations. Where fresh, the formation is a blue-grey colour, but is generally weathered to a brownish flaky rock. Residual deposits are only a few metres deep, occurring as a yellow-brown

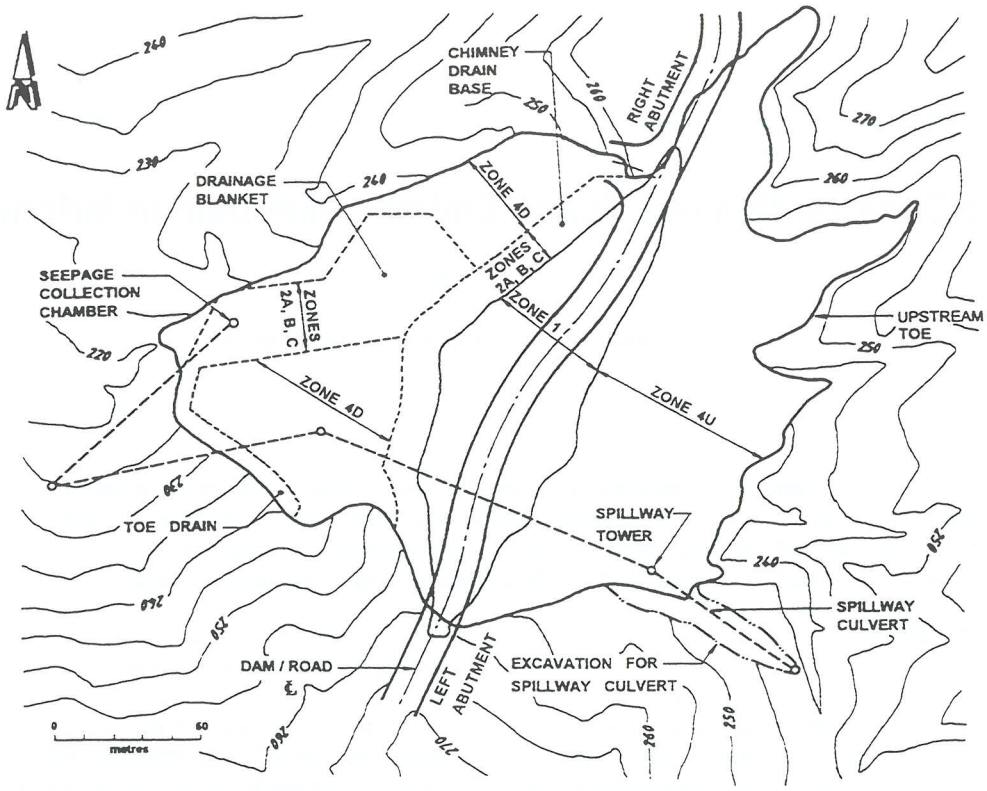

Figure 1 Dam L2 - General Arrangement

clay. The formation is generally steeply inclined and has been folded about east-west striking fold axes, with a dip to the north.

Over parts of the site (particularly the abutment slopes), the Jatilihur Formation rocks are overlain by a relatively thin (1 to 3 metres) mantle of red-brown halloysitic clays, considered to represent weathered younger Quaternary volcanics.

Zones of surficial alluvium of Recent/Quaternary origin exist along alluvial terraces in the river valleys. These include clay, silt, sand and gravel, mostly of volcanic origin.

2.3 Site Investigation

The site investigation was limited by terrain and access difficulties, and comprised four boreholes on the centerline, supplemented by test pits. Potential borrow areas were evaluated by test pits.

3. EMBANKMENT DESIGN

As with most embankments, the profile adopted for Dam L2 was governed by material availability. The client had planned to construct the dam coincident with major subdivisional works on the plateaus immediately north and east of the site, and these locations were set aside as embankment material borrow sources. Following investigation and testing of material properties, it was deemed that the clays and underlying claystone from these excavations would be suited to a zoned earth/soft rockfill embankment profile, and the typical section shown in Figure 2 was adopted.

3.1 Embankment Zoning

The central **Zone 1** Core consists of compacted medium to high plasticity clay. Extensive laboratory testing indicated that both the "upper" volcanic clay and the "lower" residual clay were suitable for use. It was revealed during the site investigation that moisture contents of the clays fluctuated considerably on a seasonal basis, but were generally wet of optimum.

Given the likelihood of the wet season encroaching on the construction period, it was considered practical to approach design in a conservative manner. Hence, design proceeded for the central clay core on the basis of undrained shear strength, with no allowance made for the dissipitation of pore pressures during construction. Stability limitations thus became the controlling factor, and are presented in the following section.

Based upon both laboratory and stability analyses, a minimum Dry Density Ratio of 93%(Standard) and moisture content range of 1% dry to 3% wet of optimum were specified. Not withstanding this compliance criteria, it was also a requirement that the vane shear strength should not be less than 60 kPa.

A design permeability of $k = 1 \times 10^{-9}$ m/sec was established for Zone 1 clay compacted in accordance with this specification. Shrinkage or cracking of the clay core was not considered to be a problem, based on the relatively flat 1:1 sides, and the thickness and low air voids content of the compacted Zone 4 rockfill shell.

Zone 2 materials form the downstream filter and drainage system. **Zone 2A** is clean, durable filter sand, and with an outer layer of geotextile forms the Chimney Drain. **Zone 2B** (nominal size 10mm) and **Zone 2C** (nominal size 20mm) are drainage materials consisting of screened gravels. These three materials together with geotextiles are incorporated in various "sandwich" arrangements to form the Chimney Drain Base, the Drainage Blanket and the Toe Drain.

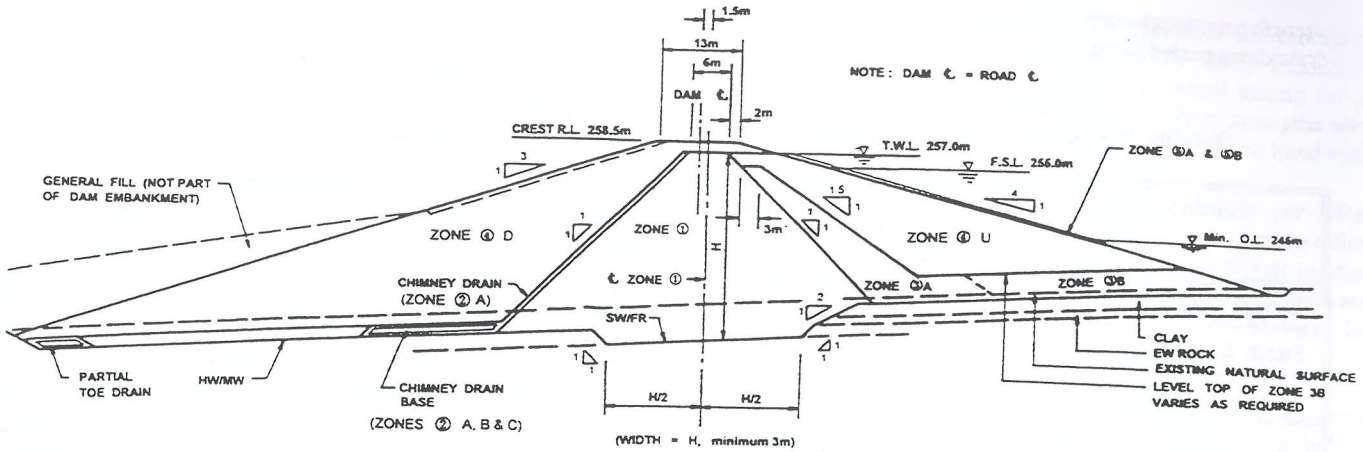

Figure 2 Dam L2 - Typical Cross Section

A Seepage Collection System comprising perforated collection pipes, concrete collection chamber and outfall pipe are located in the Blanket Drain at the downstream toe. This arrangement was necessary as the deep subdivisional fill over the downstream toe eliminated the option of conventional toe drains.

Zone 3A formed the upstream shoulder transition, and is made up of extremely to moderately weathered claystone compacted to a Dry Density Ratio of 95% (Standard) with moisture contents in the range 2% dry to 4% wet of optimum. **Zone 3B** consisted of similar material, and was incorporated into the floor of the upstream shoulder.

Zone 4 slightly weathered to fresh claystone forms the upstream and downstream shoulders of the embankment. It was identified during site trial compactions that the fresh claystone forms a weak rockfill which breaks down under compaction to form a soil-like material. It was thus considered appropriate to use soil-type methodologies for fill placement and testing.

The claystone is not durable and was found to deteriorate rapidly upon exposure. When dried it cracks and shatters, and also exhibits pronounced slaking and softening in contact with water.

The shoulders were hence designed as soft rockfill, with a compacted Dry Density Ratio of 98% (Standard) and a maximum allowable air voids of 10%. This was primarily to minimise "collapse" settlements caused by the wetting up of loose, dry fill.

The upstream slope is protected by **Zone 5A** geotextile and **Zone 5B** volcanic rock rip-rap.

3.2 Embankment Stability

Embankment stability analyses were conducted on the maximum height section, as well as the critical topographic upstream and downstream sections. Three loading conditions were considered, namely:

- during construction
- steady state seepage during operating conditions
- rapid draw-down from full supply level (25 day and three month durations)

As the island of Java is seismically active the steady state maximum height section was also analysed with a pseudo-static earthquake load. Existing seismicity data for the area were used to calculate horizontal acceleration versus Average Recurrence Interval (ARI). Each stability condition was then solved for "a_{yield}": the acceleration producing a Factor of Safety of 1.0 for a full depth failure surface passing through the crest.

Finite element modelling of pore water pressure dissipation in the clay fill was conducted using the computer program SEEP/W, to obtain pore pressures for use in rapid draw-down stability analyses. The embankment piezometric surfaces generated during these analyses were also used as the basis for the design of the downstream filters and drains.

Laboratory testing conducted during the site investigation phase provided a basis for the selection of the design parameters presented in Table I.

Table I
Adopted Design Parameters

Unit Description	Strength Parameters				Bulk Density
	Steady State		During Construction		
	c' kPa	ϕ' deg	c_u kPa	ϕ_u deg	t/m³
Embankment -					
Zone 1	0	31	50	5	1.85
Zone 3A	6	31	35	10	1.95
Zone 4	5	29	60	0	2.02
Foundations -			c_r	ϕ_r	
Surface Clay	5	20	0	12	1.85
HW - MW Rock	50	25	-	-	2.10
SW - Fr Rock	100	28	-	-	2.20

Critical Factors of Safety determined during the stability analysis are presented in Table II.

Upstream failures through the residual clay foundations were considered. The Zone 1 clay was assumed to exhibit undrained

strength parameters during earthquake loading. The critical rapid draw down period identified by SEEP/W was 25 days.

Table II
Stability Analysis - Critical Factors of Safety

Condition	Downstream		Upstream	
	Factor of Safety			
During Construction	1.71		1.30	
Steady State Seepage	1.83		1.94	
Rapid Draw Down	-		1.27	
	a_{yield} & equivalent ARI			
Seismic Steady State	0.24g	600	0.22g	450

4. EMBANKMENT CONSTRUCTION

4.1 Construction Progress and Timing

Construction of Dam L2 commenced with the clearing and stripping of topsoil in early April 1995. Actual fill placement began in early May and was practically completed in early November, a total period of approximately seven months. A total of 290,000 m^3 of fill was placed in this time.

The construction process is presented graphically in Figure 3. The construction time was of longer duration than originally forecast, and this can be attributed to three main factors:

- *Weather* - unseasonably wet weather during the normally drier months of April to August caused significant delays. This pattern continued into the wet season with consistent rain falling in the afternoons and evenings. Working days were shortened, with the first and last few hours of each day usually devoted to cleaning-up after a night's rain and then sealing-off in anticipation of the next.

- *Filter Material* - delays in provision of Zones 2B and 2C filter materials were a great concern during the first few months of construction, as evident in Figure 3. Random quality of materials, poor roads, long haulage distances and small, inappropriate trucks resulted in extremely slow delivery rates and the eventual postponement of all earthworks on the core and upstream shoulder for four weeks.

- *Abutment Foundations* - foundation conditions in the right (northern) abutment were poorer than expected, and subsequently required the excavation of greater quantities of unsuitable material than originally forecast. This often resulted in lengthy delays in the placement of the clay core (Zone 1).

4.2 Foundation Preparation

The embankment design specified different types of surface preparation for the core trench, upstream and downstream

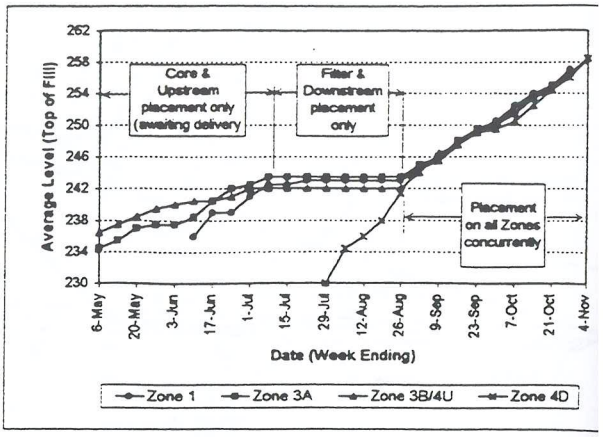

Figure 3 Dam L2 - Progress of Rasing

foundation areas. Soil condition / degree of weathering was as the basis for foundation stripping, as the variable subsur conditions proved the depths encountered during the investigation to be indicative only. Stripped materials incorporated into the embankment zones wherever practical. works conducted in preparing the foundations, separated into three categories, can be summarised as follows:

Type A (Upstream) - the specification called for the strippin topsoil and the insitu compaction of the exposed clay. In prac however, the upstream ground consisted of a layer of very wet up to 2 metres thick over relatively thin zones of weathered r This clay was unsuitable as a foundation material and subsequently removed. This resulted in the majority of upstr Zone 4 material being founded on moderately weathered clayst

Type B (Downstream) - this type of preparation required removal of all soils and extremely weathered rock, expos moderately weathered claystone. The claystone weathering pro was found to be very shallow, with layers of suitable modera weathered material generally being too thin to be distinguished excavation plant. Thus most of the downstream Zone 4 is foun on slightly weathered rock.

Although the actual Type A and B foundation works give impression of an over-engineered design, they are in fact dire attributable to the limited coverage of the original investigation and the dryer conditions in which it was conduct

Type C (Core) - Type C stripping beneath the Zone 1 core wa slightly weathered to fresh claystone. After bulk excavation o weathered material, the surface was scraped with the bucket small excavator, hand cleaned and air blasted. Provided clay placed within the next few hours a good surface was held, longer exposure periods would result in rapid deterioration of rock surface. Air blasting would then be required to be repeat whilst the total cleaning sequence was repeated in cases where placement delay exceeded 24 hours. Deterioration after this ti would generally take the form of extensive shrinkage cracking fissuring such that lumps exceeding one kilogram could removed by hand.

Due to the variability of the weathering profile there w numerous places where it was not considered viable to comp

clay against the excavated and cleaned surface. Good rock was either therefore removed to provide a working area for compaction equipment, or alternatively dental concrete was poured. The biggest such problem, which was exacerbated by poor workmanship, was in the area of the spillway culvert.

The spillway culvert was constructed by a separate contactor prior to the commencement of embankment works. It was designed to be cast-in-situ, in a trench excavated into fresh rock. Subsequent excavation at the south abutment in the area adjacent to the spillway culvert showed that in some areas the culvert had not been built to specification. Fresh rock had generally not been encountered during trenching and, presumably as a result of excavation instability, the culvert had been constructed against formwork. The resulting gap was then backfilled with loose material. This formed a potential seepage path beneath the embankment, and it was necessary to remove some 180 m³ of loose material and replace it with concrete. Constant supervision was then required during the preparing of foundations and placement of core material against the sides of the concrete culvert encasement.

4.3 Zone 1 - Clay Core

During the Zone 1 construction, the two different medium to high plasticity clay types were utilised. The"lower" yellow residual clay type, sourced from various subdivisional works, was the primary source of core material during the early stages of construction, and was utilised in approximately 75% of the core.

During construction of the upper third of Zone 1 the reserves of "lower" clay became very limited, hence requiring the use of "upper" red-brown clay deposits. Being of volcanic origin, these contained many basalt floaters which had to be removed, usually by hand at the dam site.

Compactors and vibrating sheeps foot rollers proved to be the most efficient means of placement. Isolated or confined areas resulting from foundation preparation had their initial layers placed and compacted with a wheel-loader to avoid damage to the underlying rock foundations. In especially confined areas, such as adjacent to the spillway culvert, a whacker-packer was employed. Once all zones were at a consistent level, scrapers were used to increase placement efficiency.

As expected, most clay used was found to have a moisture content wet of optimum. The upper limit of the moisture content specification was removed during the final third of the core construction (provided all other requirements were met) to assist with the problem of increasing moisture content in the available materials as the wet season set-in. An analysis of post-construction consolidation settlements indicated that the impact of this relaxation would be negligible.

Ultimately, however, placement of the "upper" red clays had to be abandoned during the final 2 metres and "lower" yellow clay employed from a new source as moisture contents in the former were too high for required shear strengths to be obtained.

Quality control for the construction of Zone 1, as with all other zones, was the jurisdiction of the author, who determined the timing and location of all tests, and supervised site laboratory practices. The laboratory was staffed by three Indonesian technicians, who undertook compaction control testing for all earthworks using the Hilf Rapid Method. Shear strengths were determined at each Zone 1 test location using a Pilcon hand vane.

The specified testing frequency for Zone 1 was 1 test per 500m³ of fill, but this frequency was ultimately almost doubled to reflect the smaller representative lots placed as a result of poor weather conditions. Compliance testing comprising Atterberg Limits and Soil Particle Density (the latter also for Zone 4) was also conducted at a nominal rate of one per week.

The distribution of Zone 1 compaction control testing is presented in Figure 4. The density ratio histogram indicates that, of the 348 tests conducted, only 19 results fell below 92%, hence requiring recompaction and retesting. The variable field moisture contents are demonstrated in the second histogram. It can, however, be seen that only 12% of results fell outside the original specification.

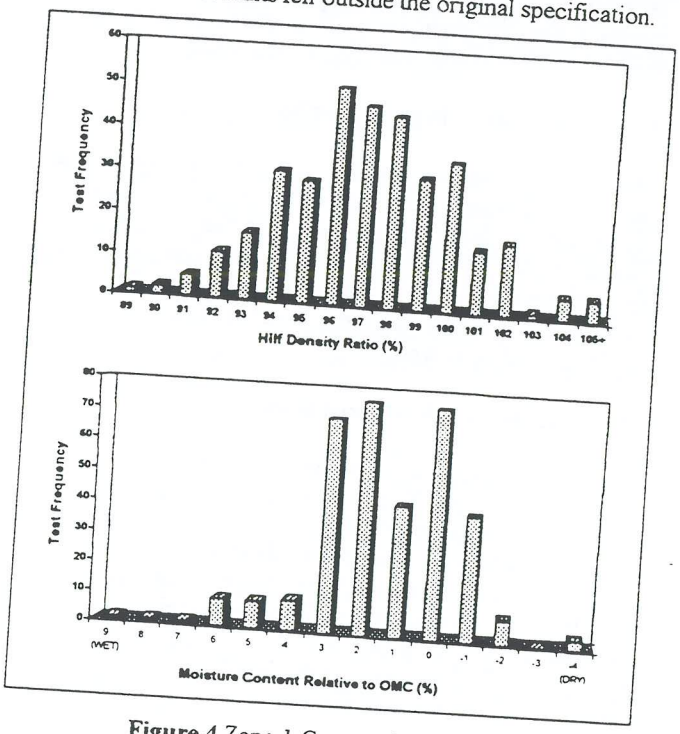

Figure 4 Zone 1 Compaction Control

4.4 Zone 2 - Filters and Drains

4.4.1 Zone 2A - Sand

This Zone consisted of fine to medium silica sand and was obtained off-site from a number of processed natural sand suppliers. Selection methods and quality control were based on the specification particle size distribution, with sampling and laboratory testing being carried out upon delivery as supplier quality control was poor. Very fine sand was often encountered and many of the initial deliveries had to be rejected.

Zone 2A was required in the Chimney Drain, the Chimney Drain Base and the Blanket Drain and as such required two main methods of placement. The chimney drain was placed in lifts of approximately 500 mm, with levels kept uniform with adjacent

Zones 4D and 1 for the majority of placement. Contamination was kept to a minimum by the geotextile layer and by hand removal of clay prior to subsequent lifts. Compaction was by lateral passes of the vibrating smooth drum roller. The Chimney Drain Base and Blanket Drain was placed in single lift horizontal layers with a wheel-loader, spread generally by hand and compacted with the smooth drum roller.

4.4.2 Zone 2B/2C - Crushed Rock Aggregate

Initially, these zones were to consist of washed river gravels obtained on site. However, project politics resulted in these gravels becoming unavailable, resulting in the filters being redesigned, using crushed rock aggregates from varies quarries around West Java. The primary quality concern was with regard to consistency of supply, with samples presented for testing often bearing little resemblance to delivered material. The most common problem was crusher-dust and the apparent inability of suppliers to remove it from the aggregate. This was particularly the case with the finer Zone 2B material, resulting in much material being rejected, often simply on a visual basis.

4.4.3 Seepage Collection Chamber

The seepage collection chamber, together with the 8 collector pipes, was constructed 2.5 m higher than originally designed. The reason for this change in elevation was that unseasonably wet weather during foundation preparation and construction of the downstream toe forced the contractor to build-up Zone 4D to a level higher than the existing creek invert in order to eliminate the continual ponding of water.

4.5 Zone 3A - Weathered Rockfill

This shoulder transition zone consisted of extremely and highly weathered claystone. Dam abutment excavations did at times produce material suitable for Zone 3A, and this was incorporated into the dam whenever practicable. Material selection was on the basis of visual inspection, as a broad range of material types were considered to be within the specification parameters. Placement was generally in conjunction with the two adjacent zones so that "soft spots" would not occur at the interfaces due to insufficient compaction across the zone boundaries.

4.6 Zone 4 - SW/Fresh Rockfill

This Zone made up the upstream and downstream shells of the dam. The majority of material was borrowed from Northridge roadworks whilst all suitable rock from the dam foundation excavations was also recovered and utilised.

The high degree of variability in rock size and strength made compaction requirements very difficult to assess and various placement methods were experimented with during the early stages of construction. The breaking-up of individual rocks was often very time consuming, but it was found that a Caterpillar 825 compactor working in tandem with a bulldozer provided the most efficient results. Once the rock was sufficiently crushed, the vibrating sheeps-foot rollers proved effective in completing the layer to the specified compaction standard. Resultant particle sizes were predominantly gravel-sized or smaller, and hence air voids compliance was generally always achieved. Quality contro centred on the maintenance of adequate layer thicknesses, with many rock fragments being of greater size than the required laye depth. Rain was also a concern, as an uncompleted laye subjected to a heavy downpour often resulted in waterlogging an the need for subsequent material removal.

4.7 Zone 5 - Upstream Slope Protection

The upstream slope protection consisted of Zone 5A and Zone 5B "Zone" 5A was Bidim A29 geotextile which formed the base laye for the rip-rap, and Zone 5B was the rip-rap itself. It was made up of the basalt floaters which occur in the "upper" clays in abundant quantities throughout Northridge. All such stones removed from the Zone 1 clay were stock-piled at the upstream toe of the dam for use as rip-rap. The material was hand-broken to manageable sizes and hand placed over the underlying geotextile in several layers to ensure adequate coverage.

5. EMBANKMENT MONITORING

Seven vibrating wire piezometers were installed in various locations in the dam embankment. Five of the piezometers were installed at RL 240 m; three in Zone 1, one in Zone 3A and one in Zone 4U. The two remaining piezometers were installed in Zone 4U at RL 247 m.

As the dam design had proceeded on the basis of undrained parameters, the main purpose of the piezometers was to provide data which would be of assistance in the design and construction of the considerably larger Dam L1.

The build-up of pore pressures within the embankment were monitored by reading each piezometer and recording its associated depth of fill twice a week. The piezometers in Zone 4U showed little fluctuation due to the depth of rockfill above them; instead their fluctuations reflected rainfall patterns. Zone 1, and to a lesser extent Zone 3A showed a steady, almost linear increase in pore pressure with depth of fill, which was not unexpected, given the wet placement conditions. This increase can be seen for the Zone 1 piezometers in Figure 5. These results indicate the pore pressure parameter; $r_u > 0.5$, which retrospectively justifies the design based on undrained strength. Note also how pressures began to level out upon completion of fill placement.

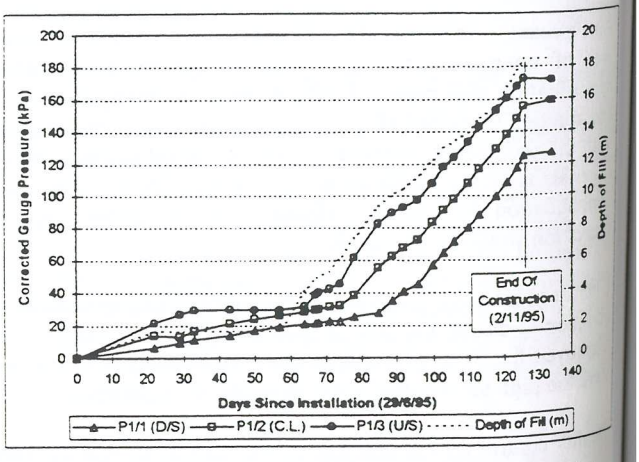

Figure 5 Zone 1 Piezometer Readings During Construction

6. PRACTICAL PROJECT ISSUES

As can be expected, supervising a construction project such as this in a developing Asian country results in a range of practical issues not usually encountered in Australia. Even the day to day issues which are normally expected to arise take on a new context when combined with different cultures, work ethics and languages.

6.1 Standards and Practices

The first major issue confronting the supervision team was the establishment of satisfactory standards and practices. Laboratory personnel supplied by the contractor were found to be excellent workers, but despite their basic understanding of testing procedures, quality control aspects of their work was initially lacking. However, once required standards were implemented, the staff demonstrated a sound willingness to learn, such that by the third construction month supervision could be lessened appreciably.

A similar situation was encountered with the construction personnel. The contractor was an Australian-Indonesian joint venture, with predominantly Australian management. Plant operators and foremen were all Indonesians, however, whose work practices and standards were found to vary considerably. This was found to be easily overcome, mainly due to the Indonesian worker's ability to put potential ego conflicts aside and their strict adherence to project hierarchies. The expatriate engineer is generally awarded the highest respect, and procedural suggestions and directives were usually eagerly implemented.

One of the biggest challenges facing the expatriate engineer is in adapting to construction practices still based largely on manual labour. Maintenance of machinery in Indonesia is generally considered optional, and man-power is cheap and abundantly available. Teams of village men and children would be on site daily for manual tasks such as foundation preparation, filter material placement, rock removal from the clay core and rip-rap breaking and placement.

Quarried material suppliers do not generally own tip trucks, so a common site would often be up to a dozen trucks encircling the filter material stockpiles, each with 10 to 15 shovel-armed Indonesians unloading by hand.

6.2 The Site Engineer - Client Relationship

The client filled their many levels of management predominantly with Indonesians, as well as a scattering of expatriates. During the course of the project the author liaised with many staff members of different nationalities, enabling an assessment of the various managerial styles to be made.

The Indonesian Manager, after demonstrating an initial period of caution regarding the new "foreign" site engineer, would generally prefer to step back from the decision making process, hence requiring a much more broadly based site supervisory role to be filled. This would often involve direct liaison with contractor management on specific issues, and subsequently reporting back, often on a daily basis to the project manager.

6.3 Tropical Weather Patterns

Although a vague awareness of the influence tropical weather has on large construction projects was gained during the design phase, the author was quite unprepared for the scale of the impact on construction methods and productivity. A warning period for imminent rain of at least thirty minutes was essential in order to complete compaction of all working layers, and to form and seal a self-shedding profile. Local knowledge was one's greatest asset, especially during periods of unseasonably early wet weather. Wet season rainfall was somewhat more predictable, but could never-the-less be devastating in its intensity. During the early stages of construction of the Dam L1 treatment plant platform in January, 420mm of rain was received over a seven day period, engulfing stranded plant in up to four metres of water.

6.4 Living in a Foreign Country

Probably the most challenging and ultimately rewarding aspects of the project was learning to adapt to a whole new way of life. Little can be done to prepare the inexperienced traveller, other than to ensure that a language dictionary and malaria tablets are packed. Communication was not the hurdle initially expected; a basic understanding of the Indonesian language proved sufficient when combined with the varying degrees of English familiarity expressed by most locals.

Residence was initially in a hotel in the small city of Bogor, hence requiring a 30 minute drive to site. The Indonesian way of driving is certainly 'different', and driving ones' self was made all the more interesting by frequent break-downs and flat tyres.

Exposure to the predominantly Muslim culture was another valuable experience as its effect on day to day life is all-encompassing. The suspension of work five times a day for prayer sessions was at first frustrating, especially on occasions when wet weather was closing in.

It could in fact be concluded that the experiences gained in life-skills throughout the period of the project were equally as valuable as those of a technical nature.

7. ACKNOWLEDGEMENT

MPA Williams and Associates acted as sub-consultants to Bukit Sentul project engineers CMPS&F Pty. Ltd. (Melbourne) who, together with PT CMPS (Indonesia) were responsible for water supply and sewerage infrastructure design. The author wishes to thank CMPS&F for permission to publish this paper.

Third A-NZ Young Geotechnical Professionals Conference, Cameron, Collingwood & Slatter (eds), Feb. 1998, Melbourne, Australia.

A Preliminary Assessment of the Behaviour of Drag Anchors in Layered Soils

M. P. O'Neill
Research Student, The University of Western Australia

Summary: This paper presents the results of a series of model drag anchor tests performed in the centrifuge on a saturated sample comprised of normally consolidated kaolin clay overlying dense silica sand. The initial focus of the paper is on the description of the test equipment and arrangement, outlining the model anchors used in the tests and the manufacture of a model instrumented anchor chain. A method of determining the orientation and embedment depth of the model anchor within the soil during each test, utilising a tracking probe attached to the anchor and "in-flight" video cameras, is also described. The results highlight the importance of the shank angle of the anchor in relation to the holding capacity and stability of the anchor/chain system.

1 INTRODUCTION

With the recent emergence of FPSO (Floating Production, Storage and Offloading) facilities as a preferred method of offshore hydrocarbon extraction, and the gradual shift of hydrocarbon discoveries towards deeper waters, greater attention has been focussed on appropriate anchoring and mooring systems. Drag embedment anchors provide a simple and economical anchoring solution, and can possess holding power to weight ratios exceeding 20.

Until recently, drag anchor design was largely empirical and based primarily on design charts developed from field test data. Furthermore, these charts describe the performance of drag anchors in homogeneous soils classified broadly as "sand" or "clay". They do not cater for drag anchor behaviour in layered soil profiles, like those encountered on the North Sea where silica sands underlie normally consolidated clays.

This paper outlines a procedure for testing model scale drag anchor and chain systems. The paper also presents the results of a number of model anchor tests using anchors with different fluke-shank angles. These tests were performed in the centrifuge in soil samples comprised of normally consolidated kaolin clay overlying dense silica sand.

2 EXPERIMENTAL DETAILS

2.1 The Centrifuge

The centrifuge at The University of Western Australia (UWA) is an Acutronic Model 661 Geotechnical Centrifuge and is rated at 40 g-tonnes, equating to a maximum payload of 200kg at an acceleration of 200 g. A swinging platform located at a radius of 1.8 m seats rectangular "strong boxes" which have internal dimensions of 650 mm long by 390 mm wide by 325 mm high, representing a prototype test bed of up to 130 m long by 80 m wide by 60 m depth. The headroom of 900 mm allows for mounting actuators which sit on top of the box and permit vertical and horizontal movements to be imposed on models.

2.2 Model Anchors and Anchor Chain

The anchor tests described in this paper were conducted using two 1:160 scale model anchors with principle dimensions similar to 32 tonne Vryhof Stevpris anchors with fluke-shank angles of 30° and 50° (Vryhof, 1990), as shown in Figure 1 (dimensions are in mm). Note that both the 30° and 50° model anchors have a fluke length of 31 mm.

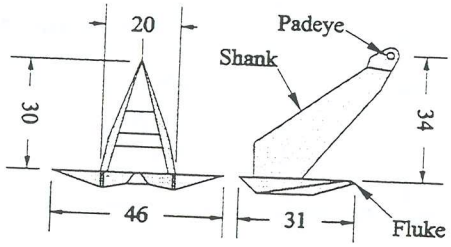

Model anchor (50° shank)

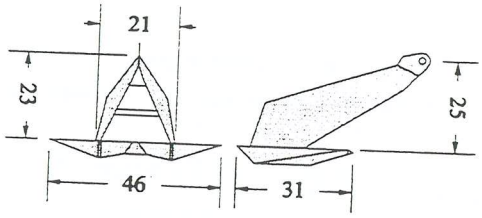

Model anchor (30° shank)

Figure 1: Model anchors

A novel model anchor chain was fabricated for the anchor tests. The chain consisted of 4 strands of 0.5 mm diameter fishing trace which were plaited in such a way as to produce a cable which has a good resemblance to a real anchor chain. The weaving of the two pairs of sinusoidal type profiles at right angles to each other results in bumps along the length of the chain which model chain links well.

In order to measure the load capacity of the model anchor as it was dragged through the test sample without disturbing the accuracy of the anchor/chain system model, a load cell was incorporated into the connection between the anchor and the chain. A miniature load cell was designed and built with four holes drilled at one end to allow attachment of the four strands of fishing trace that made up the chain. A pinned connection was located at the other end to enable the model anchor to be easily attached. The thin electrical cable from the load cell was strapped to the model chain for the first 200 mm to avoid damage to the cable.

The arrangement for each anchor test is shown in Figure 2. From the anchor, the chain is laid on the sample surface along the length of the strong box and wrapped 180 degrees around a pulley located at the end of the box. In order that the anchor chain correctly forms an inverse catenary curve from the anchor to the soil surface, where the angle of the chain with the horizontal at the surface is equal to or close to zero (Neubecker, 1995), the vertical position of the end pulley is adjustable to ensure that the chain meets the pulley at the sample surface. The chain then comes back along the length of the box and is wrapped 90 degrees around a pulley located at the base of the actuator, where it is then orientated vertically. From here the chain is wrapped 180 degrees around a third pulley located in the actuator carriage, brought back down and anchored to a padeye fixed to the actuator.

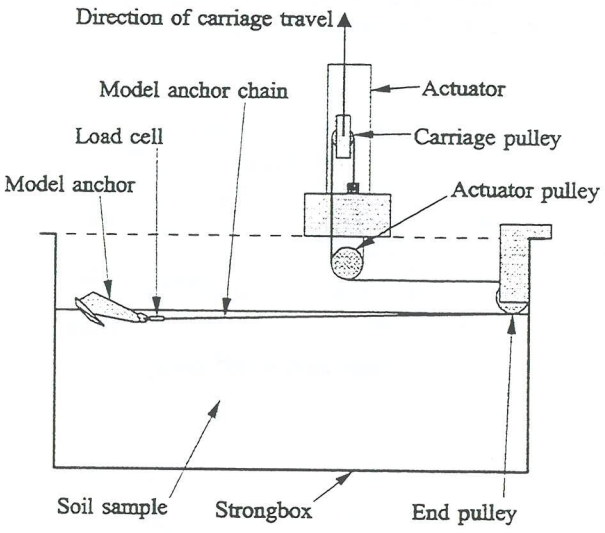

Figure 2: Testing arrangement

During an anchor test the actuator carriage is moved up, and hence there is a gearing ratio of 2:1 between the displacement of the anchor and the actuator carriage. All anchor tests presented in this paper were conducted at a carriage speed of 0.1 mm/s (corresponding to a model anchor drag speed of 0.2 mm/s).

2.3 Tracking Probe

In order to determine the position of the model anchor in the soil during the test, a tracking system developed by Neubecker (1995) was employed. A 0.6 mm steel rod was attached to the anchor just behind the padeye, as shown in Figure 3. A board consisting of two parallel black and white scales 50 mm apart was mounted horizontally and directly above the line of travel of the anchor padeye. The probe was approximately 160 mm in length to ensure that it protruded a significant distance from the soil. Hence, during the test the tracking probe would travel close to the horizontal scales, allowing the orientation and drag distance of the anchor to be determined. The tracking probe was also marked with a black and white scale to indicate distance from the anchor padeye, and enabled the embedment depth of the anchor padeye to be calculated.

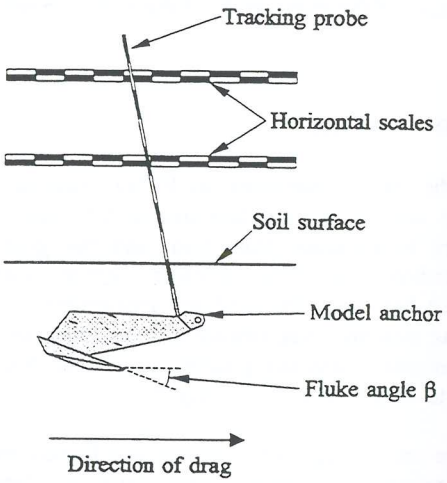

Figure 3: Tracking probe

Two video cameras were mounted on top of the strong box at approximately the same level as the horizontal scales to enable observation of the tracking probe as it moved past the scales. The signals from both cameras were recorded on video tape to allow a detailed analysis of the movement of the anchor to be conducted after the test. The scope of each video camera was such that only about half of the full drag length of each test could be observed before the tracking probe went out of range. Hence, the cameras were carefully positioned to ensure that the probe was always within the viewing range of one of the cameras, and that there was an overlap in the views of both cameras as the probe moved from the range of one camera to the other.

After each test the movement of the tracking probe past the scales was digitised. This involved the use of a frame-grabbing computer to save an image from the recorded video signals as an image file every 30 seconds during the test. The saved images were then put into a graphics program. Two points along the length of the tracking probe which were within view of the cameras during the entire test were

selected. Each image was analysed separately to allow the x-z coordinates of the selected points to be determined. Additional information from each image was also gathered in order to correct for parallax effects. The data from all images was then syncronised with the data obtained from the anchor chain load cell.

2.4 Sample Preparation

The anchor tests described in this paper were conducted in a fully saturated sample comprised of dense silica sand underlying normally consolidated kaolin clay. The depth of the clay layer for the first two tests was 14 mm (2.2 m at prototype scale), while for the last two tests it was 35 mm (5.6 m at prototype scale).

Initially, a fine mesh and a thin layer of coarse sand was placed over a drainage hole at the base of the strong box. In order that the silica sand layer possess as high a density as possible, the silica sand was placed dry into the strong box by slow raining using an automatic sand rainer. At the conclusion of the raining, the sand surface was vacuum levelled to the required height of 185 mm. The strong box was then weighed in order to determine the density of the sand, which came out to be 16.7 kN/m^3. This compares reasonably well with the maximum dry density of 17.0 kN/m^3 (Neubecker, 1995).

The sand sample was then saturated by slow upwards percolation of water through the base drainage hole. Saturation was continued until there was at least 50 mm of water above the sand surface.

The kaolin clay was prepared as a slurry which was mixed under a vacuum for several hours to de-air the soil. The slurry was then carefully placed in the strong box over the silica sand to the required height, ensuring that no air was trapped in the slurry and that the surface of the sand was not disturbed. A miniature pore pressure transducer was placed within the clay slurry to allow measurement of the dissipation of pore pressure during consolidation in the centrifuge.

The strong box was placed in the centrifuge, where the sample underwent a slow consolidation procedure designed to minimise infiltration of the clay layer into the sand. This process involved a gradual ramp-up at acceleration levels of 10 g, 20 g, 40 g and 80 g before reaching the target acceleration level of 160 g. At each level, the sample was allowed to consolidate until the pore pressure reached a plateau.

At the conclusion of the second anchor test (Test 7.3), additional de-aired kaolin slurry was added to the test sample, and the sample allowed to reconsolidate at the full target acceleration of 160 g.

3 EXPERIMENTAL RESULTS

3.1 Sample Details

Four anchor tests using the 30° and 50° model anchors were conducted in the test sample, covering two different normally consolidated clay layer depths as shown in Table 1. Each test was adequately spaced along the width of the strong box to avoid clashing of the failure zones of soil.

Test Number	Anchor Type	Clay Depth (m)
7.1	50° shank	2.2
7.3	30° shank	2.2
7.4	30° shank	5.6
7.5	50° shank	5.6

Table 1: Anchor test summary

Prior to Tests 7.1 and 7.4, cone penetration tests (CPT 1 and CPT 2 respectively) were conducted in order to determine the friction angle of the test sample. The method for its calculation was proposed by Robertson and Campanella (1983), and involves an empirical correlation between the bearing capacity factor, N_q, and the friction angle, ϕ'. Figure 4 shows the cone resistance profiles obtained from both cone tests, which indicated a friction angle of approximately 42°.

Prior to Test 7.4 and in addition to the cone test (CPT 2), the undrained shear strength (s_u) profile of the 5.6 m normally consolidated clay layer was determined using a t-bar apparatus (Stewart and Randolph, 1991). As indicated in Figure 4 (T-bar 1), the shear strength gradient was approximately 1.1 kPa/m. No t-bar test was performed prior to Test 7.1 because the clay layer was relatively shallow (14 mm at model scale), making it difficult to gather any strength data. However, it is reasonable to assume that the undrained shear strength gradient of the 2.2 m clay layer was also approximately 1.1 kPa/m.

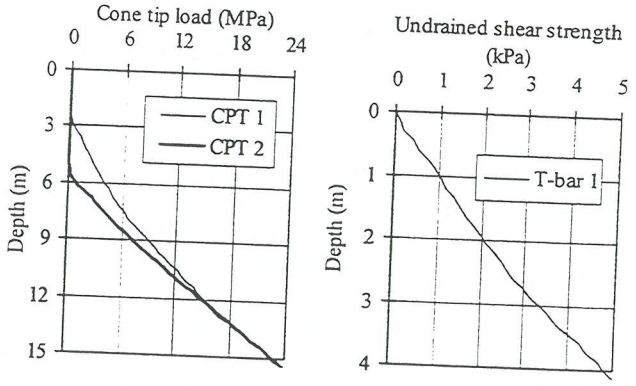

Figure 4: Cone penetrometer and t-bar tests

3.2 Anchor Tests

Figure 5 shows the plots of anchor capacity against horizontal padeye displacement (in fluke lengths) for Tests 7.1 and 7.3 (using the 50° and 30° anchors respectively). The anchor capacity is expressed in terms of anchor efficiency, which is the ratio of the holding power of the anchor to the anchor dry weight. Note that displacement data was gathered at 30 second intervals, and therefore the curves appear stepwise in nature. Both tests show a steady increase in capacity in the first fluke length of drag. By 2 fluke lengths the capacity

developed by the 50° anchor had leveled out at an efficiency of approximately 6.7, and remained at that level for the rest of the drag. The capacity of the 30° anchor peaked at an efficiency of 9.4 at 2 fluke lengths of drag, before dropping slightly to 7.5 at 5 fluke lengths. This capacity was maintained until the conclusion of the test.

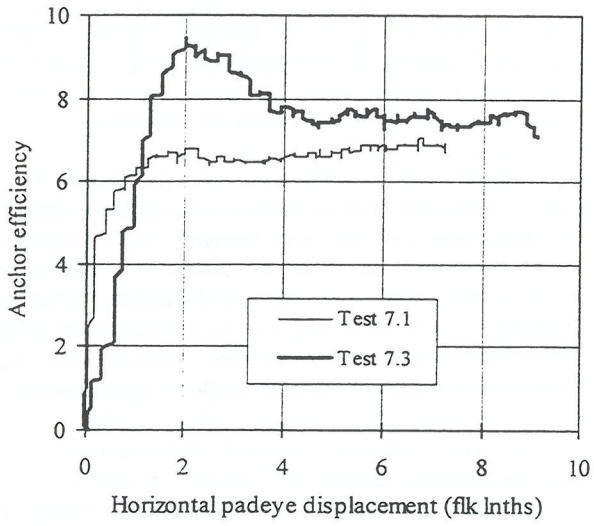

Figure 5: Anchor efficiency vs horizontal padeye displacement - Tests 7.1 and 7.3

Similar efficiency curves plotted against horizontal padeye displacement for Tests 7.4 and 7.5 are shown in Figure 6. The capacity of the 50° anchor (Test 7.5) leveled out at an efficiency of approximately 8.6 after a drag length of 2 fluke lengths, and then proceeded to decrease slightly over the rest of the drag to an efficiency of 7.6. The 30° anchor peaked at an efficiency of 12.4 after a little over 2 fluke lengths of drag, before steadily dropping to 9.8 at 8 fluke lengths.

The results show that the capacities of the anchors were significantly higher in the tests conducted in the sample with a deeper clay layer. Furthermore, the capacity of the anchor with the 30° shank was markedly higher than the anchor with the 50° shank in both clay depths.

Figure 7 shows the anchor fluke angle β plotted against horizontal padeye displacement for Tests 7.1 and 7.3, where β is measured as the angle of the upper surface of the anchor flukes to the horizontal (Figure 3). Prior to dragging in both tests, the anchor was orientated with the front tips of the flukes and the anchor padeye approximately level (β values of 80° and 58° for the 50° and 30° anchors respectively). At the commencement of dragging, both anchors began to rotate with the fluke angle β decreasing. However, within the first half a fluke length of drag, the rate of rotation of the 50° anchor dropped substantially, and by 2 fluke lengths of drag had ceased rotating altogether at a fluke angle of 66°. On a number of occasions during the rest of the drag, the 50° anchor rotated backwards slightly (β increase) before re-orientating itself back to a fluke angle of around 65°.

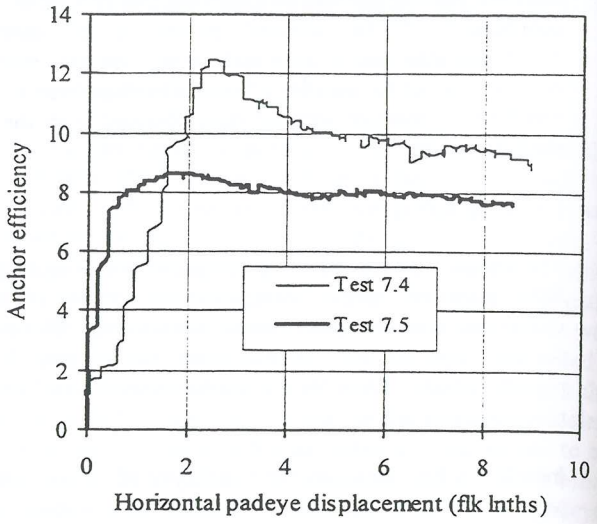

Figure 6: Anchor efficiency vs horizontal padeye displacement - Tests 7.4 and 7.5

Unlike the 50° anchor, the 30° anchor continued to rotate with β decreasing at a steady rate down to a value of 22° at 2 fluke lengths of drag, then decreasing further but at a slower rate to a value of 12° at 9 fluke lengths of drag. Note that the point of change in the rate of rotation corresponds approximately with the maximum anchor capacity measured (Figure 5).

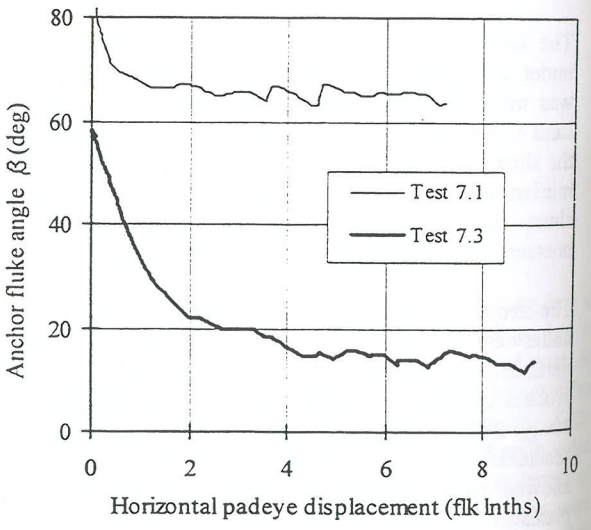

Figure 7: Anchor fluke angle β vs horizontal padeye displacement - Tests 7.1 and 7.3

The curves showing the fluke angle β of the model anchors during the drags in the sample comprised of the deeper clay layer (Tests 7.4 and 7.5) are featured in Figure 8. The small gap in the curve for Test 7.4 is the result of unclear video images and the inability to obtain accurate x-z coordinates from these images. As with Tests 7.1 and 7.3, these drags commenced at relatively high fluke angles. Both anchors rotated with β reducing in the early stages of each test. The

rotation rate of the 50° anchor (Test 7.5) reduced significantly at approximately half a fluke length of drag, but unlike Test 7.3 which was conducted in a shallower clay layer, the anchor continued to rotate, with the fluke angle reaching 51° after 8 fluke lengths of drag. In Test 7.4, the anchor rotated to a lower β value of 16° after 3 fluke lengths, and remained at 16° to 22° for the rest of the test.

In both 30° anchor tests, a relatively low fluke angle was reached and maintained, accompanied by good development of holding capacity. For the case of the 50° anchor tests, less rotation was observed, and on occasion the anchor rotated back to a higher fluke angle, suggesting that the anchor was attempting to "dig" into the sand but became unstable when β became too low.

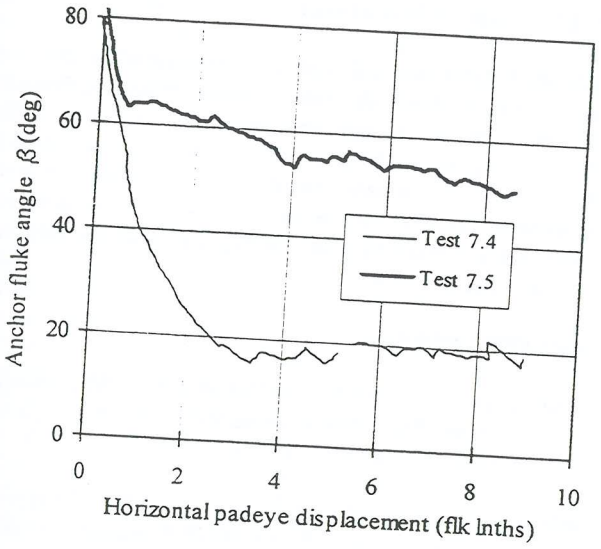

Figure 8: Anchor fluke angle β vs horizontal padeye displacement - Tests 7.4 and 7.5

The embedment depths of both the anchor padeye and the front fluke tips plotted against horizontal padeye displacement for Tests 7.1 and 7.3 are shown in Figure 9. For these tests, the sand/clay interface was at a depth of 2.2 m (prototype scale) or 0.45 fluke lengths. At the commencement of each test, the anchor padeye and fluke tips were at approximately the same level. In both tests the anchor padeye reached the sand/clay interface within the first 2 fluke lengths of drag, but upon further dragging did not penetrate into the sand layer.

The fluke tips in Test 7.1 (50° anchor) penetrated partially into the sand, reaching a depth of 0.60 fluke lengths (or 0.15 fluke lengths into the sand) at a little under 2 fluke lengths of drag. However, as the anchor ceased to rotate (Figure 7) the depth of the fluke tips within the sample quickly decreased back to approximately 0.54 fluke lengths, just below the sand/clay interface. Again, the fluke tips were attempting to dig into the sand, but this quickly caused the anchor to become unstable. Upon further dragging, the fluke tips continually embedded and pulled out of the sand, unable to embed deeper than 0.70 fluke lengths into the sample (0.25 fluke lengths into the sand layer). In Test 7.3 (30° anchor), the fluke tips reached a sample depth of 1.00 fluke length (0.55 fluke lengths into the sand) within the first 2 fluke lengths of drag. Further embedment of the fluke tips was observed during the remainder of the test (up to 1.1 fluke lengths), and was due mainly to small rotations of the anchor.

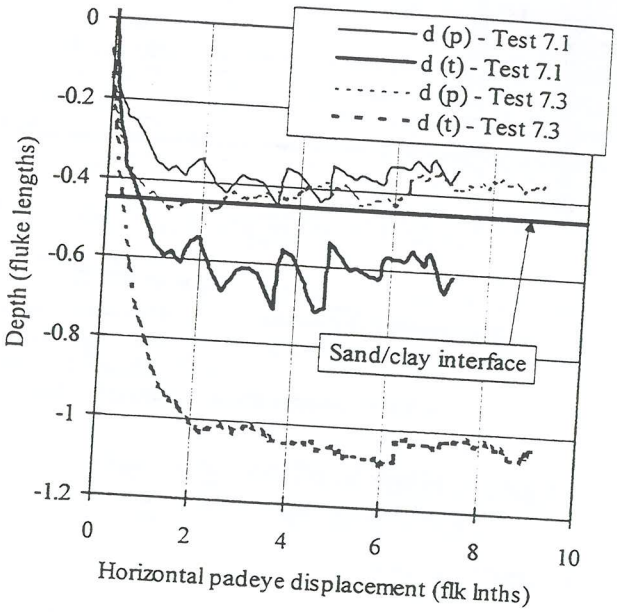

Figure 9: Padeye (p) and fluke tip (t) depth vs horizontal padeye displacement - Tests 7.1 and 7.3

The anchor padeye and fluke tip embedment plots for Tests 7.4 and 7.5 are shown in Figure 10. In these tests, the sand/clay interface was located at a depth of 5.6 m (prototype scale) or 1.13 fluke lengths. As before, the anchor padeye in both tests quickly reached the interface, but did not penetrate into the sand in any significant way during further dragging. The fluke tips of the 30° anchor (Test 7.4) again showed reasonable embedment, reaching a maximum depth of 1.74 fluke lengths (0.61 fluke lengths into the sand layer) within a little over 2 fluke lengths of drag. Despite a minor reduction in embedment depth at around 4.4 fluke lengths of drag the fluke tips remained relatively stable at a depth of approximately 1.65 fluke lengths for the remainder of the test.

Unlike Test 7.1, where the fluke tips of the 50° anchor made no significant penetration into the sand layer, in Test 7.5 the tips embedded at a steady rate to approximately 1.55 fluke lengths (0.51 fluke lengths into the sand) after 4 fluke lengths of drag. The tips then remained at an embedment depth of 1.50 fluke lengths for a further 2 fluke lengths of drag. Towards the end of the test, the tips were observed to increase in depth, reaching 1.70 fluke lengths at the conclusion of dragging. It would have been interesting if the drag could have proceeded a further few fluke lengths, in order to determine whether the tips would have embedded further, whether the anchor had reached a point of stability or whether the anchor was on the verge of pulling out.

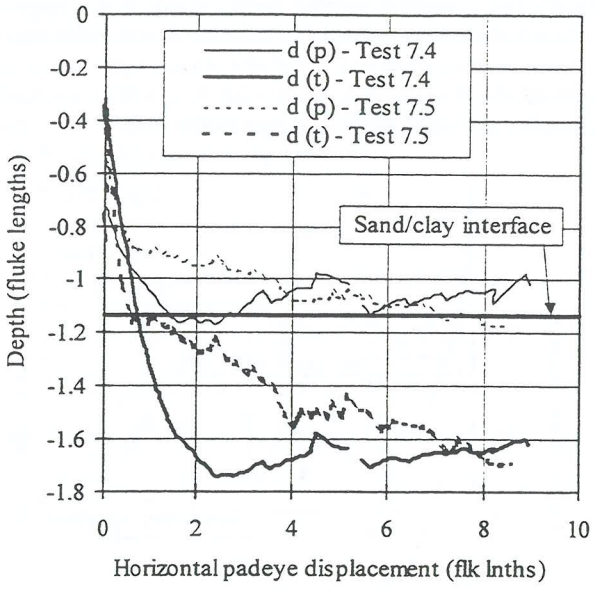

Figure 10: Padeye (p) and fluke tip (t) depth vs horizontal padeye displacement - Tests 7.4 and 7.5

4 CONCLUSIONS

Results have been presented from a series of model drag anchor and anchor chain tests performed in the centrifuge at The University of Western Australia in saturated samples comprised of a thin layer of normally consolidated clay overlying dense silica sand.

By incorporating a miniature load cell into the anchor chain without disturbing the accuracy of the anchor/chain system, and by employing a tracking system in order to determine the orientation and embedment of the model anchor during testing, a comprehensive description of both the development of anchor holding power and the anchor kinematics was obtained.

The model anchor with the 30° shank was able to rotate to shallower fluke angles and embed further than the anchor with the 50° shank. This in turn led to the 30° anchor generating higher holding capacities and remaining more stable with continued dragging.

In many instances, the experimental data showed the anchor continually digging into the sand layer, becom unstable and partially pulling out. This result was expec since the 30° anchor is used predominantly in sand, while 50° anchor is used in softer soils. Interestingly, experimental data showed that in those tests where the fl tips did embed into the sand, only minimal embedment of shank into the sand was achieved.

Further tests will be conducted covering a wider range of c layer depths and soil conditions. The results, together with anchor theory developed by Neubecker (1995), will be used develop a simulation program to predict drag anch embedment and capacity in layered cohesive and n cohesive soils

5 ACKNOWLEDGEMENTS

The work described in this paper forms part of the activities the Special Research Centre for Offshore Foundati Systems, funded through the Australian Research Counci Research Centre's Program. The author is supported by University Postgraduate Award. Special thanks are due to t workshop and centrifuge staff at UWA, without who excellent technical support the experimental research wou not have been possible.

6 REFERENCES

Neubecker, S. R. (1995), The behaviour of drag anchor a chain systems, PhD Thesis, Department of Civil Engineerin The University of Western Australia.

Robertson, P. K. and Campanella, R. G. (1983), Interpretatio of cone penetration tests. Part 1: Sand. Canadian Geotechnic Journal, 20, 718-733.

Stewart, D. P. and Randolph, M. F. (1991), A new sit investigation tool for the centrifuge, *Centrifuge 91*, Balkema Rotterdam, pp531-538.

Vryhof Anchors. 1990. *Anchor Manual*. Krimpen ad Ysse The Netherlands.

Third A-NZ Young Geotechnical Professionals Conference, Cameron, Collingwood & Slatter (eds), Feb. 1998, Melbourne, Australia.

Ground Support Design for Olympic Dam Expansion Project

Jason Rivalland, BFP Consultants Pty Ltd

Summary: Olympic Dam is currently undergoing an expansion project, costing an estimated $AUS 1.5 billion. Included as a part of the expansion project is 24km of tunnels as well as 6km of underground rail system. BFP is currently working under contract to Western Mining Corporation (WMC), to provide ground support design and advice relating to the expansion project. The two main approaches being used for the support design was an overall rockmass one using the Rock Tunnelling Quality Index, Q by Barton et al. (1974) and a structural failure one using the geotechnical programs DIPS and UNWEDGE. Both these approaches have been used to derive a support design for all the proposed development drives, shafts and chambers located in varying orientations, depths and geological materials for the Olympic Dam Expansion Project.

1. INTRODUCTION

Olympic Dam, so named after a livestock watering dam on the Roxby Downs pastoral lease, was first discovered in 1975 by the Western Mining Corporation (WMC). It was not until 1976 however that drill hole RD10 producing an intersection of 170 metres containing 2.1% Cu and 0.6kg/t U308 that the economic potential of the deposit was realised.(1) Estimated ore reserves are currently put at 569 million tonnes of mineralisation, requiring a mine life of 100 years. The expansion project will triple the output of the Olympic Dam Mine from 3 MT a year to 9 MT a year, making it one of, if not the largest uranium mine in the world.

Design of the tunnels and associated chambers has resulted in varying levels of support using rock bolts, cable bolts and fibre reinforced shotcrete. The actual design process will be detailed further in the following sections.

The proposed crusher and associated development are located in massive granite and granite breccias, having an average UCS value of 129 MPa. The major openings are located well away from the ore body.

2. DESIGN APPROACH

The BFP support design, technical specification and contract drawings were required by WMC and the contractor well in advance of any major openings or exposure. Hence the data provided to BFP consisted of structural mapping information from the decline which was advancing towards the area of interest and some specific geotechnical holes drilled from the decline towards two proposed crusher sites.

From the database provided, the BFP ground support approach accounted for two discrete failure modes, i.e. an overall rockmass failure or discrete structural wedge failures. The rock mass approach used the rock mass classification system of Barton et al (1974) (2) together with the latest support classification chart of Grimstad and Barton (1993). In contrast the structural approach used the Canadian program UNWEDGE to examine the occurance, size and weight of potential wedges in the roof and sidewalls of all openings.(3)

The two methods vary significantly in their philosophy, with the Q system being primarily concerned with overall rockmass properties such as rock strength, block size and inter-block shear strength while UNWEDGE is primarily concerned with the formation of discrete structural wedges.

3. POTENTIAL ROCK MASS FAILURES

Rock mass classification schemes have been continuously developing for over 100 years, with the first reported use of a classification system for the design of tunnel support in a paper by Terzaghi (1946).

The Rock Tunneling Quality Index or Q system as it is more commonly known is used for the determination of rock mass characteristics and tunnel support requirements. The numerical value of Q varies on a logarithmic scale from 0.001 to a maximum of 1000 and is defined by:

$$Q = \frac{RQD}{J_n} \times \frac{J_r}{J_a} \times \frac{J_w}{SRF}$$

Where:

RQD	: is the Rock Quality Designation.
J_n	: is the joint set number.
J_r	: is the joint roughness number.
J_a	: is the joint alteration number.
J_w	: is the joint water reduction factor.
SRF	: is the stress reduction factor.

This equation can be broken down into three components relating to both geology and geometry as follows:

- Block Size (RQD/J_n)
- Inter-block shear strength (J_r/J_a)
- Active Stress/Strength (J_w/SRF)

The first quotient (RQD/J_n), can be seen as a crude measure of block or particle size with a maximum value of 200 and minimum value of 0.5.

The second quotient (J_r/J_a) represents the roughness and frictional characteristics of the joint walls or filling materials. The quotient is heavily weighted in favour of rough unaltered joints in direct contact.

The third quotient (J_w/SRF) can be regarded as the total stress parameter. It is a complex empirical factor describing the 'active stress'. (4)

In order to obtain Q, either logging of core on site, or underground exposure mapping is required to obtain a figure for RQD and the various J factors. The value of the aforementioned factors may vary throughout the same drill hole or opening as different materials are intersected. In

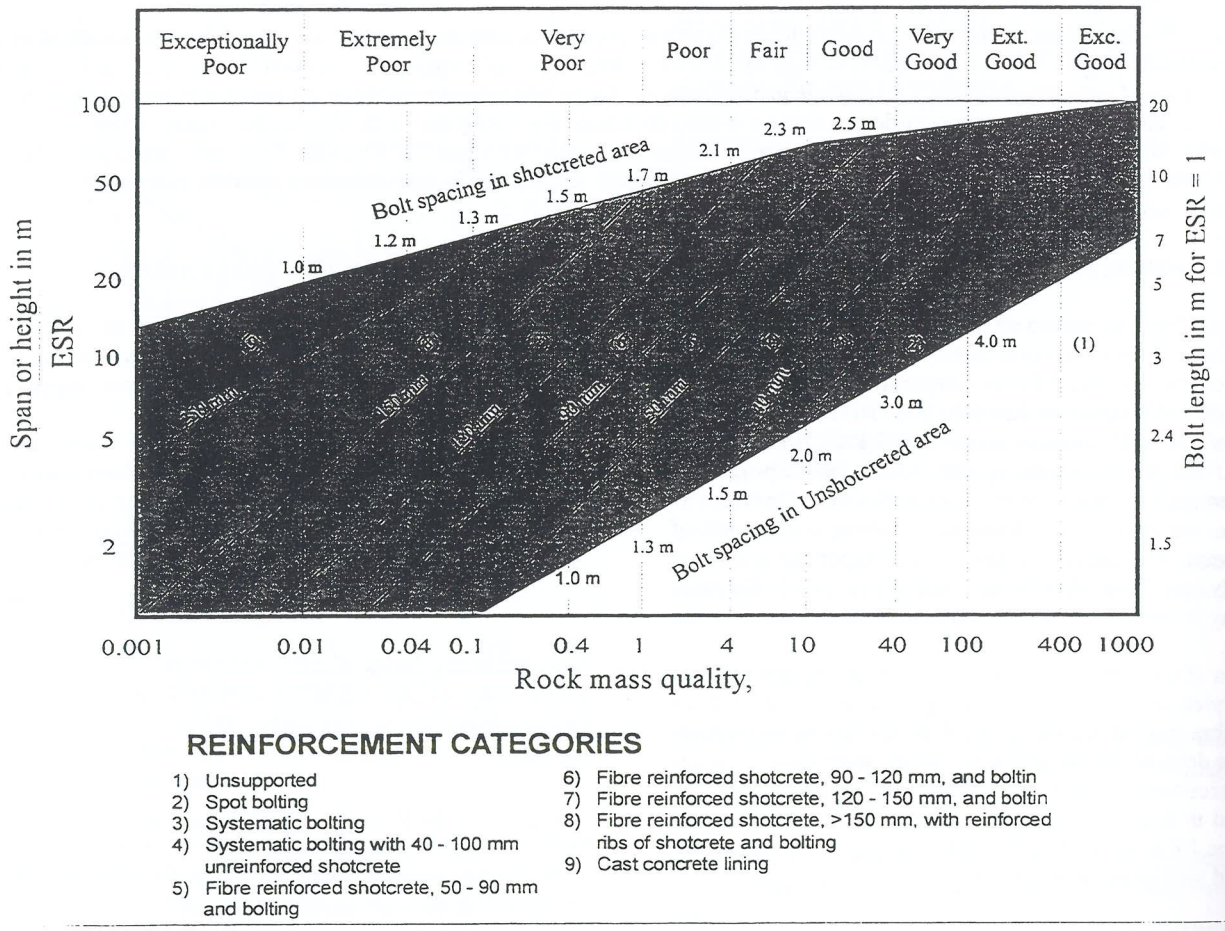

REINFORCEMENT CATEGORIES

1) Unsupported
2) Spot bolting
3) Systematic bolting
4) Systematic bolting with 40 - 100 mm unreinforced shotcrete
5) Fibre reinforced shotcrete, 50 - 90 mm and bolting
6) Fibre reinforced shotcrete, 90 - 120 mm, and boltin
7) Fibre reinforced shotcrete, 120 - 150 mm, and boltin
8) Fibre reinforced shotcrete, >150 mm, with reinforced ribs of shotcrete and bolting
9) Cast concrete lining

Figure 1. Estimated support categories based on Q (After Grimstad and Barton, 1993)

designing a large opening for example, the data from one drill hole might be separated into different regions. The core from the sidewall and roof would be geotechnically logged at intervals governed by the material encountered whilst drilling. This geotechnical logging includes such information as;

- Core loss
- Rock type
- Weathering
- Alteration
- RQD
- Number of defects
- Number of defect sets
- Defect type
- Roughness
- Infill
- Infill width

Once the core has been logged the values for the various Q factors can be obtained from the tables produced by Barton et al.

Once Q is established, the next step is to determine the *Excavation Support Ratio* or ESR. The value of ESR is related to the intended use or duty of the excavation and to the degree of security which is demanded of the support system to maintain the stability of the excavation. Barton et al. (1974) suggested the following values:

they are planar and continuous, ensuring that the largest possible wedges are enabled to form. UNWEDGE assigns a factor of safety to each potential wedge, allowing the design engineer to make an assessment of the support required. UNWEDGE allows the user to select one of the wedges, starting with the wedge with the lowest factor of safety and re-running the program with various ground support options simulated (end anchored bolts, shotcrete, etc.). Normally the first run will simulate the effect of the "first pass" support design as determined from the rockmass approach outlined in Section 3. UNWEDGE then provides a new Factor of Safety, taking into account the increased resisting force provided by the support. Multiple analyses are performed until a suitable Factor of Safety is reached (normally ≥ 1.5).

Despite the advantages in using UNWEDGE to perform structural analyses there are also disadvantages. UNWEDGE is primarily designed for use where the in situ stresses are low and where their influences can be neglected without the introduction of significant errors. In cases of high in situ stresses, the factor of safety provided by the program may be too high or too low, depending on the shape of the wedge. In the case of a long thin wedge, the high in situ stress will tend to clamp the wedge in place, the result being a factor of safety too low. The reverse is true for shallow flat wedges which may be forced out by the high stresses.

The following case study will more clearly illustrate the methodology behind the Barton et al. Q system and UNWEDGE.

5.0 CASE STUDY

5.1 Rock Mass

The following example is taken from the Olympic Dam Crusher Chamber Geotechnical Investigation produced for WMC by BFP Consultants Pty Ltd.

A total of six holes were drilled with the geotechnical logging of 1000m of BQ core. Samples were selected for Uniaxial Compression Strength tests (UCS). From this data, the following values for the various components of the Q system were obtained;

RQD: almost of the logged core had an RQD of 100%. The lowest RQD value recorded was 93%.

J_n: varied from 0.5 to 9 (i.e. massive rock with no defined joint sets to 3 for well defined joint sets).

J_r: most of the observed defects had undulating rough surfaces. Occasional slicksides were noted, a value of 3 was used for J_r.

J_a: the majority of defect surfaces were unaltered or contained hard rock infills that would not be likely to weaken the rock mass. A value of 1 was used for J_a.

J_w: very low water flows were observed at the drilling site. J_w has therefore been set to 1 for all Q calculations.

SRF: for the sake of this example, SRF has been set to 150 based on the recent work by Grimstad and Barton (1993).

The mean value for Q 3.8 was selected for use in the rock mass design.

In order to use the chart in Figure 1, the Span/ESR factor is required. The initial unsupported span is 7.0 m while an ESR figure of 1.3 was used from Category C, Table 1. These two values provide a Span/ESR figure of 5.4.

Using the mean value for Q and the Span/ESR of 5.4, the support design from Figure 1 is rockbolts about 2.8 metres in length at about 2 metre spacing with 50mm of fibre reinforced shotcrete.

5.2 Structural Analysis

This case study involves the design of the Crusher Chamber at Olympic Dam, Roxby Downs. A plan view of the crusher chamber is shown in Figure 2.

As the dimensions in Figure 3 indicate, the crusher opening is very large and surrounded by development. The crusher's orientation was selected to minimize any stress effects. Previous insitu stress measurements in the area resulted in a predominately NE-SW principal stress direction, hence the long axis of the crusher was aligned in this direction. Due to the size, orientation and location of the crusher several additional problems needed to be overcome, primarily;

- The length and location of any rock bolts would be governed by the location of surrounding openings as well as any potential structural and rock mass requirements.
- The crusher excavation sequence.

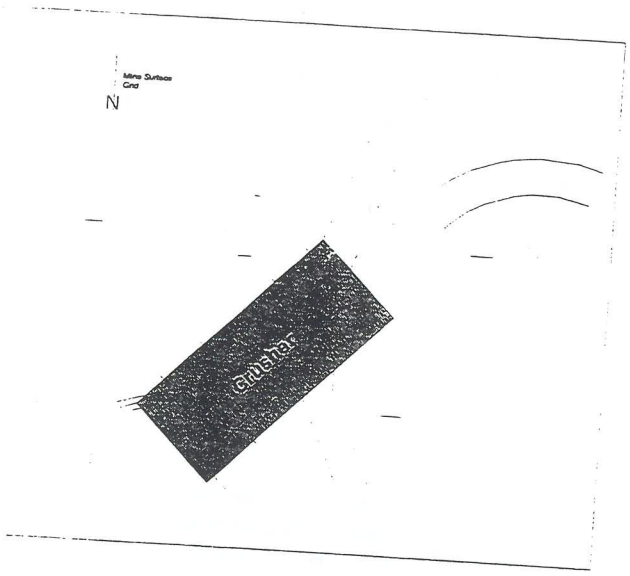

Figure 2. Crusher Chamber – Plan Elevation

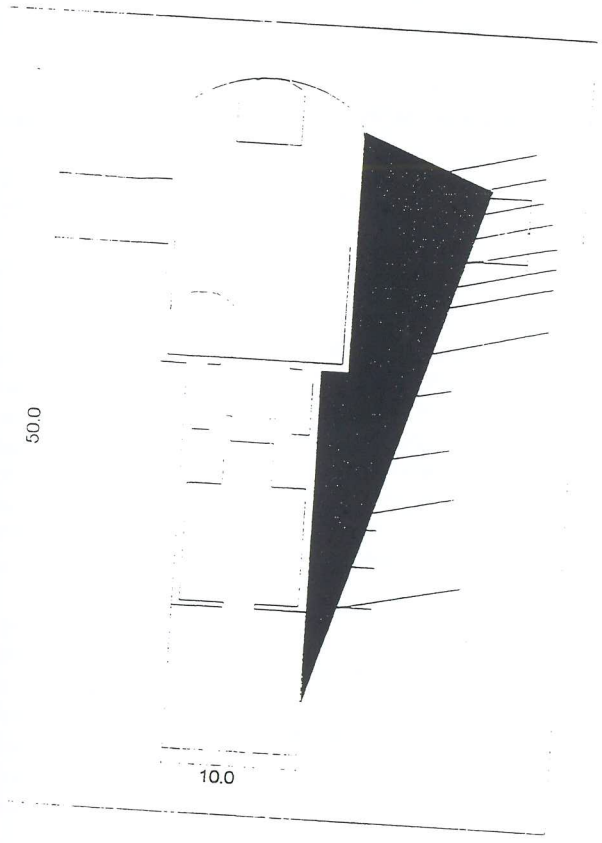

Figure 3 Crusher Chamber – Cross Section

Having being provided with structural mapping data by WMC from the nearby decline, a DIPS structural file provided the following result

Joint Set	Dip (degrees)	Dip Direction (degrees)
1	50	241
2	84	350
3	26	90

The UNWEDGE analysis indicated the potential for a large wedge on the South-East wall of the crusher chamber. Due to the size and shape of this wedge (see Figure 3), the primary concentration of bolts would have to be in the upper chamber as most of the mass of the wedge is contained in the upper portion. The maximum depth of the potential wedge in this region is approximately 8 metres, and this potential wedge meant that cable bolts would need to be used to ensure adequate anchorage length into solid rock. Cable bolts however do not offer immediate support and usually require the time taken for the grout to cure, before offering their maximum level of support.

The use of end anchored rock bolts was also recommended in conjunction with shotcrete. These end anchored rock bolts offer immediate support of the surface skin, allowing men and machinery to safely operate in the supported openings. The shotcrete provides additional safety against block failures between the rock bolts.

As can be seen in Figure 2, there are drives and openings located on the South-East wall. The bolting pattern was also tailored to suit the location of these openings. Another practical consideration was the excavation stages. The crusher chamber was to be excavated using a "top down" approach. With this method, the support would have to be installed as excavation progressed, hence the use of the end anchored bolts to ensure immediate support particularly in the roof.

Ultimately, the support installed consisted of cable bolts, end anchored bolts and shotcrete, with a concentration of cable bolts in the top of the South- East wall to support the potential wedge.

The ground support is performing well but the design process has not stopped. All openings are geologically mapped, not only for filing records but with the purpose of checking against the original DIPS master file and UNWEDGE analyses. In this way the insitu structures for a particular opening are used to update and change, if necessary, the UNWEDGE input data. Further analysis can then be re-run so that the original support design is checked and the "design loop" is closed off.

6. CONCLUSIONS

Analyses using both a structural and rock mass approach have a significant role to play in the design of underground openings. The contrast between the two, i.e. the *rockmass approach* based on the inherent properties of the rock, ie. rock strength, the presence of water, the number of joints and defects etc.. and a *structural* analysis based on the potential formation of wedges caused by the intersection of

joints and/or bedding planes. Both of these methods are required to cover all potential failure modes when designing any underground opening in rock.

7. REFERENCES

1. OLYMPIC DAM CORPORATION, " Olympic Dam Information Handbook"

2. Barton, N.R., "A review of the shear strength of filled discontinuities in rock.", 1974

3. Rock Engineering Group, University of Toronto, "UNWEDGE Users Manual", 1992

4. E. Hoek, "Support of Underground Excavations in Hard Rock", 1995

5. Grimstad, E., and Barton N., "Updating of the Q system for NMT", 1993

6. Rock Engineering Group, University of Toronto, "DIPS " Users Manual

7. Barrett Fuller & Partners, "Olympic Dam Crusher Chamber – Geotechnical Investigation", July 1997

8. ACKNOWLEDGEMENTS

The WMC Olympic Dam Expansion Project design team for permission to present the paper and Mr. K. J. Dugan of BFP Consultants for assistance in the writing, presentation and review of this paper.

Third A-NZ Young Geotechnical Professionals Conference, Cameron, Collingwood & Slatter (eds), Feb. 1998, Melbourne, Australia.

ANALYSIS OF FOUNDATION STABILITY OF MARINE RETAINING BUNDS, DURING CONSTRUCTION STAGES, USING EFFECTIVE STRESS

Bruce Symmans. GRADIPENZ
Riley Consultants Ltd, Auckland

Summary

Staged construction uses controlled rates of loading to enable soil strengthening via consolidation, in order to increase the foundation stability. The use of total stress analysis assuming instantaneous loading can sometimes lead to excessive conservatism as it makes no allowance for an effective strength gain that will occur during staged construction.

Experimental determination of consolidation parameters CV and A can allow an estimate to be made of the excess pore water pressure dissipation for any given length of time. The designer can then calculate the stability of the foundations at any given stage of construction using an appropriate effective stress stability analysis method.

Using effective stress analysis allows for an efficient design solution in which load timing can be manipulated to maintain adequate foundation stability. With an effective stress method design assumptions can be verified using piezometers to monitor the excess pore water pressures during construction.

Studies of three marine reclamation bund failures have verified that the effective stress method of analysis does give reasonable predictions of the actual factor of safety.

INTRODUCTION

As a load is placed on to a soil it induces excess pore water pressures (EPWP) within the soil. As the EPWP dissipates the load induced by construction is transferred from the pore water within the foundation soil, to the soil skeleton. This transfer of load from the water to the soil increases the effective stress in the soil which will generally increase the foundation stability. In terms of total stress, the consolidation that occurs as a result of EPWP dissipation will increase the undrained shear strength of the soil as the soil becomes denser.

Typically a design can be achieved that has a sufficient factor of safety (FOS) for the long-term (drained) condition. Difficulties can arise when trying to achieve an adequate FOS during construction. Total stress stability methods assuming instantaneous loading do not account for this strength gain and so can lead to excessive conservatism when construction is staged.

This paper describes a method of determining the rate at which the foundation strength gain occurs, making it possible to assess the structures stability at various stages of construction. This allows the construction rate to be timed so that adequate factors of safety are maintained at all times during the construction sequence.

The effective stress analysis method described is based on a combination of various classical soil mechanics principles. This method was used in order to study three marine reclamation retainment bund failures that have occurred around the Auckland, Waitemata harbour between 1995 and 1996. Each of the three failures of the rock retainment bund occurred during the period that the reclamation behind the bund was being filled. All three failures have subsequently been shown to exhibit adequate long term (drained) stability.

DISCUSSION

Bishop and Bjerrum (1) proposed that an effective stress analysis "is a generally valid method for analysing any stability problem and is particularly valuable in revealing trends in stability that would not be apparent from total stress methods" and advocated its use for analysing staged construction.

Calculation of effective stress

As the EPWPs induced by the applied load dissipate there is a decrease in water uplift pressures and hence an increase in effective vertical stress. All else being equal this increase in effective vertical stress will normally increase the frictional resistance along any shear surface and so will increase the stability of the bund.

In order to assess the rate at which the effective stress increases, the designer must assess:

- The excess pore water pressures induced within the foundation material due to initial and any additional loadings placed.
- The rate at which the pressures will dissipate at any given point within the soil foundations.

The designer can then use the EPWPs to analyse the stability of the bund and reclamation using conventional effective stress methods.

EPWP due to loading

The vertical stress (total) distribution induced by the loads can be estimated using contours of equal stresses or pressure bulbs from Teng (2).

The amount of EPWP initially induced by the increased vertical load will depend on the load's lateral distribution and the preconsolidation history of the foundation soils.

When an undrained saturated soil is loaded, a proportion of the load is initially supported by the pore fluid with the remainder being supported by the soil skeleton. The proportion of load supported by the pore fluid (i.e EPWP) is given by the pore pressure parameter A.

$$\text{i.e } \Delta u = A \Delta \sigma$$

where Δu = Change in excess pore water pressure

and $\Delta \sigma$ = Change in total stress

The pore pressure parameter A can be determined experimentally see Lamb and Whitman (3). Table 1 shows some typical vales for A.

Material (saturated)	Pore pressure parameter A
Very sensitive soft clays	>1
Normally consolidated clays	½ to 1
Over consolidated clays	¼ to ½
Heavily over consolidated sandy clays	0 to ¼

Table 1 Pore pressure parameter A, from Skempton and Bjerrum (4)

For saturated, soft, normally consolidated to slightly over consolidated soils all or most of the applied loading will initially be transmitted to EPWP rather than the soil structure. It is therefore a conservative approximation to assume that the EPWP induced within the foundation soils will be equal to 100% of the applied vertical load distribution (i.e A=1.0).

For a laterally confined, saturated material where no lateral displacement of the soil is possible, A will be 1.0 regardless of the soil properties.

Material densities

The use of soil and rock densities in calculating the applied loadings needs careful consideration. The effective load of the porous bund will vary because uplift pressures within the bund will vary due to tidal fluctuations. Eventually the soils will consolidate under the maximum load applied which occurs at low tide. During the finite period of construction the foundation soils will probably only consolidate towards the mean load applied. Densities should therefore be calculated using:

- Bulk density for material placed above mean sea level
- Buoyant density for any material placed or removed from below mean sea level

Once the initial EPWP distribution has been calculated the rate at which the EPWPs dissipate should be determined.

EPWP dissipation

The EPWP dissipation within the soil foundation can be estimated in a number of ways. The most accurate is by using a finite difference model. The finite difference model can be calculated using a simple spreadsheet but more specialised commercial software is also available. For a quick check or for less detailed projects where dissipation can be assumed to be in a vertical direction only, a one dimensional finite difference model can be adopted. For a uniform initial EPWP distribution, vertical dissipation can be approximated using "degree of consolidation" curves from Lambe and Whitman (3).

Dissipation modelling equations

Based on Terzaghi's Consolidation theory the governing differential equation relating excess pore-water pressure, position and time can be derived as:

$$\frac{\partial u}{\partial t} = Cv \frac{\partial^2 u}{\partial z^2} \qquad (1)$$

where CV = coefficient of consolidation
u = excess porewater pressure
t = time
z = drainage distance

This equation can be developed into a model with dissipation in one dimension. The EPWP in the cell x=n, y=n at t=n+1

assuming vertical dissipation only, is given by equation (2).

$$u(y_n,t_{n+1}) = u(y_n,t_n) + \beta\left(u(y_{n+1},t_n) + u(y_{n-1},t_n) - 2u(y_n,t_n)\right) \quad (2)$$

and with two dimensional dissipation

$$u(x_n,y_n,t_{n+1}) = u(x_n,y_n,t_n)+\beta\left(u(x_{n+1},y_n,t_n)+u(x_{n-1},y_n,t_n) +u(x_n,y_{n+1},t_n)+u(x_n,y_{n-1},t_n)-4u(x_n,y_n,t_n)\right) \quad (3)$$

where β is a dimensionless coefficient

$$\beta=\frac{Cv\,\Delta t}{z^2} \quad (4)$$

and z = the distance between cell centres

The coefficient of consolidation (CV) can be directly measured from an oedometer test, described in NZS 4402:1986.

As for all finite difference models accuracy is proportional to the time step (Δt). Appropriate selection of boundary conditions is also essential. The excess porewater pressures will be zero at any free surface and will be zero a large horizontal distance from the applied load. The designer must also assess whether double or single drainage is occurring within the foundation layers. If single drainage is occurring, at the horizontally impervious boundary dissipation will only occur horizontally and vertically away from the boundary. The EPWP in the model cells above the horizontal impervious boundary can be modelled using equation (5).

$$u(x_n,y_n,t_{n+1}) = u(x_n,y_n,t_n)+\beta\left(u(x_{n+1},y_n,t_n)+u(x_{n-1},y_n,t_n) +u(x_n,y_{n+1},t_n)-3u(x_n,y_n,t_n)\right) \quad (5)$$

The initial loading and any subsequent lifts in bund or reclamation height should be added to the model at the appropriate time steps.

The uplift pressures within the soil foundations at a given time can be determined by adding the EPWP to the static background water pressures. For soils below mean low water, the static water pressures will closely correspond to a piezometric level at mean sea level.

Figure 1 shows the EPWP calculated beneath a marina bund 13 months after the rock bund was placed. The reclamation fill was progressively raised over the same 13 month period. Single drainage was assumed to occur because of the underlying lower permeability mudstone.

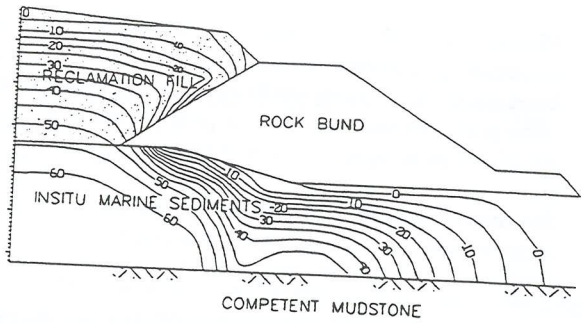

FIGURE 1: EPWP beneath a marina bund 13 months after bund placement

Calculation of FOS

The construction should be staged so that easy checks can be made on stability and the rate of construction can be controlled by the designer. The FOS at any of the proposed stages can be easily calculated using an effective stress stability analysis. Estimates of uplift pressures at each stage can be derived from the method described above.

Effective strength parameters can be established by:

- confined triaxial testing
- preloading a test structure to failure

The critical case for bund stability will occur at low tide when the water surcharge on the toe is at a minimum. This case should be analysed using the lowest tide likely to occur during the construction period, noting that barometric pressures can further reduce the predicted low tide levels significantly. All of the failures studied occurred at or very close to low tide.

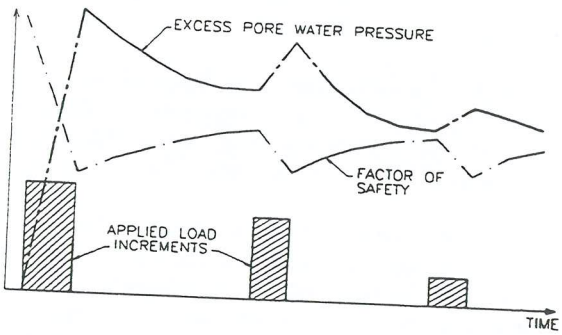

FIGURE 2: Schematic relationship between staged load application, EPWP and FOS.

As the EPWP increase immediately as further load increments are applied, critical times during construction will be as the loadings are applied. Figure 2 schematically shows how the FOS changes relative to the load sequencing.

Monitoring

Piezometers with low water volume requirements such as pneumatic piezometers, should be installed, preferably prior to bund construction. Early installation will give background pore water pressures and will show the peak pressures as well as the initial and most rapid excess pore pressure decrease.

Standpipe piezometers are not suitable for this situation as they require large fluid volume changes to register small changes in pressure which will affect the pressures in the surrounding soils.

Settlement monitoring is a good indication that pressures are dissipating or increasing (ie. settlement will stop) as expected, it is however difficult to get a correlation of EPWP from settlement.

It is important that the piezometers are installed by, or at least supervised by an experienced geotechnical engineer who is familiar with piezometer installation and understands the implications of defective monitoring equipment.

To achieve the best results from piezometer monitoring, the piezometer tips should be installed close to the most likely failure plane were EPWPs are expected to be greatest.

Alarm levels should be set on piezometer pressures, and construction of any stage should not commence or proceed until pressures have dissipated to pre-established safe levels.

Construction programming

It is important to consider the amount of time which will be required for pressure dissipation during the construction programme. If possible the construction programme should be flexible to allow for delays in construction should slower than anticipated pore pressure dissipation occur.

Accuracy of determining FOS

For the actual failures studied the degree of field testing was reasonably good and the model used was reasonably detailed. The factors of safety calculated using the described method were in the range of 0.93 to 0.98 for each of the study failures.

The greatest uncertainty exists in estimating the rate of pore pressure dissipation from consolidation theory, see Bishop and Bjerrum (1). The observed rate of settlement of structures is invariably quicker than that calculated from oedometer test results carried out on small samples, see Simons and Menzies (5). This is because thin layers or lenses of sand or rootholes can result in higher permeabilities which will cause faster than expected dissipation of EPWP.

The assumptions made during design can and should be verified during construction using piezometer monitoring.

If the settlements of the structure are anticipated to be large the following factors may affect the rate at which dissipation occurs.

- Drainage length will shorten with time as the soil compresses.
- As the structure settles a larger proportion of the load will become buoyant and so may reduce the effective vertical stress.
- As the soils consolidate and become more dense there may be a decrease in permeability.

The significance of each of the above factors will be project specific and so should be considered independently by the designer.

Conclusions

Invariably the critical time for the stability of structures placed over soft saturated foundations is during construction, when excess pore water pressures induced by applied loading remain high within the foundation soils.

The use of total stress analysis assuming instantaneous loading can sometimes lead to excessive conservatism as it makes no allowance for an effective strength gain due to dissipation of excess porewater pressures.

Experimental determination of consolidation parameters CV and A can allow an estimate to be made of the EPWP dissipation at any given time. The designer can then calculate the stability of the structure at any given stage of construction using an appropriate effective stress analysis.

Using effective stress analysis allows for an efficient design solution where the rate of construction can be controlled to maintain adequate foundation stability. The assumptions made in design can be verified using piezometers to monitor the excess pore water pressures during construction.

References

1 Bishop, A.W. and Bjerrum, L. (1960). " The relevance of the triaxial test to the solution of stability problems." Proc. Res. *Conference on shear Strength of cohesive soils*, ASCE, 437-501.

2 Teng, W.C. (1962) Foundation Design. Prentice Hall, New Jersey.

3 Lambe, T.W and Whitman, R.V. (1979). Soil Mechanics, SI Version. John Wiley & Sons, New York.

4 Skempton, A.W. and Bjerrum, L. (1957). " A Contribution to the settlement Analysis of Foundations on Clay," Geotechnique, Vol. 7, p. 168.

5 Simons, N.E. and Menzies, B.K.(1977). A Short Course in Foundation Engineering, Newnes - Butterworths, London.

Analysis of Offshore Foundations Subjected to Storm Loading

Hossein A. Taiebat
Centre for Geotechnical Research, The University of Sydney

Summary: The potential for liquefaction of seabed sand underneath an offshore foundation subjected to cyclic storm loading is investigated. A semi-analytical approach has been adopted in the formulation of three dimensional finite element method for consolidation analysis. The effects of densification due to cyclic loading are also considered in the formulation. Results of experimental studies on sand samples are used to evaluate the effect of cyclic loading at different points in the soil. As an illustration of the method, the possibility of liquefaction of calcareous sand around a hypothetical offshore foundation under storm loading is investigated.

1 INTRODUCTION

The stability of foundations for offshore structures can be strongly affected if the seabed sediments have the potential to liquefy under wave-induced cyclic loading. The potential for liquefaction of seabed soils, particularly loose sands, is therefore a major issue that should be considered by the designers of offshore facilities on granular materials.

Foundations of marine structures are generally subjected to two kinds of loadings; ambient loads due to submerged weight and cyclic loads due to waves applied during a storm. Cyclic loads include a large number of cycles of short to medium periods (*5* to *15sec.*). Laboratory tests on sands have shown that the application of a large number of cyclic loads with moderate amplitude could produce a progressive degradation of the soil resistance and buildup of pore water pressures, which can alter the stability of marine structures founded on such soil. The pore pressure at various places within the soil profile may build up to a stage where it becomes equal to the mean effective stress resulting in cyclic liquefaction and leading to possible instability.

1.1 Liquefaction phenomena

The most important feature of cyclic loading on sands is the cumulative densification which is responsible for such phenomena as liquefaction and loss of strength. Numerous experiments on various sands show that cyclic stresses or strains cause slip at grain to grain contacts. This inter-granular slip, in dry sands, would lead to volumetric compaction. In saturated sands where the drainage path is long or cyclic loads are applied at high frequencies, the volumetric compaction is retarded because water can not drain instantaneously to accommodate the volume change. Consequently, the sand skeleton transfers some of its inter-granular or effective stresses to the pore water and the pore water pressures increase. Reduction in effective stresses leads to a structural rebound in the sand skeleton and reduces shearing resistance of the soil. In extreme cases, the pore water pressure developed during cyclic loading may increase until all the inter-granular or effective stresses acting on the soil skeleton are eliminated from the system. In this case the soil flows like a viscous liquid and liquefaction is said to have occurred (Finn *et al*, 1976).

1.2 Experimental studies of liquefaction

In laboratory undrained tests, liquefaction is characterized by a rise in pore water pressure to a value equal to the consolidation pressure in triaxial tests or to the initial vertical stress in simple shear tests. Excessive strains accompany the high pore water pressure rise and the sample collapses within a few cycles after the pore pressure becomes equal to the initial consolidation stress.

The knowledge of pore pressure response to a cyclic loading and its interaction with the soil skeleton is an important feature for a liquefaction analysis. The results of experimental tests on saturated sand are usually expressed in term of the number of cycles required for liquefaction, N_l, under various levels of cyclic stress ratio, q_{cyc}/p', where q_{cyc} is the cyclic deviatoric stress applied to the sample and p' is the mean consolidation stress. Typical results of experimental studies which were conducted on samples of calcareous sand under cyclic loading and undrained conditions (Kaggwa, 1988) are presented in Fig. 1.

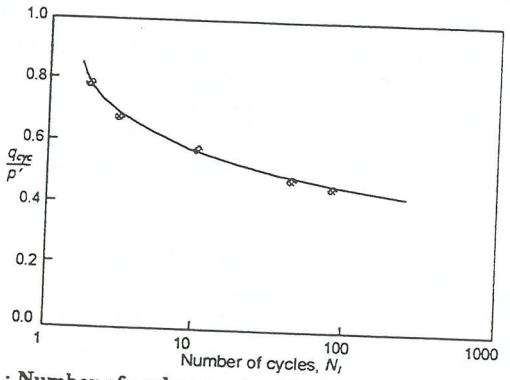

Fig. 1 : Number of cycles required for liquefaction versus cyclic stress ratio

The rate of pore pressure generation is usually related to the cyclic ratio, N/N_l, by a pore pressure generation function (Seed and Idriss, 1982). The rate of pore pressure generation can be expressed as :

$$\frac{u_g}{p'} = \frac{2}{\pi} Arc\sin\left(\frac{N}{N_l}\right)^{1/2\theta} \quad (1)$$

where u_g is the pore pressure developed due to cyclic loading, N is the number of stress cycles applied to the sample, and θ is a factor related to the type of material and the magnitude of initial deviatoric stress, q. A value of θ was proposed by Kaggwa (1988) for calcareous sands as:

$$\theta = 1.68\, e^{6.79q/p'} \quad (2)$$

A family of curves which represent the pore pressure generation function with different values of θ is plotted in Fig. 2.

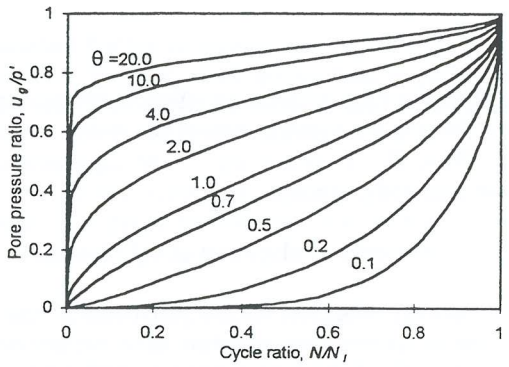

Fig. 2 : Rate of pore pressure generation for various θ

1.3 Evaluation of liquefaction of soils under foundations

Application of cyclic loading to a foundation will also generate pore pressures in the soil. However, the net increase in pore pressure will be the resultant of the pore pressure generation due to cyclic loading, the diffusion of pore pressure within the soil, and the dissipation of the pore pressure through drainage boundaries.

Development of pore pressures and strains resulting from cyclic loading can be predicted mainly by two numerical approaches. The first one is an incremental analysis in which the whole stress path is followed for every individual load cycle by using a hysteritic stress-strain relationship. Application of this method for evaluation of liquefaction in the field is not practical since it requires a large computational effort. In the second approach, the tendency to accumulate strain and its subsequent effects on pore pressure generation are considered at the end of one or more cycles. The results of physical experiments are used to correlate the accumulation of strain and pore pressure due to cyclic loading. Depending on the availability and level of sophistication of experimental and numerical tools, various methods for liquefaction analysis have been developed. Most of the studies on liquefaction potential of offshore foundations are based on the second approach, some of them are summarized below.

One of the earliest evaluations of the possibility of liquefaction was performed by Bjerrum (1973). Based on results of undrained simple shear tests, he estimated the excess pore pressure increment of every single wave and determined the excess pore pressure at the end of a storm by summing up the pore pressure increments. The effect of dissipation of pore water pressure during the storm was ignored. Lee and Focht (1975) consider the effect of pore pressure dissipation in a pragmatic manner by modifying the experimental procedure.

Rahman *et al* (1977) presented a more rigorous solution to the problem by considering the effects of stress distribution in the soil profile and dissipation of pore pressure using a finite element analysis based on Darcy's Law. Chugh and Thun (1985) used the same procedure for one dimensional dynamic analysis of a liquefiable soil. In both methods, the stress distribution in the soil profile was obtained from independent sources.

Reese *et al* (1988) analysed a pile subjected to lateral load generated by storm waves. The results of strain-control cyclic tests on sand samples were used to calculate the pore pressure. The deflection of the pile due to lateral load was obtained using the p-y method. The strain field was calculated by employing a "hybrid, finite-element-type formulation". The dissipation of pore pressure was then evaluated using an axi-symmetric finite element model.

1.4 Procedure for analysis of liquefaction

A procedure for the analysis of liquefaction based on the second approach is used in this study. The procedure incorporates the generation of pore water pressure due to cyclic loading under undrained conditions, followed by an analysis of pore pressure dissipation both during and after a storm event. Experimental test data on the sand are used to evaluate the pore water pressure generated at any point in the soil during cyclic loading.

The analysis includes a number of steps, viz.
1-definition of storm and the resulting loads that act on the foundation,
2-computation of initial and cyclic stresses within the soil,
3-estimation of excess pore water pressures resulting from the cyclic loading under undrained conditions,
4-incorporation of the cyclic load effects in a finite element program and solving for dissipation of pore water pressures.

2 NUMERICAL FORMULATION

The three dimensional nature of the stress and strain fields in the soil under a foundation subjected to lateral cyclic loading is one of the main difficulties in a liquefaction analysis. A numerical tool is required, capable of performing a three dimensional consolidation analysis. The numerical tool should be efficient and quick, because in a liquefaction analysis, the whole process of generation and dissipation of pore water pressure must be followed thousands of times during a storm.

In the present paper, the procedure described in section 1.4 is used to analyse the possibility of liquefaction in soil. A unique feature of the analysis is that the effect of excess pore pressure is explicitly taken into account. An efficient finite element program has been developed based on a semi-analytical approach (Zienkiewicz and Taylor, 1989). The method presented originally by Zienkiewicz *et al* (1982) has been used to include an additional accumulation of strain due to cyclic loading into the finite element formulation.

2.1 Effects of cyclic loads

The cyclic loading on saturated sands can be viewed as an agency that causes a reorientation and repositioning of sand particles, which leads to a reduction in void spaces. As a consequence, in an undrained test, water pressure in the voids rises and in a drained test, displacement and volumetric strain increase. The change in the void spaces due to cyclic loading can be considered as a change in strain, $d\varepsilon^c$, within the samples.

A reasonable approximation to the cyclic strain generated by cyclic load, $d\varepsilon^c$, is to consider it to be isotropic, i.e.:

$$d\varepsilon^c = e.d\varepsilon_v^c/3 \tag{3}$$

where $d\varepsilon_v^c$ is the change in the volumetric strain due to the change in the voids volume, and $e=(1,1,1,0,0,0)^T$.

The total strain, $d\varepsilon^t$, can be regarded as the sum of strain changes related directly to stresses, $d\varepsilon^s$, and strain changes which are generated by cyclic loads, $d\varepsilon^c$, i.e.

$$d\varepsilon^t = d\varepsilon^s + d\varepsilon^c \tag{4}$$

The general stress-strain relationship can be given as:

$$d\sigma' = \boldsymbol{D}(d\varepsilon^t - d\varepsilon^c) \tag{5}$$

in which $\boldsymbol{D}$ is the stiffness matrix of the solid skeleton.

The definitions of effective and total stresses and their link with pore pressure gives:

$$d\sigma = d\sigma' + e.du \tag{6}$$

where $d\sigma$ denotes the change in total stress in the soil, and u is the excess pore water pressure.

Substituting equations (3) and (6) into equation (5) yields:

$$d\varepsilon^t = e.d\varepsilon_v^c/3 + \boldsymbol{D}^{-1}(d\sigma - e.du) \tag{7}$$

For an undrained test, $e^T.d\varepsilon^t=0$, and in such tests where the average stress level is held constant, $d\sigma=0$, the pore water pressure will rises to du_g due to cyclic loading. Therefore equation (7) gives:

$$d\varepsilon_v^c = e^T.\boldsymbol{D}^{-1}.e.du_g \tag{8}$$

where du_g represents the pore pressure generated by cyclic loading alone.

Equation (8) relates the pore pressure generated in an undrained cyclic test to the volumetric strain in a drained cyclic test. By this expression the volumetric strain and the pore water pressure can interchangeably be used in all computations (provided the inverse of $\boldsymbol{D}$ can be evaluated). The use of the latter is convenient as it represents the most direct connection between the experimental data and subsequent calculations.

Substituting equation (8) in (7) results in a general stress-strain relationship that can be used in the formulation of finite element method, i.e.

$$d\varepsilon^t = e.e^T.\boldsymbol{D}^{-1}.e.du_g/3 + \boldsymbol{D}^{-1}(d\sigma - e.du) \tag{9}$$

or in a more general form:

$$d\sigma - e.du = \boldsymbol{D}.d\varepsilon^t - \boldsymbol{D}.d\varepsilon^c \tag{10}$$

in which:

$$d\varepsilon^c = e.e^T.\boldsymbol{D}^{-1}.e.du_g/3 \tag{11}$$

Computationally, the term $d\varepsilon^c$ (or $\boldsymbol{D}.d\varepsilon^c$) in equation (11) can be regarded as an initial strain (or initial stress) in the standard finite element formulation. This term can be included in the right hand side force vector, f_r, in the coupled finite element equations.

2.2 Coupled finite element formulation

The fully coupled finite analysis of consolidation has been described previously in the literature (see for example, Small *et al*, 1976). The governing system of equation may be written as:

$$\begin{pmatrix} \boldsymbol{K} & -\boldsymbol{L}^T \\ -\boldsymbol{L} & -\Delta t.\beta.\boldsymbol{\Phi} \end{pmatrix} \begin{pmatrix} \Delta\delta \\ \Delta v \end{pmatrix} = \begin{pmatrix} f_r \\ f_p \end{pmatrix} \tag{12}$$

where δ represents the nodal displacements, v denotes the nodal pore pressures, $\boldsymbol{K}$ is the stiffness matrix, $\boldsymbol{L}$ is the coupling matrix, β is an integration constant, $\boldsymbol{\Phi}$ is the flow matrix, f_p are the flow terms, and f_r is the vector of body forces and surface tractions, which includes the initial strains due to cyclic loading.

It is assumed that the process of application of wave loads on the system is so slow that the associated dynamic effects do not change the results of analysis significantly and thus may be ignored.

2.3 Finite element program

A semi-analytical approach in finite element method has been used to develop a quick and efficient finite element program. The program has the capability of three dimensional consolidation analysis. The formulation of the finite element program is based on the assumption that the field quantities such as displacements and pore pressure can be given by their discrete Fourier representation. In this method advantage is taken of the axi-symmetric nature of the problem geometry, and only one wedge from a cylinder of the soil-foundation media is modelled (Fig. 3). Instead of solving a very large number of algebraic equations, a smaller number of equations arising from a substitute problem will be solved (Taiebat, 1998). This method reduces the computational time below 5% of the time required for a standard three dimensional finite element analysis (Lai and Booker, 1991).

3 STEPS IN THE LIQUEFACTION ANALYSIS

In the liquefaction analysis, the duration of the storm is divided into a number of wave parcels. Within each parcel, the waves are assumed to be of equal height and the cyclic loads they induce to the foundation have the same amplitude. Each parcel is further divided into small time steps, of length Δt, which may include one wave or several waves.

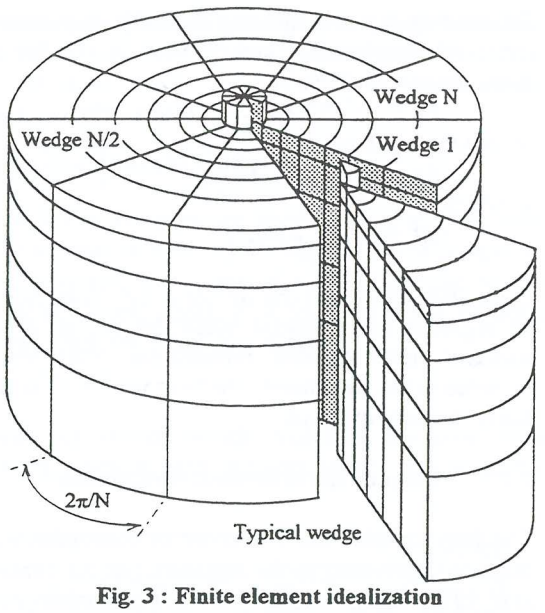

Fig. 3 : Finite element idealization

At the beginning of each time step, the pore pressure generated by the cyclic loads acting during the time interval Δt is calculated. This can be achieved by the knowledge of the number of cyclic loads applied to the foundation during the time interval, the cyclic stress ratio, q_{cyc}/p', and the experimental data such as those presented in Fig. 1 and equations (1) and (2). The effects of cyclic loads are then incorporated in the finite element program, using equation (10). The problem is then solved by computing the dissipation of pore pressure that is generated within the time increment being considered. The analysis is continued by marching forward in time, computing the pore pressure generated by cyclic loading and the dissipation by soil consolidation, until all parcels of wave loading have been considered and the end of storm is reached.

The initial mean and deviatoric stresses, p' and q, and cyclic deviatoric stress, q_{cyc}, are evaluated by the program whenever any change in loading occurs during the storm.

4 ILLUSTRATIVE EXAMPLE

Prediction of the liquefaction potential of the seabed soil around a single pile subjected to cyclic loading was investigated as an illustration of the proposed method. The finite element program and the procedure described in the previous section have been used in the analysis.

4.1 Definition of the problem

A single pile with a length of *80m* and a diameter of *2m* embedded in calcareous sand was considered. The Young's modulus of the pile is *200GPa*. The soil layer was assumed to be essentially elastic. The soil Young's modulus was defined as $E'=1.0\,z$ *(MPa)*, where z is the depth in metres below the mudline. The soil has a coefficient of permeability of $k=5.4\times10^{-6}m/sec$, a submerged unit weight of $\gamma_{sub}=7kN/m^3$, and a coefficient of in situ lateral pressure of $K_o=0.3$. The cyclic properties of the calcareous soil are described by Fig.1, equations (1) and (2).

The magnitude of the ambient axial and lateral loads on th pile are *25,000 kN* and *2,000 kN*, respectively. Also mudmat with a radius of *4m* exerts a uniform pressure *100kPa* on the surface of the soil. It is assumed that th ambient loads remain constant during the storm.

The storm loading considered in this analysis has bee generated for cyclones with *100* and *10,000* year retur periods. The wave composition and their duration are show in Table 1. The storm was assumed to have a simple wav load composition, increasing in magnitude from zero to i maximum value at the peak of the storm, and reducin gradually to zero after the peak. Fig. 4 shows the storm histogram adopted in this analysis. The peak of storm for *10* and *10,000* year return period is *24hrs* and *20hrs* after th start of the storms, respectively.

It was assumed that the storms generate only a lateral cyclic loa on the pile. The cyclic loads, H_{cyc}, is a function of wave height i.e. $H_{cyc}=0.268h^{2.6}$ *(kN)*, where h is the wave height in metres.

Table 1 : Composition of wave heights for storms

Wave Height (*m*)	Period (*sec.*)	No. of waves	
		100 yr.	*10,000 yr.*
0 - 1	4.6	4254	4227
1 - 2	5.8	3490	3196
2 - 3	7.0	3054	2012
3 - 4	8.2	2290	1514
4 - 5	9.4	1964	1125
5 - 6	10.6	1310	931
6 - 7	10.7	982	717
7 - 8	10.9	796	680
8 - 9	11.1	644	525
9 - 10	11.3	436	467
10 - 11	11.5	306	363
11 - 12	11.7	208	381
12 - 13	11.9	142	284
13 - 14	12.1	88	228
14 - 15	12.3	54	140
15 - 16	12.5	34	118
16 - 17	12.7	20	120
17 - 18	12.9	10	66
18 - 19	13.1	6	34
19 - 20	13.4	4	20
20 - 21	13.6	2	17
21 - 22	13.6	0	19
21.8	**13.8**	**1**	0
22 - 23	14.0	0	13
23 - 24	14.2	0	7
24 - 25	14.4	0	4
25- 26	14.6	0	4
26 - 27	14.8	0	1
28.4	**15.0**	0	**1**

4.2 Results of the analysis

Excess pore pressures were predicted around the pile during the storm. For the storm with *100* year return period, the magnitude of the pore water pressure is not significant during the first *13* hours of the storm. Application of larger waves generates increasing excess pore pressures up to the peak of the storm, after which the excess pore pressures steadily reduce to zero. Similar trends can be observed during the analysis for *10,000yr.* storm. The variations of the maximum values of the excess pore pressures generated during the

storms are shown in Fig. 5. The maximum pore pressure in the soil is not sustained for more than *30* minutes.

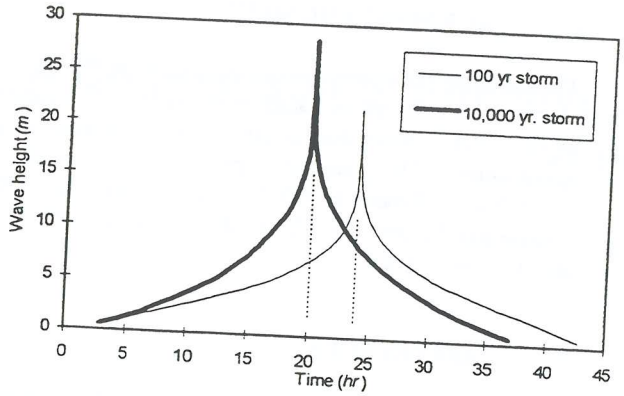

Fig. 4 : Storm histogram

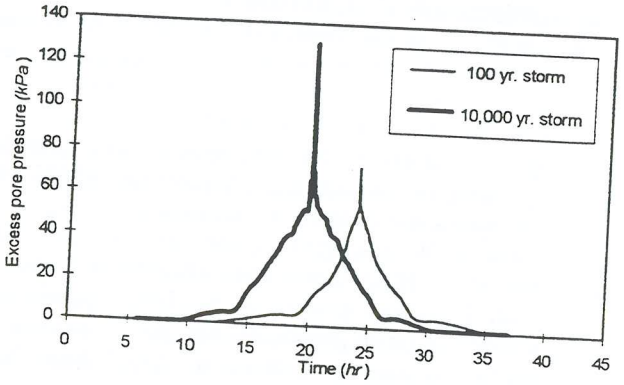

Fig. 5 : Variations of the maximum excess pore pressure during the storms

The distribution of predicted excess pore pressure in the vertical plane containing the applied lateral load, at the peak of storm, is illustrated in Fig. 6 and Fig. 7, for the *100yr.* and *10,000yr.* storms, respectively. These figures show that the zone of high pore pressure is limited to a small area around the pile. Application of the *10,000yr.* storm loading results in a wider and deeper zone of excess pore pressure around the pile, as expected.

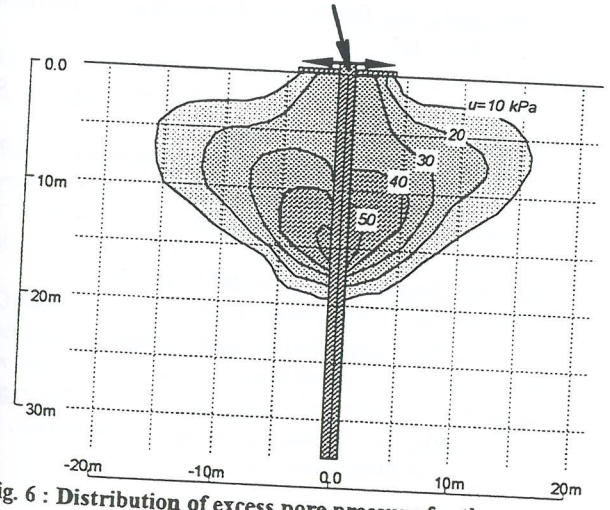

Fig. 6 : Distribution of excess pore pressure for the storm with *100* year return period at the storm peak

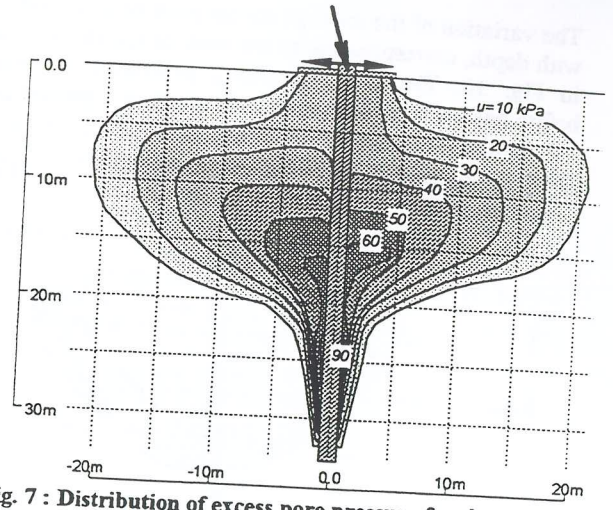

Fig. 7 : Distribution of excess pore pressure for the storm with *10,000* year return period at the storm peak

Representative values of pore pressure have been obtained by averaging the pore pressures in a region adjacent to the pile to a distance of four diameters from the pile and over the horizontal angular range from the direction of applied lateral load to *90°* from this direction. The variation of these average values with depth at the peak of the storm is shown in Fig. 8.

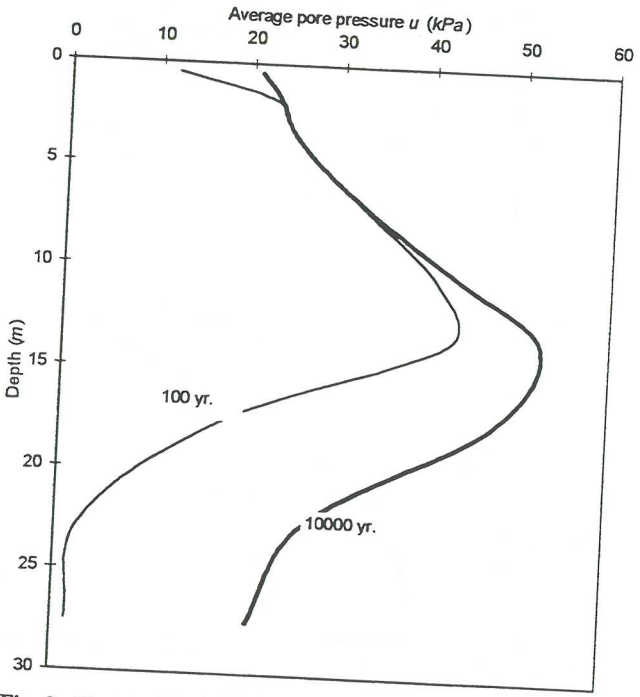

Fig. 8 : Variation of the average excess pore pressure with depth at the strom peak

If liquefaction is deemed to occur when the value of pore pressure reaches the same magnitude as the mean initial stress, then the results of analyses for both storms indicate the development of liquefaction in the soil around the pile. The extent of liquefied zones in the vertical plane of the applied lateral load is shown in Fig. 9. It can be seen that the liquefied zones in this section extend to a depth of *12.5m* for the *100yr.* storm and *17m* for the *10,000yr.* storm.

The variation of the average excess pore pressure ratio, *u/p'*, with depth, corresponding to the peak of the storm, is shown in Fig. 10. The same averaging procedure as explained before has been used. Fig. 10 indicates that a general zone of liquefaction covers the top layer of the soil, which has a thickness of about *8m* for the *100yr.* storm and *13m* for the *10,000yr.* storm.

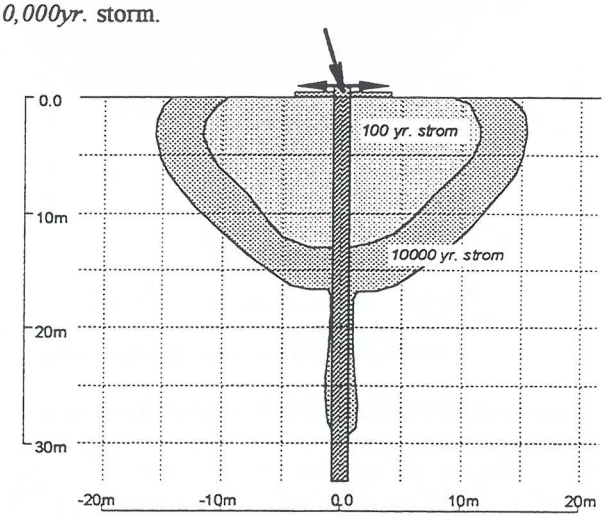

Fig. 9 : Liquefied zone at the storm peak

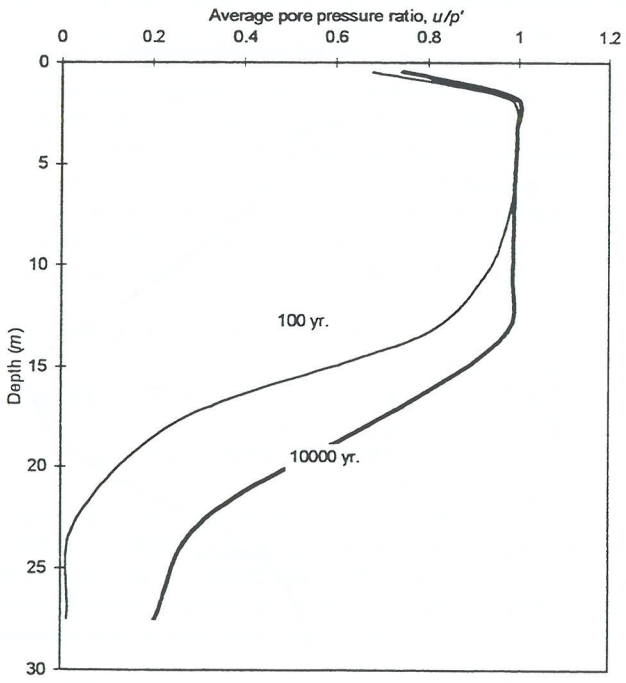

Fig. 10 : Variation of the average excess pore pressure ratio with depth at the storm peak

5 CONCLUSION

A method of analysis was presented which can be used for three dimensional liquefaction analysis of offshore foundations subjected to cyclic wave loading. The method was used to analyse a hypothetical single pile subjected to cyclic loading. The results of study on the pile show that the possibility of liquefaction of the soil around the top section of the pile is high. Therefore, the resistance of that part of the soil should be ignored in the design procedures.

6 ACKNOWLEDGMENT

The material published herein is a part of Ph.D. research program currently undertaking by the writer. The supervision of Prof. John Carter during the course of studies is greatly appreciated. The support provided by Centre for Geotechnical Research (CGR) and Centre for Offshore Foundation System (COFS) at the University of Sydney is also acknowledged.

7 REFERENCES

1. Bjerrum, L. (1973) "*Geotechnical problems involved in foundations of structures in the North Sea*", Geotechnique, 23, 3, 319-358
2. Chugh, A. K. and Thun, J. L. V. (1985) "*Pore pressure response analysis for earthquakes*", Canadian Geotech. J., 22, 466-76
3. Finn, W. D. L., Lee, K. W. and Martin, G. R. (1976) "*An effective stress model for liquefaction*", Liquefaction Problems in Geotechnical Engineering, ASCE, Annual convention and exposition, Philadelphia.
4. Kaggwa, W. S. (1988) "*Cyclic behaviour of carbonate sediments*", Ph.D. thesis, The University of Sydney.
5. Lai, J. Y. and Booker, J. R. (1991) "*Application of discrete Fourier series to the finite element stress analysis of axi-symmetric solids*", Int. J. Num. Methods in Engineering, 31, 619-47
6. Lee, K. L. and Focht, J. A. (1975) "*Liquefaction potential at Ekofisk tank in North Sea*", J. Geotech. Division, ASCE, GT1, 1, 18
7. Rahman, M. S., Seed, H. B. and Booker, J. R. (1977) "*Pore pressure development under offshore gravity structures*", J. Geotech. Division, ASCE, GT12, 103, 1419-36
8. Seed, H. B. and Idriss, I. M. (1982) "*On the importance of dissipation effects in evaluating pore pressure changes due to cyclic loading*", Soil mechanics-Transient and cyclic loads, Ed. Pande and Zienkiewicz, John Wiley & Sons, New York
9. Small, J. C., Booker, J. R. and Davis, E. H. (1976) "*Elasto-plastic consolidation of soil*", Int. J. Solids Structures, 12, 431-88
10. Taiebat, H. A. (1998) "*Numerical analysis of offshore foundations*", Ph.D. thesis, The University of Sydney
11. Zienkiewicz, O. C. and Taylor, R. L. (1989) "*Semi-analytical finite element processes*", The finite element method, Chapter 6, McGraw-Hill, New York
12. Zienkiewicz, O. C., Leung, K. H., Hilton, E. and Chang, C. T. (1982) "*Liquefaction and permanent deformation under dynamic conditions- Numerical solution and constitutive relations*", Soil Mechanics-Transient and cyclic loads, Ed. Pande, G. N. and Zienkiewicz, O. C., John Wily & Sons, New York

Third A-NZ Young Geotechnical Professionals Conference, Cameron, Collingwood & Slatter (eds), Feb. 1998, Melbourne, Australia.

A Comparison of Site Investigation Practice in the UK and Queensland

John Theos, Arup Geotechnics, Brisbane

Summary: A number of differences in specific areas of site investigation practice in the UK and Queensland are identified and discussed. These include, the use of desk studies, soft ground drilling, the procurement and the specification of site investigations. The main difference is perhaps the manner in which site investigations are procured, and it is concluded that this has probably resulted from the way the industries have evolved in the respective countries.

1 INTRODUCTION

Following a recent secondment to Arup Geotechnics' Brisbane office from Leeds in the UK, a number of differences in site investigation practice have been observed. This paper examines these differences from the desk study stage to the production of the interpretive report. In addition, the relative merits of the different approaches are considered and discussed. The paper is not an industry wide survey but a more personal observation of the author, reflecting his experience of working within the same organisation in two different countries.

2 DESK STUDIES

There are certain aspects which require different treatment at the desk study stage. Site investigations in the UK tend to be carried out on sites that have previously been developed. This is especially true of city centre sites where there may have been development dating back to medieval times and beyond. The need for detailed desk studies is therefore treated as a matter of course in the planning of investigations in the UK. A typical desk study would cover the following aspects:

- A site description including the results of a walk over survey;
- A history of the site;
- The geology of the site;
- An interpretation of the aerial photographs;
- A discussion on potential contamination;
- A description of previous investigations carried out on or nearby the site, if any;
- Recommendations for the site investigation.

2.1 History

This is traced through a number of different sources, the most abundant of which are maps and aerial photographs. In the UK there is a long history of detailed mapping which covers the main period of industrial expansion in the late 19th century and early 20th century. In the post Second World War period there is also frequent aerial photographic information which coincides with the last major phase of industrial expansion and then the contraction and dismantling of many industrial areas. For early industrial there are more fragmentary records in the form of private surveys and contemporary records.

2.1.1 Maps

Principally, in the UK, maps fall into two categories: Ordnance Survey and non-Ordnance Survey. The Ordnance Survey began publishing maps in 1804 at 1" to 1 mile scale. Larger scale maps are, however, of more interest for a desk study i.e. at 1:10560 (6" to 1 mile) and 1:2500 scales which show considerable detail. Most OS large scale 1st edition mapping starts from the 1860s and 1870s. 1:2500 scale maps show considerably more detail and exist for all settled areas from the 1860s and 1870s. Usually there are three and sometimes four pre-Second World War editions at roughly 20 year intervals. The maps are readily available either from the Ordnance Survey themselves, at the British Library (in London) or through the reference library local to the site.

Non-OS maps cover all privately commissioned and speculative mapping and pre-OS mapping. The accuracy, quality and scales vary with such maps. The principle maps of interest include early town plans, parish tithe maps, fire insurance plans and mine plans. These maps are generally found in municipal and county archives.

Maps from different periods are available for most areas of Queensland. However, regular mapping of the same area for a number of different dates may only be available for urban

centres such as Brisbane and the Gold Coast. It is therefore more difficult to trace a relatively reliable history of a particular site with these large gaps in information.

The first period of extensive mapping in Queensland was carried out by the Australian Army in the 1930s and 40s at 1" and 4" to 1 mile scales. The next major period of mapping commenced in the 1960s and has been ongoing ever since. Early cadastral maps dating from about the 1860s are held in the State Archives, but these are of limited value when tracing developments as they only really show property boundaries.

A fairly extensive amount of historical information and maps are available for Brisbane, but a large number of different sources have to be checked (for completeness): Brisbane City Council's (BCC) Heritage Section, the Department of Environment's Heritage Unit, the John Oxley Library (part of the State Library) and the State Archives.

2.1.2 Aerial Photographs

Aerial photography provides a more detailed record of the landscape than topographic mapping. The entire United Kingdom was flown in the three years following the Second World War. Since then there have been several smaller blocks of cover which in an ad hoc way provide at least one additional date of cover and in urban and industrial parts of the country upwards of a dozen dates of aerial photographic cover from the late 1940s to the present. This is all vertical cover which can be viewed in three dimensions through a stereo scope. Scales are typically from 1:3000 to 1:10000.

Aerial photographs are available for most areas of Queensland from the 1940s. Brisbane and the Gold Coast are particularly well covered for a number of different dates and scales. In addition, as a result of the work of the Beach Protection Authority, the whole of the Queensland coast has been photographed at least once in recent years. In general photographs of 1:12000 scale are available for coastal areas, 1:25000 for inland areas and 1:40/80000 for central areas of the state.

Orthophotos, which are 1:10000 vertical aerial photographs with contours marked on them are available for the Moreton Bay area (around Brisbane). These do not allow for stereo viewing, but are a very useful nonetheless.

The Department of Natural Resources in Brisbane hold the most complete record of photographs although there are a number of private companies which have their own collection.

2.2 Geological Maps and Memoirs

Complete coverage of the UK is available either at 1:50000 scale or at 1" to 1 mile (1:63360). 'Solid' and 'drift' editions are generally available. The 'solid' editions show the bedrock types only whereas the 'drift' maps show the nature and distribution of glacial, alluvial and other recent materials in addition to the solid geology. Most areas are also covered by 6" to 1mile (1:10560) which contain much more detailed information and even include brief details of deep boreholes and wells. There are a series of Handbooks of British Regional Geology for England, Wales and Scotland which describe the general geology of each region. For more detail there are memoirs available for many of the 'one inch' sheets. These were written by the geologists who first produced those maps. The smallest scale maps available Queensland are at 1:100000, although map commentaries (the equivalent to the hanbooks available in the UK) are available for some of these.

2.3 Other Geotechnical Data

Other sources of geotechnical data include mining reports and borehole information held by the British Geological Survey. On behalf of the Department of the Environment, Arup Goetechnics have produced a "Review of Mining Instability in Great Britain"[1] which provides information on areas of potential instability due to mining and is usually referred to. For coal mining areas in particular, reports are available from the Coal Authority.

Another good source of information is the British Geological Survey (BGS), which keeps a database of borehole records for the entire UK. There is an obligation to supply borehole records to the BGS on completion of site investigations. For a small fee, a search can be conducted and copies of the borehole records made available.

Unfortunately, there is no such body mandated to collect borehole data in Queensland, although some public bodies like Main Roads and Queensland Rail, do hold a certain amount of geotechnical information.

2.4 Contamination

A large number of site investigations in the UK are being carried out on sites that have previously been developed. A useful by-product of a historical desk study is that by tracing the development of a site it could also identify potential sources of contamination. This has become increasingly important and contributes to vulnerability reduction for site workers, plant and structures by identifying possible hazards in advance of the work.

2.5 Summary

Desk studies are carried out as a normal precursor to a site investigation in the UK. There is a vast amount of readily available historical and geological information for the majority of areas in the UK. Because of the scale of mapping (topographic and geological) and aerial photography, a considerable amount of detail can be gleaned at desk study stage. This is probably the reason why desk studies play a considerably more important role in the planning of site investigations in the UK.

3 INVESTIGATION TECHNIQUES

In general the methods adopted in the fieldwork and laboratory testing are essentially very similar. The way in which soils and

rocks are logged is, however, slightly different according to the respective code of practice for each country. The main area of difference is with regard to the soft ground drilling techniques.

In the UK soft ground drilling is usually carried out by light cable percussion (shell and auger) type rigs. This method uses a simple lightweight rig developed from old well boring techniques and towable by a Land Rover type vehicle. It consists of a tripod fitted with a diesel powered winch with a clutch and brake. The winch is used to lift and drop a variety of tools down the hole in a percussive action. Hole diameters are usually 6"to 8" (150-200mm) in diameter. A clay cutter tool is used for dry cohesive soils, a shell (or baler) for granular soils and a chisel for breaking up rock or other obstructions. Casing can be installed to support caving ground or seal off groundwater.

The equivalent drilling in Queensland is carried out by mechanical auger drilling or wash boring with hole diameters generally at 75mm. Without frequent sampling it is often difficult to obtain an accurate log of the soil profile with either of these two techniques. Changes in stratum and water ingress are more easily detected in a light cable percussive bore. In addition, as larger diameter holes are drilled in the UK, larger diameter undisturbed samples are obtained. The standard undisturbed sample tube is 100mm in diameter in the UK as opposed to 50mm in Queensland. However, both augering and wash boring are faster techniques than light cable percussion boring.

4 PROCUREMENT

Perhaps the most obvious difference in site investigation practice is the manner in which site investigations are procured and in the way that geotechnical information is presented. Current UK practice is to present separate factual and interpretive reports. The factual report, which is prepared by a specialist site investigation contractor, is the only report submitted during the tender process for the main works. The interpretive report is written by the consultant to the client's specific instructions and generally only used by the design team.

The Institution of Engineers, Australia, in their 'Guidelines for the Provision of Geotechnical Information in Construction Contracts'[2] recognise the two approaches in the provision of geotechnical data in tender documents:

"(a) provide only incontestable fact, with no interpretation or subjectivity which could be legally challenged, and which could lead to acceptance of responsibility, and having provided this limited information disclaim any liability as to its accuracy;

(b) allow for competent interpretation to a certain level (based on reason and a community standard of accepted engineering practice), with free acceptance by all parties that the interpretation has only a likelihood, not a certainty, of veracity. In addition, recognise the need for the fair apportionment of risk between the parties."

The recommendation given later in the guide is that "full disclosure of all known information or reports relevant to site conditions be made to tenderers on a contractual basis". As such current practice in Queensland is in line with item (b) above i.e. both the factual and interpretive information are provided in one report.

Current practice in the UK is essentially that described in (a) above. The reason for the difference of approach is probably related to the way in which the site investigation industries have evolved in the respective countries. The consultant's role in the UK is to carry out the following tasks on behalf of his client in relation to the procurement of the factual information:

- Ensure that an adequate desk study and walk-over survey is carried out;
- Define the scope of the investigation and provide the client with a cost estimate;
- Draw up the appropriate contract documents, including a specification and bill of quantities for the investigation;
- Obtain competitive tenders from at least three appropriate specialist site investigation contractors;
- Report on the tender prices to the client and make a recommendation;
- Administer the contract once it has been signed by the client and the contractor;
- Supervise the work to ensure that the technical standards are met;
- Ensure that the work is competently reported.

An advantage with the approach adopted in Australia for clients is that they only have to go to one firm for their geotechincal 'package'. In addition, the geotechnical engineers who will evetually provide the advice will have first hand experience of the ground conditions during the site investigation. This should enable them to provide a more efficient service.

5. SPECIFICATIONS

In the UK, all fieldwork and laboratory testing is carried out by specialist site investigation contractors who either have their own drillers and laboratories or subcontract to others. The consultant decides upon the scope of the investigation and on that basis draws up the specification and bill of quantities. This process was somewhat simplified in 1993 by the publication of the Site Investigation Steering Group's 'Specification for ground investigation'[3] (the so called 'yellow book'). This is a specification intended for general application to site investigation work, and sets out in detail the procedures to be adopted. Schedules are provided which set out the scope of the investigation and any modifications to the specification. A bill of quantities is provided which details the items which

correspond to the investigation.

The specification not only sets out the procedures to be adopted for the drilling of boreholes and insitu testing but also for the laboratory testing of soils and rocks. The relevant British Standard is usually referred to with regard to laboratory testing. Before the 'yellow book' each consultant had its own particular specification and bill of quantities. The site investigation contractors therefore had to make themselves familiar with each particular specification prior to pricing and carrying out the work.

The need for such specifications in the UK is really a function of the procurement process whereby the specialist contractor has a contract directly with the client. Site investigation specifications are not as necessary in Queensland as mostof the work is directed first hand by the geotechnical consultant. The guidance given in AS 1726 (Geotechnical site investigations)[4] is typically used to conduct the work.

6. CONCLUSIONS

This paper has identified three main differences in site investigation practice between the UK and in Queensland:

i. The extensive use of desk studies in the UK which is not as apparent in Queensland. Desk studies play such an important role in the UK simply because of the amount of information potentially available for the majority of the country. There are very few 'green-field' sites available for development and regeneration of derelict land is on the increase. Desk studies are therefore an extremely useful tool in not only providing a preliminary geotechnical model for the site but also its potential for contamination.

ii. Soft ground drilling techniques are another difference. The relative merits of the light cable percussive method used in the UK and mechanical augering and wash boring have been discussed. It is considered that the geotechnical benefits of the light cable percussive method far outweigh those of the speed of augering/wash boring. It is not hard to see how augering/wash boring is so prevalent in Queensland. The majority of drillers are self employed, and so speed and ease of drilling will be their priority.

iii. Perhaps the greatest difference in site investigation practice is with regard to the way in which investigations are procured and how the information is reported. The method adopted in the UK is recognised by the Institution of Engineers, Australia, but not recommended. The reason for the difference of approach is probably related to the way in which the site investigation industries have evolved in the respective countries.

7. REFERENCES

1. Arup Geotechnics, "Review of Mining Instability in Great Britain", Department of the Environment, 1991.

2. A Construction Industry Committee convened by the Institution of Engineers, Australia, "Guidelines for the Provision of Geotechnical Information in Construction Contracts", The Institution of Engineers, Australia, 1987.

3. Site Investigation Steering Group, "Site Investigation in Construction", Thomas Telford, 1993.

4. Standards Australia, "AS 1726-1993, Geotechnical site investigations", Standards Australia, 1993.

Thermal Modelling of Soil in Earth-Sheltered Structures

F. Thiele,
Department of Civil and Environmental Engineering, The University of Melbourne.

Abstract - This paper introduces a research project, which aims to model the effect of a flame front on a saturated earth berm sheltering a structure. FLAC 3.3 software is to be used to develop the theoretical models. Earth-sheltered structures are known for their energy efficiency. They offer other advantages including protection from natural hazards. Models simulating the behavior of earth sheltered structures in wildfires (bushfires) will be studied. Monitoring of the soil and atmospheric conditions at an earth-sheltered house in Gembrook, Victoria is soon to begin. Other sites may be monitored as the project develops. This data will be used to calibrate the theoretical models. This study should produce guidelines as to the dimensions of a berm, constructed from a "real" soil, which will keep a structure habitable during a bushfire. Risk assessment of this mode of construction in fire prone areas will be quantified. This study may also lead to the modelling and design of earth-sheltered storage structures for fuels or chemicals in fire prone areas.

1. Introduction

In North America, FLAC 3.3 software is used to model the freezing and evaporation of water in soil and optimise basement design for depth and insulation thickness. It is proposed to model the inverse of this situation, the effect of a flame front on a saturated earth berm sheltering a structure.

FLAC (Fast Lagrangian Analysis of Continua) is a two-dimensional, explicit finite difference code. It is capable of transient and steady state thermal analysis using implicit or explicit methods. (1) It is anticipated that a combination of both implicit and explicit methods will be utilised to produce the optimum model

2. Earth-sheltered Buildings

Earth-sheltered buildings, while not yet common in Australia, are steadily becoming more popular. Notable large scale examples include the New Parliament House in Canberra and the Brewarrina Aboriginal Cultural Museum. Currently under construction, in Sydney, is the new earth sheltered Woollahra City Council Chambers. This is being constructed adjacent to the existing historic building. There are also a small number (at least 30-50) of earth-sheltered homes being built each year. (2) These are usually built in rural or semi-rural (and often bushfire-prone) areas.

Earth-sheltered buildings offer many benefits including:

- Energy Efficiency -- little or no heating and cooling costs.
- Unobtrusive, blending into the landscape; there is an earth-sheltered Rangers Residence at Lake St. Clair National Park (Tasmania) which is effectively invisible until you are almost on top of it.
- Low maintenance.
- Preserves open space; earth-sheltered buildings have been designed and built in Europe and the USA for schools, museums, university buildings
- Protection from noise pollution; a public housing project in Minneapolis was successfully designed to minimise noise from an expressway directly behind the development. (3)
- Protection from hazards such as high-intensity storms, earthquakes and wildfires. Underground structures provide resistance to seismic movement due to a number of factors inherent in their design; large earth loadings used in design and the natural movement of the structure with ground motion lessens the "amplification of ground motions by structural oscillation". (4)
- Studies on earthquake effects on underground structures [Gao, (1984) (5) and Loofbourow, (1985) (6)] and earth-sheltered buildings [Lowing, (1984) (7)] support the superior resistance of subsurface structures. Eighty percent of the recently completed Miho Museum in Japan is below ground, chiefly because of the strict local seismic and environmental regulations. (8)

3. Wildfires

Wildfires (bushfires) cause immense damage to people, property and the environment every year. The 'Ash Wednesday' fires in 1983 resulted in the death of 76 people and property damage in excess of $440 million. (9) Wildfires also regularly threaten life and property in the US, Canada, South Africa and the Mediterranean countries.

Earth-sheltered buildings have been given qualitative approval for use in bushfire prone areas by Standards Australia, CSIRO (10) and other sources. (11) This approval is primarily based on the non combustible characteristics of soils. Few, if any, quantitative studies appear to have been performed.

Krarti and Claridge (1990) developed a semi-analytical method for analysing heat exchange between soil and rectangular earth-sheltered buildings. (12) A number of studies have been performed on the thermal performance of these structures, but the emphasis tends to be on heat loss in cool climatic conditions. How does a heat front from an intense, transient source move through an earth wall?

4. The Gembrook House Project

An associated project is the monitoring of an earth sheltered house in Gembrook, Victoria. This project involves the monitoring of soil temperature and moisture levels in the earth berm and roof of the house. External and internal air temperature and humidity both internally and externally will also be monitored.

Thermocouples and Buriable TDR (Time Domain Reflectometry) Wave guides were installed during construction. The thermocouples were laid in 15 mm diameter UPVC conduit to give additional protection from impact or flexural damage. Where instruments were buried at any depth, the necessary pits were backfilled and compacted in layers. A final layer of bentonite was used to mitigate any concentration of moisture due to changed drainage conditions in the disturbed soil. Instrumentation to measure air temperature and humidity both internally and externally is also to be installed. Monitoring is expected to commence in late 1997.

The monitoring program should provide soil temperature and moisture profiles, which will aid in the calibration (matching) of the models. Should a bushfire occur during the monitoring period, some extremely useful data will be obtained.

The body of the house is constructed of reinforced concrete, monolithically poured using a patented reusable modular form work.

The design of the Gembrook house incorporates a number of Passive Annual Heat Storage (PAHS) principles. Passive Annual Heat Storage is a series of techniques designed to maintain a desirable average air temperature. The structure and the surrounding earth interact in such a way as to ensure that internal temperatures remain within a few degrees of the desired temperature at all times. (13) This can eliminate the need for supplementary heating and cooling even in extreme climates. After construction, a 'settling' period is necessary for the earth/structure to stabilise. Existing sources (14) make recommendations only for North American conditions. Data from this project is also to be used in a study of PAHS stabilisation for Australian conditions.

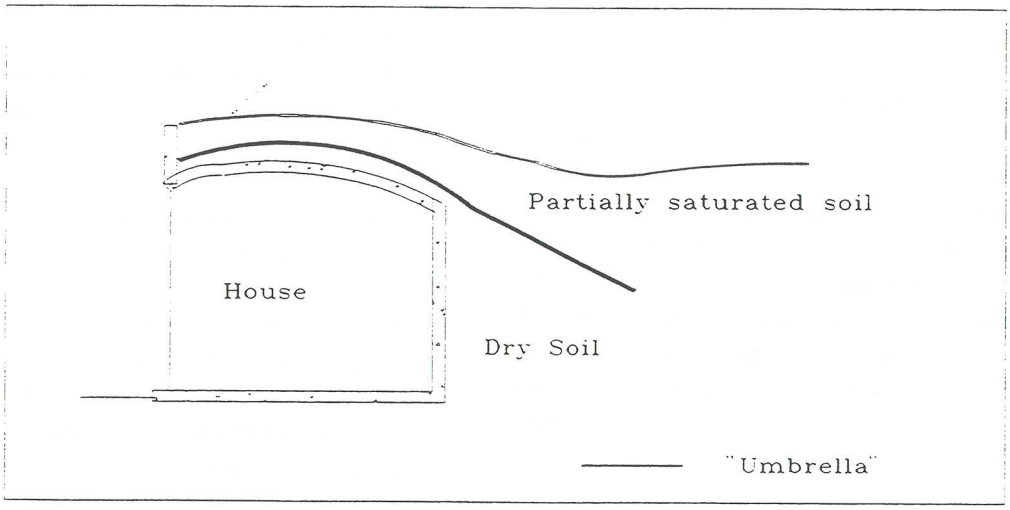

Figure 1 – Section through Earth-sheltered House in Gembrook, Victoria.

The design of the Gembrook House involves an insulating "umbrella" laid over a layer of compacted soil, during the construction process, forming a dry soil "heat bank" after a suitable period of drainage. This will result in a layered soil profile comprising, from the concrete structure of the roof upwards:

- dry (or nearly dry) soil,
- insulating layer (2 layers of heavy duty builders plastic sandwiching a thick layer of spoiled hay), and
- Partially saturated soil subject to normal surface conditions. (Refer Figure 1, below.)

There are many variations of wall profile possible. Further models for a representative sample of wall profiles are envisaged. These would include models for earth sheltered structures and possibly other earth wall types such as pise (rammed earth) and adobe (mud brick).

5. Conclusion

This study should result in a greater understanding of the movement of heat fronts through earth walls. Guidelines will be produced as to the dimensions of a berm, constructed from a "real" soil, which will keep a structure habitable during a bushfire. The "real" soil properties used in this modelling will include porosity, density, and initial degree of saturation.

Risk assessment of this mode of construction in fire prone areas will be quantified. This study may also lead to the modelling and design of earth-sheltered storage structures for fuels or chemicals in fire prone areas.

(1) "Fast Lagrangian Analysis of Continua Version 3.3", Volume III: Appendices Itasca Consulting Group, Inc. Minneapolis 1995

(2) Baggs, D.W., ECA Space Design Pty. Ltd., Castle Hill, NSW, pers. comm.

(3) BAGGS, S.A., BAGGS, J.C., BAGGS, D.W. "Australian Earth-covered Building," New South Wales University Press, Rev. Ed., 1991, p101

(4) CARMODY, J, and STERLING, R, "Underground Space Design: a guide to subsurface utilization and design for people in underground spaces," Van Nostrand Reinhold, 1993, p28.

(5) GAO, Q, "The destructive effect of Earthquake on Surface and Underground Constructions," in "Advances in Tunnelling Technology and Subsurface Use", Vol. 4, No. 4, 1984, pp. 195-200.

(6) LOOFBOUROW, R.L., "Effects of Seismic Movement on Underground Space, With Special Reference to Kansas City, Missouri," in "Underground Space," Vol. 9, 1985, pp. 225-229.

(7) LOWING, A.N., "Earthquake Considerations for Earth-Sheltered Residential Buildings," in "Underground Space," Vol. 8, 1984, pp. 169-173.

(8) LUFTY, C, "Spirit of Place," in "Time," December 1, 1997, pp. 73-75.

(9) RAMSAY, G.C., and DAWKINS, D, "Building in bushfire-prone areas - Information and advice," CSIRO, Division of Building, Construction and Engineering, and Standards Australia, SAA HB 36-1993.

(10) RAMSAY, G.C., and DAWKINS, D, ibid.

(11) BOYER, L.L., and GRONDZIK, W.T., "Earth Shelter Technology," Texas A & M University Press, 1987, p 184-85, 193.

(12) KRARTI, M, and CLARIDGE, D.E., "Two-Dimensional Heat Transfer from Earth-Sheltered Buildings," in "Journal of Solar Engineering" Vol. 112, February 1990, pp. 43-50.

(13) HAIT, J, "Passive Annual Heat Storage, Improving the Design of Earth Shelters," Rocky Mountain Research Center, USA, 1983.

(14) HAIT, J, ibid.

Third A-NZ Young Geotechnical Professionals Conference, Cameron, Collingwood & Slatter (eds), Feb. 1998, Melbourne, Australia.

Determining Strength of Calcareous Sediments in a Geotechnical Centrifuge

P.G. Watson
Geomechanics Group, The University of Western Australia

Summary This paper presents results obtained from centrifuge testing of calcareous sediments in order to determine their monotonic and cyclic strength properties. The focus of the paper is on the description of a new testing device for use in the centrifuge facility at The University of Western Australia. Capable of applying torsional loads to various probes, at speeds ranging from 0.2 to 340 deg/s, the equipment has been used to examine the monotonic strength of calcareous sediments through vane shear testing. The results of such tests are compared to those obtained from alternative strength characterisation methods. In addition, a new testing device called the Torsional Plate Load Test is introduced as a means of investigating the monotonic and cyclic properties of the soil.

1 INTRODUCTION

In the design of foundations for offshore structures, one of the primary areas is the determination of *insitu* soil properties. Such soil properties include those used to characterise the type of material, as well as monotonic and cyclic strength parameters, and consolidation coefficients. Typically, an *insitu* site investigation is conducted at the proposed location, and coupled with a detailed laboratory test program to determine the desired parameters. At present, field site investigation techniques include core sampling to determine material types and to obtain undisturbed samples for laboratory testing, and cone penetrometer (CPT) and vane testing to determine *insitu* soil strength.

The discovery of extensive oil and gas reserves in the extremely soft calcareous sediments characteristic of the North-West Shelf of Western Australia, where undrained shear strength profiles may be as low as 0.5 - 1 kPa/m, has led to engineers challenging the traditional testing techniques.

This paper details aspects of a centrifuge test program initiated at The University of Western Australia (UWA) to examine alternate types of *insitu* soil testing apparatus. Firstly, the T-bar and ball penetrometer are discussed and compared to results from traditional CPT testing in calcareous clay in the centrifuge. Discussion will then focus on the description of a new testing apparatus developed for the centrifuge able to conduct in flight rotation tests, with vane test results presented. Finally, a new rotation device is introduced and discussed as a possible device to examine both the monotonic and cyclic *insitu* strength properties.

2 EXISTING METHODS

As mentioned previously, existing *insitu* testing devices for offshore soil strength determination are the vane test and CPT. However, limitations of both apparatus has led to alternative testing devices being examined. Before discussing the proposed alternative testing devices, a brief mention is made of the vane shear test and CPT.

2.1 Vane Tests

With respect to the vane test, the apparatus is only used in soft to medium strength soils due to the sensitivity of the equipment. This becomes a problem when testing in calcareous sediments, where soft soil layers are often separated by thin crusts of cemented material of variable strength.

To deduce undrained shear strength (s_u) from vane tests, the torque (T) required to rotate a cylinder of soil sheared by the vane probe is measured, and can be directly correlated to s_u using

$$s_u = \frac{T}{\pi d^2 (h/2 + d/6)} \qquad (1)$$

where h represents the height of the cylinder (equal to the height of the vane probe) and d represents the diameter of the cylinder (equal to the diameter of the vane probe). A full discussion is provided in Scott (1). The geometry of the centrifuge vane used in the research program is further discussed in Section 4.2.

2.2 Cone Penetrometer

Unlike the vane test, the cone penetrometer is not subjected to limitations due to material layering. However, the use of CPT testing becomes questionable in extremely soft sediments. This can be explained by examining the corrections required in the analysis of CPT data.

Firstly, a correction must be made for the pore pressure at the shoulder of the cone (defined as the pore pressure area correction), and an estimate of the excess pore pressure generated during penetration of the cone is required. In the water depths typical of the new oil and gas fields (often > 300 m) this correction can be significant, and errors in estimating the excess pore pressure can lead to errors in interpreting the CPT results.

Secondly, to deduce net bearing pressure (q_{net}) the measured CPT results (q_m) must be corrected for the overburden stress (σ_v) due to the weight of the soil. In many cases the net bearing pressure may be roughly equivalent to the overburden pressure, which implies that small errors in deducing overburden pressure can result in significant errors in the deduced q_{net}.

In its simplest form, the relationship between measured cone resistance, net bearing pressure and overburden pressure can be expressed as (after Robertson and Campenella (2))

$$q_{net} = q_m - \sigma_v \quad (2)$$

Including the effect of area correction, where α is the area correction factor defined by Almeida and Parry (3), equation (2) becomes

$$q_{net} = q_m - \sigma_v + \alpha(u_0+\Delta u) \quad (3)$$

where u_0 is the hydrostatic pore pressure and Δu represents the excess pore pressure generated during penetration of the cone penetrometer.

Further, excess pore pressure can be determined using

$$\Delta u = \beta q_{net} \quad (4)$$

where β represents the ratio of excess pore pressure to net bearing capacity. Combining equations (3) and (4), and acknowledging that $\sigma_v = \sigma'_v + u_0$, a general equation of the form

$$q_{net} = \frac{q_m - \left[\sigma'_v + u_o(1-\alpha)\right]}{1-\alpha\beta} \quad (5)$$

can be derived to deduce q_{net} from q_m.

Having determined q_{net} from equation (5), the undrained shear strength (s_u) is then calculated using (after Davies et al, (4))

$$q_{net} = N_{CPT} s_u \quad (6)$$

where N_{CPT} is a cone factor deduced from a combination of numerical and experimental testing. For this research program, N_{CPT} is approximately 10-12 which agrees well with other researchers. Field values of N_{CPT} are somewhat arbitrary, with reported values ranging from between 9 and 15 depending on over-consolidation ratio, soil structure and sensitivity, and cone design.

Given uncertainties in the various factors used to derive s_u, Randolph (5) demonstrated how even moderate errors in q_m, α, β, σ'_v and N_{CPT} can lead to errors in predicting s_u betwee +35 % and -25 %. This fact has been the driving force behin the design of alternative testing devices for offshore soils.

3 NEW PROBES

To overcome the shortcomings of the CPT in soft soils (suc as the calcareous sediments typical on the North-West Shelf) two alternative probes have been examined as part of th centrifuge research program at UWA. These are the T-ba and ball penetrometer. Both penetrometers consist of a prob located at the end of thin shaft. The probe is penetrated int the soil stratum, and a load - displacement response generated The two new probes are illustrated in Figure 1, which als shows the CPT and approximate soil mechanisms of the thre devices during penetration. For this research project, the T bar probe consists of a 5 mm diameter bar 20 mm in length penetrated into the soil in a direction perpendicular to th length of the bar. In the case of the ball penetrometer, th probe is simply a 12 mm ball located at the end of the shaft In both cases the probe is sandblasted to generate a surface roughness.

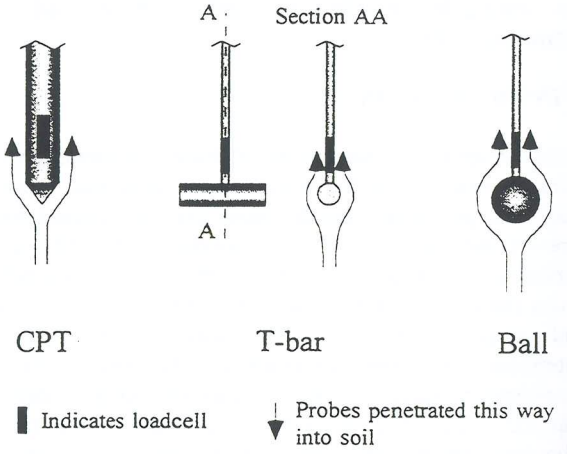

Figure 1 CPT, T-bar and ball penetrometer

As indicated in Figure 1, soil flows above the new probes during penetration, thus allowing equilibrium of the *insitu* vertical stress. Although a small correction is required for the area of the shaft in a similar manner to the CPT, no significant correction is required and the measured bearing pressure (q_m) is equivalent to the net bearing pressure (q_{net})

Thus q_m can be directly correlated to the undrained shear strength using

$$q_m = (N_{Ball} \text{ or } N_{T\text{-}bar})s_u \quad (7)$$

where $N_{T\text{-}bar}$ and N_{Ball} are factors derived from numerical analysis and experimental research. For the case of the T-bar, an exact solution was derived for N_{Tbar} by Randolph and Houlsby (6) using plasticity analysis, with values ranging from 9.14 for a fully smooth analysis to 11.94 for a fully rough case. In this project an intermediate value of 10.5 has been adopted, with support for this coming from Stewart and Randolph (7) where results were reported from field tests of a prototype scale T-bar penetrometer, and a value of 10.5 was proposed.

In the case of the ball penetrometer, disagreement exists between current numerical solutions and experimentally derived values. A value of 10.5 is recommended, and this is further discussed in Watson et al (8).

As will be demonstrated in section 5.2, the T-bar and ball penetrometer provide alternative means of estimating monotonic undrained shear strength. Although the tests have been conducted using model probes under centrifuge test conditions, it is expected that the results would be equally valid under field conditions, with testing currently ongoing to examine this further.

4 ROTARY ACTUATOR

As mentioned previously, a new device was developed as part of this research program. The new apparatus (refered to as the *rotary actuator*) can be used for traditional vane shear tests in flight in the centrifuge, but has primarily been developed to accommodate the new Torsional Plate Load Test (TPLT) discussed below. With the exception of some specific components, the entire actuator was designed and constructed at the Department of Civil Engineering at UWA. A description of the equipment and its features is now presented.

4.1 General Description

Illustrated in Figure 2, the rotary actuator is designed to be housed within existing actuators on the centrifuge, and is supported using clamps (I). The existing actuators enable vertical and lateral movement of the foundation or probe, while torsion (and thus rotation) is applied using the new apparatus.

Torque is applied to the foundation (or probe) using a Motor-Tacho-Gearbox combination (A) purchased from Portescap© to design specifications. Having a mass of less than 500 g (note that weight is an important factor in the design of all equipment on the centrifuge), the inline system utilises at 100:1 gear ratio to provide up to 10 Nm of torque at rotation speeds up to 1 rev/s. A flexible coupling (B) links the gearbox with the lead shaft (C), which also supports a purpose designed and built slip ring assembly (D).

Specially designed within an insulated cell, the slip ring passes the analog signal from load cells located just above the soil probes (see section 4.2) during continuous rotation, thus eliminating the need for cables located along the shaft. Power for the motor and tachometer feedback for velocity control during testing, as well as signals from the load cells and encoder (see below) are passed through a single connection (J), which is connected to a patch box which distributes the various signals for processing and data aquisition.

A detachable connection (E) is located at the base of the lead shaft, which allows multiple shaft extensions to be connected to the apparatus, and a variety of foundation types to be tested. Axial load generated during penetration is prevented from reaching the slip ring / motor assembly by passing the lead shaft through two angular contact bearings (F).

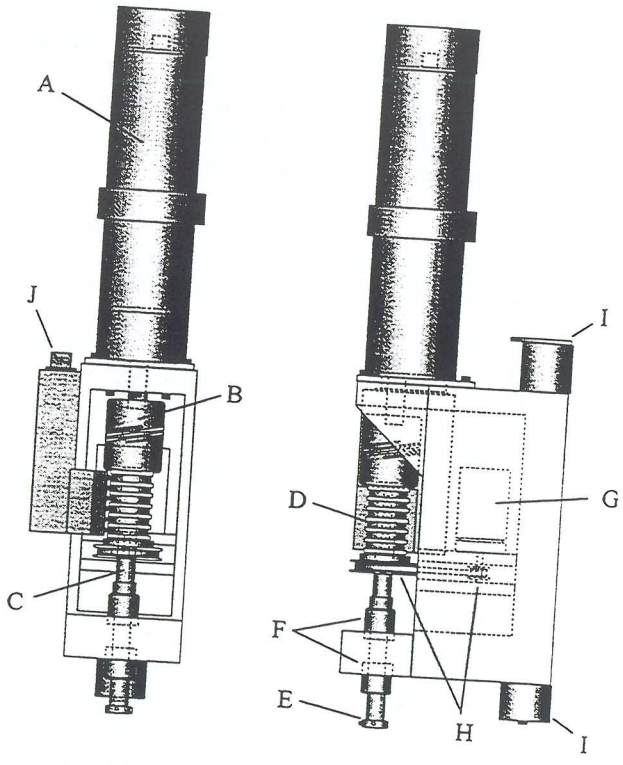

Figure 2 Rotary actuator

Position and velocity is measured using an encoder (G) coupled to the lead shaft via a 4:1 flexible gear and pulley system (H). The encoder signal (consisting of three out-of-phase signals) is processed using electronics developed at UWA, and produces output for rotation and angular velocity during continuous rotation. Sensitivity of the encoder signal is rated at 0.094 deg/bit for rotation angle and 0.1696 deg/s/bit for angular velocity, giving precision control over both position and velocity defined loading events.

The entire apparatus is housed within a clear perspex shield (not illustrated in Figure 2), which provides protection for the various internal components.

4.2 Foundation Types

At present two types of foundation / probes are being examined using the apparatus. These are illustrated in Figure 3, and are the vane and TPLT apparatus.

Compared to those used *insitu*, the vane fabricated at UWA is somewhat squatter in profile, with an aspect ratio (=h/d) of 2/3. This maximises the number of tests that can be done in a centrifuge sample that is only 200 - 250 mm high, and to minimise the effect of strength gradient on observed results. However, the geometry of the vane has a significant influence on the results obtained (discussed further is Section 5.1).

The TPLT consists of a model foundation 30 mm in diameter with skirts 10 % of the diameter. The TPLT can be used to predict the monotonic undrained shear strength of the soil

either through back analysis of the penetration response of the foundation, or through an examination of the response to torsional loading (similar to the vane test, discussed in Section 5.3.1). In addition, the cyclic behaviour of the soil can be examined by applying cyclic loads to the foundation and observing the behaviour (Section 5.3.2).

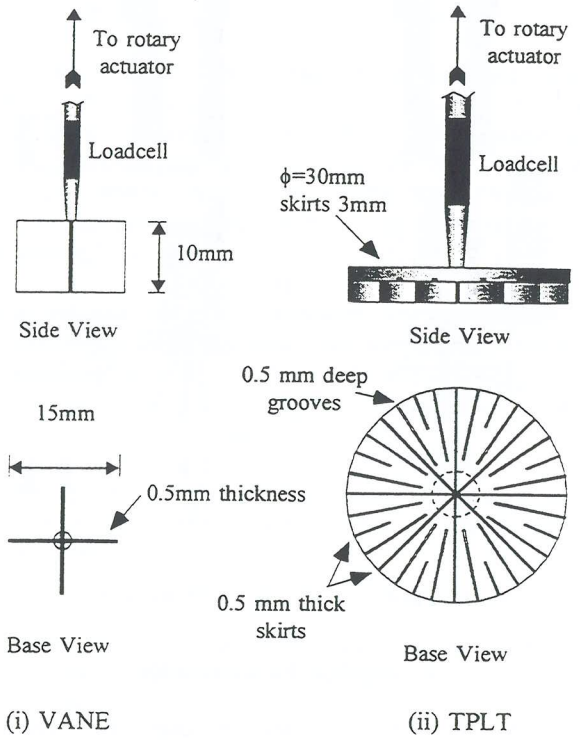

Figure 3 Rotary actuator foundation / probe devices

4.3 Software Development

In addition to the various mechanical components, a full complement of electronic equipment and computer software has been developed to support the rotary actuator.

At present the software (written in QuickBasic format) allows the following tests to be conducted :

Mode 1 Standard vane shear test. This test mode involves rotation of the vane at a selected rate under torsion load and/or rotation limit control.

Mode 2 Cyclic loading. This test mode allows the model foundation to be cycled between torsion limits while maintaining a chosen vertical stress. Limits are set on the rotation speed and the amount of rotation allowed.

Mode 3 Sideswipe test. This test mode involves continuous one way rotation of the foundation under torsion load and/or rotation limit control. Prior to rotation a selected vertical stress is achieved, and the rotation is carried out under conditions of zero vertical strain.

Mode 4 Probe test. This test mode involves continuous one way rotation of the foundation under torsion load and/or rotation limit control. Prior to rotation a selected vertical stress is achieved, which is maintained during rotation.

Test modes 2-4 are designed to be used with the TPLT apparatus, with mode 2 being used to investigate the cyclic behaviour of the foundation, and mode 3 and mode 4 being used to investigate the relationship between torsional load and vertical stress.

5 RESULTS

5.1 Vane Shear Tests

As mentioned previously, CPT, T-bar and ball penetrometer tests have been conducted in calcareous clay at 120 g. In addition, vane tests have been conducted in the same calcareous clay to provide a direct comparison of undrained shear strength deduced from the various test devices.

Figure 4 presents the results obtained from vane tests at increasing depth in the calcareous clay. At each depth the vane was rotated at a constant velocity of 12 deg/s, with a wait time of 30 seconds after insertion of the vane prior to rotation. Although not discussed here, further research has shown that the effect of rotation rate and wait time on the observed undrained shear strength is minimal.

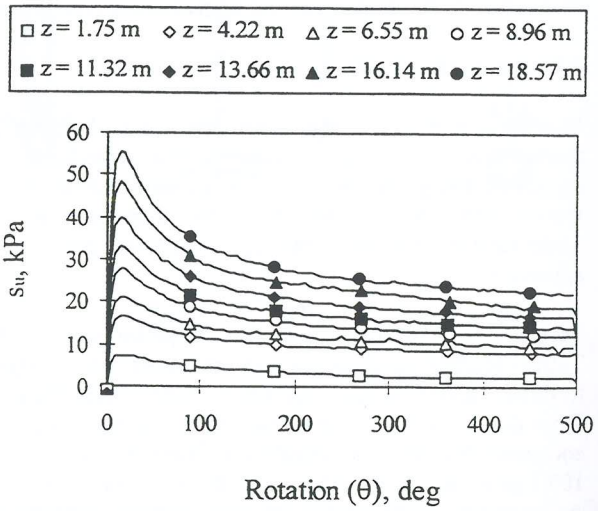

Figure 4 Example of vane testing in calcareous clay

As can be seen from the figure, a peak is observed after approximately 15 degrees rotation, followed by considerable strain softening. Although the results are presented as undrained shear strength, a direct comparison with CPT, T-bar and ball penetrometer results indicated that the observed vane results were approximately 20 % higher. Possible reasons for this are explained in more detail in Watson et al (8), and relate to the geometry of the model vane and soil strength anisotropy. Factoring the results by 83 % provides an excellent fit with the other test devices (see Section 5.2). This is recommended as the vane factor for the UWA vane, and is supported by tests conducted in several other soil types.

5.2 Comparison of s_u

Figure 5 presents a comparison of s_u profiles for the calcareous clay using the various devices. In the analysis it was assumed that $N_{T\text{-}bar} = N_{Ball} = 10.5$, and that $N_{CPT} = 11$. In addition it was determined that for processing the CPT data :

σ_v ~ 15 kPa/m (from water contents determined at the end on testing), α = 13 % (determined from laboratory calibration) and β = 1.0 (based on experience with similar materials). The vane results have been factored by 83 % as explained in section 5.1.

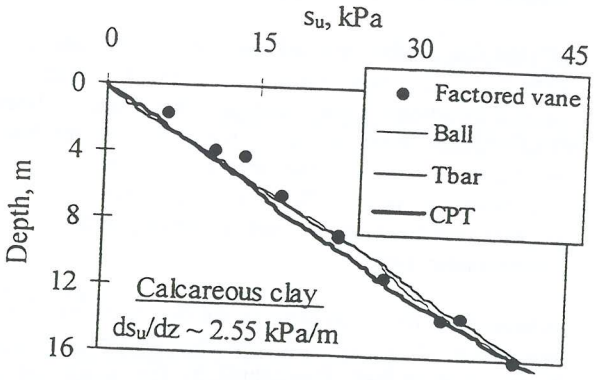

Figure 5 Comparison of s_u profiles from various test devices

As can be seen, an excellent comparison can be made between the various test devices in estimating the undrained shear strength of calcareous clay in the centrifuge.

5.3 Torsional Plate Load Tests

As previously mentioned, the TPLT can be used as a tool for investigating both the monotonic and cyclic properties of a soil.

5.3.1 Monotonic loading

The monotonic shear strength of the soil can be determined from either the penetration response of the TPLT, or from an examination of the torsional response generated by rotating the foundation at depth (similar to the vane).

Since soil flows above the TPLT (similar to the T-bar and ball penetrometers), no correction is required for overburden pressure and the net bearing pressure is equal to the measured bearing pressure (q). The measured bearing pressure can then be used to generate an s_u profile using

$$s_u = q/N_c \qquad (8)$$

where N_c is the bearing capacity factor. By considering the TPLT as a shallow foundation bearing on the surface of soil with strength varying linearly with depth, a profile of N_c can be determined from solutions presented in Houlsby and Wroth (9).

Houlsby and Wroth deduced that for surface footings bearing on soil with strength proportional to depth such that s_u = kd (where k is the strength increase per metre and d is the depth below the foundation), the bearing capacity factor is a function of the ratio kD/s_{uo} (where s_{uo} is the undrained shear strength at the soil surface and D is the foundation diameter). By excluding depth effects and considering s_{uo} as being the shear strength at the depth of the TPLT during penetration, it can be shown that

$$\frac{kD}{s_{uo}} = \frac{D}{d} \qquad (9)$$

From this a continuous profile of N_c can be determined from the Houlsby and Wroth solutions for the range of D/d occuring during penetration of the TPLT.

Note that the above analysis assumes an infinitely thin footing, and a correction has been made to N_c to allow for side shear acting over the full depth of the TPLT. Assuming a fixed percentage of the soil shear strength (δs_u) at the plate/soil interface and 100 % of s_u where there is soil/soil shearing, this amounts to adding roughly 0.5 to the value of N_c deduced using the original Houlsby and Wroth solutions. Figure 6 shows the observed bearing response, and the deduced N_c relationship considering the TPLT to be a shallow footing.

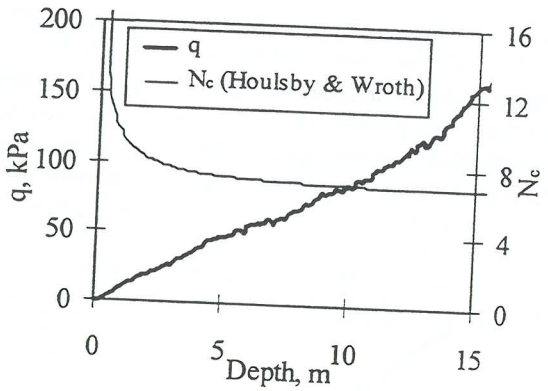

Figure 6 q and N_c

However, as indicated the above analysis ignores the effect of embedment on the foundation response. As such, bearing capacity factors determined using the above method are likely to significantly underestimate the bearing capacity at high embedment. Using a constant value of N_c for the full penetration (similar to that used for the penetrometer devices outlined above) can also be used, and a comparison is made using a constant value of N_c equal to 10.5.

To deduce shear strength from the torsion response, a similar expression is used to that applied to the vane test. However, allowance must be made for shear along the top plate. The equation used to deduce s_u from rotation of the TPLT at depth was

$$s_u = \frac{T}{2\pi r^2 (r/3 + r\delta/3 + t\delta + h)} \qquad (10)$$

where T is the measured torque, t is the thickness of the top cap, h is the skirt height, r is the radius of the TPLT and δ a defined above for monotonic penetration of the TPLT. An average shear strength is assumed to act over the TPLT depth.

Figure 7 presents results obtained using the TPLT apparatus to deduce shear strength in calcareous silt at 150 g. As can be seen, good agreement exists between the shear strength deduced from the monotonic push (using N_c = 10.5) and the torsion results (using δ = 0.4). The shear strength obtained using the bearing capacity factors shown in Figure 6 is

significantly higher, and use of a constant value of 10.5 is recommended.

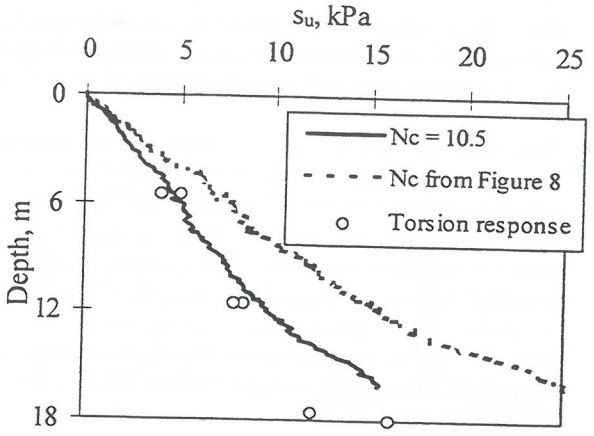

Figure 7 Monotonic s_u from TPLT tests

Figure 8 shows the shear strength profiles derived from TPLT testing in comparison with T-bar and ball penetrometer tests conducted in calcareous silt. As can be seen, an excellent agreement exists between the various testing methods.

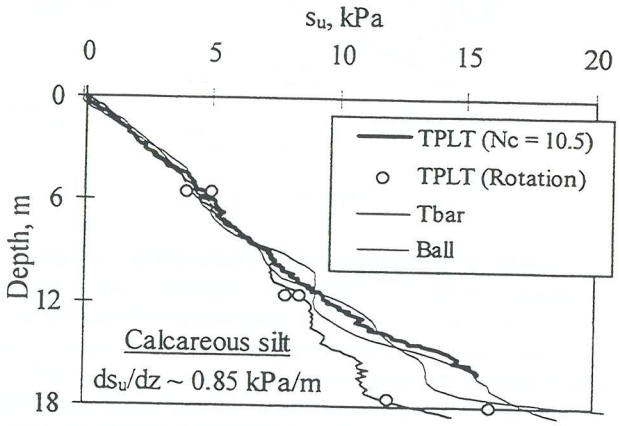

Figure 8 s_u profiles from various tests

5.3.2 Cyclic loading

In addition to the monotonic shear strength, TPLT testing can be used to investigate the cyclic performance of soils. Although only in the preliminary stage, it is hoped that cyclic torsional loading (T_{cyc}) about an average torsion load (T_a), applied at different levels of constant vertical stress (V_a), will provide insight into the behaviour of real foundations subjected to cyclic loading induced by wave or storm loading.

6 CONCLUSIONS

Results have been presented from inflight centrifuge testing of two calcareous materials typical of soil types found on the North-West Shelf of Western Australia. The focus of the work has been directed toward the development of alternative soil testing apparatus to overcome shortcomings associated with the existing *insitu* testing devices for the centrifuge.

T-bar and ball penetrometer testing has been shown to provide results comparable with CPT results, but which can be obtained without the corrections for excess pore pressure and *insitu* stress required to process the CPT data. The results are supported by inflight vane testing using the new rotary actuator described in detail in this paper.

A new test device, named the Torsional Plate Load Test (TPLT) has also been introduced. The TPLT can be used to predict monotonic shear strength either from analysis of the load response observed during penetration of the foundation, or from analysis of the torque required to rotate the foundation at depth. Both methods have been shown to produce results which compare favourably with T-bar and ball penetrometer tests.

Although the focus has been on the development of laboratory equipment, it is expected that the results will have field applications as well, highlighted by the recent use of T-bar testing apparatus at an offshore site in the Timor Sea.

7 ACKNOWLEDGEMENTS

The author is supported by an Australian Postgraduate Research Award and a F S Shaw Memorial Postgraduate Scholarship. The efforts of workshop and centrifuge staff, in particular Mr Mike McCarthy, in developing and testing the apparatus described in this is gratefully acknowledged.

8 REFERENCES

1. Scott, C.R. (1980). *An Introduction to Soil Mechanics and Foundations*,. Third Ed., Applied Science Publishers.
2. Robertson, P.K. and Campanella, R.G. (1983) Interpretation of cone penetration tests. Part II : Clay. *Canadian Geot. J.*, Vol. 20, No.4, 734-745.
3. Almeida, M.S.S. and Parry, R.H.G. (1984) Penetrometer apparatus for use in the centrifuge during flight. *Proc. Symp. Application of Centrifuge Modelling to Geotechnical Design*, Manchester, 47-66.
4. Davies, M.C.R., Almeida, M.S.S. and Parry, R.H.G. (1989) Studies with centrifuge vane and penetrometer apparatus is a normal gravity field. *Geotechnical Testing J.*, GTJODJ, Vol. 12, No. 3, 195-203.
5. Randolph, M.F. (1997). Modelling of offshore foundations. *E H Davis Memorial Lecture 1997.*
6. Randolph, M.F. and Houlsby, G.T. (1984). The limiting pressure on a circular pile loaded laterally in cohesive soil. *Geotechnique*, Vol. 34, No. 4, 613-623.
7. Stewart, D.P. and Randolph, M.F. (1994). T-bar penetration testing in soft clay. *J. Geot. Eng. Div., ASCE*, Vol. 120, No. 12, pp 2230-2235.
8. Watson, P.G., Newson, T.A. and Randolph, M.F. (1997) Strength profiling in soft offshore soils. *First Int. Conf. On Site Characterisation*, (submitted Sept. 1997).
9. Houlsby, G.T. and Wroth, C.P. (1983). Calculation of stresses on shallow penetrometers and footings. *Proc. IUTAM/IUGG Symp. On Seabed Mechanics*, Newcastle, 107-112.

Third A-NZ Young Geotechnical Professionals Conference, Cameron, Collingwood & Slatter (eds), Feb. 1998, Melbourne, Australia.

Design and Construction of Sand Dam to Float Dredge over Buried Pipelines

Peter W Wright Geotechnical Engineer/Hydrogeologist Douglas Partners Pty Ltd

SUMMARY

Mineral sands mining by dredging is carried out within the Tomago Sand-beds aquifer, which is also used to supply potable water to the Newcastle region. In order to transfer a floating dredge and separator plant over twin 1 m diameter water supply pipelines, a large temporary lock system was constructed of sand, comprising 4 m high dam walls. The water level was raised to 3 m above original ground level to enable the mining plant to float across the pipelines.

Engineering design and construction of the lock system was required to prevent damage to the strategically important pipelines. The design included slope stability and seepage analyses as well as analysis of stresses imposed on the pipeline by the embankment. The necessity to control stress on the pipeline required spanning over the pipeline with a steel plate structure underlain by a void. The presence of the void within the embankment placed particular emphasis on the control of piping, which had potential to cause both filling of the void and embankment failure. After consideration of both cut-off walls and lining systems, piping was controlled using a combination of sand and gravel toe berms underlain by filter fabric, as well as baffles along the steel plate. A void was maintained below the steel plate utilising reinforced filter fabric.

1 INTRODUCTION

The aim of the project was to design and construct a lock system to enable safely floating a sand mining dredge over strategically important water supply pipelines. The primary constraint on the project was the necessity to use the sands on site for construction of the dam walls. This constraint required the design to overcome some interesting problems as discussed in the following sections.

Involvement in the project comprised three main stages as follows:

- preliminary design;
- detailed design;
- construction testing.

The Tomago Sand Beds are a major source of potable water for the Newcastle Region. Douglas Partners has had extensive involvement in water quality management of the aquifer over the last 20 years and thus have significant data on the site as discussed in the following section.

2 SITE CHARACTERISTICS

The Tomago Sand Beds comprise an extensive unconfined sand aquifer. The aquifer has an average thickness of around 20 m and is underlain by clay and sedimentary bedrock. The sands are generally fine to medium grained, in-situ and laboratory testing suggests a typical hydraulic conductivity of 1×10^{-4} m/s to 2×10^{-4} m/s.

Antecedent groundwater levels at the crossing location are generally between one and three metres below ground level. Hydraulic gradients in the area were generally in the range 0.003 to 0.004.

The site contains both previously mined and natural unmined sand. Cone penetration testing undertaken in the sandbeds indicates that areas of hydraulically placed mine tailings are generally in a very loose to loose condition. Unmined ground is typically in a medium dense to dense condition.

Existing twin 1.0 m diameter water supply pipelines cross the site. The pipelines are of concrete lined steel construction with their obvert level 1 m below ground surface level.

2 PRELIMINARY DESIGN

2.1 General

The preliminary stages of design work comprised assessment of the practicality to construct the dam walls from clean sands. Assessment of seepage flows through the relatively permeable sands was a primary consideration together with slope stability analysis.

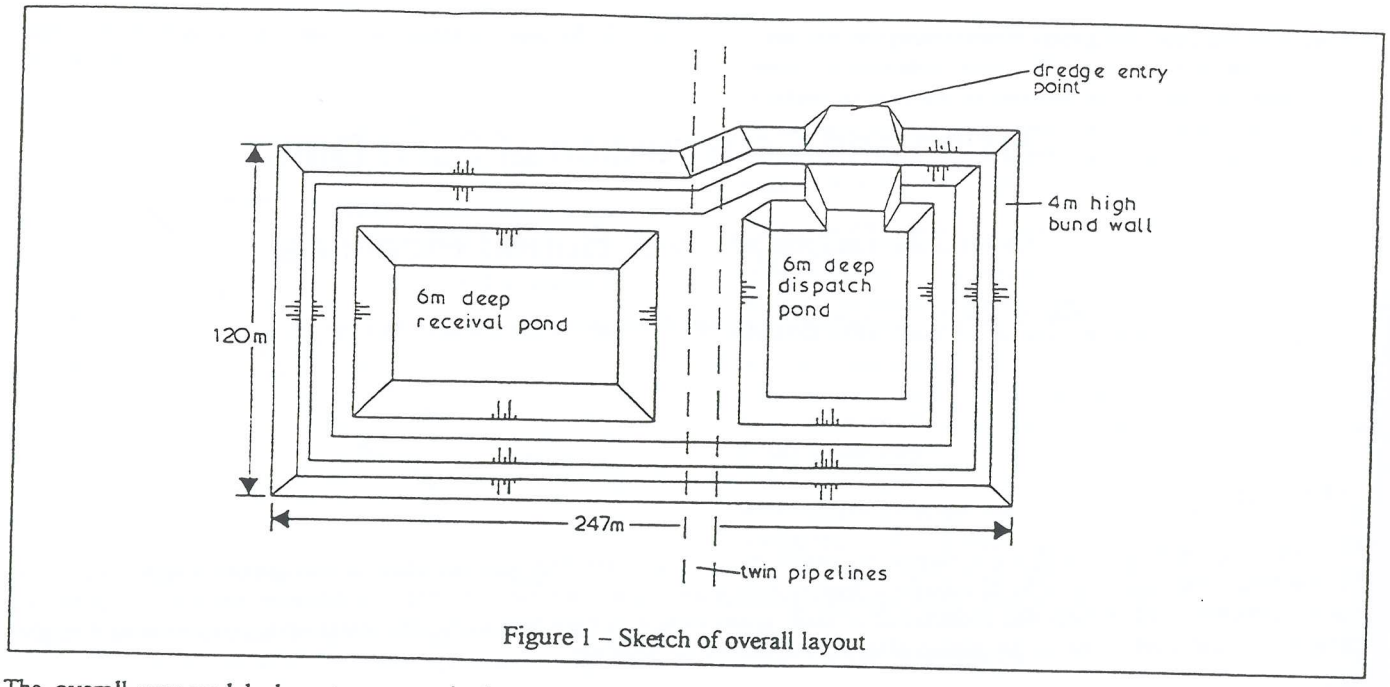

Figure 1 – Sketch of overall layout

The overall proposed lock system comprised a rectangular dam 240 m long and 115 m across, with ponds excavated within the bunded area either side of the pipeline. The overall scheme layout is shown on Figure 1. The mining plant required at least 3 m depth of water, thus dam walls were 4 m high to allow 1 m freeboard, the ponds required excavating to approximately 6 m below existing ground level.

2.2 Seepage

The seepage analyses was carried out using the computer modelling package SEEP/W, which allows transient analyses and unsaturated flow. In order to model unsaturated flow the program makes use of functions to relate both hydraulic conductivity and volumetric water content to pore pressure. Standard library functions appropriate for a fine to medium grained sand were used, and are presented in Figure 2 below. The functions take into account the reduction in hydraulic conductivity and water content for negative pore pressures (unsaturated conditions).

The seepage analyses and stability analyses are somewhat interdependent and preliminary seepage analyses were based on batter slopes of 2H : 1V. The cross section was assumed homogeneous and isotropic. A sensitivity analysis was performed on the saturated hydraulic conductivity, ranging it from $1x10^{-4}$ m/s to $2x10^{-4}$ m/s whilst retaining the general shape of the function appropriate for unsaturated conditions.

Steady state modelling indicated that with the dam full, hydraulic gradients were less than the critical gradient appropriate for piping of the sands. The primary concern was surface erosion of the sands at the toe, due to seepage exiting the lower slopes of the batter. As such, the seepage analyses concentrated on the time taken for seepage to surface at the downstream toe.

It was estimated a period of at least twelve hours was required to fill the dam and the transient analyses indicated that the wetting front was likely to reach the downstream toe within six to eight hours of the dam being full. Both partial lining of the upstream batters and a cut-off wall 10 m to 15 m deep were modelled. Each case still allowed propagation of the wetting front to the toe within the period required to transfer the dredge, however hydraulic gradients at the toe were significantly reduced thus reducing the likelihood of piping.

Due to the uncertainty of the effect of seepage at the toe, as well as cost and construction considerations, a third option was adopted which involved placing filter fabric at the toe beneath a 1 m high berm constructed of sand. The

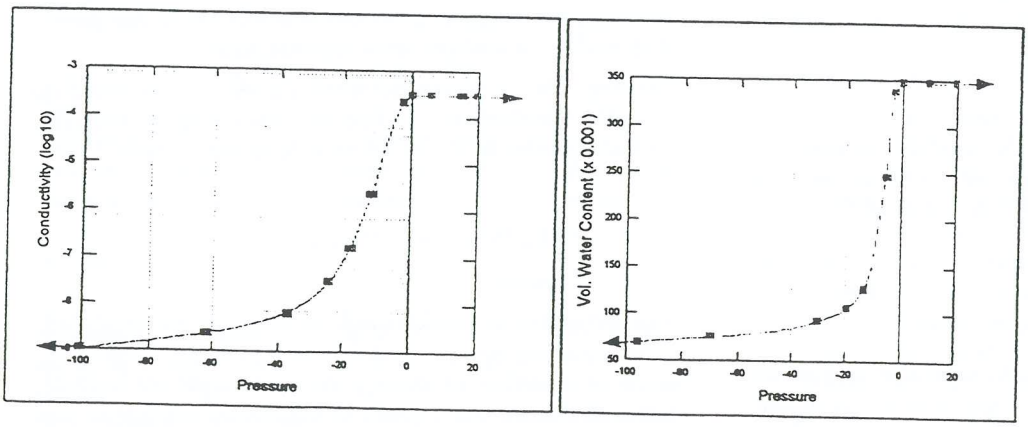

Figure 2 – Hydraulic conductivity and volumetric water content functions

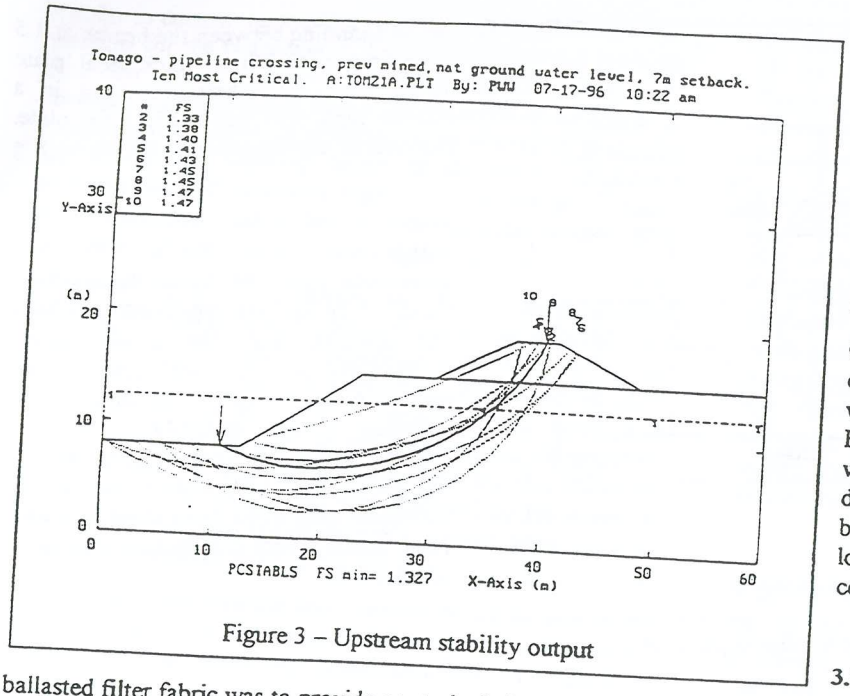

Figure 3 – Upstream stability output

ballasted filter fabric was to provide control of piping and the berm provided enhanced down stream stability of the embankment.

Steady state modelling of the toe berm option indicated seepage rates in the range 10 to 20 litres/min/m run of the dam. The estimated seepage rates were then used for preliminary assessment of pumping requirements to fill the lock system.

2.3 Stability

Stability analyses was carried out using the slope stability model PCSTABL 6.0, using the following strength parameters;

- Previously mined ground : $\phi' = 28°$
- Natural unmined ground : $\phi' = 30\text{-}32°$
- Constructed bund wall : $\phi' = 32\text{-}34°$

The strength parameters were considered relatively conservative, however they were based on limited site specific data, and allowed for refinement of the analyses during final design work if required. A minimum density index of 75 % was assumed for the constructed bund wall. A minimum acceptable factor of safety of 1.2 was adopted based on the temporary nature of the works. Slip circle type analyses was carried out based on various seepage conditions.

The modelling indicated that the antecedent water levels were critical for upstream stability and the elevated water levels, calculated from the seepage analyses, were critical for downstream stability. For 2H:1V batters of the constructed dam, downstream stability was acceptable particularly if the 1 m high berm discussed in the previous section was constructed at the toe.

The upstream profile was assessed based on a batter slope of 1.5H:1V for the excavated pond walls and a 2H:1V for the constructed dam wall. The modelling indicated that a setback distance between the toe of the bund and the edge of the pond was required, varying from 2.5 m for unmined ground to 7 m for previously mined ground. A typical stability output is presented on Figure 3. Minor slumping of the saturated pond walls was not considered to be critical to overall stability.

3 DETAILED DESIGN

3.1 General

Once the viability of the project was confirmed detailed design was undertaken. Particular attention was placed on protection of the buried pipelines. Fretting and overall stability of the excavated pond walls adjacent to the pipelines; the effect of the dredge landing above the pipeline in the event of a breach of the dam; and the effect of the surcharge load on the pipeline from the embankment were all considered.

3.2 Stability

A ten metre setback between the edge of the pond and the edge of the pipelines was adopted to provide protection from fretting but more particularly to increase stability in the case that the dredge landed above the pipelines.

2.3 Stress on Pipelines

Stress analyses on the pipeline, undertaken by the civil consultants involved in the project Advitech Pty Ltd, estimated that the pipelines could sustain a safe applied load equivalent to approximately 1 m thickness of sand without cracking of the concrete liner occurring. The ratio of vertical to horizontal stress on the pipelines was found to be particularly important. As 4 m of compacted sand was to be

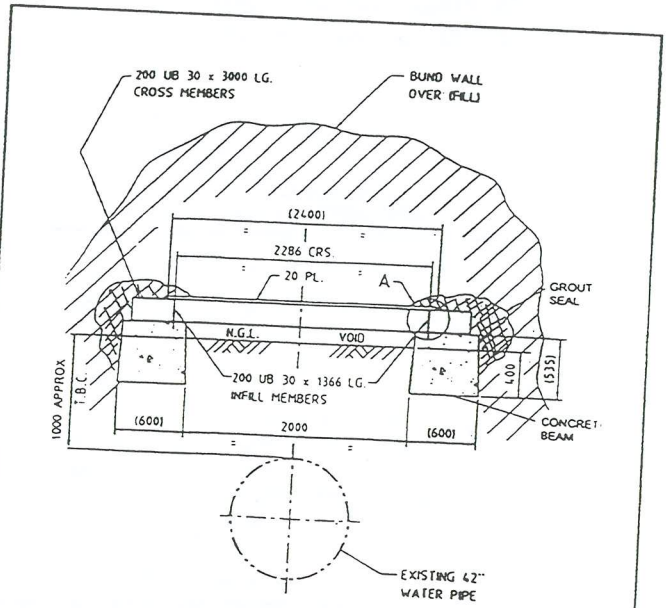

Figure 4 – Section of structure over pipelines

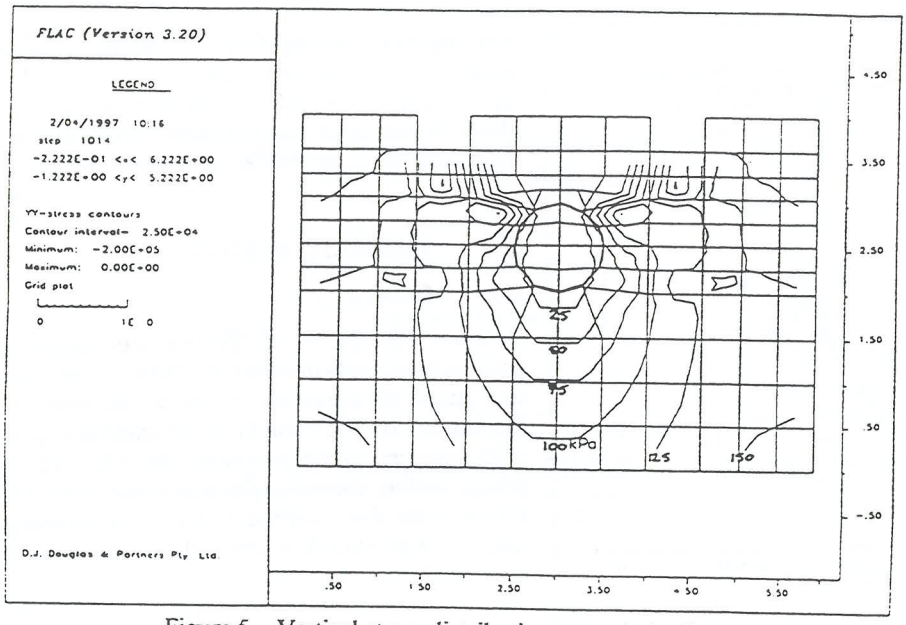

Figure 5 – Vertical stress distribution around pipeline

placed over the pipelines, measures to reduce stress on the pipelines were required.

Several options were considered to control stress on the pipelines including concrete encasement of the pipeline, however the Hunter Water Corporation, owners of the pipeline, required that excavation around the pipelines was kept to a minimum.

The preferred option was the construction of a structure which spanned across the pipelines, distributing the load of the overlying embankment either side of the pipeline. The structure comprised a concrete beam placed each side of each pipeline, in parallel, 2.5 m apart. Steel beams were then placed spanning between the beams at 1.5 m centres, with 20mm thick steel plate placed over the beams, resulting in a 300mm high void below the steel plate. The overall configuration is shown on Fig 4.

Analyses of the resulting stress distribution around the pipeline was undertaken using the modelling package FLAC. A Mohr-Coulomb/Elastic analysis was adopted and the pipeline was incorporated into the model as a solid with an equivalent modulus. The modelled stress distribution indicated maximum vertical total stresses at the pipeline of 50 kPa and a vertical to horizontal total stress ratio close to unity. The vertical stress distribution is shown on Figure 5.

3.4 Seepage

The restriction that no more than one metre of filling could be unsupported above the pipeline meant the void ran almost the full width of the embankment. The continuation of the void close to the downstream toe significantly increased the risk of piping. The void would provide a preferred path for flow beneath the embankment resulting in high hydraulic gradients at the toe. The impermeable steel plate above the void would force seepage flowing through the embankment to be concentrated at toe where the height of the embankment above the steel plate was less than a metre. This would increase the hydraulic gradient as well as force the seepage exit point further up the embankment.

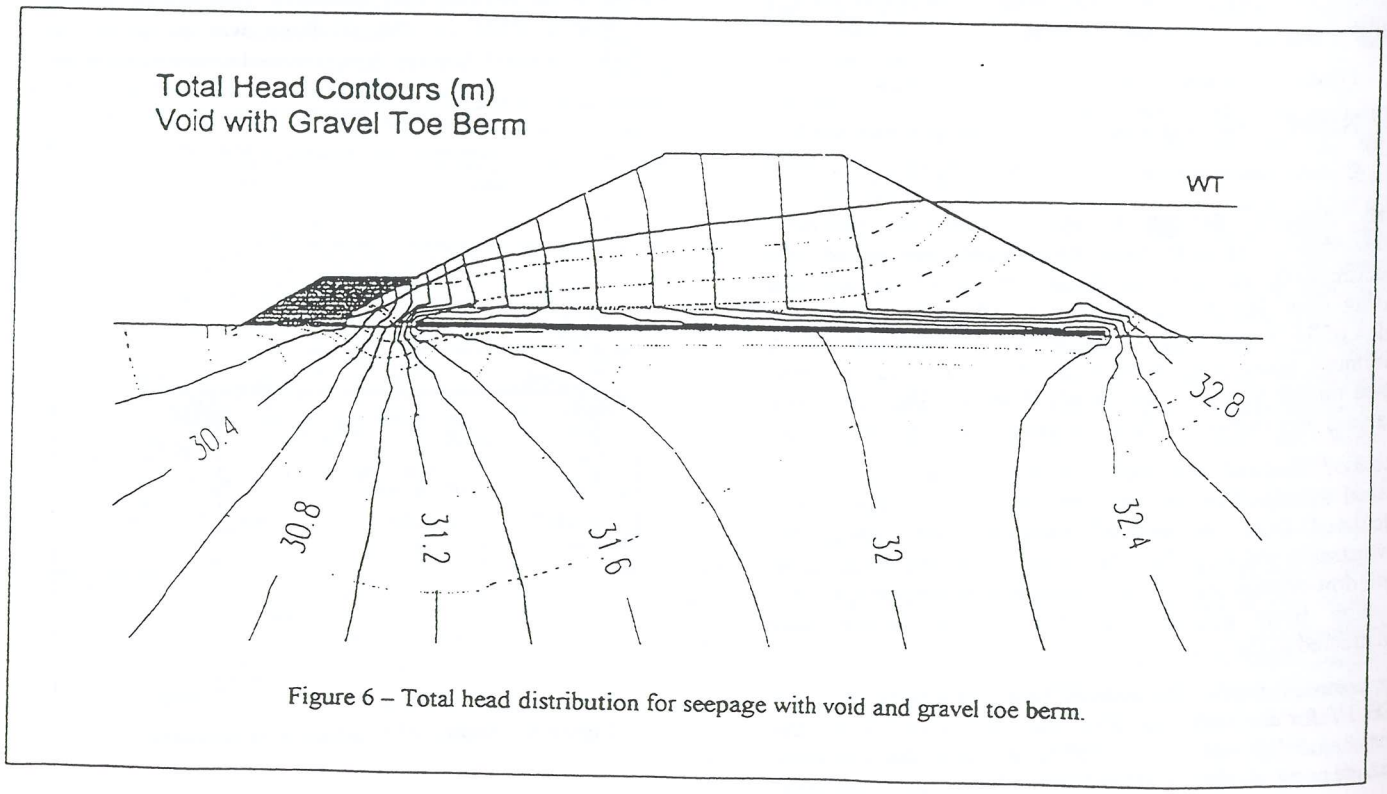

Figure 6 – Total head distribution for seepage with void and gravel toe berm.

In order to control the seepage exit point, the sand toe berm as specified for the remainder of the embankment was replaced by a free draining gravel, underlain by filter fabric. The seepage regime modelled with SEEP/W is shown on Figure 6. A distinct draw-down of the water table is evident at the toe due to the free draining nature of the gravel. Hydraulic gradients are still relatively high, however the gravel berm allowed the use of a higher critical hydraulic gradient and thus an acceptable factor of safety against piping.

Additional measures to reduce the risk of piping included welding 300 mm high baffle plates to the top of the steel plate where the smooth interface otherwise provided potential for piping to develop. Due to the constraint that the gravel berm could only be one metre high, additional filter fabric was placed along the surface of the batter slope immediately above the berm in case the seepage did exit the face above the gravel berm. The filter fabric was anchored by the gravel at the bottom end and anchored between sand layers, during embankment construction, at the top end.

A secondary consideration was mobilisation of the sand at the upstream end of the void such that it filled the void, thereby transferring load from the embankment onto the pipelines. This concern was addressed by spanning reinforced filter fabric between the concrete girders such that it held the underlying sand in place. Figure 7 shows the details of preventative measures used to stabilise the sands.

CONSTRUCTION

Performance of the lock system was very much dependant on careful construction of the bund walls and attention to detail at the pipelines. Full time construction supervision was provided by Advitech Pty Ltd, with Douglas Partners providing earthworks inspections and testing.

Compaction was primarily checked using dynamic penetrometer testing. Calibration of the penetrometer was undertaken under laboratory conditions using sand from site placed at a controlled density index within a 200 litre mould. Ongoing correlation of penetrometer testing against field density testing and laboratory compaction was undertaken throughout construction.

The construction of the steel structure resulted in the ends of the void being open, as well a number of openings along the side of the void. The need for a low shrinkage, low cost and reasonably high strength sealing material, which could be placed with practical ease, resulted in the use of a dry mix of sand, cement and fly-ash. The material was placed dry to reduce shrinkage and was compacted using a vibrating plate, then overlain with wet sand to allow hydration. A cement/fly-ash content of 20% was used to provide sufficient strength to inhibit cracking due to deflection of the steel plate, the fly-ash content reducing shrinkage and cost.

CONCLUSIONS

The mining equipment was successfully floated over the pipeline in March 1997. Subsequent camera inspection inside the pipeline confirmed no damage to the concrete lining of the pipelines. Observation made while the water level was at full height confirmed that the seepage and piping control measures had worked. Seepage was observed emanating from the gravel toe berm and elsewhere only minor slumping of the sand occurred at one corner of the dam. The dam has since been removed.

The project provided a number of challenging problems, which required practical engineered solutions to allow simplicity of construction and control of costs. Dam design and construction always provides interesting design issues, however the necessity to use relatively permeable sands for construction of the lock system and the added complexity of controlling stresses on the pipeline made this project particularly unusual.

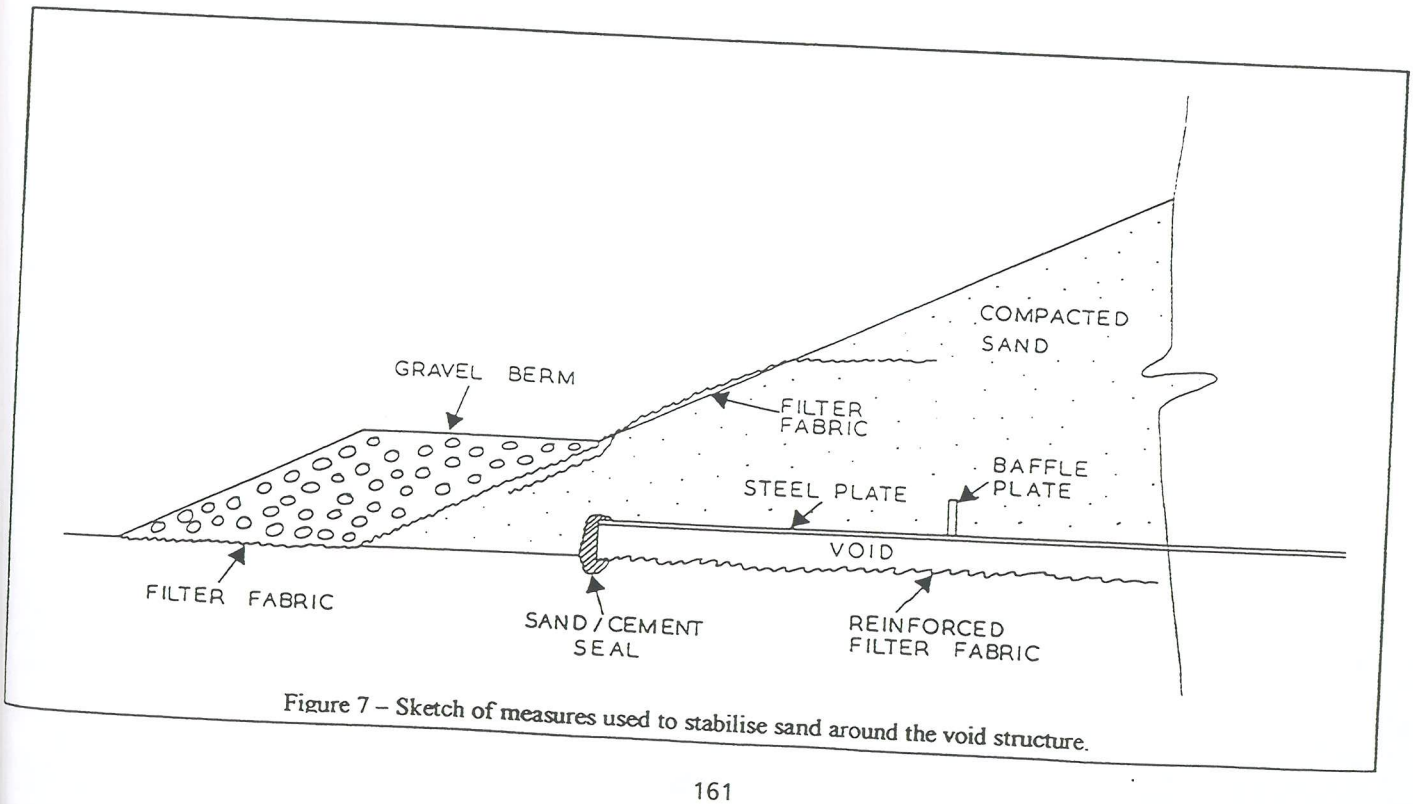

Figure 7 – Sketch of measures used to stabilise sand around the void structure.

BIBLIOGRAPHY

- Carter M, "Geotechnical Engineering Handbook", Pentech Press.
- Douglas Partners Pty Ltd, "Report on Geotechnical Assessment, RZM Pipeline Crossing, Tomago", Project no 18471, March 1996.
- Douglas Partners Pty Ltd, " RZM Pipeline Crossing, Tomago", Project no 18471A, August 1996.
- Douglas Partners Pty Ltd, " RZM Pipeline Crossing, Tomago", Project no 18471A/1, February 1997.
- Geoslope International, "SEEP/W user manual", Ver 4.0, 1996.
- Lee, White & Ingles, "Geotechnical Engineering",1983, Pitman.

Cameron, Grant; Collingwood, Ben; Slatter, Jim editors.
PROCEEDINGS OF THE THIRD AUSTRALIA-NEW ZEALAND YOUNG GEOTECHNICAL

Sponsored by:

COFFEY PARTNERS INTERNATIONAL PTY LTD

FRANKIPILE AUSTRALIA PTY LTD

GEOTECHNICAL SYSTEMS AUSTRALIA PTY LTD

GEOTEST PTY LTD

GOLDER ASSOCIATES PTY LTD

MONASH UNIVERSITY, DEPARTMENT OF CIVIL ENGINEERING

RUST PPK CONSULTANTS PTY LTD

THE NEW ZEALAND GEOTECHNICAL SOCIETY

UNIVERSITY OF NSW, SCHOOL OF CIVIL ENGINEERING

UNIVERSITY OF WA, DEPARTMENT OF CIVIL ENGINEERING

VIBROPILE (AUST.) PTY LTD

WOODWARD-CLYDE CONSULTANTS PTY LTD